Preparation and Characterisation of Binder-Free All-Cellulose Composites

A THESIS SUBMITTED TO THE UNIVERSITY OF LONDON
FOR THE DEGREE OF DOCTOR OF PHILOSOPHY

December 2013

By
Raquel Arévalo Peces
School of Engineering and Materials Science
Queen Mary, University of London
Mile End Road, London E1 4NS

I declare that the work presented in this thesis is performed entirely by myself during the course of my PhD studies at Queen Mary, University of London and has not been submitted for a degree at this or any other university.

Raquel Arévalo Peces

A mis padres,

hermana y sobrina.

Abstract

A recent emerging concept of all-cellulose composites within the field of environmentally friendly materials has received increasing attention. The main advantage of these materials is the lack of using additional bonding agents such as polymer resins as in the case of e.g. phenolic resin based panel products or natural fibre reinforced plastics that increase their environmental impact. Two different routes for the production of all-cellulose composites have been followed. The obtained materials were characterised by scanning electron microscopy, X-ray diffraction, flexure and tensile mechanical tests, thermogravimetric analysis, pycnometry and water absorption tests.

The first strategy makes use of the selective dissolution method where the cellulose fibre skins are partially dissolved to form a matrix phase that bonds the fibres together, while the strong core fibres are maintained and impart a reinforcing effect to the composites. The influence of the dissolution time, activation time and the fibre source were assessed. It was found that a dissolution time of 18 h led to materials with the best overall mechanical performance (5.5 GPa and 145 MPa for Young's modulus and tensile strength, respectively), as this time allowed for the dissolution of a sufficient amount of fibre surface to obtain good interfacial bonding between fibres, while keeping a considerable amount of remaining fibre cores that provide a strong reinforcement to the composite, leading to materials that outperform natural fibres reinforced polypropylene composites.

Still, the previous methodology has the drawback of using chemical substances of high environmental impact (solvents). In order to overcome this, a new concept in the production of all-cellulose composites is proposed in this work, which makes use of the intrinsic bonding capability between cellulose fibres to enhance the hydrogen bond network in order to produce materials of good mechanical performance. A new experimental procedure was developed, based on the refinement

of cellulose fibres in order to increase their specific surface area, thus increasing the interfibre bonding capability, and achieving materials with excellent mechanical properties, up to 17 GPa and 119 MPa for flexural modulus and strength, respectively, and low water absorption. These new high-performing environmentally friendly materials are based on renewable resources and are 100% recyclable and biodegradable.

Acknowledgements

Financial support from the Engineering and Physical Sciences Research Council through a Technology Strategy Board project REFLECT no. MATH1E2R, under the Design & Manufacture of Sustainable Products Call, is gratefully acknowledged. In addition, I would like to thank all the partners involved in this research work incluiding Omodo GmbH, InterfaceFLOR, Brunel University, BioRegional Development Group, Heineken UK, Hemp Technology, and the UK's National Non-Food Crop Centre (NNFCC).

I wish to thank my supervisor Prof. Ton Peijs (my dear Tonito) for giving me the opportunity to carry out this PhD study in his group (despite my first English interview), but also for his support, guidance, advice, help and care. Moreover, I would like to thank Dr. Stergios Goutianos for his great contribution in the research work described in Chapter 8 but especially for his constant encouragement and support throughout this study.

Most of the experiments have been carried out at Queen Mary, Materials Department, in an exceptional friendly environment. I wish to thank all the group members and support staff for their kind help, fruitful discussions and advices and more importantly for their friendship. Thanks to Dr. Z. Luklinska and Mr. M. Willis for SEM assistance, Dr. R. Wilson for XRD assistance and discussions, Mr John Caufield, Mr Mick Willis, Mr Colin Langdown, Mr Danny Neighbour, Mr Bill Godwin, Mr Vince Ford and Mr Hugh MacGillivray for their technical assistance with the manufacturing and testing of the specimens. Thanks are especially given to all of the members in Prof. Ton Peijs´s group for making me feel part of this great family: Emiliano Bilotti, Chris Reynolds, Hua Deng, Rui Zhang, Zhujuan Wang, Nattakan Soykeabkaew, Jianmin Zhang, Saharman Gea, Antonio Scherillo, Manuela Russo, Marc Simonet, Jia Ma, Doris Wai Yin Wong, Mohammed Baklar, Dhanushka Hapuarachchi, Rahul Gaba, Russell Bailey, Fianti Noor, Mónica Pino, Inés Jimenez

Palomar, Pelin Yilmaz, Urszula Stachewicz, Beatriz Cortés Ballesteros, Sara Rita Agnese Cammarano. I would like to acknowledge Beimeng Qi, Olivier Picot, Linjiang Chen, Alvaro García Rodríguez and Iffat Fatima Patel for assistance with the experimental work.

I would like to thank all the friends I made during my stay in London for their friendship, hospitality and unconditional support: Ana María Borreguero, María del Pilar García Souto, Choothum Jeenjitkaew, Maurizio Zaccagnino, Said Hamad, Alicia Viruel, Rocío, Alessia Annibale, Ricardo Grau-Crespo, Hector, Antonio Torrisi, Tzu Chun Chen, Francisco Rafael García García and Dafne Zuleima.

All support, endless love and understanding from all my Spanish friends are deeply appreciated: Gema Aguilar, Joana Aguilar, Isabel Galán, Violeta Lucas, Macarena de los Ríos, Marta Robles, Charo Escribano, Ruth Ortiz, Salomé Del Castillo, Virginia Aguilar, Virginia Ramos, Eugenia Angulo, Isabel Rodríguez, Silvia Álvez, Mercedes Alonso, Raquel García, Mercedes Abengózar y Raquel Moreno. I love you!!!

Special thanks to Luis Gómez-Hortigüela for his unconditional support and encouragement from the beginning to the end of this adventure. I would never have been able to finish this thesis without you. Every word of this thesis has inside the constant support, admiration and love you have provided me during these years. This thesis has been a joint creation.

Quiero expresar mi más profundo agradecimiento a Guillermo Rubio por su paciencia y cariño mostrados durante los meses de escritura de esta tesis, sin duda, uno de los momentos más duros de mi vida. Gracias por acompañarme en esta etapa de mi vida con tu comprensión y ánimo constantes, y sobre todo, por enseñarme que todo esfuerzo lleva consigo su recompensa. Gracias de verdad.

Finalmente, quiero dedicar esta tesis a mis padres, Ramón y Luisa, por haberme apoyado desde el principio en esta aventura y haber demostrado una paciencia infinita durante la escritura de la tesis. A mi hermana, Luisi, y sobrina, Andrea que las quiero con locura. A Andrea, la niña de mis ojos, por haberme proporcionado tanta alegría y cariño, pero sobre todo, por haberme transmitido tu entusiasmo por la vida. Cuánto te eché de menos en Londres, pequeñita. Te quiero hasta el infinito y más allá princesita.

Table of Contents

List of Figures

List of Tables

1

Introduction

Nowadays, problems associated with the environment such as the shortage of landfill space, the depletion of petroleum resources, the emissions during incineration and hazards to living beings combined with the growing environmental awareness have spurred an extensive research into environmentally friendly materials in order to replace materials considered harmful to the environment. Natural fibres represent exceptional candidates for the production of biobased materials due to their low cost, worldwide availability, low density, competitive specific mechanical properties, sustainability, combustibility and biodegradability[1]. In conventional natural fibre reinforced plastics, natural fibres serve as reinforcement and are embedded in a polymeric matrix. Thermoplastic materials that currently dominate as matrices for natural fibres are polypropylene, polyethylene, and poly(vinyl chloride) while for thermosets, phenolics and unsaturated polyesters are most common[2]. One of the main advantages of natural fibres is related to their intrinsic lightweight

properties compared to traditional glass fibres, which implies a potential reduction of fuel consumption together with the related reduction of gas emissions, making these materials very suitable for transport applications such as the automotive industry (Figure 1.1). However, one of the main drawbacks of the use of natural fibres as reinforcements in polymer composites is their poor compatibility with polymer matrices due to the hydrophilic nature of these biofibres and the reinforced hydrophobic polymers[3]. In order to improve the adhesion between natural fibres and polymeric matrices, the use of compatibilisers or coupling agents is often required[4-6]. In certain cases, a modification of the fibre surface and/or the matrix is necessary to improve the compatibility between fibres and matrices[7]. Nevertheless, in many cases the different strategies followed to achieve an improvement in fibre-matrix adhesion also involve an increase in processing cost and time[8], as well as an increase in environmental impact. Another disadvantage related to the use of natural fibres in polymer composites is the relatively low composite processing temperature range required, due to the possibility of thermal degradation of natural fibres and/or the possibility of volatile emissions that could affect composite properties. Typically, processing temperatures for most natural fibres are thus restricted to about 200 °C, which limits the choice of the polymers as well as their subsequent recyclability[9].

Figure 1.1. Elements of a Mercedes-Benz A-class car made with flax fibre mat reinforced polypropylene.

A desirable solution to overcome such limitations is provided through the development of "all-polymer composites" or "self-reinforced polymer composites" derived from mono-material based *eco-design* concepts. All-polypropylene composites were found to be highly competitive with traditional glass fibre reinforced plastics for a number of applications, notably the automotive industry, due to their recyclability, lightweight properties and eco-friendly nature[10-12]. An important advance in this field was recently introduced by the development of all-cellulose composites[13]. The production of all-cellulose composites was based on a selective dissolution method where the cellulose fibre skins were partially dissolved to form a matrix phase that bonds the fibres together, while the strong core fibres were maintained to impart a real reinforcing effect to the composites. The fact that in these composites both the fibre and the matrix are cellulose, renders an excellent interfacial compatibility, hence providing fully recyclable and environmentally friendly materials with good mechanical properties[8,14]. Due to the environmental benefits and the high mechanical performance of these materials, this approach has been followed for the production of all-cellulose composites in Chapter 4, using cotton as natural fibre source. The effect of the activation time, dissolution time and cotton source on the performance of the obtained materials will be reported.

However, although this method provides a great advance towards the production of environmentally friendly high-performing materials, it still presents an important disadvantage: the use of environmentally harmful and expensive chemical substances or solvents such as N,N-dimethyl acetamide. Therefore, it is proposed that the ideal biobased composite material would be solely based on natural fibres and hence have no polymer matrix so that a 100% biobased material is obtained, consequently decreasing its environmental impact, while at the same time creating a fully recyclable material which requires neither the addition of coupling agents, binders nor fibre treatments, which would all increase the environmental impact. Such a new concept for all-cellulose composites is proposed in Chapter 5. The binder-free all-cellulose composites presented here are made entirely from plants and biobased waste sources and use no pre-treatment, no solvents and, most importantly,

no resins or bonding agents as in the case of e.g. phenolic resin based medium density fibreboards (MDF) or natural fibre reinforced plastics. Instead bonding between fibres is achieved solely through Van der Waals or hydrogen-bonding. To produce high-performing composites without the need of a matrix, the Van der Waals or hydrogen-bonded fibre network should be significantly enhanced by increasing the fibre specific surface area. Therefore, Chapter 5 also reports the development of a new environmentally friendly processing protocol for large scale production of binder-free all-cellulose composites based on the increased inter-fibre bonding capability of cellulose fibres through an extensive refining process, where the initial cellulose fibres with diameters of about 20 μm are reduced to fibrils with diameters in the nanometer range. Unlike conventional panel-board products like MDF, binder-free all-cellulose composites are fully recyclable similar to paper, as well as biodegradable with excellent mechanical properties outperforming natural fibres reinforced plastics, thus providing an exceptional alternative to wood fibre composites and other chipboards or panel products for building applications, such as walls or flooring (Figure 1.2).

Figure 1.2. Binder-free all-cellulose composites for flooring application.

Different raw materials can be use for the production of binder-free all-cellulose composites, such as flax fibres and blends of recycled paper fibres and hemp/bleached kraft fibres as will be demonstrated in Chapters 5 and 6, respectively.

Finally, a study of the fracture behaviour of binder-free all-cellulose composites through the measurement of its fracture resistance and the observation of failure mechanisms during crack growth will be presented in Chapter 7.

1.1 Aim of the work

The aim of the current research work is to produce high-performance all-cellulose composites by following the two strategies explained above. Different processing parameters will be analysed in an attempt to optimise the mechanical performance of the obtained materials and establish the validity of a new concept for binder-free cellulose composites. The structure, morphology and mechanical properties of these composites will be characterised by scanning electron microscopy, X-ray diffraction, mechanical tests, thermogravimetric analysis, pycnometry and water absorption tests.

1.2 References

[1] L. A. Berglund and T. Peijs, Materials Research Society Bulletin 35 (3), 201 **(2010)**.

[2] R. Malkapuram, V. Kumar, and Y. S. Negi, Journal of Reinforced Plastics and Composites 28 (10), 1169 **(2009)**.

[3] M. Q. Zhang, M. Z. Rong, and X. Lu, Composites Science and Technology 65 (15-16), 2514 **(2005)**.

[4] A. Espert, F. Vilaplana, and S. Karlsson, Composites Part a-Applied Science and Manufacturing 35 (11), 1267 **(2004)**.

[5] S. Mohanty and S. K. Nayak, Journal of Reinforced Plastics and Composites 23 (18), 2047 **(2004)**.

[6] S. Mohanty, S. K. Nayak, S. K. Verma, and S. S. Tripathy, Journal of Reinforced Plastics and Composites 23 (6), 625 **(2004)**.

[7] A. K. Bledzki and J. Gassan, Progress in Polymer Science 24 (2), 221 **(1999)**.

[8] N. Soykeabkaew, N. Arimoto, T. Nishino, and T. Peijs, Composites Science and Technology 68 (10-11), 2201 **(2008)**.

[9] D. N. Saheb and J. P. Jog, Advances in Polymer Technology 18 (4), 351 **(1999)**.

[10] N. Cabrera, B. Alcock, J. Loos, and T. Peijs, Proceedings of the Institution of Mechanical Engineers Part L-Journal of Materials-Design and Applications 218 (L2), 145 **(2004)**.

[11] T. Peijs, Materials Today 6 (4), 30 **(2003)**.

[12] I. M. Ward and P. J. Hine, Polymer Engineering & Science 37 (11), 1809 **(1997)**.

[13] T. Nishino, I. Matsuda, and K. Hirao, Macromolecules 37 (20), 7683 **(2004)**.

[14] T. Nishino and N. Arimoto, Biomacromolecules 8 (9), 2712 **(2007)**.

2

Cellulose fibres and cellulose based microcomposites

2.1 Native Cellulose Fibres

Native cellulose fibres are known to occur in a wide variety of living species from the world of plants, animals and bacteria. The most abundant are those coming from plants, which are usually called ligno-cellulosic fibres since their main constituents are cellulose and lignin, hydrocarbon polymers whose structure will be explained below.

2.1.1 Ligno-cellulosic fibres from higher plants

Chemical composition

Ligno-cellulosic materials are widely distributed in the biosphere in the form of trees (wood), plants and crops. A classification of these ligno-cellulosic fibres is shown in Figure 2.1. There exists a wide variety of ligno-cellulosic fibres, which can be subdivided into non-wood and wood fibres. Non-wood natural fibres, in turn, can be grouped into, depending on their origin, fibres from leaf, bast, seed and fruit, grass fibres and straw fibres. With respect to wood fibres, it is common to classify them as either softwood or hardwood, depending on the particular tree of origin; for every tree species there is a range of densities for the wood it yields. Softwood comes from a type of tree known as a gymnosperm, which reproduces by forming cones which emit pollen to be spread by the wind to other trees; some examples of softwood include pine, redwood, fir, cedar, and larch. A hardwood is an angiosperm, which means that it makes enclosed seeds or fruits; hardwoods include maple, balsa, oak, elm, mahogany, and sycamore. These names, however, are a bit misleading, as hardwoods are not necessarily hard, and softwoods are not necessarily soft.

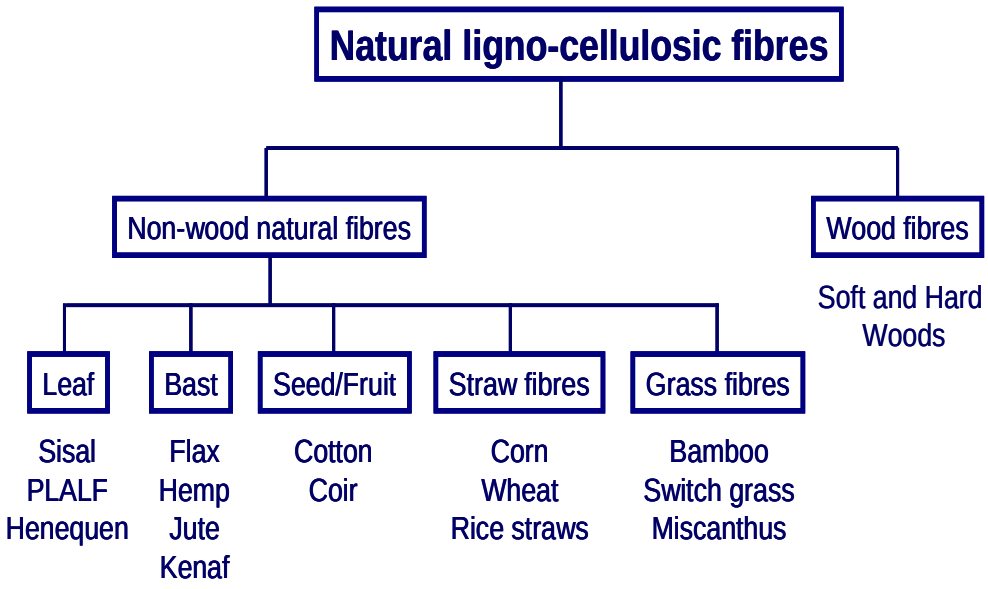

Figure 2.1. Classifications of natural ligno-cellulosic fibres.

Natural ligno-cellulosic materials are the most abundant renewable biomaterial of photosynthetic origin on earth. In terms of mass units, the net primary production per year is estimated to be $2x10^{11}$ tons, a much higher value compared to the production of synthetic polymers, $1.5x10^{8}$ tons[1]. By far, the most abundant ligno-cellulosic materials are obviously wood fibres from trees[2], however, other fibre types are emergent in use. Table 2.1 contains the world production of fibre materials originating from annual crops (in 1996). Cotton is the dominant fibre among fibres obtained from annual crops, with a share of 80%. The world production of cotton in 2001 was about 21.2 million tons, which accounted for about 38% of the world's cellulosic fibre production of 54.0 million tons. Apart from cotton, only jute (approximately 13% share, corresponding to 3.1 million tons) significantly contributes to the world production. Furthermore, the production rates of fibres such as hemp, jute, ramie or others are of minor importance when compared to the total fibre world market. However, these fibres are becoming more and more important today. For example, in Germany the production rate of hemp grew from 2,600 tons in 1999 to 23,800 tons in 2005[3].

Table 2.1. World production of fibre materials originating from annual crops in 1996[3].

Name	Code	World production (10^6 tons)	Portion (%)
Cotton	CO	18.8	79.0
Jute	JU	3.1	13.0
Flax	LI	0.56	2.4
Sisal	SI	0.29	1.2
Coir	CC	0.12	0.5
Abaca	AB	0.11	0.5
Kapok	-	0.11	0.5
Hemp	HA	0.08	0.3
Ramie	RA	0.07	0.3
Agave	-	0.07	0.3
Other fibre crops	-	0.43	1.8
Total	-	23.8	100.0

The main components of natural ligno-cellulosic fibres are cellulose, hemicellulose, lignin, pectin and waxes[4]. The amount of cellulose in ligno-cellulosic systems can vary depending on the species and age of the plant/species[1]; Table 2.2 shows the chemical composition of different cellulose based natural fibres[5].

Table 2.2. Chemical composition of different cellulose based natural fibres[5].

Component	Cotton	Jute	Flax	Ramie	Sisal
Cellulose	82.7	64.4	64.1	68.6	65.8
Hemi-cellulose	5.7	12.0	16.7	13.1	12.0
Pectin	5.7	0.2	1.8	1.9	0.8
Lignin	-	11.8	2.0	0.6	9.9
Water soluble	1.0	1.1	3.9	5.5	1.2
Wax	0.6	0.5	1.5	0.3	0.3
Water	10.0	10.0	10.0	10.0	10.0

Cellulose is a polydisperse linear homopolymer, consisting of regio- and enantioselective β-1,4-glycosidic linked D-glucopyranose units (Figure 2.2). The repeat unit of cellulose polymer, known as cellobiose, comprises of two β-D-glucopyranose rings rotated with respect to each other[6].

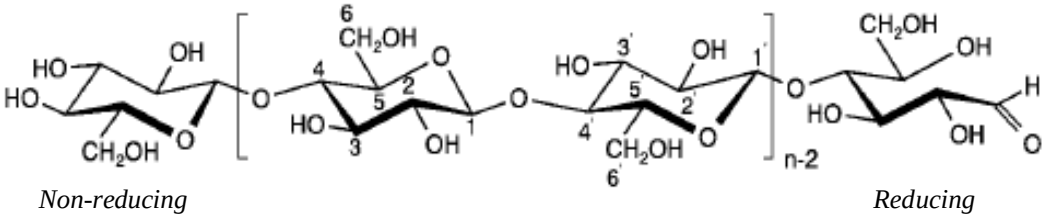

Figure 2.2. Molecular structure of cellulose.

^{1}H-NMR spectroscopy[7] and several X-ray diffraction and other physicochemical studies[8] have shown that the β-D-glucopyranose adopts the $^{4}C_{1}$ chair conformation, corresponding to the lowest free energy conformation of the

molecule. As a consequence, the hydroxyl groups (OH groups) are positioned in the ring plane (in equatorial positions), while the hydrogen atoms are in the vertical (axial) position. The repeating unit of the cellulose macromolecule (cellobiose) (Figure 2.2) includes six hydroxyl groups and three oxygen atoms. Therefore, the presence of six hydrogen bond donors – six hydroxyl groups – and nine hydrogen bond acceptors – six hydroxyl groups and three oxygen atoms – provides a wide range of possibilities for forming different hydrogen-bonded systems. The polymer contains free hydroxyl groups at the C2, C3, and C6 atoms. Based on the OH groups and the oxygen atoms of both the pyranose ring and the glucosidic bond, ordered hydrogen-bonded systems can be formed, leading to various types of supramolecular semi-crystalline structures. Besides, due to the existence of different mutual arrangements of the pyranose rings as well as different possible conformations of the hydroxymethyl groups, cellulose chains can exhibit different crystal packings leading to different crystalline polymorphs[9]. Cellulose displays six different polymorphs, namely I, II, III_I, III_{II}, IV_I and IV_{II} with the possibility of conversion from one form to another.

The crystal structure of crystalline native cellulose, typically called cellulose I, comprises of two different crystalline forms (allomorphs), namely cellulose I_α and I_β, as a result of different hydrogen-bonding patterns of the glycosidic linkages. The I_α allomorph is described as a triclinic P-1 structure, with one cellulose chain per unit cell, whereas the I_β phase is assumed to be a monoclinic unit cell with space group $P2_1$ and two chains per unit cell[10]. These two different crystalline cellulose I modifications can be found alongside each other, with a I_α/I_β ratio depending on the origin of the cellulose. The I_α phase prevails in the major part of cellulose isolated from bacteria (bacterial cellulose) and in cellulose from fresh-water and marine algae (Valonia cellulose)[11-13] whilst in ramie, cotton, wood and animal celluloses (tunicate cellulose), the I_β is the dominating allomorph[11,14,15].

According to Yamamoto and Horii[16], the I_α phase is meta-stable and can be almost completely transformed into the thermodynamically more stable I_β phase by

annealing at 260°C to 280°C. Initial details of the crystalline structure of these two allomorphs were reported by Kono et al.[17] using ^{13}C NMR. Nishiyama et al. reported the first crystallographic structure for cellulose I_α (from Glaucocystis) and for cellulose I_β (from tunicate) using synchrotron X-ray and neutron diffraction[12,14], nevertheless modelling studies had already predicted these structures[18-20]. The availability, for the first time in 2003, of crystallographic coordinates for both I_α and I_β allowed a detailed comparison of the structures and hydrogen-bonding arrangements in these two phases. Figure 2.3 shows the crystal structure of cellulose I_α and I_β. The projections of the crystal structures the two cellulose allomorphs down the chain axes (Figure 2.3: a-b) are remarkably similar. In the projection perpendicular to the chain axis and in the plane of the hydrogen bonded sheets (Figure 2.3: c-d), the main difference between I_α and I_β is the relative displacement of the sheets in the chain direction. In both I_α and I_β, the second sheet, labelled as II, is shifted in the "up" direction by ~c/4 relative to the first sheet, labelled as I. The third sheet, labelled as III, is similarly shifted with respect to II by ~c/4 in I_α but in I_β it is shifted by a ~c/4 in the "down" direction[12].

In both celluloses I_α and I_β the planes of the glucopyranose units in the chains are identical, and the chains cross-linked by hydrogen bonds form two-dimensional sheets, which are arranged in stacks in crystallites. An important fact concerning the two polymorphs is that there are no strong intermolecular interactions between the sheets. The absence of strong hydrogen bonds between the sheets allows for the sheets to be shifted with respect to each other under certain actions, resulting in the polymorphic transition of cellulose I_α into cellulose I_β[12].

Although the chemical structure of cellulose from different natural fibres is the same, the degree of polymerisation (DP) varies; for example, cotton, flax and ramie fibres have degrees of polymerisation of 7000, 8000 and 6500, respectively[5]. The major presence of cellulose in natural fibres makes them hydrophilic in nature (8-12.6%)[21] due to the high amount of hydroxyl groups present in cellulose macromolecules.

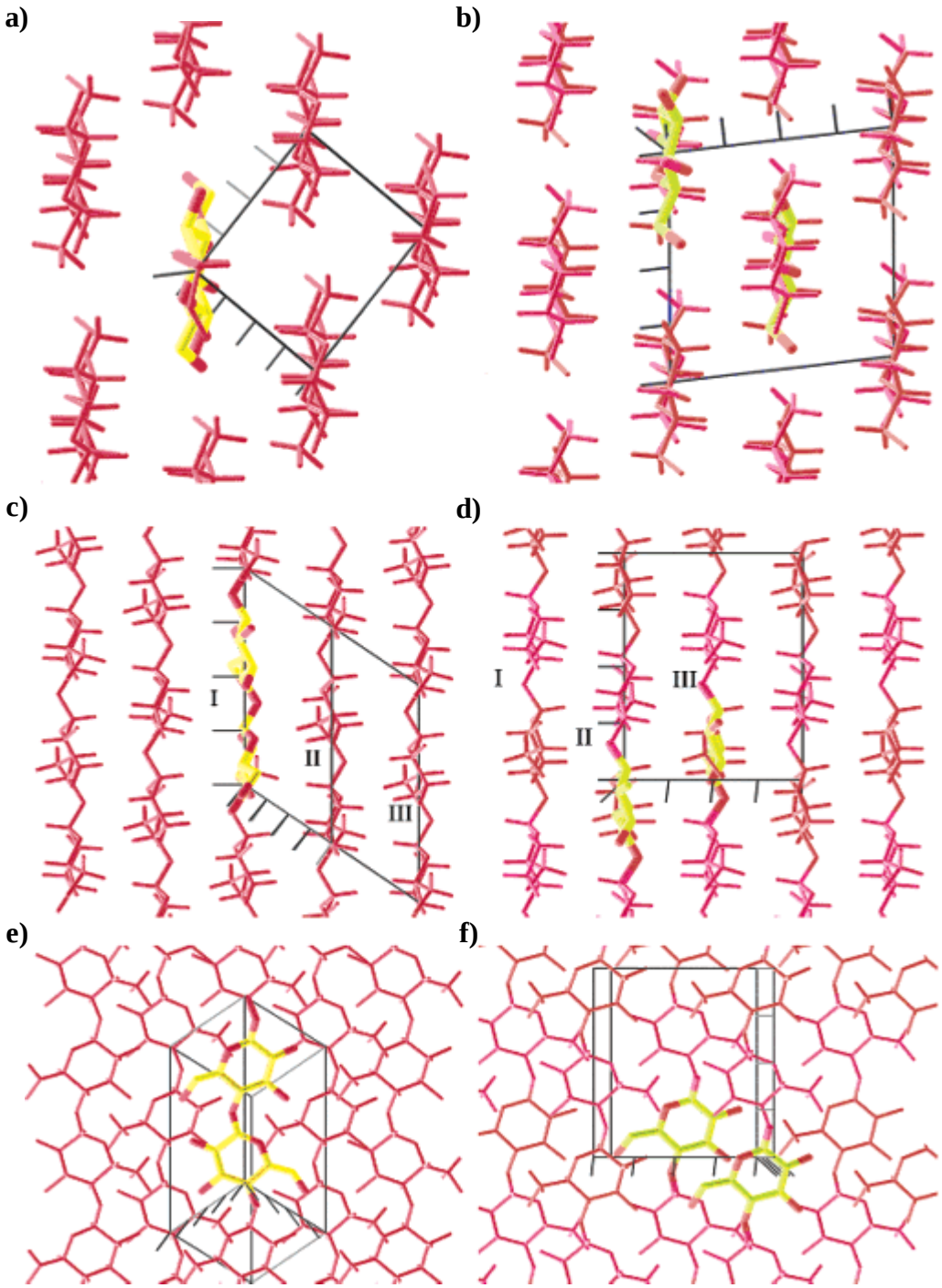

Figure 2.3. Projections of the crystal structures of cellulose I_α (a, c, e) and I_β (b, d, f) down the chain axes (a-b), perpendicular to the chain axis and in the plane of the hydrogen bonded sheets (c-d), and perpendicular to the hydrogen bonded sheets (e-f). The cellulose chains are represented by red skeletal models. The asymmetric unit of each structure is also represented in thicker lines with carbons in yellow. The unit cell of each structure is shown in grey[12].

Hemicellulose is a highly branched polymer, in contrast to the linear chain of cellulose (Figure 2.4). The pendant side groups of this branched polymer results in its non-crystalline structure. Hemicellulose molecular structure contains a variety of sugar units, whereas cellulose contains only 1,4-β-D-glucopyranose units, and its degree of polymerisation is 10-100 times lower than that of cellulose. Unlike cellulose, the constituents of hemicellulose differ from plant to plant. Hemicellulose is very hydrophilic, soluble in alkali and easily hydrolysed in acids[4].

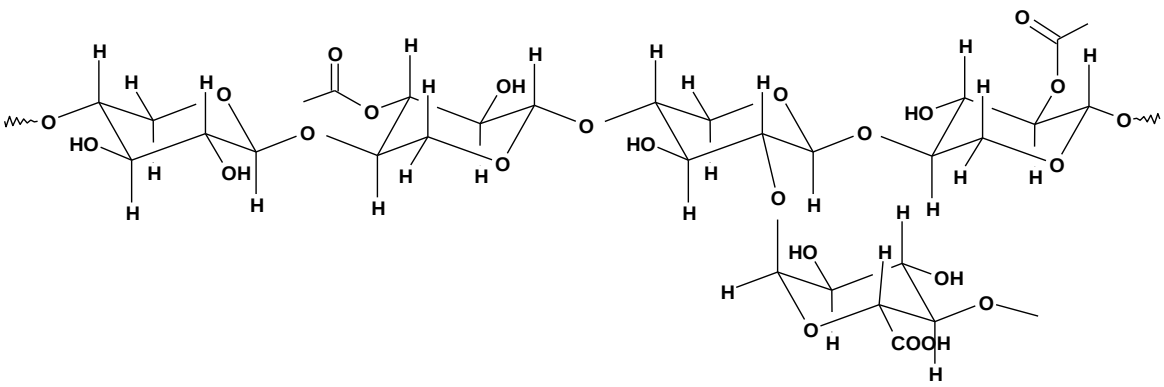

Figure 2.4. Molecular structure of hemicellulose.

Lignin is a complex hydrocarbon polymer with both aliphatic and aromatic constituents[5] (Figure 2.5). It is thought to be a complex, three-dimensional copolymer with very high molecular weight. The main difficulty in lignin chemistry is that no method has been established so far to isolate lignin in its native state from the fibre. Although the exact structural formula of lignin in natural fibres has not yet been established, most of the functional groups and units which make up the molecules have been identified. The high carbon and low hydrogen content of lignin suggest that it is highly unsaturated or aromatic in character. Hydroxyl, methoxyl and carbonyl groups have been identified, and ethylenic and sulfur-containing groups have also been found in lignins. It is believed that the structural units of lignin molecule are derivates of 4-hydroxy-3-methoxy phenylpropane[1,4]. The structural details differ from one source to another. Lignin is totally amorphous and

hydrophobic in nature[4]. Moreover, lignin is considered to be a thermoplastic polymer exhibiting a glass transition temperature of ~90 °C and a melting temperature of around 170 °C[22]. Lignin is the compound that provides rigidity to plants. In addition, lignin is not hydrolysed by acids, but it is soluble in hot alkali, readily oxidised, and easily condensable with phenol[23].

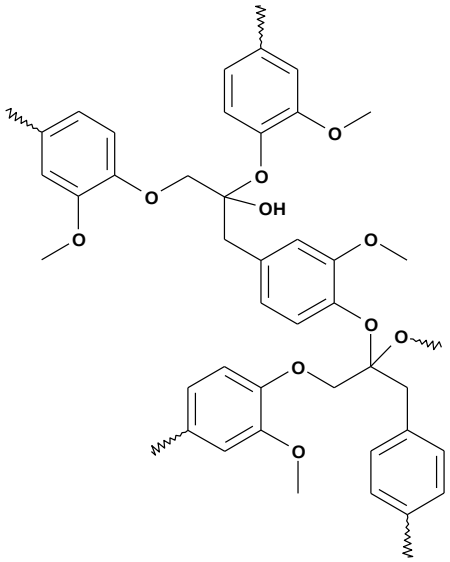

Figure 2.5. Molecular structure of lignin[5].

Pectins are a collective name for heteropolysaccharides, which consist of α-1, 4-linked galacturonic acid units, sugar units of various composition and their respective methyl esters[2]. Pectins are soluble in water only after a partial neutralisation with alkali or ammonium hydroxide[5]. Pectins are responsibility for giving flexibility to plants[4]. Finally, waxes consist of various alcohols which are insoluble in water as well as in several acids (palmitic acid, oleaginous acid, stearic acid). Waxes form a small percentage of the structure and can be extracted with organic solutions[2,5].

Hierarchical structure of natural fibres

There are several hierarchical levels of the structural organisation of natural fibres, from the macroscopic to nanosized levels[9]. In non-wood natural fibres (Figure 2.6)[24], the elementary fibres or plant cells are glued together by an interphase mainly consisting of pectin and hemicellulose to form the technical fibre. This technical fibre consists of about 10-40 elementary fibres in cross section. Few technical fibres, in turn, are bonded together by a relatively weak interphase, mainly consisting of pectins, to build up a bast fibre bundle. These fibre bundles can be separated into technical fibres through hackling and combing. Finally, these fibre bundles form a ring around the outer part of the stem[25]. In contrast to non-wood natural fibres, the stem of wood fibres is organised in annual rings with alternating layers of thin- and thick-wall cells, creating a fairly complex structure with layers of alternating density[26] (Figure 2.7).

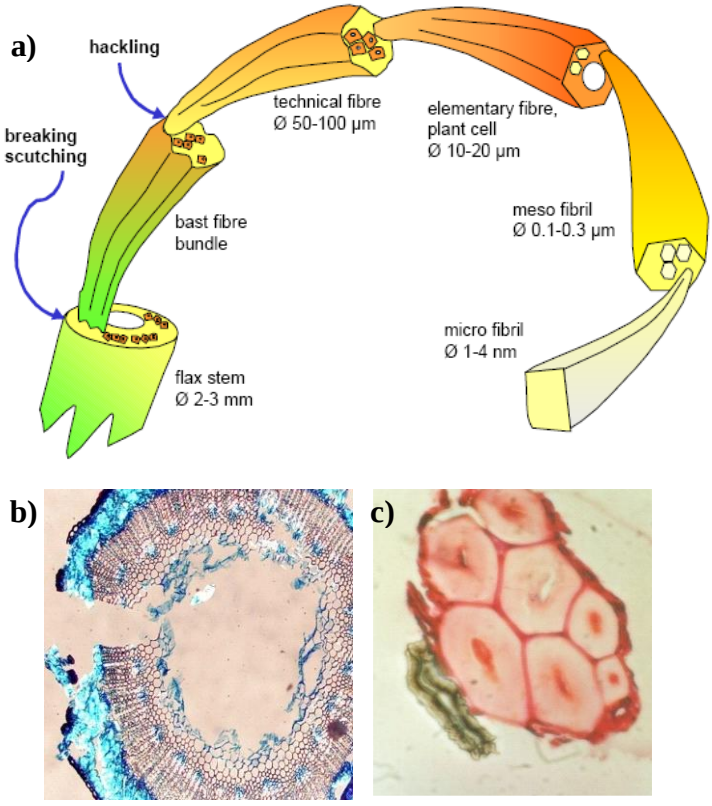

Figure 2.6. Hierarchical structure of flax stem to microfibril (a); photographs of a cross section of flax stem (b) and a technical fibre bundle (c)[24].

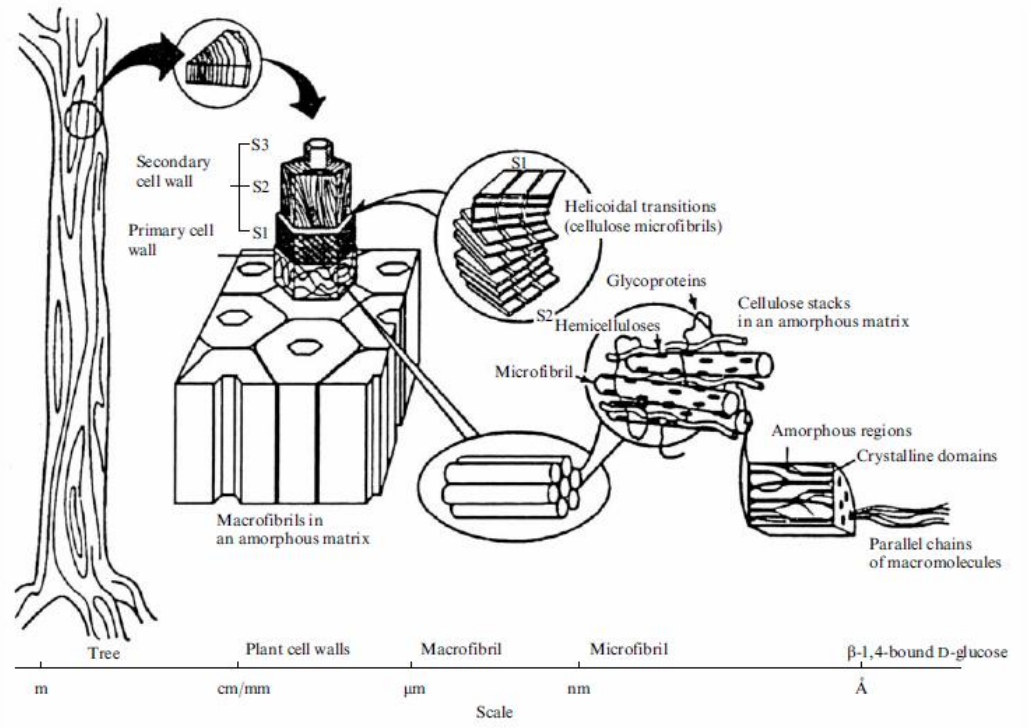

Figure 2.7. Hierarchical structure of wood.

In fibre cell walls or elementary fibres, cellulose chains biosynthesised by enzymes are deposited in a continuous fashion and aggregated into repeated crystalline structures to form microfibrils[27], which is the basic structural unit of the plant cell wall[6]. In natural fibre cells, cellulose is found not to be uniformly ordered, but there are regions of low order (so-called amorphous regions) as well as of very high crystalline order[28]. According to this, microfibrils consist of crystalline regions or domains alternated with amorphous regions[9]. The microfibril of native cellulose is considered to be the smallest well-defined morphological unit[6]. Such microfibrils have typically a diameter of about 2 to 30 nm and are made up of 30-100 cellulose molecules in extended chain conformation; with these microfibrils providing the mechanical strength to the plant[29]. Recently, electron microscopic and WAXS investigations indicated that its diameter may differ in the range of 3 to 35 nm depending on the cellulose source[30] (Table 2.3). The length of the microfibril also

depends on the source of cellulose and can reach several tens of microns. At the microfibril level, the principal physical and physico-mechanical properties of cellulose are manifested[9]. The degree of crystallinity and the dimensions of the crystallites of the microfibrils of native cellulose have been the subject of extensive investigations for many years. Table 2.4 summarises some results of X-ray diffraction measurements of native celluloses[31].

Table 2.3. Range of microfibril diameter of various cellulose samples[30].

Sample	Microfibril diameter (nm)
Bacterial cellulose	4-7
Cotton linters	7-9
Ramie	10-15
Dissolving pulp	10-30
Valonia cellulose	10-35

Table 2.4. Degree of crystallinity (χ_C), crystallite sizes ($D_{(hkl)}$), and lateral dimensions (d) of microfibrils of native celluloses[31].

Cellulose source	χ_C (%)	Crystallite sizes (nm)			d (nm)
		D(1$\bar{1}$0)	D(110)	D(020)	
Algal cellulose	> 80	10.1	9.7	8.9	10-35
Bacterial cellulose	65-79	5.3	6.5	5.7	4-7
Cotton linters	56-65	4.7	5.4	6.0	7-9
Ramie	44-47	4.6		5.0	3-12
Flax	44	4-5	4-5	4-5	3-18
Hemp	44	3-5	3-5	3-5	3-18
Dissolving pulp	43-56			4.1-4.7	10-30

Single or elementary fibres are single plant cells, which can be considered to be composites of semicrystalline cellulose microfibrils embedded in a pliable amorphous matrix of lignin and hemicellulose[32] (Figure 2.8). The fibre cell wall is not a homogenous membrane, but consists of a layered structure, where two different walls and a lumen (open channel in the centre of the fibre) can be identified (Figure

2.8-c). These layers or cell walls differ in their composition (ratio between cellulose/lignin/hemicellulose) and in the orientation of the cellulose microfibrils[5].

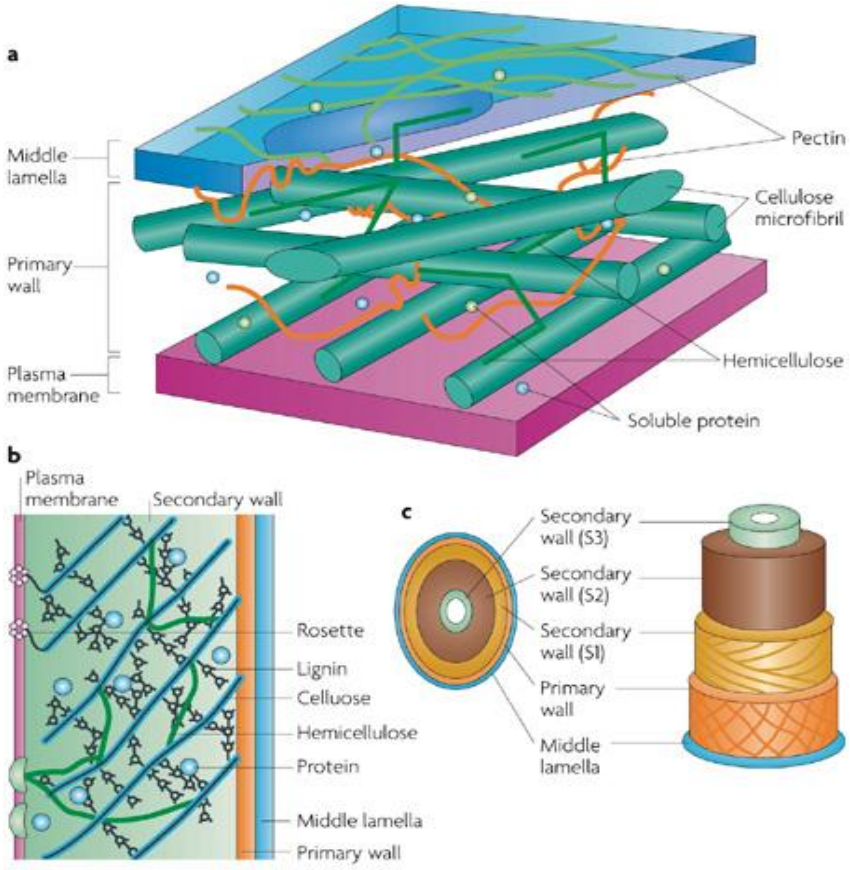

Figure 2.8. Schematic representation of the cell wall structure. a) Cell wall containing cellulose microfibrils, hemicellulose, pectin, lignin and soluble proteins. b) Components of the secondary wall. c) Organisation of primary and secondary walls[33].

The first layer deposited during cell growth is known as primary wall. Primary walls have to be rigid to withstand the internal and external stresses and at the same time have to be compliant to be able to expand during cell growth[34]. In this relative thin layer (~50 nm) the almost transverse (90°) orientation of cellulose microfibrils (orientation related to the cell axis) provides enough flexibility to allow

the cell expansion during growth. The matrix of primary walls consists mainly of hemicelluloses (e.g. xyloglucan, arabinoxylan), lignin, pectins, and structural cell wall proteins, which build a complex assembly with the cellulose microfibrils[32] (Figure 2.8-a). The secondary wall is deposited after the differentiating cell has reached its final shape and size (Figure 2.8-b). This wall is made up of three layers (S1, S2, S3) (Figure 2.8-c) with different orientations of cellulose microfibrils toward the cell axis, as can be seen in detail in Figure 2.9.

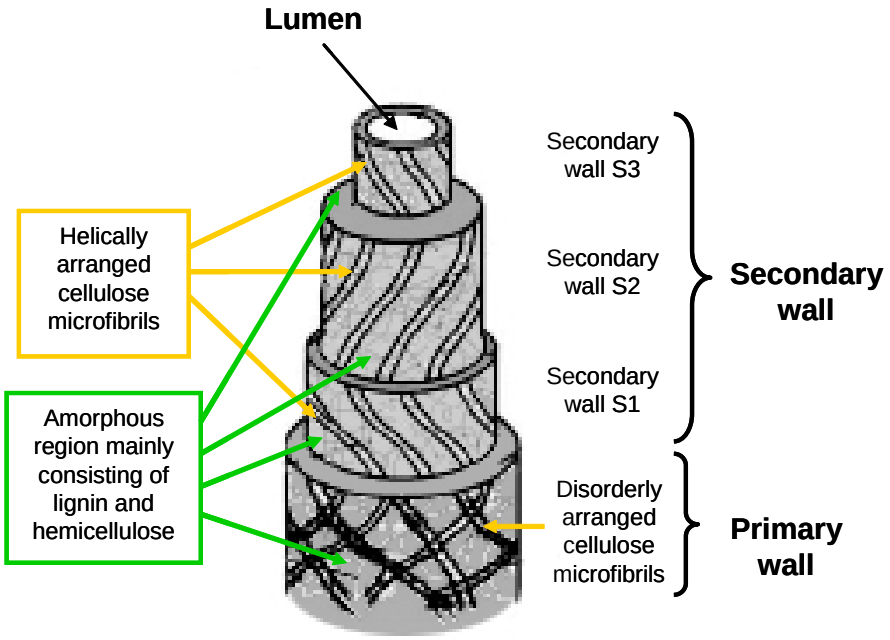

Figure 2.9. Orientation and ordering of cellulose microfibrils in a natural fibre[4].

The thick middle layer (S2) consists of a series of helically wound cellulose microfibrils oriented to the fibre axis. The angle between the cellulose microfibrils and the fibre axis is known as the microfibrillar angle (S2) and its value varies from one fibre to another[4] (ranging from 0° to about 45°) (Table 2.5). The cellulose microfibrils aligned along the length of the fibre render maximum tensile and flexural strength, in addition to providing rigidity. An increase of the microfibrillar angle implies a decrease of the cell wall stiffness, but an increase of the strain to

fracture. This interrelation enables natural fibres to adjust both stiffness and toughness of their tissues by shifting the cellulose microfibril orientation in the cell wall[35]. For instance, wood cell walls of young trees have a rather high microfibrillar angle which makes their wood flexible and enables the plant to reduce wind loads by bending. Cell walls of adult wood, however, present lower microfibrillar angles, making their wood much stiffer in order to withstand wind loads[36]. The microfibrillar angle plays an important role in the mechanical properties of fibres.

Table 2.5. Chemical composition (wt.%) and microfibrillar angle (degrees) of some natural fibres[1].

Type of fibre	Cellulose	Lignin	Hemicellulose	Pectin	Wax	Angle	Moisture
Bast							
Jute	61-71.5	12-13	13.6-20.4	0.2	0.5	8	12.6
Flax	71	2.2	18.6-20.6	2.3	1.7	10.0	10.0
Hemp	70.2-74.4	3.7-5.7	17.9-22.4	0.9	0.8	6.2	10.8
Ramie	68.6-76.2	0.6-0.7	13.1-16.7	1.9	0.3	7.5	8.0
Kenaf	31-39	15-19	21.5	-	-	-	-
Leaf							
Sisal	67-78	8-11	10.0-14.2	10.0	2.0	20.0	11.0
PALF	70-82	5-12	-	-	-	14.0	11.8
Henequen	77.6	13.1	4-8	-	-	-	-
Seed							
Cotton	82.7	-	5.7	-	0.6	25[37]	-
Fruit							
Coir	36-43	41-34	0.15-0.25	3-4	-	41-45	8.0

In general, the mechanical properties of cellulose based natural fibres are determined by the microfibrillar angle and the cellulose content[2,5,38] (Table 2.5). Coir shows the least tensile strength among all the natural fibres listed, which is attributed to its low cellulose content and considerable high microfibrillar angle, as shown in Table 2.5. Instead, the high tensile strength of flax fibre can be attributed to its high cellulose content and comparatively low microfibrillar angle. However, it is not possible to correlate the fibre strength exactly with the cellulose content and the

microfibrillar angle because of the very complex structure of natural fibres, as shown in Figure 2.6.

Elementary fibre properties in non-wood and wood based natural fibres can vary widely depending on the source, age, separating technique, moister content, history of fibre, etc, as can be observed in Table 2.6. The lignin content of fibres also influences its structure, properties and morphology. The waxy substances present in natural fibres generally affect their wettability and adhesion characteristics[1].

Table 2.6. Comparative properties of some natural fibres with conventional man-made fibres[1].

Fibre	Density (g/cm^3)	Diameter (µm)	Tensile strength (MPa)	Young's Modulus (GPa)	Elongation at break (%)
Cotton	1.5-1.6	-	250-800	6-12	7.-8.0
Jute	1.3-1.45	25-200	300-400	10-30	1.16-1.5
Flax	1.50	-	800-1500	40-70	2.7-3.2
Hemp	-	-	690	-	1.6
Ramie	1.50	-	400-900	60-80	1.2-3.8
Sisal	1.45	50-200	600-700	10-40	3-7
PALF	-	20-80	410-1600	35-80	1.6
Coir	1.15	100-450	130-170	4-6	15-40
E-glass	2.5	-	2000-2500	73	2.5
S-glass	2.5	-	3600	86	2.8
Aramid	1.4	-	2700	60-125	3.3-3.7
Carbon	1.8	-	3200	230-400	1.4-1.8

In terms of specific mechanical properties, natural fibres are exceptional candidates as load bearing constituents in composite materials. Therefore, the competitive mechanical properties together with the superior environmental benefits of the cellulosic fibres has motivated their exploitation as an alternative to conventional reinforcements in composite materials, notably glass fibres, over the last few years.

The next section describes the introduction of natural fibres in the composites field and provides an overview of recent methods and approaches developed to address the different shortcomings found in these biocomposites and to enhance their properties with the aim to produce a sustainable, eco-efficient and competitive material into the current composite market.

2.2 Micro-cellulose based biocomposites

2.2.1 Historical development of composites

Composite materials have been known in various forms throughout the history of mankind. For example, the ancient Israelite workers during their tenure under the Pharaohs incorporated chopped straw in bricks as a means of enhancing their structural integrity[39] (Figure 2.10). All the initial applications of composite materials were mainly related to building materials[40].

Figure 2.10. Brick-making in ancient Egypt (from Tomb of Rekhmire).

However, the use of composites throughout history has not only concentrated on building tasks, but also on weapon designs. It is worth mentioning the powerful archery bows made by Mongols in the 12th century. These bows were composites structures made by combining cattle tendons, horn, bamboo, and silk which bonded with natural pine resin. The tendons were placed on the tension side of the bow, the bamboo was used as a core, and sheets of horn were laminated to the compression side of the bow. The entire structure was tightly wrapped with silk using the rosin adhesive.

While the concept of composites has been in existence for several millennia, the incorporation of fibre reinforced plastic (FRP) technology into the industrial world is less than a century old. Spurred on by the needs of electronics, defense and eventually space technologies, researchers created materials with properties that seem to defy known principles. The first known FRP product was a boat hull manufactured in the mid 1930's as part of a manufacturing experiment using a fibre glass fabric and polyester resin laid in a foam mould. Since then, FRP applications have revolutionised entire industries, including aerospace, marine, electrical, chemical, corrosion-resistance and transportation. Immediately following World War II, composite materials emerged as a major engineering material. The composites industry developed rapidly through the 1950s. In fact, most of the composite processing methods used today such as open moulding, hand lay-up, spray-up, compression moulding, filament winding, resin transfer moulding, vacuum bagging, and vacuum infusion were developed and used between 1946 and 1955. The products manufactured from composites during this period included: boats, car bodies (Corvette), truck parts, aircraft components, underground storage tanks, cladding for buildings, and many other familiar products.

Since the 1960s, innovations in modern composite materials have dramatically changed the materials landscape. New high-performance composite materials (notably aramid, carbon and glass reinforced plastics) now dominate the aerospace, leisure, automotive, construction and sporting industries[41]. However,

problems associated with the environment like the persistence of plastics, the shortage of landfill space, the depletion of petroleum resources, the emissions during incineration, combined with the growing environmental awareness, have triggered the development of novel biomaterials, specifically cellulose-based composites, for replacing the current ones[42]. Through this, natural fibres are emerging as a feasible alternative to conventional reinforcing fibres in composites for non-structural or semi-structural applications. The biodegradable nature of plant fibres can contribute to the formation of a healthy eco-system as well as their high performance fulfills the economic interest of industries[43]. The main drivers for the exploitation of cellulose fibres as reinforcement in plastics have been their low density combined with competitive mechanical properties, environmental benefits, worldwide availability and low cost[44]. Examples of cellulose based materials and applications are presented in Figure 2.11.

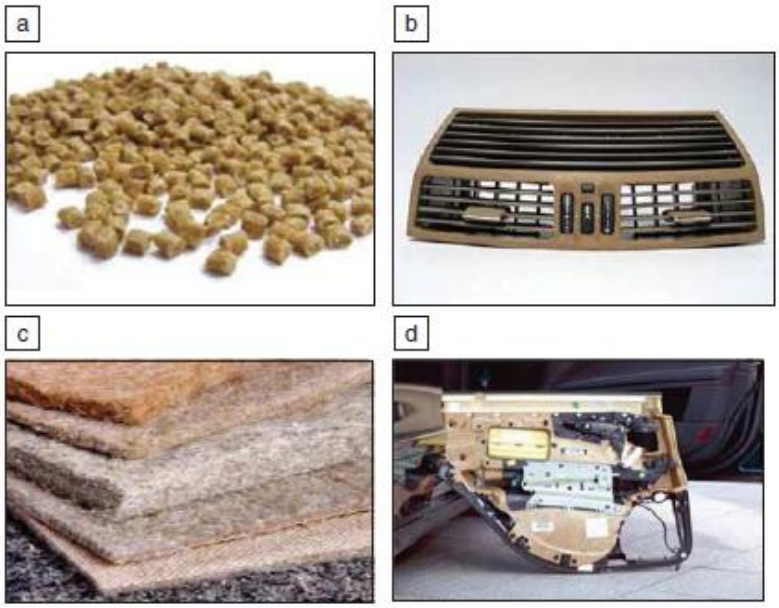

Figure 2.11. Examples of industrial biocomposite material forms and applications. (a) Thermoplastic/natural fibre granules for injection moulding; (b) section of a dashboard panel; (c) fibre mats for press-moulding; and (d) a BMW door panel. Images courtesy of Nova–Institute, Germany[44].

2.2.2 Biocomposites based on cellulose microfibres

Wood plastic composites (WPCs) include both thermosetting- and thermoplastic composites. The techniques of producing wood thermosetting composites have been well established since 1900[45]. Phenol formaldehyde (PF) and Urea formaldehyde (UF) are the most common thermosetting resins used as adhesives for wood composite products such as plywood, particleboard, fibreboard, and oriented strand board (OSB)[46-49].

Wood thermoplastic composites are manufactured by dispersing wood fibres and wood flour (WF) into molten plastics to form composite materials by processing techniques such as extrusion, thermoforming, and compression or injection moulding. Although wood thermoplastic composites have been developed in the United States since 1980s, they have been only recently experienced a dramatic growth[50]. WPCs are mixtures of wood fibre, often waste wood at high loadings (50–80 wt.%) and synthetic resins. WPCs take advantage of both wood and plastics, in other words, they can be worked like wood and yet processed like plastics, and they offer greater durability and moisture resistance than softwood[44]. The most commonly used thermoplastics in manufacturing WPCs are polyethylene (PE), polypropylene (PP), polyvinyl chloride (PVC) and their recycled materials[51]. They have been hugely successful in North America in decking, railing, siding, and other construction applications because of their low lifecycle costs and the environmental benefits they offer over chromated copper arsenate treated lumber[45,52].The north American market share of PE based wood composites in 2002 was around 83%, 9% for PVC, and 7% for PP based wood composites. Most of PE wood based composites are used for decking, which makes up 50% of the market for the total number of WPC applications. PVC wood composites can also be used for decking, but they are more often applied to windows and doors, which represent 22% of market[50]. While in the United States, decking has been the biggest growth area for WPCs, in Europe the automotive industry is the main user of WPCs for interior applications. For this

reason, the most popular resin for WPC in Europe is not polyethylene but virgin polypropylene[44].

Challenges in WPC technology have been mainly centred on maximizing dispersion, while minimizing mechanical or thermal damage to the wood fibres during compounding[53] and also overcoming difficulties in obtaining good interfacial adhesion[54]. Swelling due to moisture absorption by the wood fibres[5,55-57] also raises concern with respect to property degradation and attack by micro-organisms.

Where wood flour or waste wood is principally used as a low cost alternative to mineral fillers in commodity plastics such as polyethylene and polypropylene resin or for the upgrading of post-consumer recycled plastics, plant fibres such as flax, hemp, jute, coconut fibres, and kenaf have recently been considered as load-bearing constituents in composite materials[4,58-60]. Plant fibres from annual crops have a higher aspect ratio than wood fibres and therefore are more effective as reinforcements for composites.

In natural fibres reinforced plastics (NFRPs), natural fibres serve as reinforcement and are embedded in a polymeric matrix. Thermoplastic materials that currently dominate as matrices for natural fibres are polypropylene (PP), polyethylene (PE), and poly-vinyl chloride (PVC) while for thermosets, phenolics and unsaturated polyesters are most common[61]. Natural fibres represent environmentally friendly alternatives to conventional reinforcing fibres such as glass, carbon and aramid fibres[42]. Glass fibres are the most widely used to reinforce plastics due to their low cost (compared to aramid and carbon fibres) and fairly good mechanical properties. Therefore, NFRPs are aimed at the replacement of glass fibre reinforced plastics (GFRPs), apart from the inherent environmental reasons, for the following advantages:

- Plant fibres are a renewable and biodegradable raw material and their availability is more or less unlimited.

- Their low density (~40% lower density than that of glass fibres[62]) results in a higher specific strength and stiffness compared to glass fibres.
- The hollow cellular structure of natural fibres provides good acoustic insulating properties.
- Depending on the exact quality of fibre required, natural fibres are in most cases cheaper than glass fibres.
- Due to their non-abrasive nature, their easy processing (reduced tool wear) allows higher filling levels with significant cost reductions.
- The processing environment of natural fibres is friendly with better working conditions, resulting in a reduction of skin and respiratory irritations for the people producing the composites[4]. This becomes especially an issue since the discussion on whether very small glass fibres can cause lung cancer.
- NFRPs require higher fibre loadings for equivalent performance of GRPs, reducing the amount of polluting polymer[62].
- One of the main advantages of the use of NFRPs is related to their intrinsic lightweight compared to traditional glass fibres, which implies a potential considerable reduction of fuel consumption together with the consequent reduction of gas emissions, making these materials very suitable for transport applications such as the automotive industry[25,63,64] .

The application of NFRPs in railways, aircraft, irrigation systems, furniture industries and sports and leisure items is growing rapidly[65]. An especial interest in NFRPs has been awakened in the automotive sector as a result of attractive mechanical and physical properties of natural fibres (NFs), specially, the one related to the environmental benefits resulting from their lightweight, such as significant fuel consumption reduction, which in turn leads to gas emission reductions. These interesting properties together with the introduction of environmental legislation in European Union; Asian countries and Japan, triggered activities in the area of NFRPs in the automotive industry. In a large research program, Daimler AG led the way in the 1990's in introducing natural fibres such as flax and hemp in a number of automotive applications[60], with the current Mercedes E-class containing as many as

50 parts based on natural fibres, with a total weight of 32 kg[44] (Figure 1.1, Chapter 1). Uses of natural fibre reinforcements have proven viable in a number of automotive parts. Flax, sisal, and hemp are processed into door cladding, seatback linings, and floor panels. Coconut fibre is used to make seat bottoms, back cushions, and head restraints, while cotton is used to provide sound proofing. For example, the BMW Group incorporates a considerable amount of renewable raw materials into its vehicles, including 10 kton of natural fibres in 2004. At General Motors, a kenaf and flax mixture has gone into package trays and door panel inserts for the Saturn L300s and European-market Opel Vectras. Toyota has interest in using kenaf to make Lexus package shelves, and has incorporated it into the body structure of Toyota's *i-foot* and *i-unit* concept vehicle. Rieter Automotive was awarded the top prize at the 2005 JEC Composite Showcase for its Acaba (banana) fibre continuous processing development, where the primary energy savings is estimated at 60% or more[66]. Although NFRPs were originally developed to replace GRPs since they are 40% lighter than glass fibres, they turned out – at least in the German and Austrian car industry - to replace WPCs. The advantages associated to the use of longer natural fibres instead of wood fibres are found in achieving significant weight reduction through improved mechanical propertiest[25]. Despite the strong potential of NFRPs in the automotive industry, so far, most of their use has been limited to interior components, and few applications are found in more structural parts.

As mentioned previously, polypropylene dominates as a matrix for natural fibres, but thermosets such as phenolics, polyurethanes, and polyesters also are used. In recent years, research efforts have shifted to biobased and biodegradable polymers[1,67] such as polylactic acid (PLA)[68,69] polyhydroxybutyrate[70,71] and starch[72]. Japanese industries, in particular, have been actively pursuing the idea of fully biodegradable parts. Toyota, as pointed out above, introduced kenaf (a fibrous African *hibiscus*) as a door trim base material in 2000, first in combination with polypropylene and, since 2003, in combination with PLA for the Toyota Raum spare tire cover. PLA and kenaf are used for the casings in electronic devices, such as in NEC's Eco Mobile phone. Biobased thermosetting resins also have been used,

including resins derived from soybean oil[73] and cashew nut shells[74]. The use of bioderived resins in automotive applications is not a new idea. In 1938, Henry Ford already made his first fibre-reinforced car body panel using a plastic matrix derived from soybean products. If it had not been for the long material cure time, and the difficulty in moulding, Ford´s idea for alternative materials may have been implemented.

Although NFRPs are likely to be environmentally superior to GRPs in most applications, their eco-friendly character should not be taken for granted, and a comparative life cycle assessment (LCA) study is required. LCA is the most widely accepted method to assess the environmental aspects and potential impacts associated with a product. This method studies environmental impacts from the extraction of raw materials and fuels, followed by all conversions steps through production, the use phase and at end of life, the waste management options[25,62]. Figure 2.12 illustrates simplified the generic life cycle stages of a NFRPs.

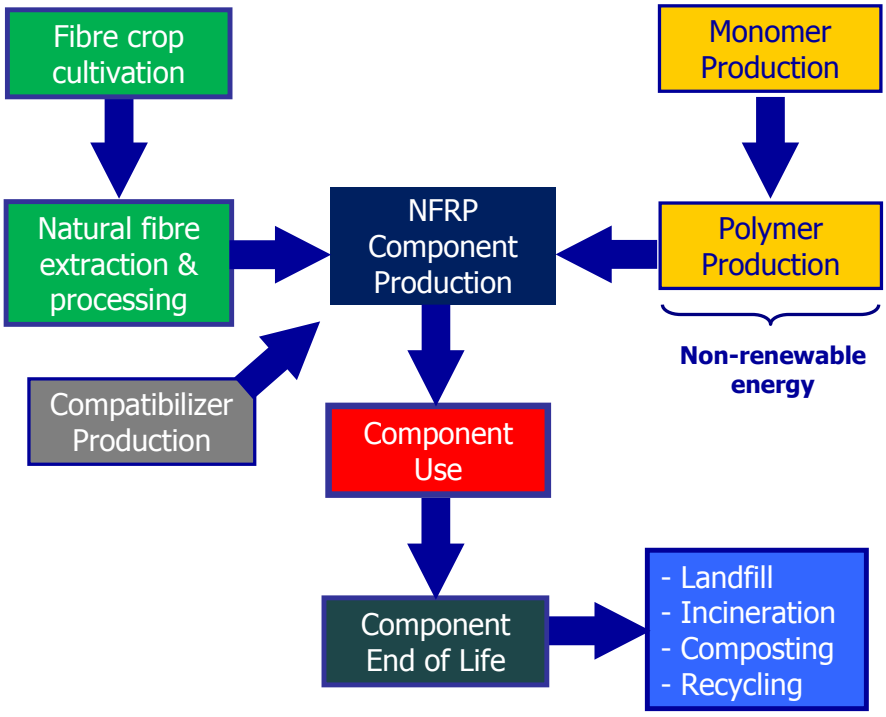

Figure 2.12. Generic life cycle assessment of natural fibre reinforced composites.

It is worth noting that most of the non-renewable energy used and greenhouse gas emissions up to the production of the composites is mainly determined by the polymer matrix material which demonstrates that the polymer matrix is the real polluter in these composites. An evidence of this statement is presented in Table 2.7 where a comparative life cycle environmental impacts from the production of glass fibre, china reed fibre, epoxy resin, ABS and polypropylene are shown. Regardless of fibre type, the environmental impacts associated to the different polymer production processes are notably higher than those of fibre (natural or man-made) production processes.

Table 2.7. Life cycle environmental impacts for production of GF, china reed fibre (ChRF), Epoxy resin (Epoxy), ABS and polypropylene (PP)[62,75].

Environmental impact	**GF**	**ChRF**	**Epoxy**	**ABS**	**PP**
Energy use (MJ/kg)	48.33	3.64	140.71	95.02	77.19
CO_2 emissions (kg/kg)	2.04	0.66	5.90	3.10	1.85
CO emissions (g/kg)	0.80	0.44	2.20	3.80	0.72
SO_x emissions (g/kg)	8.79	1.23	19.00	10.00	12.94
NO_x emissions (g/kg)	2.93	1.07	35.00	11.00	9.57
Particulate matter (g/kg)	1.04	0.24	15.00	2.90	1.48
BOD to water (mg/kg)	1.75	0.36	1200.00	33.00	33.94
COD to water (mg/kg)	18.81	2.27	51000.00	2200.00	178.92
Nitrates to water (mg/kg)	14.00	24481.00	1.00	71.00	18.78
Phosphates to water (mg/kg)	43.03	233.60	220.00	120.00	3.39

This comparative study shows that the environmental impact for the production process of thermosetting polymers (epoxy resins) is higher than for thermoplastic polymer production (ABS and PP). According to this table, the most environmentally friendly polymer corresponds to the thermoplastic PP, followed by another thermoplastic, ABS, and finally, the thermosetting epoxy resins[62]. In order to assess, from an environmental point of view, if natural fibres are superior to glass fibres, the estimated non-renewable energy requirements for production of glass fibre and two natural fibres are presented in Table 2.8. As can be seen glass fibre production requires 5–10 times more non-renewable energy than natural fibre

production. Natural fibre cultivation depends mainly on solar energy and fibre production and extraction use small quantities of fossil fuel energy; therefore, the global non-renewable energy required for its production is quite low. On the other hand, glass production and high-temperature glass fibre production are both energy intensive processes depending mainly on fossil fuels. As a result, the pollutant emissions from glass fibre production are significantly higher than from natural fibre production (columns 2 and 3 of Table 2.7).

Table 2.8. Non-renewable energy requirements for production of different fibres (MJ/kg)[75,76].

Non-renenewable energy requirements (MJ/kg)					
Glass fibre mat[76]		**Flax fibre mat[76]**		**China reed fibre[75]**	
Raw materials	1.7	Seed production	0.05	Cultivation	2.50
Mixture	1.0	Fertilizers	1.0	Transport plant	0.40
Transport	1.6	Transport	0.9	Fibre extraction	0.08
Melting	21.5	Cultivation	2.0	Fibre grinding	0.40
Spinning	5.9	Fibre separation	2.7	Transport fibre	0.26
Mat production	23.0	Mat production	2.9		
Total	**54.7**	**Total**	**9.55**	**Total**	**3.64**

The life cycle environmental impacts from glass fibre and china reed fibre production processes are thoroughly broken down in Table 2.7. Except for nitrate emissions associated with fertilizer use in china reed production, all other emissions are much lower for natural fibres. Increased nitrate emissions can lead to eutrophication of water bodies, which is a significant water quality problem in many areas. However, Corbière et al.[75] found that life cycle eutrophication impacts of NFRPs are lower than life cycle eutrophication effects of GRPs, when they include contribution of atmospheric NOx emissions to eutrophication. These observations are likely to be valid across different natural fibres, since their production processes are very similar. Hence, substitution of glass fibres by natural fibres of equal weight normally improves environmental performance of the component, with possible exceptions of local eutrophication effects[62]. The results obtained from the

comparative study performed by Bos[25] and others[77] confirm the conclusions presented above. In this study, the environmental impact (cradle-to-factory gate) of beams made from NFRPs, designed based on a stiffness-limited criteria, were analysed and compared with GRPs. The influence of the fibre content of different composites on the environmental impact is displayed in Figure 2.13. The environmental impact is expressed as eco-indicator, where lower values indicate lower environmental impacts. As expected, the composites reinforced with natural fibres are more environmentally friendly than their counterparts reinforced with glass fibres for the same fibre weight fractions. In addition, the environmental impact of the composites decreases with fibre content, evidencing that the polymeric matrix is the real polluter in this type of materials. Finally, the analysis showed that the eco-indicator is much higher for composites based on thermosetting matrixes.

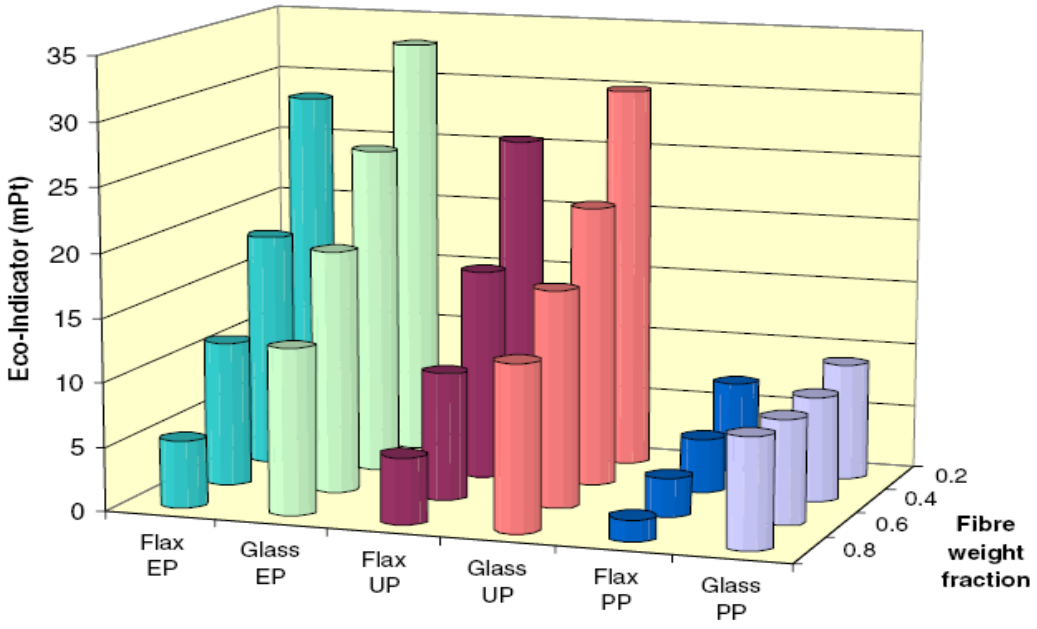

Figure 2.13. Environmental impact (eco-indicator) as a function of the fibre weight fraction for several natural fibre reinforced plastics[77].

NFRPs require higher fibre volume fractions compared to GRPs for equivalent mechanical performance, because glass fibres have superior mechanical

(especially strength) properties than natural fibres. This higher fibre volume fraction reduces the volume and weight fraction of the polluting polymer matrix used in the composite. Hence replacement of base polymer by higher natural fibre loadings will improve the environmental performance of NFRPs composites compared to equivalent GRPs. Moreover, as mentioned previously, the higher volume fraction of lower density natural fibres in NFRPS, reduces significantly the weight of the final composite (Table 2.9), which in turn, involves improvement in fuel efficiency and therefore, a great reduction of emissions during the material use phase, especially in automotive applications[62].

.

Table 2.9. Weight reduction with natural fibre composites[62].

Component	Conventional composites	Weight (g) of component	NFRPs	Weight (g) of NFRP component	Weight reduction (%)
Auto side panel	ABS	1125	Hemp-Epoxy	820	27
Auto insulation panel	GF-PP	3500	Hemp-PP	2600	26
Transport pallet	GF-PP	15000	China reed-PP	11.770	22

At the end-of-life stage of the composite, in the disposal phase, the LCA will assess the waste management options as a function of the polymeric matrix. With regard to NFRPs, four disposal options can be considered: landfill, incineration, composting and recycling. According to the waste management hierarchy (Figure 2.14), the least favoured option is landfilling; indeed, due to lack of space and the high environmental impact associated, this option is banned in many countries, especially in Europe[77]. Unlike glass fibres, natural fibres can be incinerated after the NFRP has served its useful life. In fact, if natural fibres are combined with thermosets, incineration with energy recovery is a good option for NFRPs since it keeps the CO_2 balance; nevertheless the combustion process can release toxic emissions from the polymeric matrix and/or coupling agents and, in addition, the

ashes generated during combustion needs to be disposed. However, the toxic air emissions generated from NFRP incineration will be fairly low since these composites are based on lower mass of polluting polymer matrix. The low calorific value of natural fibres needs to be considered and most importantly, incineration does not lead to closed loop waste management systems and, as a result, is not a fully sustainable option. If natural fibres are combined with a biodegradable matrix, such as polyhydroxybutyrate (PHB), polylactic acid (PLA) and starch, an additional disposal option becomes available through composting. In the case of natural fibres based on thermoplastics, the last and most favoured option for waste management is recycling; however, this option is limited due to a possible cumulative fibre thermal degradation during reprocessing[71].

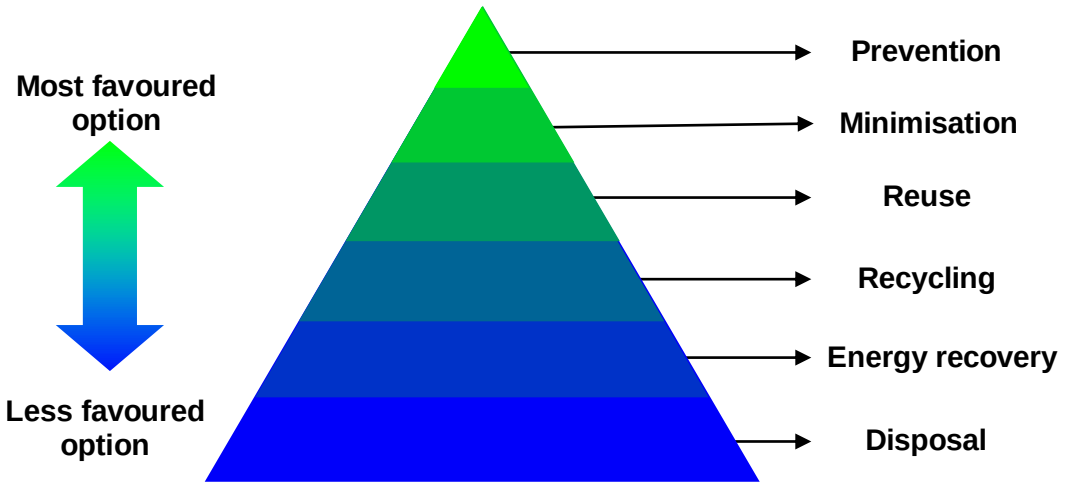

Figure 2.14. Waste management hierarchy.

Potential problems with mechanical recycling are highly significant for the automotive industry in light of the new environmental legislation introduced by European Union; Asian countries and Japan. European Union legislation implemented in 2006 has expedited recent NFRPs automotive insertion; by 2006, 80% of a vehicle must be reused or recycled and by 2015 it must be 85%. Japan requires 88% of a vehicle to be recovered (which includes incineration of some

components) by 2005, rising to 95% by 2015. As a result, today most automakers are evaluating the environmental impact of a vehicle's entire life cycle, from raw materials to manufacturing to disposal[66].

In conclusion, NFRPs are environmentally superior to GRP in most applications for the following reasons: natural fibre production results in lower environmental impacts compared to high-temperature glass fibre production; NFRPs require higher fibre content for equivalent performance, reducing the amount of polluting polymer matrix; lightweight NFRPs improve fuel efficiency and reduce emissions during their use phase, especially in automotive applications; and end-of-life incineration of natural fibres results in energy recovery. Despite the advantages of NFRPs over GRP, there are several unsolved issues that must be addressed for their wide-scale acceptance, as will be discussed in the following section.

2.2.3 Challenges in cellulose microcomposites

Despite the attractive properties of cellulose based composites; the use of cellulose reinforcements is limited in industrial practice due to the difficulties associated with composite processing. Common challenges in WPCs and NFRPs have been related to the low thermal stability of lignocellulose fibres; difficulties in fibre feeding, fibre dispersion, and breakage during compounding; moisture absorption; flame-retardant properties; and especially the creation of a strong interfacial bond with the polymer matrix[44].

Natural fibres contain amorphous polysaccharides and lignin that start to degrade near 230 ºC, therefore, the processing temperature of NFRPs is restricted to about 200 ºC due to the possibility of fibre thermal degradation and/or the possibility of volatile emissions that could affect the composite properties. Thermal degradation does not only limit the number of polymers that can serve as a matrix since the

processing temperature of most thermoplastics is near or exceeds thermal fibre degradation, but also gives particular concern with respect to reprocessing and recycling[58]. Attempts have been made for the improvement of fibre thermal stability such as coating the fibres and/or grafting the fibres with monomers. Grafting is possible since lignin can react with the monomers. Mohanty et al.[78] have reported that grafting of acrylonitrile on jute improved the thermal stability as evidenced by the increase in the degradation temperature from 170 to 280 ºC. Sabaa[79] has also reported improved thermal stability for acrylonitrile-grafted sisal fibres as confirmed by the increased initial degradation temperature, lowering of the rate of degradation, and the total weight loss. In another study by Yap et al.[80] wood polymer composites were prepared *in situ* by polymerisation of various monomers and it was observed that the maximum rate of degradation was substantially reduced for phosphonate-treated wood flour.

The degradation of natural fibres leads to poor organoleptic properties such as odour and colour and also deterioration of their mechanical properties[58]. Gonzalez and Myers[81,82] have studied the effect of thermal degradation on the mechanical properties of wood plastic composites. The temperature range of study was from 220 to 260 ºC and the exposure time varied from 4 to 4096 min. It was observed that although, in general, the mechanical properties decayed as a result of thermal degradation of wood flour, toughness and bending strength were more affected. In another study of wood flour polypropylene composites, similar loss in properties was reported after extrusion at 250 ºC[83].

Another drawback of the use of natural fibres to reinforce plastics is their high tendency to absorb moisture. The fibre moisture content varies between 5 and 10%. The absorption of moisture during composite processing leads to fibre swelling and presence of voids at the interface fibre/polymer matrix, which results in poor mechanical properties and reduces the dimensional stability of the composites. This problem can be overcome by applying surface treatments on these fibres aimed to decreasing the amount of surface hydroxyl groups that can interact with water

molecules. For instance, acetylation is a well-known esterification method that consists of the substitution of hydroxyl groups of the fibre cell wall with acetyl groups by the reaction of cellulosic fibres with acetic or propionic anhydride at elevated temperature. As a result, acetylation reduces substantially the moisture absorption of natural fibres, which in turn, improves their dimensional stability and environmental degradation[84]. Hydrothermal treatment is another approach to reduce moisture absorption of natural fibres since it increases the crystallinity of cellulose and therefore, contributes to a reduced moisture uptake. Moreover, on hydrothermal treatment, a part of the hemicelluloses is extracted thereby decreasing the moisture absorbance[29]. According to Stamboulis et al.[85] moisture absorption and swelling of treated flax fibre composites is ~30% lower than that of composites with untreated flax fibres. Strong intermolecular fibre-matrix bonding decreases the rate of moisture absorption in biocomposites. However it is difficult to eliminate totally the moisture absorption without using expensive surface barriers on the composite surface[42].

An additional restriction to the successful exploitation of natural fibres for durable composites is their low microbial resistance and susceptibility to rotting. These properties pose serious problems during shipping, storage and composite processing. The non-uniformity and variation of dimensions and of their mechanical properties (even between individual plants in the same cultivation) poses another serious problem[4].

From the development of natural fibre reinforced plastics the optimisation of the biofibre-matrix interface has been of pivotal importance. The fibre-matrix interface plays an important role in the physical and mechanical properties of composites. Many times, biofibres behave as filler rather than a real reinforcement due to ineffective stress transfer from matrix to fibre as a consequence of a poor adhesion at the fibre-matrix interface. Attempts to improve the interfacial properties have been made through modification of fibre surface with traditional methods. For instance, alkali and heat treatments of plant fibres have been used to clean fibre surface, reduce moisture absorption, and increase the surface roughness[86]. The

removal of surface impurities on cellulose fibres as well as the increase of fibre surface roughness leads to an improvement of fibre-matrix adhesion as they favour the mechanical interlocking adhesion mechanism.

The main challenge for the use of natural fibres as reinforcements in composites has been related to the creation of a strong interfacial bond with the polymeric matrix due to their poor compatibility between the hydrophilic nature of these biofibres and the often hydrophobic thermoplastic matrices[61,87]. This incompatibility favours fibre-fibre interactions over fibre-matrix interactions what results in the formation of fibre aggregates within the matrix and, therefore, a non-uniform fibre dispersion in the matrix. The poor wettability of the hydrophilic fibres with the hydrophobic matrix, as a consequence of their different surface tensions, leads to mixing difficulties that also give place to heterogeneous distribution of fibres within the matrix, which impairs the efficiency of the composite. The use of additives such as stearic acid or mineral oil can reduce the fibre-fibre interactions and therefore, enhance the fibre dispersion in the matrix[58].

In order to improve the adhesion between natural fibres and thermoplastic matrices, the use of compatibilisers or coupling agents is often required[44,88-90]. These compatibilisers or coupling agents act as a bonding bridge between fibre and matrix. The coupling agents are tetrafunctional organometallic compounds based on silicon, titanium, and zirconium and are commonly known as silane, zirconate, or titanate coupling agents[58]. The effect of silane coupling agents on the interface performance of NFRPs is reported in many publications. Silanes are fixed on the fibre surface by covalent and hydrogen bonding. The long hydrocarbon chains provided by silanes reduce the fibre polarity and therefore, increase the fibre-matrix compatibility favouring the fibre-matrix adhesion. Silane treatment leads to an increase of the composite tensile strength due to improved interfacial load transfer efficiency as a result of better fibre-matrix adhesion. Moreover, the effect of moisture on composite properties is minimised with this kind of treatment[5,42].

There are also physical methods to optimise the fibre-matrix interface such as corona and cold plasma surface treatments. These plasma treatments are very interesting techniques for surface oxidation activation but add significant cost. Depending on type and nature of the used gases, a variety and degree of surface modification can be achieved including introduction of surface crosslinking; increasing or decreasing the surface energy; and production of free radicals and groups[5,29].

However, compatibilisation routes based on modified matrices are often more suitable for natural fibres. Maleated polyolefins such as maleic anhydride-grafted polypropylene (MAH-g-PP) are the most commonly used coupling agents. Such matrix modifications allow interactions between the acidic anhydride groups of maleated coupling agents and the hydroxyl groups of cellulose leading to a strong fibre-modified matrix adhesion by the covalent and hydrogen bonds established between anhydride and hydroxyl groups[5]. As previously mentioned compatibilisation can lead to significant improvements in properties, particularly in terms of tensile and flexural strength and also moisture resistance, since an improvement in fibre-matrix adhesion enhances the load transfer from matrix to fibre and decreases the rate of moisture absorption in composites. However, in many cases the different strategies followed to achieve an improvement in fibre-matrix adhesion also involve an increase in processing cost and time[91] as well as an increase in environmental impact. Research on a cost-effective method to improve the interfacial properties of NFRP is necessary, since the main market attraction of these materials is the competitive cost of NFs[42].

A very desirable solution to enhance the fibre/matrix interface in composites has been the development of self-reinforced polymer composites. The fact that in these composites both fibre and matrix are chemically identical renders an excellent interfacial compatibility, hence providing fully-recyclable and environmentally friendly materials with good mechanical properties. For example, fully recyclable all-polypropylene or self-reinforced polypropylene composites have been proposed

to replaced traditional glass fibre reinforced plastics for a number of applications, notably in automotive industry[92]. Following the success of these self-reinforced composites, all-cellulose composites have been recently introduced. Nishino and co-workers have developed a new route to produce all-cellulose composites based on the partial dissolution of cellulose fibres. During composite preparation, the surface layer of cellulose fibres is partially dissolved to form the matrix phase that bonds the fibres together. This selective dissolution method results not only in very high fibre volume fractions, but also in a gradual interphase which minimises voids and stress concentrations of all-cellulose composites[92-95]

Following interface-based optimisation routes for NFRPs, new developments also include the use of longer fibres such as in long-fibre thermoplastics[86,96] or textile composites based on spun yarns[97-99]. The latter materials allow the introduction of fibre orientation through the use of textile preforms such as woven or non-crimp multi-axial fabrics. The use of low twist yarns, as in the case of the recently introduced Biotex flax/PLA commingled yarns, is essential for improved fibre efficiency compared to highly twisted yarns, as used in conventional textile applications[99].

Despite the optimisation routes developed, NFRPs still present limitations such as low strength, low strain to failure and high tendency to absorb moisture. In addition, odour and discolouring problems usually arise due to thermal decomposition of hemicelluloses and lignin during composites processing. A promising approach to address these problems is through the use of nanocellulose instead of cellulose microfibres for the production of composites. The properties of nanocelluloses depending on their origin and the new methods used to obtain nanocellulose from wood/ natural fibres are presented in the next chapter.

2.3 References

[1] A. K. Mohanty, M. Misra, and G. Hinrichsen, Macromolecular Materials and Engineering 276-277 (1), 1 **(2000)**.

[2] S. J. Eichhorn, C. A. Baillie, N. Zafeiropoulos, L. Y. Mwaikambo, M. P. Ansell, A. Dufresne, K. M. Entwistle, P. J. Herrera-Franco, G. C. Escamilla, L. Groom, M. Hughes, C. Hill, T. G. Rials, and P. M. Wild, Journal of Materials Science 36 (9), 2107 **(2001)**.

[3] A. Bartl, B. Mihalyi, and I. Marini, Chemical and Biochemical Engineering Quarterly 18 (1), 21 **(2004)**.

[4] M. J. John and S. Thomas, Carbohydrate Polymers 71 (3), 343 **(2008)**.

[5] A. K. Bledzki and J. Gassan, Progress in Polymer Science 24 (2), 221 **(1999)**.

[6] D. Klemm, H. Schmauder, and T. Heinze, *Cellulose*, in *Biopolymers*, ed. A. Steinbüchel. Weinheim, Wiley-VCH. 6, 275-285, **(2003)**

[7] H. A. Krassig, *Cellulose: structure accesibility and reactivity*, in *Polymer Monographs*, ed. Amsterdam, Gordon and Breach Science Publishers 11, 167-323 (1993).

[8] P. E. Marszalek, A. F. Oberhauser, Y. P. Pang, and J. M. Fernandez, Nature 396 (6712), 661 **(1998)**.

[9] V. I. Kovalenko, Russian Chemical Reviews 79 (3), 231 **(2010)**.

[10] R. H. Atalla and D. L. Vanderhart, Science 223 (4633), 283 **(1984)**.

[11] I. M. Saxena and R. M. Brown, Annals of Botany 96 (1), **(2005)**.

[12] Y. Nishiyama, J. Sugiyama, H. Chanzy, and P. Langan, Journal of the American Chemical Society 125 (47), 14300 **(2003)**.

[13] R. Witter, U. Sternberg, S. Hesse, T. Kondo, F. T. Koch, and A. S. Ulrich, Macromolecules 39 (18), 6125 **(2006)**.

[14] Y. Nishiyama, P. Langann, and H. Chanzy, Journal of the American Chemical Society 124 (31), 9074 **(2002)**.

[15] Y. Nishiyama, G. P. Johnson, A. D. French, V. T. Forsyth, and P. Langan, Biomacromolecules 9 (11), 3133 **(2008)**.

[16] H. Yamamoto and F. Horii, Macromolecules 26 (6), 1313 **(1993)**.

[17] H. Kono, S. Yunoki, T. Shikano, M. Fujiwara, T. Erata, and M. Takai, Journal of the American Chemical Society 124 (25), 7506 **(2002)**.

[18] R. J. Vietor, K. Mazeau, M. Lakin, and S. Perez, Biopolymers 54 (5), 342 **(2000)**.

[19] A. Aabloo, A. D. French, R. H. Mikelsaar, and A. J. Pertsin, Cellulose 1 (2), 161 **(1994)**.

[20] A. P. Heiner, J. Sugiyama, and O. Teleman, Carbohydrate Research 273 (2), 207 **(1995)**.

[21] A. K. Bledzki, S. Reihmane, and J. Gassan, Journal of Applied Polymer Science 59 (8), 1329 **(1996)**.

[22] P. O. Olesen and D. V. Plackett, Perspectives on the performance of natural fibres, in Natural fibres performance forum, Copenhagen **(1999)**.

[23] A. K. Mohanty, M. Misra, and L. T. Drzal, *Natural fibers, Biopolymers, and Biocomposites*.CRC Press, Boca Raton**(2005)**

[24] H. L. Bos, M. J. A. Van Den Oever, and O. C. J. J. Peters, Journal of Materials Science 37 (8), 1683 **(2002)**.

[25] H. L. Bos, The potential of flax fibres as reinforcement for composites materials. PhD thesis, Eindhoven University of Technology, Eindhoven **(2004)**.

[26] P. Fratzl and R. Weinkamer, Progress in Materials Science 52 (8), 1263 **(2007)**.

[27] S. Kamel, Express Polymer Letters 1 (9), 546 **(2007)**.

[28] J. W. S. Hearle, Journal of Polymer Science 28 (117), 432 **(1958)**.

[29] K. Susheel, B. S. Kaith, and K. Inderjeet, Polymer Engineering & Science 49 (7), 1253 **(2009)**.

[30] H. P. Fink, D. Hofmann, and H. J. Purz, Acta Polymerica 41 (2), 131 **(1990)**.

[31] B. H. D. Klemm, H. P. Fink, and A. Bohn, Angewandte Chemie-International Edition 44 (22), 3358 **(2005)**.

[32] I. Burgert, American Journal of Botany 93 (10), 1391 **(2006)**.

[33] M. B. Sticklen, Nature Reviews Genetics 9, 433 **(2008)**.

[34] L. Taiz, Annual Review of Plant Physiology and Plant Molecular Biology 35 (1), 585 **(1984)**.

[35] P. Fratzl, I. Burgert, and H. S. Gupta, Physical Chemistry Chemical Physics 6 (24), 5575 **(2004)**.

[36] H. Lindstrom, J. W. Evans, and S. P. Verrill, Holzforschung 52 (6), 573 **(1998)**.

[37] F. Busnel, Contribution à l'étude des matériaux composites à matrice organique renforcés par des fibres de lin – Influence des traitements chimiques sur la liaison interfaciale fibre/matrice. PhD thesis, Université de Bretagne Sud, France **(2006)**.

[38] A. Stamboulis, C. A. Baillie, and T. Peijs, Composites Part A: Applied Science and Manufacturing 32 (8), 1105 **(2001)**.

[39] J. R. Vinson and R. L. Sierakowski, Introduction to Composite Materials, in The Behavior of Structures Composed of Composite Materials, Edited G.M.L. Gladwell, Springer Netherlands. vol. 105 pp.1-38 **(2002)**.

[40] A. Moropoulou, A. Bakolas, and S. Anagnostopoulou, Cement & Concrete Composites 27 (2), 295 **(2005)**.

[41] P. Wambua, J. Ivens, and I. Verpoest, Composites Science and Technology 63 (9), 1259 **(2003)**.

[42] G. Bogoeva-Gaceva, M. Avella, M. Malinconico, A. Buzarovska, A. Grozdanov, G. Gentile, and M. E. Errico, Polymer Composites 28 (1), 98 **(2007)**.

[43] A. Kaushik and M. Singh, Carbohydrate Research 346 (1), 76 **(2011)**.

[44] L. A. Berglund and T. Peijs, Materials Research Society Bulletin 35 (3), 201 **(2010)**.

[45] C. Clemons, Forest Products Journal 52 (6), 10 **(2002)**.

[46] D. P. Kamdem and B. Riedl, Colloid and Polymer Science 269 (6), 595 **(1991)**.

[47] D. P. Kamdem and S. T. Sean, Forest Products Journal 44 (2), 65 **(1994)**.

[48] S. Hiziroglu and D. P. Kamdem, Forest Products Journal 45 (11-12), 66 **(1995)**.

[49] J. M. Munson and D. P. Kamdem, Forest Products Journal 48 (3), 55 **(1998)**.

[50] H. H. Jiang and D. P. Kamdem, Journal of Vinyl & Additive Technology 10 (2), 59 **(2004)**.

[51] A. K. Bledzki, S. Reihmane, and J. Gassan, Polymer-Plastics Technology and Engineering 37 (4), 451 **(1998)**.

[52] R. M. Rowell, Journal of Polymers and the Environment 15 (4), 229 **(2007)**.

[53] A. K. Bledzki, M. Letman, A. Viksne, and L. Rence, Composites Part a-Applied Science and Manufacturing 36 (6), 789 **(2005)**.

[54] J. Z. Lu, Q. L. Wu, and H. S. McNabb, Wood and Fiber Science 32 (1), 88 **(2000)**.

[55] A. K. Bledzki and O. Faruk, Composites Science and Technology 64 (5), 693 **(2004)**.

[56] S. H. Huang, P. Cortes, and W. J. Cantwell, Journal of Materials Science 41 (16), 5386 **(2006)**.

[57] A. Viksne, A. K. Bledzki, L. Rence, and R. Berzina, Mechanics of Composite Materials 42 (1), 73 **(2006)**.

[58] D. N. Saheb and J. P. Jog, Advances in Polymer Technology 18 (4), 351 **(1999)**.

[59] T. Peijs, Materials Technology 15 (4), 281 **(2000)**.

[60] T. Schlosser and J. Knothe, Kunstoffe: Plast Eur. 87 **(1997)**.

[61] R. Malkapuram, V. Kumar, and Y. S. Negi, Journal of Reinforced Plastics and Composites 28 (10), 1169 **(2009)**.

[62] S. V. Joshi, L. T. Drzal, A. K. Mohanty, and S. Arora, Composites Part A: Applied Science and Manufacturing 35 (3), 371 **(2004)**.

[63] A. C. N. Singleton, C. A. Baillie, P. W. R. Beaumont, and T. Peijs, Composites Part B-Engineering 34 (6), 519 **(2003)**.

[64] J. George, M. S. Sreekala, and S. Thomas, Polymer Engineering and Science 41 (9), 1471 **(2001)**.

[65] A. S. Herrmann, J. Nickel, and U. Riedel, Polymer Degradation and Stability 59 (1-3), 251 **(1998)**.

[66] J. Holbery and D. Houston, JOM: Journal of the Minerals, Metals and Materials Society 58 (11), 80 **(2006)**.

[67] K. G. Satyanarayana, G. G. C. Arizaga, and F. Wypych, Progress in Polymer Science 34 (9), 982 **(2009)**.

[68] K. Oksman, M. Skrifvars, and J. F. Selin, Composites Science and Technology 63 (9), 1317 **(2003)**.

[69] T. Nishino, K. Hirao, M. Kotera, K. Nakamae, and H. Inagaki, Composites Science and Technology 63 (9), 1281 **(2003)**.

[70] E. Bodros, I. Pillin, N. Montrelay, and C. Baley, Composites Science and Technology 67 (3-4), 462 **(2007)**.

[71] N. M. Barkoula, S. K. Garkhail, and T. Peijs, Industrial Crops and Products 31 (1), 34 **(2010)**.

[72] L. Averous and N. Boquillon, Carbohydrate Polymers 56 (2), 111 **(2004)**.

[73] A. O'Donnell, M. A. Dweib, and R. P. Wool, Composites Science and Technology 64 (9), 1135 **(2004)**.

[74] E. T. N. Bisanda and M. P. Ansell, Journal of Materials Science 27 (6), 1690 **(1992)**.

[75] T. Corbière-Nicollier, B. Gfeller Laban, L. Lundquist, Y. Leterrier, J. A. E. Månson, and O. Jolliet, Resources, Conservation and Recycling 33 (4), 267 **(2001)**.

[76] J. Diener and U. Siehler, Die Angewandte Makromolekulare Chemie 272 (1), 1 **(1999)**.

[77] L. Shen and M. K. Patel, Journal of Polymers and the Environment 16 (2), 154 **(2008)**.

[78] A. K. Mohanty, S. Patnaik, B. C. Singh, and M. Misra, Journal of Applied Polymer Science 37 (5), 1171 **(1989)**.

[79] M. W. Sabaa, Polymer Degradation and Stability 32 (2), 209 **(1991)**.

[80] M. G. S. Yap, Y. T. Que, L. H. L. Chia, and H. S. O. Chan, Journal of Applied Polymer Science 43 (11), 2057 **(1991)**.

[81] C. Gonzalez and G. E. Myers, International Journal of Polymeric Materials 23 (1-2), 67 **(1993)**.

[82] G. E. Myers, I. S. Chahyadi, C. Gonzalez, C. A. Coberly, and D. S. Ermer, International Journal of Polymeric Materials 15 (3-4), 171 **(1991)**.

[83] S. Takase and N. Shiraishi, Journal of Applied Polymer Science 37 (3), 645 **(1989)**.

[84] S. Mishra, M. Misra, S. S. Tripathy, S. K. Nayak, and A. K. Mohanty, Polymer Composites 23 (2), 164 **(2002)**.

[85] A. Stamboulis, C. A. Baillie, S. K. Garkhail, H. G. H. van Melick, and T. Peijs, Applied Composite Materials 7 (5-6), 273 **(2000)**.

[86] J. Gassan and A. K. Bledzki, Composites Science and Technology 59 (9), 1303 **(1999)**.

[87] M. Q. Zhang, M. Z. Rong, and X. Lu, Composites Science and Technology 65 (15-16), 2514 **(2005)**.

[88] A. Espert, F. Vilaplana, and S. Karlsson, Composites Part a-Applied Science and Manufacturing 35 (11), 1267 **(2004)**.

[89] S. Mohanty and S. K. Nayak, Journal of Reinforced Plastics and Composites 23 (18), 2047 **(2004)**.

[90] S. Mohanty, S. K. Nayak, S. K. Verma, and S. S. Tripathy, Journal of Reinforced Plastics and Composites 23 (6), 625 **(2004)**.

[91] N. Soykeabkaew, N. Arimoto, T. Nishino, and T. Peijs, Composites Science and Technology 68 (10-11), 2201 **(2008)**.

[92] S. J. Eichhorn, A. Dufresne, M. Aranguren, N. E. Marcovich, J. R. Copadona, S. J. Rowan, C. Weder, W. Thielemans, M. Roman, S. Renneckar, W. Gindl, S. Veigel, J. Keckes, H. Yano, K. Abe, M. Nogi, A. N. Nakagaito, A. Mangalam, J. Simonsen, A. S. Benight, A. Bismarck, L. A. Berglund, and T. Peijs., Journal of Materials Science 45 (1), 1 **(2009)**.

[93] T. Nishino and N. Arimoto, Biomacromolecules 8 (9), 2712 **(2007)**.

[94] C. Qin, N. Soykeabkaew, N. Xiuyuan, and T. Peijs, Carbohydrate Polymers 71 (3), 458 **(2008)**.

[95] N. Soykeabkaew, C. Sian, S. Gea, T. Nishino, and T. Peijs, Cellulose 16 (3), 435 **(2009)**.

[96] N. M. Barkoula, S. K. Garkhail, and T. Peijs, Journal of Reinforced Plastics and Composites 29 (9), 1366 **(2010)**.

[97] S. Goutianos and T. Peijs, Advanced Composites Letters 12 (6), 237 **(2003)**.

[98] S. Goutianos, T. Peijs, B. Nystrom, and M. Skrifvars, Applied Composite Materials 13 (4), 199 **(2006)**.

[99] B. Madsen and H. Lilholt, Composites Science and Technology 63 (9), 1265 **(2003)**.

3

Nanocelluloses and cellulose based nanocomposites

The persistence of plastics in the environment, the depletion of petroleum resources and the growing environmental concern as well as new strong regulations for a cleaner and safer environment have spurred the development of biobased materials. In this way, natural fibres (NFs) become attractive environmentally friendly alternatives to conventional reinforcing fibres in composite materials. As previously described in Chapter 2, cellulose based composites have been successfully applied in the automotive industry since their lightweight properties can lead to improved fuel efficiency as well as a reduction of greenhouse gas emissions. Potential applications of cellulose based composites in railways, aircraft, furniture industries, and sports and leisure items are currently being evaluated.

Despite the promising potential of cellulose based composites, there are still unsolved issues such as low thermal stability of NFs, difficulties in fibre dispersion and composite processing, moisture absorption, relative low strength and the lack of proper interfacial adhesion between biofibres and polymeric matrix due to the inherent hydrophilic character of NFs. In addition, the thermal decomposition of hemicelluloses and lignin during composite processing leads to poor organoleptic properties such as odour and discolouring problems. Moreover, NFs exhibit considerable variability in diameter, along with the length of individual fibres. This non-uniformity and variation of dimensions and of their mechanical properties (even between individual plants in the same cultivation) poses a serious problem[1]. The quality and overall properties of fibres depend also on factors such as size, maturity, and processing methods adopted for the extraction of biofibres[2,3]. Additionally, NFs contain defects or dislocations such as pores, nodes and compression failures that act as starting points for cracks, which reduces the mechanical performance and reinforcing capability of these fibres.

A promising way to address these shortcomings is through nanocelluloses of high cellulose purity. These nanocelluloses present outstanding properties due to their high crystallinity and almost defect free structures as well as their nanosized dimension. Therefore, the application of nanocelluloses in the composite field opens a window of opportunity to overcome the limitations of traditional microcomposites, together with the possibility to design and create new materials and structures with unprecedented flexibility and physical properties. As a consequence of the high specific surface area of nanocelluloses, their nanocomposites will present a very large matrix-nanofibre interfacial area, providing changes in molecular mobility, relaxation behaviour and in ensuing thermal and mechanical properties. Unlike traditional composites, cellulose based nanocomposites generally involve low loadings of well-dispersed nanofibres to achieve high mechanical properties due to their superior intrinsic mechanical performance. However, from an environmental point of view, lower amounts of reinforcement yield higher polymer content, and therefore higher amount of polluter, since the polymer matrix is considered the real

polluter of these composites as demonstrated in the previous chapter. Despite the advantages of nanocelluloses in composite materials, there are still some key issues that need to be addressed. For instance, the high energy input required for their isolation is a great obstacle for their industrialisation. Although several pre-treatments have been proposed for decreasing the energy demands, they usually involve long processing times and the use of a variety of non-environmentally friendly chemical substances. In order to assess the environmental benefits of these pre-treatments a life cycle assessment should be performed. The long processing times associated with these pre-treatments also hinder their industrial application.

Moreover, as often occurs in cellulose microcomposites, the lack of compatibility among cellulose and hydrophobic polymers requires the use of coupling agents or the nanocellulose surface modification, which can lead to a loss of mechanical performance of nanocomposites. These surface treatments will involve a significant increase of the composite cost due to their high surface area per unit mass as well as a reduction of the environmental character associated with cellulose.

Another challenge associated with the high specific surface area of nanocelluloses is the achievement of good distribution of these nanofibres within the matrix due to their high tendency to aggregate. The quality of the nanofibre dispersion affects directly the mechanical properties of nanocomposite. Because of these setbacks, so far the use of nanocelluloses has been focused on the development of new multifunctional nanostructured materials for niche applications.

The need to produce at large scale fully recyclable and biodegradable materials based on the exploitation of the intrinsic high Van der Waals or hydrogen bonding capability of nanofibrillated cellulose has motivated the development of 100% cellulose based material through an environmental processing method as described in Chapter 5. These materials, termed as "binder-free all-cellulose composites" are made entirely from plants and biobased waste sources without the use of pre-treatments, solvents, resins or bonding agents. The mechanical

performance of these materials can out-perform most of conventional natural fibre reinforced plastics and wood panel products and thus, potential applications will be in building products and the furniture industry.

This chapter provides an overview of the different sources of nanocelluloses and recent methods used for their isolation. The morphology and other properties of nanocelluloses such as crystalline structure and chemical and physical properties are also described as a function of the isolation method applied. Finally, the use of nanocelluloses as reinforcement in nanocomposite materials is reviewed, including nanocomposite processing, challenges and current applications.

3.1 Nanocelluloses

3.1.1 Introduction

Nanocelluloses are cellulosic materials with one dimension in the nanometre range and are present in the form of native cellulose microfibrils in plant cell walls, including algae and tunicate sea animals, but they are also excreted by bacteria.

As previously mentioned in Chapter 2, NFs present a hierarchical structure comprising of macroscopic down to nanosized levels. In fibre cell walls or elementary fibres, cellulose chains are aggregated into repeated crystalline structure to form microfibrils[4] which also aggregate into larger macroscopic fibres. Microfibrils are considered to be the smallest well-defined morphological unit[5] and consist of crystalline regions alternated with amorphous regions[6]. Despite the term used to refer to this unit, microfibril, its dimensions are actually in the nanoscale range and vary depending on the cellulose source. Their diameters can range from 3 to 35 nm with lengths reaching several tens of microns. The degree of crystallinity and the dimensions of the crystallites of microfibrils of native cellulose from

different sources are displayed in Table 2.4 of Chapter 2. Such microfibrils are made up of 30-100 cellulose molecules in extended chain conformation that are laterally bonded by hydrogen bonds. This high molecular arrangement in microfibrils results in almost defect-free nanostructures with a high degree of crystallinity that together with their high pure cellulose content, exhibit impressive mechanical properties. In essence, the main reason for the increased interest in nanocelluloses as a reinforcing phase for composite materials is related to their consistent and outstanding mechanical properties, which are close to those of perfect cellulose crystals. Nanofibrils and nanofibres are also used as synonyms for microfibrils. Hereinafter, the term microfibril will be replaced for nanofibril or nanofibre with the aim of emphasising its nanosized dimensions.

In order to exploit the exceptional properties of cellulose nanofibrils, the hierarchical structure of wood or natural fibres needs to be deconstructed in order to isolate them. In the case of bacterial cellulose and whiskers produced by tunicates already exist in this form, making them suitable materials for niche applications.

As mentioned above, some of the drawbacks of cellulose microfibres are their dimensional inconsistencies and variability in mechanical properties. Unlike cellulose microfibres, nanocelluloses exhibit more consistent properties. The Young´s modulus of natural fibres varies according to the source of cellulose and fibre dimensions. Typical values of modulus from 40 to 60 GPa are found for natural bast fibres like flax and hemp, while it potentially increases up to 80 GPa for single cells[7] and to 100-140 GPa for nanocelluloses[8,9] since these are highly crystalline structures with very low amorphous material, making them close to perfect cellulose crystals. Despite the huge amount of literature devoted to determination of cellulose crystal modulus, so far, it is not clear what the true value is. According to experimental data gathered from X-ray diffraction measurements of crystal displacement during tensile loading of fibrous ramie plant cells, Sakurada et al.[10] reported a value of 138 GPa for cellulose crystal modulus in 1962. This paved the way for many more measurements and determinations of the crystal modulus using

X-ray diffraction[11,12] and theoretical approaches[8,13-15], all of which have obtained values ranging from 100-160 GPa[16]. An elastic modulus of 143 GPa was experimentally determined for tunicin cellulose crystal through a Raman spectroscopic technique[8]. Regardless of not knowing the accurate value of cellulose crystal modulus, it is worth pointing out that the values estimated are similar to the modulus of aramid fibres (Kevlar and Twaron). The modulus of crystalline cellulose is quite high compared to other materials, especially if its density is taken into account. Table 3.1 displays the moduli of a number of common materials used in engineering.

Table 3.1. Moduli of engineering materials compared to cellulose.

Material	Modulus (GPa)	Density ($Mg\ m^{-3}$)	Specific modulus ($GPa\ Mg^{-1}\ m^{3}$)
Aluminium	70	2.7	26
Steel	210	7.8	26
Glass	70	2.5	28
Crystalline cellulose	138	1.5	92

The strength of NFs also depends on the cellulose source, their composition and the amount and type of defects present in the fibres. Fibre bundles, so far the material of use in most composite materials, have relatively low strength of around 600 MPa[17], while the actual fibre cell is much stronger (up to 1500 MPa)[18-20], and therefore higher intrinsic strengths are expected for nanofibres due to the absence of defects at the nanosized level. Recently, the strength of individual native cellulose nanofibrils from wood and tunicate has been estimated based on a model for the sonication-induced fragmentation of filamentous nanostructures. The mean strength of the wood cellulose nanofibrils ranged from 1.6 to 3 GPa depending on the method used to measure the nanofibril diameter, whereas higher crystalline tunicate cellulose nanofibrils exhibited higher mean strengths of 3−6 GPa. These estimated strength values of cellulose nanofibrils are comparable with those of commercially available carbon fibres[21].

Another advantage of nanocelluloses is their dimensional stability in the presence of water. Unlike cellulose microfibres, nanofibrils do not swell in contact with water since the penetration of water into the crystalline structure is not energetically favoured[16].

In general, nanocelluloses have gained importance due to their unique characteristics that result from the combination of cellulose properties with the specific features of nanoscale materials. Such properties are: very large surface to volume ratio; high surface area; good mechanical properties including a high Young´s modulus, high tensile strength, very low coefficient of thermal expansion, and a broad chemical modification capacity and the formation of versatile semi-crystalline fibre morphologies. Moreover, biocompatibility, non-toxicity, and the biodegradability of cellulose nanomaterials are important features in biochemical and biomedical applications[22]. As a result, research focused on the isolation, characterisation and application of nanocelluloses has considerably increased during the last 15 years. Novel methods for their production ranges from top-down methods involving enzymatic/chemical/physical methodologies for their isolation from wood and forest/agricultural residues to the bottom-up production of cellulose nanofibrils from glucose by bacteria[23]. On the basis of their dimensions, functions, and preparation methods, which in turn depend mainly on the cellulosic source and on the processing conditions, nanocelluloses can be divided in three different types: nanocrystalline cellulose (NCC), nanofibrillated cellulose (NFC) and bacterial cellulose (BC) (Table 3.2).

As can be seen from the second column of Table 3.2, the terms used to refer to different forms of nanocelluloses are quite varied, which can lead to confusion. In order to clarify the reader, the different types of nanocelluloses with some of their synonyms that can be found in the literature are gathered in the Table 3.2. The term nanocrystalline cellulose (and its synonyms) is used to designate elongated crystalline rod-like nanoparticles whereas the term nanofibrillated cellulose (and its

synonyms) is referred to long flexible nanoparticles consisting of alternating crystalline and amorphous region.

Table 3.2. Family of nanocellulose materials.

Type of nanocelluloses	Synonyms	Typical sources	Formation and average size
Nanofibrillated cellulose (NFC)	Microfibrillated cellulose, microfibrils, and nanofibrils	Wood, sugar beet, potato tuber, hemp flax	Delamination of wood pulp by mechanical pressure before and-or after chemical or enzy-metic treatment Diameter: 5-60 nm Length: several micrometers
Nanocrystalline cellulose (NCC)	Cellulose nanocrystals, crystallites, whiskers, nanowhiskers, and microcrystals	Wood, hemp, cotton, flax, tunician, avicel, ramie, wheat straw	Acid hydrolysis of cellulose Diameter: 5-70 nm Length: 100-250 nm (NFs) 100 nm to several micrometers (tunicates, algae, bacteria)
Bacterial cellulose (BC)	Bacterial nanocellulose microbial cellulose, and biocellulose	Low molecu-lar weight sugars and alcohols	Bacterial synthesis Diameter: 20-250 nm Different types of nanofibre networks

This section is divided into three parts dealing with the three different members of the nanocelluloses family: NCC, NFC and BC. Each part includes the morphology and properties of each nanocellulose type as well as the methods used for its isolation. A comparison among the different cellulose nanostructures is also presented highlighting their similarities and differences.

3.1.2 Nanocrystalline cellulose (NCC)

Nanocrystalline celluloses, also known as whiskers, consist of rod-like cellulose crystals with widths of 5–70 nm and lengths between 100 nm and several

micrometers. They can be extracted from plant material by acid hydrolysis of the amorphous regions surrounding and embedded within cellulose nanofibrils due to the amorphous regions being more accessible to acid and more susceptible to hydrolytic action than the crystalline domains. The first report dealing with the isolation of cellulose nanocrystals via acid hydrolysis was published over 50 years ago[24].

Nanowhiskers can also be isolated from the mantle of tunicates where the cellulose nanofibrils or tunicin are embedded in a protein matrix. After deproteinisation and acid hydrolysis, tunicin breaks down in the form of whiskers[25,26].

Nanowhiskers have been isolated from a wide variety of cellulose sources including plants[27-29], microcystalline cellulose[30], animals[25,31], bacteria[32] and algae[33]. The morphology and dimensions of the nanocrystals strongly depend on their cellulose source[34], for instance, highly crystalline tunicate and algal cellulose liberate whiskers of several microns in length while less crystalline wood fibres yield to shorter whiskers. The dimensions of some nanowhiskers from different cellulose sources are listed Table 3.3[35].

Table 3.3. Characteristics of whiskers of cellulose from different sources[35].

Cellulose source	Length (nm)	Cross setion (nm)
Tunicate	100-several microns	15
Algal (Valonia)	>1000	10-20
Bacterial	100-several microns	5-10 by 30-50
Wheat straw	220	5
Cotton	200-350	5-15
Wood	100-300	3-5
Sugar beet pulp	210	15

Among the different sources of cellulose whiskers, it is worth highlighting tunicates due to the high aspect ratio and crystallinity of tunicin[31]. Tunicate nanowhiskers are reported to have moduli of ~140 GPa, but acid hydrolysed nanowhiskers are thought to have much lower moduli (50-100 GPa)[16]. However, the

widespread use of tunicin whiskers may be is restricted by high cost of harvesting and limited availability. Wood is a key source due to its natural abundance and cotton constitutes the main source among the non wood natural fibres. The main reasons are the widespread availability of cotton and their high cellulose content (94%) that results in higher yields of cellulose whiskers and avoids intensive purification of cellulose[16]. Filter paper and related products were the preferred substrate for initial basic research on cellulose nanowhiskers, because of their purity and ready availability in laboratories.

NCC Preparation

As mentioned above, cellulose nanocrystals are generated by the liberation of crystalline regions of the semicrystalline cellulosic fibres via a controlled acid hydrolysis, and often followed by ultrasonic treatment. This chemical process starts with the removal of polysaccharides bound at the nanofibril surface and is followed by the cleavage and destruction of the more readily accessible amorphous regions to liberate rod-like crystalline cellulose sections. It is ascribed to the faster hydrolysis kinetics of amorphous domains compared to crystalline ones. When the appropriate level of glucose-chain depolymerisation has been reached, the acidic mixture is diluted, and the residual acids and impurities are fully removed by repeated centrifugation and extensive dialysis. The hydrolysis is followed by a mechanical process, typically sonication, which disperses the nanocrystals as a uniform stable suspension[23]. Geometrical characteristics and properties of isolated cellulose are determined by cellulose origin and hydrolysis conditions such as type and concentration of acid employed, time and temperature; together with sonication treatment[36]. Figure 3.1 shows TEM images taken from dilute suspensions of hydrolysed cotton and tunicin. The differences present in both morphology and dimensions of cotton and tunicin whiskers are evident. The lengths and diameters are around 200 nm and 5 nm for cotton and 1 μm and 15 nm for tunicate whiskers. Therefore, tunicin whiskers are longer and thinner than cotton ones, and therefore

exhibit higher aspect ratio; a very important feature for their application in composite materials.

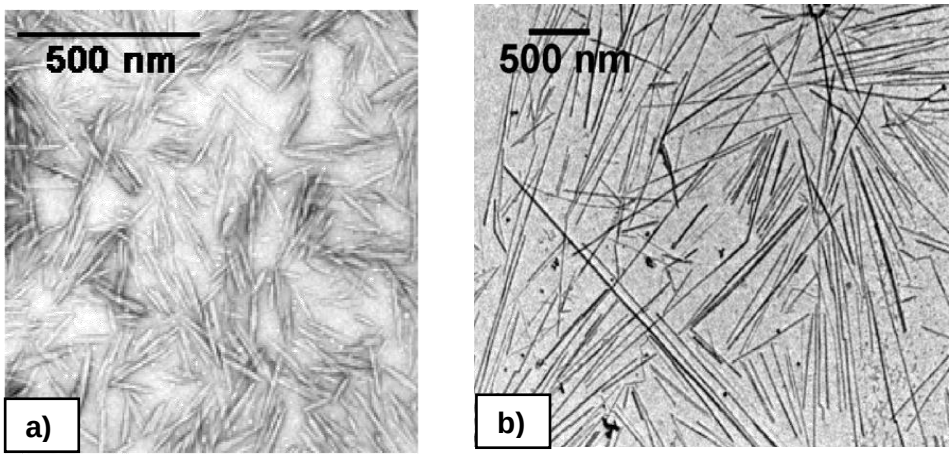

Figure 3.1. Transmission electron microscope images of dilute suspension of cellulose whiskers obtained from acid hydrolysis of (a) cotton and (b) tunicate.

The hydrolysis conditions must be adjusted depending on the substrate. However, few studies have been focusing on the effects of hydrolysis conditions. Reaction time has been identified as one of the most important parameters to be considered during acid hydrolysis process. The effects of reaction time have been studied during the preparation of nanocrystals from cotton[37], wood[38], pea hull fibres[29], microcrystalline cellulose[39], coconut husk fibres[40] and kenaf fibres[41]. Dong et al.[37] observed a decrease in cotton nanocrystal length with prolonged hydrolysis time (Figure 3.2). Similar results have been obtained from the preparation of cellulose nanowhiskers with different origin. Hydrolysis time must be adjusted so that it should be long enough to complete the hydrolysis of amorphous regions. However, very long hydrolysis times can result also in the degradation of the crystalline domains. These authors also studied the effect of temperature and ultrasound treatment on the resulting cellulose crystals.

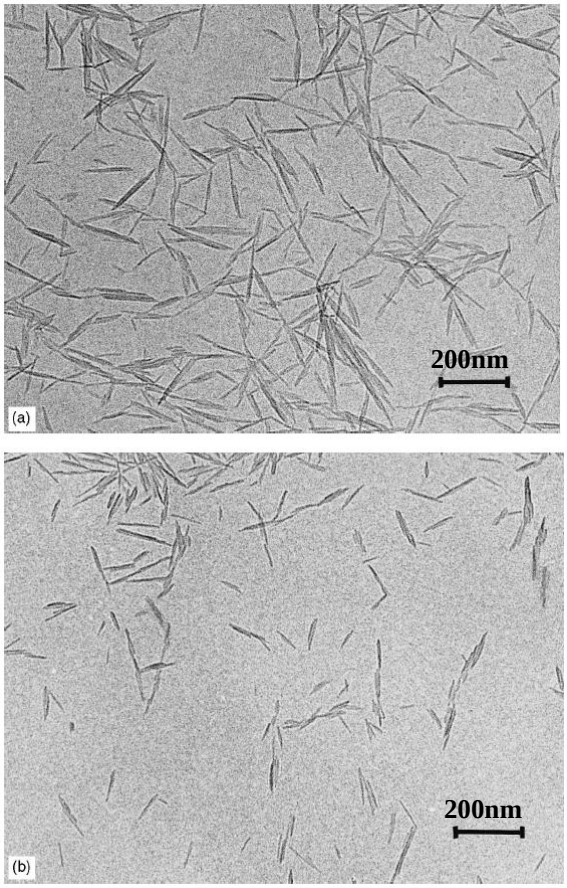

Figure 3.2. Transmission electron microscope micrographs showing the effect of hydrolysis time on the size of cotton whiskers[36]. (a) A suspension hydrolysed for 20 min at 45 °C; (b) a suspension hydrolysed for 4 h at 45 °C.

The colloidal and surface properties of nanocrystals are strongly influenced by the mineral acid used in the hydrolysis. The use of sulfuric acid for the preparation of cellulose whiskers leads to more stable crystal suspension than that prepared by hydrochloric acid, since nanocrystals hydrolysed with sulfuric acid also undergo some surface sulfation and therefore, are stabilised by strong electrostatic repulsion between the anionic sulfate ester groups at the surface[28,30]. The aqueous suspension stability of nanocrystals has therefore, an electrostatic origin. In the case of nanowhiskers generated by using hydrochloric acid, exhibit poor colloidal stability due to the absence of charge at their surface. Other ways to achieve charged whiskers

consists of the oxidation of surfaces[42,43] or an acylation process. Post-sulfation of HCl-prepared crystals is also feasible[30].

The sulfate ester groups introduced in the crystal surface with the sulfuric acid treatment bring about an increase of the hydrophilic character of cellulose whiskers leading to more stable suspensions in water over a wide range of pH values[23]. The stability of crystal suspensions is not only influenced by crystal surface properties, but also by their dimensions and their size polydispersity. Typically, smaller nanoparticles with low aspect ratio are dispersed more homogeneously in solution. In addition, the intensity of ultrasound treatment also affects the dispersion of nanocrystals in water.

Typically, the acid hydrolysis method for the generation of cellulose whiskers leads to quite low yields (2-3%): however, recent optimisation of the process has allowed reaching yields of up to 30%[35,41]. These low yields pose a problem for their production at industrial scale.

NCC Properties

Cellulose crystals show some dispersibility in aqueous-based mixtures and in organic solvents with high dielectric constants, such as dimethyl sulfoxide (DMSO) and ethylene glycol, but tend to aggregate in highly hydrophobic solutions. This poor stability of cellulose whiskers in organic media and hydrophobic thermoplastic matrices poses problems for their application in composites as will be discussed later.

In 1959, the study of acid-treated cellulose and chitin crystallite suspensions led to a discovery of their birefringent character[44]. In the early 1990s, Revol[45] and co-workers demonstrated that cellulose crystals generated by sulfuric acid hydrolysis, in fact, formed a chiral nematic liquid-crystalline phase that was preserved even after water evaporation. Following this discovery, several studies were focused on the

optical and liquid-crystalline properties of cellulose suspensions. Sugiyama et al.[46] reported the possibility to align cellulosic whiskers and form a highly ordered cellulosic by drying diluted aqueous suspensions of tunicin whiskers at room temperature under a strong homogeneous 7 T magnetic field. The microcrystal axis orientation perpendicular to the magnetic field direction was confirmed by electron and X-ray diffraction. Using this process to orient cellulose microcrystals, Revol et al. demonstrated that by varying the ionic content of cellulose crystal suspensions, films with unique optical properties can be prepared. These films consisting of solidified liquid crystals of cellulose have the capability to reflect coloured light were prepared from wood pulp nanocrystals suspensions. Optical properties of these materials depend on both the cellulose origin and the preparation conditions. The wavelength of reflected light can be controlled by adjusting the ionic strength of the suspension. These new materials have high potential for application in security papers[36].

Cellulose nanowhiskers have mechanical strengths equivalent to the binding forces of adjacent atoms leading to highly ordered structure, which produces not only unusually high strengths but also significant changes in electrical, optical, magnetic, ferromagnetic, dielectric, conductive, and even superconductive properties. The reinforcing ability of cellulose whiskers lies in their high surface area and good mechanical properties together with their ability to form rigid networks[4]. Potential applications of nanocrystalline cellulose could be in nanocomposites, paper making, coating additives, and security papers.

3.1.3 Nanofibrillated cellulose (NFC)

Nanofibrillated cellulose refers to individual or cellulose nanofibrils aggregates disintegrated from plant cell wall of cellulose source such as wood pulp fibres. Unlike NCC, NFC consists of longer and more flexible nanofibrils with a width of about 5-40 nm and a length of several micrometers. In addition, NFC exhibits both amorphous and crystalline regions and presents a web-like structure

with high surface area[47]. The typical morphology of nanofibrillated cellulose is displayed in Figure 3.3.

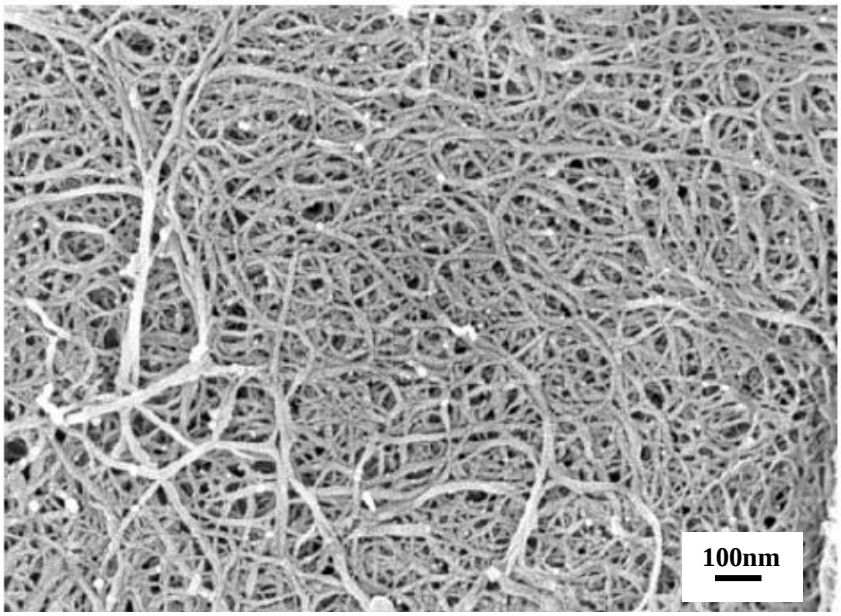

Figure 3.3. High magnification FE-SEM micrograph of the typical morphology of NFC[58].

Nanofibrillated cellulose was first produced in 1983 by Turbak et al.[48] through subjecting wood pulp slurry to high mechanical forces in a high pressure homogeniser. The high shear and impact forces promoted the disintegration of cellulose fibres into nanofibril aggregates with lengths in the micron scale and widths ranging from 10 to 100 nm. These nanofibrils had a high aspect ratio and exhibited gel-like characteristics in water, with pseudoplastic and thixotropic properties. Due to their ability to form stable aqueous suspensions, they have been applied to multiple uses such as thickeners, emulsifiers or additives in food, paints and coatings, as well as cosmetics and medical products[49].

However, the major obstacle for its successful commercialisation has been the high energy consumption (25000 KWh per ton of NFC) involved in the disintegrating process. Later, it was discovered that it was easier to produce NFC from primary-wall materials (e.g., parenchyma cells from sugar beet and citrus fruits)

than secondary-wall materials[50], as the stabilisation of these suspensions by glucuronic and galacturonic acid residues made them easier to delaminate[51]. More recently, there has been a focus on energy-efficient production methods, whereby fibres are pretreated by various physical, chemical, and enzymatic methods before homogenisation to decrease the energy consumption.

NFC Preparation

NFC is currently manufactured from a number of different cellulose sources. Wood is obviously the most important industrial source of cellulosic fibres, and is thus the main raw material used to produce NFC. Bleached kraft pulp is most often used as a starting material for NFC production, followed by bleached sulfite pulp. The high demand of such raw materials from different sectors such as building and furniture and paper industries, has led to an increasing interest in other sources such as agricultural crops and their by-products since they offer environmental benefits owing to their renewable nature and their low energy consumption in production. Unlike wood, a secondary-wall material, cellulose nanofibrils from primary-wall materials such as agricultural fibres are easier to isolate, and therefore, less energy is required for the fibrillation of these pulps[52].

Many examples of NFC obtained from non-wood sources can be found in the literature. For instance, it can be extracted from sugar beet pulp[50], wheat straw and soy hulls[53], sisal[54] or even bagasse[55], palm trees[56], etc.

Mechanical treatments

Regardless of cellulose source, NFC is manufactured from a pulp suspension mainly using a mechanical treatment. Four typical mechanical methods are currently

used for its production: homogenisation, microfluidisation, microgrinding, and cryocrushing; all of which consume different levels of energy. All these methods lead to different types of nanofibrillar materials, depending on the cellulose raw material and its pre-treatment, and more importantly, depending on the disintegration process itself.

A) High pressure homogeniser

The production of NFC is now generally performed by a mechanical treatment of pulp fibres, consisting of refining and high pressure homogenising processes[57,58]. The application of this method for the production of NFC was first reported by Herrick et al. and Turbak et al.[48]. The refining process used is common in the paper industry, and is accomplished via a piece of equipment called a refiner. In a disk refiner, the dilute fibre suspension to be treated is forced through a gap between the rotor and stator disks, which have surfaces fitted with bars and grooves, against which the fibres are subjected to repeated cyclic stresses. This mechanical treatment brings about irreversible changes in the fibres, increasing their bonding potential by modification of their morphology and size[57]. However, mechanical refining methods tend either to damage the nanofibril structure by reducing molar mass and degree of crystallinity or fail to sufficiently disintegrate the pulp fibre[59]. The refining process is carried out prior to homogenisation due to the fact that refining produces external fibrillation of fibres by gradually peeling off the external cell wall layers (P and S1 layers) and exposing the S2 layer, and also causes internal fibrillation that loosens the fibre wall, preparing the pulp fibres for subsequent homogenisation[57]. Pulp fibre slurry is treated by several passes through a disk refiner in order to get the desired fibrillation degree[60].

In the homogenisation process (Figure 3.4), dilute slurries of cellulose fibres previously treated by refining are pumped at high pressure and fed through a spring-loaded valve assembly. As this valve opens and closes in rapid succession, the fibres are subjected to a large pressure drop with shearing and impact forces. The slurry is

reintroduced in the device many times in order to increase the fibrillation degree of fibres. This combination of repeated forces promotes a high degree of fibrillation of the cellulose fibres, resulting in nanofibrillated cellulose[57]. However, an increase in the number of homogenisation cycles involves a considerable increase in energy consumption reaching values as high as 30,000 kWh/t[52]. Many studies have been performed with the aim of optimising the number of cycles in the homogeniser, and therefore the energy demand. Iwamoto et al.[61] reported that after 14 cycles, further homogenising up to 30 cycles did not improve fibrillation. This observation was supported by Malainine et al.[62] who achieved the desired fibrillation by applying 15 passes through a laboratory homogeniser operated at 500 bars. Therefore, fibre suspensions are usually homogenised approximately 10–20 times in order to achieve the desired fibrillation[63-65]. The main processing issue in the production of NFC with high-pressure homogeniser is the fibre length, since long fibres often clog the equipment. In order to reduce the clogging tendency, a mechanical treatment prior to homogenisation process is required to reduce the fibre length and/or to pre-defibrillate the fibres[49]. Alternatives for mechanical reduction of fibre size include refiners, as previously described, PFI mills, manual cutting, and Valley beaters[57,61,63,66].

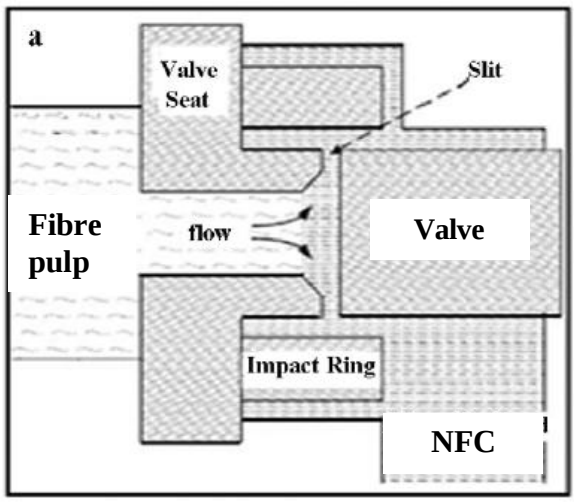

Figure 3.4. Schematic representation of a homogeniser.

Overall, it can be stated that homogenisation is an energy-intensive process. Besides the large energy consumption, the main disadvantage of the use of homogeniser is that long fibres often clog the system, particularly at the moving parts (in-line valves) which then must be disassembled and cleaned. On the other hand, the homogeniser can easily be scaled to industrial production and can be operated continuously[49].

B) Microfluidiser

Microfluidisation is a process commonly used in the cosmetic, biotechnology, and pharmaceutical industries. Compared to the homogeniser, the likelihood of clogs in a microfluidiser during fibre processing is lower since it has no in-line moving parts. In microfluidiser (Figure 3.5), the wood pulp passes through thin z-shaped chambers (with channel dimensions that are usually 200-400 µm) under high pressure, i.e., 2070 bar[67]. The shear rate applied is thus very high (up to 107 s^{-1}), which results in the formation of very thin cellulose nanofibres. The microfluidiser operates at a constant shear rate, compared to the homogeniser, which operates at a constant processing volume. The interaction chamber can be designed with different geometries to produce different sized materials and plugging can be resolved by using reverse flow through the chamber[49].

As in the previous disintegration system, the production of NFC through microfluidiser also requires a fibre pre-treatment to reduce their size and facilitate their subsequent defibrillation. Mechanical pre-treatments are common for both homogeniser and microfluidiser. Zimmermann et al.[68] and López- Rubio et al.[69] reported the mechanical fibrillation process using a microfluidiser. Such mechanical dispersion of pulp fibres leads to fibril structures with diameters between 20 and 100 nm and estimated lengths of several tens of micrometers. This equipment is increasingly being used, since it makes it possible to obtain more uniformly sized fibres[70].

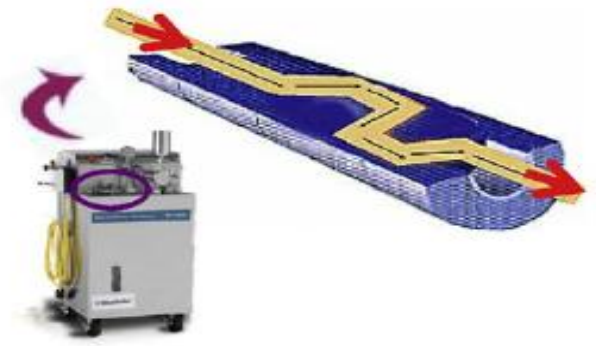

Figure 3.5. Microfluidiser processor used for the production of NFC.

C) Grinder

Modified commercial grinders with specially designed disks have been used by some researchers in order to fibrillate cellulose fibres (Figure 3.6). In such equipment the cellulose slurry is passed through a gap between a rotary and a stator disk which have bursts and grooves that contact the fibres to disintegrate them into individualised nanofibres[71]. Typically, the materials used for the disks in the grinder are non-porous resins containing silicon carbide. The disks can be produced using different grit classes and different groove configurations to alter flow patterns during processing. As an example, Taniguchi and Okamura[72] obtained nanofibrillated fibres having diameters in the range 20–90 nm by a unique super-grinding procedure. Iwamoto et al.[58] fibrillated pulp fibres from Pinus radiate with a grinder and observed the influence of multiple passes through the grinder on the NFC morphology. From one to three passes, most of the fibres were turned into sub-micron-size and nano-sized fibres. At five passes, most of the fibres became nanosized fibres with diameters ranging from 20 to 50 nm. With a higher number of passes, no significant changes were observed in the fibre morphology. Further grinding treatment led to a degradation of fibrillated fibres demonstrated by a decrease in their crystallinity and DP, which resulted in a detriment of the reinforcing potential of NFC. It was then concluded that with five passes through the grinder, the fibrillation of pulp fibres was almost complete.

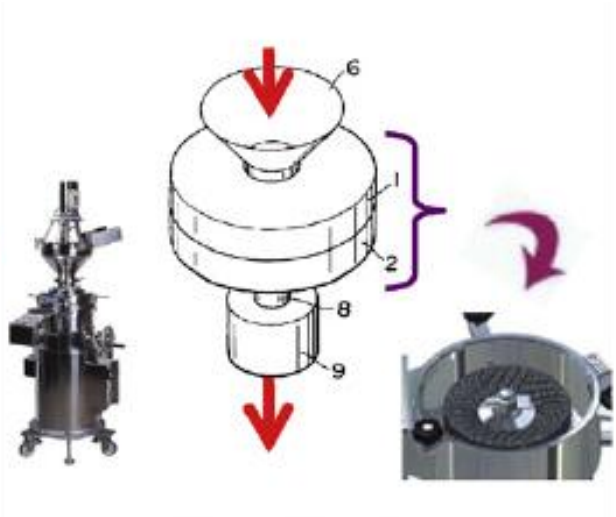

Figure 3.6. Ultra-fine friction grinder employed for the disintegration of fibre pulps into nanofibres.

As a result of the complicated multilayered structure of plant fibres and interfibrillar hydrogen bonds, a common feature of all disintegration methods is that the material obtained consists of aggregated nanofibres with a wide distribution in width. However, Abe et at.[71] also reported an efficient extraction of wood cellulose nanofibres as they exist in the cell wall, with a uniform width of 15 nm, by a very simple grinding treatment. This result was achieved by keeping the material in the water-swollen state after the removal of lignin and hemicellulose, thus avoiding the generation of strong hydrogen bonding between the cellulose bundles, which often takes place during drying processes.

A drawback of using this mechanical treatment for fibre fibrillation is the constant maintenance and replacement of grinder disks since pulp fibres often wear down the grooves and grit. On the other hand, the mechanical fibre shortening pre-treatment used with other processing techniques is not usually required for grinding treatments[49].

D) Cryocrushing

Another method, which is however very rarely used, was proposed by Dufresne et al.[73], who carried out a cryocrushing process to produce NFC from sugar beet pulp. Cryocrushing consists of applying high shear forces to fibres previously frozen with liquid nitrogen[74]. Under mechanical crushing, the ice crystals within the frozen fibre cells slash the cellular wall allowing the liberation of nanofibrils[75]. Alemdar and Sain[53] extracted NFC from wheat straw and soy hulls via mechanical treatment involving cryocrushing, followed by disintegration and fibrillation. These authors found that almost 60% of the NFC obtained had a diameter in the range 30–40 nm and lengths of several micrometers. Cryocrushing is limited for the isolation of cellulose fibrils from primary cell walls and therefore, its use is only suitable for the production of NFC from agricultural crops and by-products. Bhatnagar and Sain[76] obtained NFC from flax, hemp, and rutabaga fibres via cryocrushing (with diameters of 5–80 nm). Wang and Sain[75] applied this process to soybean stock to produce NFC with diameters in the range 50–100 nm.

In most of cases, the successful extraction of nanofibres from natural fibres requires a combination of several high intensity mechanical treatments such as high-pressure homogeniser processes followed by a grinding treatment[61] or vice versa[55]. Other equipments and methods for mechanical disintegration are currently available including blenders, sonicators, and steam explosion techniques.

Each of the previously mentioned mechanical treatments requires high energy demands. Energy consumption during production is an important aspect in the determination of the ‘‘green’’ nature of these NFC-based materials. Recently, a comparative study of the energy consumption and physical properties of NFC produced by different mechanical treatments including homogenisation, microfluidisation, and grinding has been reported[49]. They concluded that the homogeniser resulted in NFC with the highest specific surface area and films with the lowest water vapour transmission rate, in spite of its high energy consumption. In

addition, films produced by a microfluidiser and a grinder presented superior physical, optical, and water interaction properties, which suggests that these materials could be produced in a more economical way for packaging applications.

In general, the most important issue, that needs to be addressed for the industrialisation of NFC production, is the high energy consumption associated to the mechanical disintegration of the fibres into NFC, which often involves several passes through the disintegration device and the combination of different intensive mechanical treatments. Values around 20,000–30,000 kWh/tonne are not uncommon. Even higher values reaching 70,000 kWh/tonne have also been reported. By combining the mechanical treatment with certain pre-treatments (e.g., chemical or enzyme) it is possible to decrease the energy consumption significantly to the level of 1,000 kWh/tonne[52].

Pre-treatments

Several strategies have been proposed in order to obtain fibres that are less stiff and cohesive, thus decreasing the energy needed for fibrillation.

A) Alkali pre-treatment

Before mechanical processing, a number of researchers have applied alkaline treatment of fibres in order to disrupt the lignin structure and help to separate the structural linkages between lignin and carbohydrates[73]. Purification by mild alkali treatment results in the solubilisation of lignin and remaining pectins and hemicelluloses. Alkali extraction needs to be carefully controlled to avoid undesirable cellulose degradation and to ensure that hydrolysis occurs only at the fibre surface so that intact nanofibres can be extracted[75].

B) TEMPO mediated oxidation pre-treatment

Currently, the more commonly used pre-treatment is TEMPO mediated oxidation. Saito et al.[77] introduced an oxidation pre-treatment of cellulose, applying 2,2,6,6-tetramethylpiperidine-1-oxyl (TEMPO) radicals before mechanical treatment in a Warning-blender. TEMPO-mediated oxidation of cellulose fibres introduces negatively charged carboxyl groups on the fibril surface and the resulting repulsive forces between charged fibrils facilitate the disintegration process. TEMPO-oxidised wood pulp fibres can be disintegrated by a simple mechanical stirring, which considerably reduces the energy consumption. Compared to the energy consumption of repeated cycles of a high pressure homogeniser (700–1400 MJ/kg), TEMPO-mediated oxidation pre-treatment dramatically decreases the consumption to values less than 7 MJ/kg[78]. Despite the surface modification, the crystalline structure of native cellulose is preserved in the interior of the fibrils. Unlike other methods, this chemical pre-treatment followed by mechanical processes provides isolated individual cellulose nanofibres in aqueous suspension, instead of fibril bundles (Figure 3.7)[77,79,80]

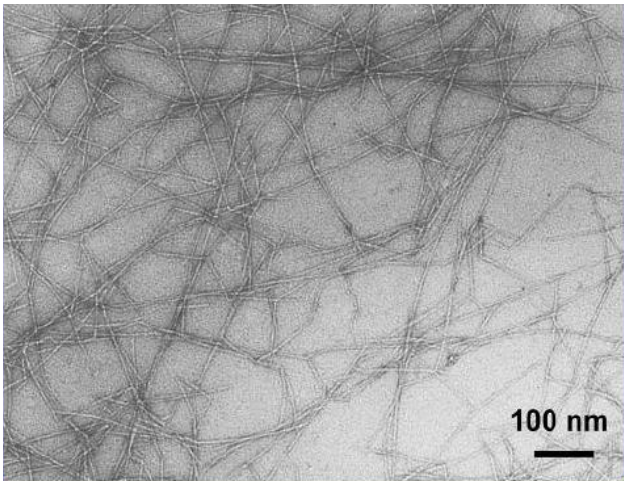

Figure 3.7. TEM image of a dispersion of TEMPO-oxidised celluloses with carboxylate content of 1.5 mmol/g. Image was taken after stirring in water for 10 days[81].

In order to avoid undesirable side reactions under alkaline conditions, such as significant depolymerisation or discoloration of the oxidised cellulose due to the presence of aldehyde group residuals, Saito et al.[82-84] applied a TEMPO/NaClO/$NaClO_2$ system under neutral or slightly acidic conditions. These authors demonstrated that the new oxidation system allowed almost complete maintenance of the original DP, uniform nanofibre distribution (~5 nm in width) and a material free of aldehyde groups.

Recently, an alternative method has been developed by A. Isogai et al.[78] and T. Isogai et al.[85]: a TEMPO electro-mediated reaction. They applied two new systems to softwood bleached kraft pulp: electro-mediated oxidation with TEMPO at pH 10, and 4-acetamido-TEMPO at pH 6.8 in a buffer solution. This is a new sustainable method to produce NFC that has carboxylate and aldehyde groups on its surface, and it could well replace the first two systems, although longer oxidation times are required. The yield is quite high (more than 80%). Moreover, it preserves the main characteristics of TEMPO-oxidised NFC produced from bleached softwood kraft pulp.

C) Carboxymethylation

Another chemical pre-treatment is carboxymethylation. This pre-treatment increases the anionic charges in the formation of carboxyl groups on the surface of the NFC. Aulin et al.[70] produced carboxymethylated NFC and compared its dimensions with that of non-pretreated NFC. The carboxymethylation treatment makes the fibrils highly charged and easier to liberate. The widths of carboxymethylated NFC obtained after microfluidisation are in 10-15 nm range. Taipale et al.[86] measured the net specific energy consumption of such treatment. They found that after carboxymethylation, the required energy of fluidisation was 2.2 MWh/tonne per pass through a microfluidiser, whereas 5.5 MWh/tonne per pass was needed to obtain NFC without pre-treatment.

D) Enzymatic pre-treatment

Enzymatic treatment of cellulose prior to defibrillation has been reported as an efficient method to facilitate their posterior disintegration, thus reducing considerably the number of cycles through homogeniser and therefore, the energy consumption for the obtaining of NFC[87]. In nature, cellulose is not degraded by a single enzyme but a set of cellulases are involved. These can be classified as A- and B-type cellulases, termed cellobiohydrolases, which are able to attack highly crystalline cellulose, and C- and D-type cellulases or endoglucanases which generally require some disorder in the structure in order to degrade cellulose Cellobiohydrolases and endoglucanases show strong synergistic effects[88]. Since the principal aim is the isolation of long and highly crystalline nanofibres, the most suitable enzymes for the pre-treament are endoglucanases. Henriksson et al.[88] successfully isolated NFC with high average molar mass and aspect ratio by pre-treating wood pulp with endogluconases in combination with mechanical beating before its disintegration in a homogeniser. Even wood pulp pretreated with a very low enzyme concentration (0.02%) was successfully fibrillated into nanofibres preserving their molecular weight and fibre length. They suggested that endoglucanase treatment increases cell wall swelling in the water suspension and, as a consequence, the cell wall is more readily disintegrated into NFC nanofibres when subjected to mechanical shearing during the homogenisation process. Henriksson et al.[88] and Pääkkö et al.[87] demonstrated that the NFC produced from enzymatically pre-treated cellulosic wood fibres showed a more favourable structure than nanofibres produced by subjecting pulp fibre to strong acid hydrolysis. After these pioneering works, studies based on the effect of different enzymatic hydrolysis parameters on the properties of isolated cellulose nanofibres have been reported[66]. Unlike other pre-treatments, enzymatic hydrolysis has a limited effect on the DP of cellulose, therefore, nanofibres isolated from this method preserve high DP, which is extremely important for achieving good mechanical properties. The importance of high DP for the mechanical properties of NFC films was demonstrated by Henriksson et al.[66].

The use of the previously described pre-treatments prior to the mechanical treatments allows the manufacture of NFC with less energy consumption. However, these pre-treatments usually consist of multi-step processes where fibres are not only subjected to several chemical treatments, but also to mechanical processes such as refining. The aim of this mechanical treatment is to increase the fibre swelling and make the cellulose more accessible for the subsequent chemical/enzymatic treatment. Therefore, mechanical treatments are commonly also used during these pre-treatments. In addition, these pre-treatment usually involve long processing times and the use of a variety of non-environmentally friendly chemical substances. Thus, these pre-treatments reduce the energy demand required for the subsequently mechanical treatment; however there is not any data reported about the environmental impact of these pre-treatments. The environmental benefits of these pre-treatments should be not only assessed based on the energy consumption of the subsequently mechanical treatment, but it is also necessary to take into account their own environmental impact. In order to assess the overall environmental impact associated to NFC production with and without pre-treatments, life cycle assessments (LCA) should be performed.

NFC Properties

Besides the interesting colloidal and rheological properties, NFC has a great potential as reinforcing medium in nanocomposites due to its high aspect ratio, modulus, and specific surface area together with its ability to form strong hydrogen-bonded networks. As a result of this impressive mechanical performance, NFC has been used for nanopaper[66,89] foams[90,91] and aerogels[92,93] and as reinforcement in a range of polymer matrices[94,95]. NFC has also been used as a substrate for functional materials including electrically conductive all-polymer batteries[96], magnetic nanopaper[97] and transparent and foldable films for display applications[98]. Moreover, due to its relatively crystallinity in combination with its ability to form networks, NFC can be acted as a barrier material[47].

3.1.4. Bacterial cellulose (BC)

Besides being the cell-wall component of plants, cellulose is also secreted extracellularly as synthesised cellulose fibres by some bacterial species. Bacterial cellulose (BC) is mainly a protective coating, whereas plant cellulose plays a structural role[99]. BC is synthesised by certain bacteria belonging to the genera *Acetobacter, Agrobacterium, Rhizobium*, and *Sarcina*[100]. The most efficient producer of BC is Acetobacter *xylinum (recently reclassified as gluconoacetobacter xylinus),* a gram-negative strain of acetic-acid-producing bacteria[101]. These bacteria are found everywhere when fermentation of sugars and plant carbohydrates take place, as on damaged fruits and flowers, or in unpasteurised or non-sterilised juice, beer and wine. Pure strains can be bought from international collection of micro-organisms[102].

BC Synthesis

In 1886, A.J. Brown discovered BC as a biosynthetic product of *Gluconacetobacter xylinus* strains. The bacteria cultivated in a culture medium containing carbon and nitrogen sources produced extracellular cellulose, an ultrafine ribbons network structure in the form of a highly hydrated pellicle, which was described by Louis Pasteur as "*a sort of moist skin, swollen, gelatinous and slippery…*"[99]. Although the solid portion in the gel-like stuff is less than one percent, it is almost pure cellulose[103], therefore no chemical treatments are needed to remove lignin and hemicelluloses, as with plant cellulose.

The biosynthesis of BC occurs between the outer and plasma membranes of the bacterial by a cellulose-synthesising complex, starting with biochemically activated dextrose. This complex is associated with pores at the surface of bacterial cell, which have diameters of about 3 nm. Cellulose synthase catalyses the addition of activated dextrose to the end of the growing cellulose chain, which exits the cell as an elementary fibril (Figure 3.8). One single cell can convert more than 100

dextroses into cellulose per hour. In the culture medium, these fibrils self-assemble to form ribbons and finally a 3D nanofibre network[102].

In a static culture, the BC is shaped as pellicles at the air/liquid interface. Biosynthesis is formed in yields up to 40% (in relation to the bacterial strain-to nanocellulose of high purity). Residual bacteria and components of the culture medium can be removed by boiling with weak basic media and subsequent washing with water[23].

The direct formation of a 3D object from cellulose by a biofabrication process is unique in the production of cellulose materials. In contrast to thermoplastic synthetic polymers, plant cellulose can only be shaped by post-processing/regeneration steps using cellulose derivatives (e.g. viscose process) or specific solvent systems (such as N-methylmorpholine-N-oxide or sodium hydroxide and urea in water)[102].

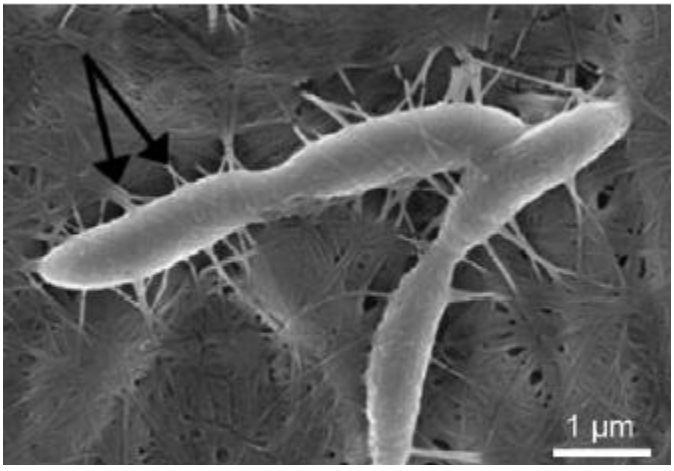

Figure 3.8. Gluconacetobacter bacteria forming cellulose nanofibres and ribbons[23].

The shape of the BC hydrogels can be designed effectively by choosing the appropriate reactor form and function (static or agitated cultivation). Under the

common static conditions in glass or polypropylene containers with circular or square profiles, the BC products are formed in the shape of the reactor; The BC hydrogel bodies adopt the dimensions of the cultivation vessel. Figure 3.9-a shows a typical BC fleece constructed of the BC nanofibre network and soaked with water in its native hydrated state formed in a circular reactor. Thinner films for technical use or patches for biomedical applications are available after shorter cultivation times. A characteristic example is demonstrated in Figure 3.9-b. Under stirring conditions, the organisation of the BC fleece is disturbed, and BC spheres or fibre bundles result with increasing agitation 0.5 mm up to centimetre-scale and with lengths of 1 to more than 20 cm can be prepared. Examples of BC spheres are demonstrated in Figure 3.9-c[23,101,102,104]. Moreover, the surface at the region of BC deposition can distinctly influence formation. Thus, the use of nematically ordered liquid-crystalline cellulose patterns as templates led to the deposition of BC along tracks defined by template[105].

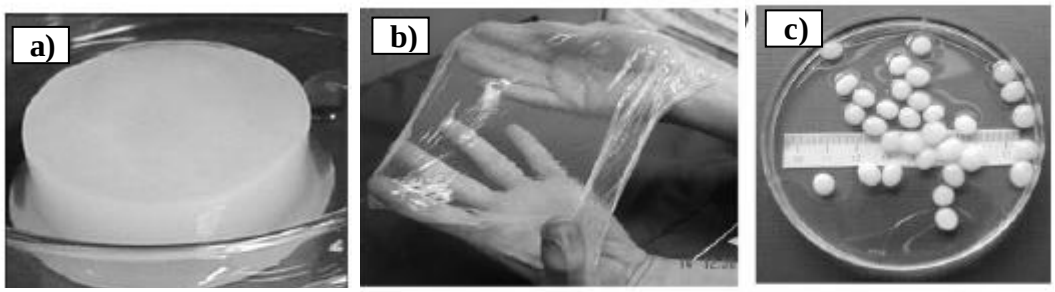

Figure 3.9. BC hydrogels formed in situ. a) Typical BC fleece formed in a circular reactor. b) Thin film of BC. c) BC spheres from agitated culture[23,102].

Controlling the structure of the nanofibre network of BC materials can be done by changing: (i) type of bacterial strain, (ii) the additives in the culture medium, (iii) the type and conditions of cultivation, and drying processes.

For commercial application, cost-efficient processes for the mass production of BC are required. During the last few years, a broad range of new concepts were investigated. Often, they were based on a combination of static and agitated cultivation. Further approaches included the continuous harvesting of cellulosic filaments, pulps, and fibres. Other examples are the linear conveyor reactor and the rotary disk reactor, developed by Bungay and Serafica[106]. These approaches lead to rather non-uniform material owing to the bundling and aggregation of thin layers or filaments. Frankenfeld et al.[107] developed a process for the production of specifically moulded shapes or layers. Levy et al.[108] and Farah et al.[109] suggested the production of sheets and membranes of BC. The sheets are collected from the surface of the culture medium and are then submitted to processes of purification. When these types of reactors are used, the homogeneity of the material can be retained, but the widths and lengths of the cultured sheets are still restricted by the dimensions of the culture vessel[23].

By manufacturing with a novel horizontal lift reactor (HoLiR), an efficient process could be developed for the (semi-)continuous cultivation of planar BC fleeces and films of freely selectable length and adjustable height. Comprehensive investigations demonstrated the comparability of the BC harvested with that gained from static cultivation under batch conditions[110]. The large number of control elements also provides problems in terms of the reproducibility of the method and comparability of the products. However, reliable control of these specific factors enables access to novel materials for applications in medicine, the life sciences, and technology.

BC Properties

There are important structural differences between BC and, for example, wood cellulose. BC is secreted as a ribbon-shaped fibril, less than 100 nm wide, which is composed of much finer 2–4 nm nanofibrils[103]. In contrast to the existing

methods for obtaining nanocellulose through mechanical or chemo-mechanical processes, BC is produced by bacteria through cellulose biosynthesis and the building up of bundles of microfibrils[99].

A recent model of the BC structure in the never-dried state was given by Fink et al.[111]. Anhydrous nano-fibrils in the range 7x13 nm appear hydrated as a whole and are aggregated to flat microfibrils with a width of 70–150 nm. This means that the water is outside of the crystalline cellulose nano-units and between these elements. A shell of non-crystalline cellulose chains passes around neighbouring microfibrils to produce a microfibril band (ribbon) with a width of about 0.5 μm. The arrangement of these microfibrils and ribbons is shown in Figure 3.10-b[111].

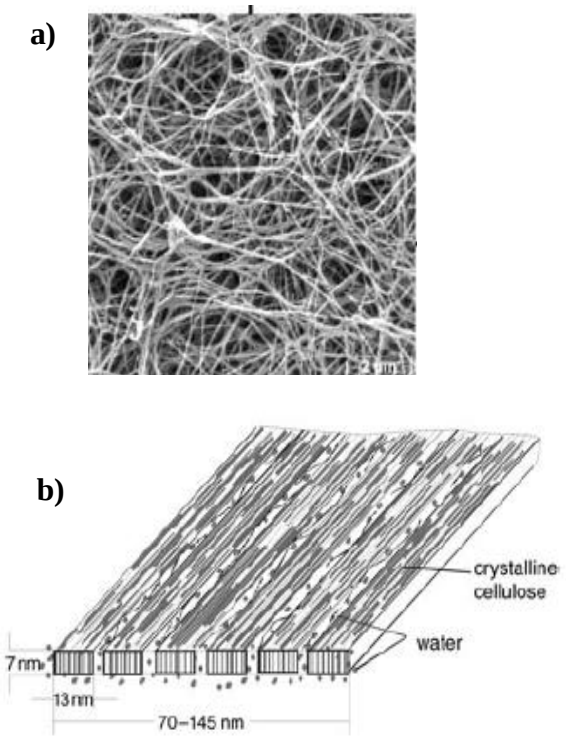

Fig. 3.10. a) SEM image of freeze-dried nanofibre network (magnification 10.000x). b) Model of initially hydrated BC fibrils[111].

The properties of bacterial cellulose are denominated by the nanoscale cellulose fibre network architecture. The main effect of the nanosize dimensions of their fibrils is an increase in surface area of the BC network, which is reflected in strong interactions with the surrounding environment. Therefore, BC binds large amounts of water up to 99% during biosynthesis in the aqueous culture media. The nanofibre structure of the hydrogel also allows strong interactions with other polymers, including extracellular matrices of living tissue and the fixation of nanoparticles of different types[23].

In terms of the molecular formula, BC is identical to cellulose of plant origins, however, important structural features and properties are quite different. Such unique properties of BC are high purity, high degree of polymerisation (up to 10000 anydroglucose units), high crystallinity (of 70 to 80% up to 84-89[112]), high water content up to 99% and high mechanical properties. The tensile strength of BC single nanofibre is equivalent to Kevlar fibres (2 GPa).and its Young´s modulus has a similar high value of 134 GPa. It also possesses a low thermal expansion coefficient (similar to that of glass). The latter is again in the range of aramid fibres. As previously mentioned, these specific parameters are caused by their particular supramolecular structure as a network of nanofibres formed during self-assembly of the cellulose molecules in the aqueous culture medium, free from potential composite partners as in wood biosynthesis[101].

These unique properties of BC together with their good biocompatibility and high porosity have made it found a multitude of applications in paper, textile, and food industries, and as a biomaterial in cosmetics and medicine[113,114]. New applications are as a thickener to maintain viscosity in food, cosmetics, etc., as nonwoven fabric or paper for old document repair, as food additives and others. The use of cellulose films as a temporary substitute for human skin in the case of burns, ulcers, decubitus and others has been reported. Biofill®, Bioprocess® and Gengiflexm® are products of BC that now have wide applications in surgery and dental implants[113]. Bacterial cellulose is also used in hi-fidelity loudspeakers and

headphones because of two essential properties: high sonic velocity and low dynamic loss[103]. Due to their high mechanical properties BC is considered highly effective reinforcement to produce high performance and transparent nanocomposites. A very important aspect in the development of BC materials concerns the design of BC composites by either in-situ or post-modification, as it will be discussed in the next section.

3.2 Cellulose based nanocomposites

In essence, the principle reason to utilise cellulose nanofibres in composite materials is because one can potentially exploit the high stiffness of the cellulose crystal for reinforcement. As previously discussed, the disintegration of natural fibres leads to highly crystalline nanocelluloses with low amount of defects and amorphous material. Due to their high aspect ratio (length/diameter) and mechanical performances, nanocelluloses exhibit great reinforcing capabilities what makes them very suitable for composite materials. Due to the intrinsic higher performances of nanocelluloses compared to cellulose microfibres, their use as a reinforcement should provide an enhancement of stress transfer and therefore of the final composite modulus. The origin of the mechanical advantage of using nanocelluloses over conventional cellulose microfibres as reinforcements in composite materials can be explained through the Halpin-Tsai model[115]. This mechanical model has been extensively used to predict the elastic properties of short-fibre composites as a function of the aspect ratio of the filler. In this approach, short fibres are assumed to be homogeneously dispersed in a continuous matrix. The model also supposes a perfect interface between fibre and matrix, without taking into account filler-filler interactions and therefore, possible formation of filler percolated networks, which can take place in high loading cellulose nanocomposites. The constituent properties and the volume fraction of the matrix and filler must be known. Figure 3.11 shows Halpin-Tsai micromechanical predictions for polypropylene matrix composites filled

with 50% of aligned cellulose fibres as a function of different fibre aspect ratios and Young´s moduli.

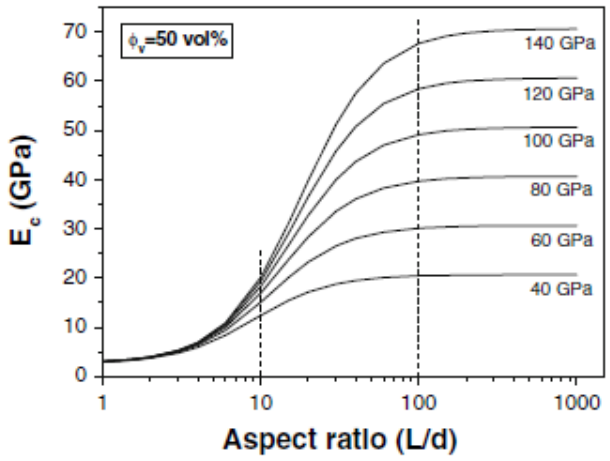

Figure 3.11. Graphic based on Halpin-Tsai model predictions where the composite modulus E_c is a function of the reinforcement aspect ratio for a range of fibre moduli. The composite consists of a polypropylene matrix and a 50% of aligned cellulose.

As can be deduced from the chart, the maximum reinforcing effect of nanocelluloses in nanocomposites can only be reached if their aspect ratio is high enough. Nanocelluloses with low aspect ratio will not provide greater reinforcing effects than conventional microfibres. Therefore, an efficient reinforcement effect can be only achieved for nanocelluloses with aspect ratios greater than 50.

With regard to aspect ratio, nanofibrillated cellulose exhibits higher reinforcing potential compared to nanocrystalline cellulose. Nanowhiskers are stiff, crystalline rods with the lowest aspect ratio of the nanocelluloses as a result of the aggressive acid hydrolysis applied for their preparation. NFC, on the other hand, consists of longer and more flexible nanofibrils and forms extensively entangled networks, resulting in more efficient reinforcements at low concentrations[87]. The effect of whiskers and NFC in thermoplastic composites has been studied. In

comparison with nanowhiskers, NFC usually results in a stronger material with higher modulus and lower elongation at break due to the possibility of NFC to form entanglements[54,116]. A comparative study of the mechanical properties of poly(caprolactone) (PCL) reinforced with sisal NFC and nanowhiskers confirmed these results[54]. The differences between nanowhiskers and NFC are related to their processing conditions. Such differences will affect the overall state of dispersion and residual stresses in the resulting nanocomposite.

As occurs with cellulose microcomposites, the properties of cellulose nanocomposites depend on nanofibre and matrix properties, morphological aspects of filler (size, shape, aspect ratio), nanofibre volume fraction and orientation, and adhesion between matrix and reinforcement. Due to the huge number of parameters that influence the mechanical properties of nanocomposites, together with the differences in the reinforcing effect according to the nanocellulose type, a comparision between different nanocellulose composites is quite complicated. For this reason, the properties of cellulose based nanocomposites will be described as a function of the nanocellulose type used as reinforcement.

3.2.1 NCC based nanocomposites

Three main parameters were reported to affect the mechanical properties of cellulose whisker reinforced nanocomposites: geometrical aspect ratio, processing method and nanowhisker-matrix and nanowhisker-nanowhisker interactions.

A) The geometrical aspect ratio

The geometrical aspect ratio: this parameter depends on the cellulose source and the conditions employed for whisker preparation. As previously mentioned, the higher the aspect ratio of nanowhiskers, the greater the reinforcing effect in

composites. This statement was clearly demonstrated by Favier[31,117] through their study of the mechanical behaviour and thermal stability of poly(S-co-BuA) nanocomposites reinforced with nanowhiskers from different sources and therefore different aspect ratios. The highest modulus increase in the rubbery state of the matrix and thermal stability were obtained for tunicin whiskers (L/d ~67) in comparison with bacterial (L/d ~60) or Avicel whiskers (L/d ~10). The crystallinity of these nanowhiskers is directly linked to their aspect ratio which in turns, depends on their origin, demonstrating that the cellulose origin governs the resulting reinforcing effect via its degree of crystallinity.

Eichhorn and Young[118] reported the effect of crystallinity on the Young´s modulus of cellulose whiskers. A decrease in whisker crystallinity leads to a lower value of Young´s modulus. Moreover, Dubief et al.[119] compared the mechanical behaviour of nanocomposites based on amorphous poly(β-hydroxyoctanoate) reinforced with tunicin and starch nanowhiskers. More than 10 wt.% of starch whiskers (L/d ~1) was needed to achieve a reinforcing effect comparable to that provided by only 1 wt.% of tunicin whiskers. Several aspect ratios of cellulose whiskers from different sources are tabulated in Table 3.4.

Tabla 3.4. Geometrical characteristics and percolation threshold (Φc) of some cellulose nanocrystals[67].

Source	Length (nm)	Diameter (nm)	L/d	*Φc*
Cotton	171.6	14.6	11.8	5.9
Ramie	200	7	28.6	2.5
Sugar beet pulp	210	5	42	1.7
Palm tree	260	6.1	43	1.6
Wheat straw	225	5	45	1.6
Tunicin	1000	15	67	1.0

B) The processing method

Processing techniques have an important incidence on the final properties of the composites. These techniques are conditioned by both intrinsic properties of whiskers and polymeric matrix (solubility, dispersibility, and degradation) and the desired final properties such as geometrical shape. As occurs with cellulose microfibres, the main drawbacks of using cellulose nanofibres as reinforcement in polymer nanocomposites are based on their intrinsic hydrophilic character. Therefore, the common challenges in cellulose based nanocomposites are related to achieving a good dispersion within hydrophobic polymer matrix and to create a strong interfacial bond between nanofibre and matrix. For this reason, the incorporation of nanocelluloses as a reinforcement has so far been mainly limited to aqueous or polar environments. The technique most commonly used for the cellulose based nanocomposites consists of water or organic evaporation by solvent casting. With regard to this technique, three systems can be distinguished depending on the polymer matrix: water soluble polymers, polymer emulsions and non-hydrosoluble polymers[67] (Figure 3.12). Although these techniques will be described for nanowhisker based nanocomposites, they are common for any nanocellulose based systems.

Water is the preferred processing medium because of the high stability of aqueous cellulose whisker dispersions and the expected high level of dispersion of the filler within the host matrix in the resulting composite film[36]. It simply consists in mixing this suspension with the polymer previously dissolved in water, and evaporating the liquid. The choice of the matrix is restricted to hydrosoluble polymers[36]. In addition, these polymers usually are highly sensitive to humidity so that special care should be taken in order to avoid the water absorption since it would be detrimental to the nancomposite mechanical performance[67].

A first alternative to achieve good dispersions of nanowhiskers within hydrophobic matrices consists of using the polymer in the latex form, so that it

allows an aqueous media for nanocomposite processing. Favier et al.[31,117] adopted the technique of solution casting using a synthetic latex obtained by the copolymerisation between styrene (35 wt.%) and butyl-acrylate (65 wt.%) (poly(S-co-BuA)). These authors mixed the whisker aqueous suspension with the polymer latex. The nanocomposite films were obtained by water evaporation at room temperature. Following this work, this technique has been used for the processing of many nanocomposites based on matrices such as poly(β-hydroxyoctanoate) (PHO)[26], polyvinylchloride (PVC)[120,121].

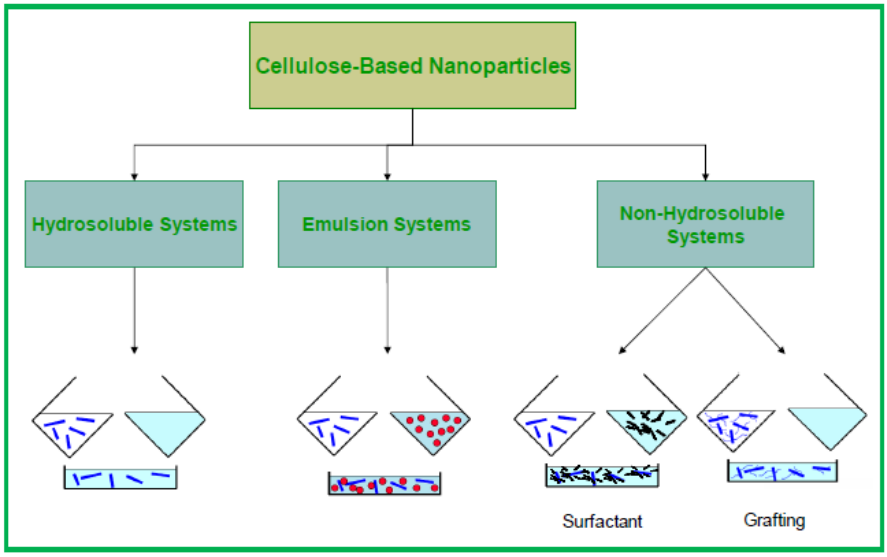

Figure 3.12. General scheme of strategies used for preparation of cellulose based nanocomposites by solvent casting[67].

A second alternative consists of dispersing cellulose whiskers in an adequate (with regard to matrix) organic medium. This was made possible by coating the whiskers surface with a surfactant[122] or by chemically modifying their surface[43,123]. The use of a surfactant is the simplest method. However, the high amount of surfactant required to coat the high specific surface area of whiskers[122] prevents the use of this expensive technique in composite applications due to the high cost associated. The chemical surface modification of cellulose whiskers is another way

to disperse cellulose whiskers in organic solvents. The same surface modifications applied to cellulose microfibres in order to improve their compatibility with hydrophobic thermoplastic matrices have been used for nanocelluloses. Those methods include surface hydrophobisation by silylation or acylation[124-126], carboxylation[43], esterification[127], polymer grafting (PCL, poly(ethylene glycol) (PEG)[43], poly(ε-caprolactone)[128]). However, the mechanical performances of the resulting composites were found to strongly decrease after chemical modification as reported for chitin whiskers from crab shell[129]. Moreover, these chemical surface treatments involve an increase in processing cost and time as well as an increase in environmental impact of nanocomposite processing.

Recently, polymer nanocomposites reinforced with cellulose whiskers have been prepared by dispersing the whisker suspensions in an organic solvent, N,N-dimethylformamide (DMF), without any surface chemical modification or coating surfactant. This approach, reported by Dufresne's group[130], involves freeze drying of the initial aqueous suspension of the nanowhiskers, and then further redispersion in DMF. The stable nanowhisker suspension in DMF was subsequently incorporated in different polyurethane matrices. This approach allowed the study of the effect of reinforcing a shape memory PU with cellulose whiskers. The efficiency of the dispersion resulted in nanocomposite films where the original transparency of PU was preserved. The cellulose whiskers were introduced before or after PU reaction and the shape memory properties of the resulting nanocomposites were studied. It was concluded that PU can be reinforced preserving their shape memory properties with cellulose nanowhiskers only if their incorporation is performed after PU synthesis to avoid their covalent attachment to the polymer.

Apart from solvent casting, two more techniques have been used for the preparation of whiskers based composites: freeze-drying and hot-pressing; or freeze-drying, extruding and hot-pressing. Composite films were also obtained by cross-linking in situ an unsaturated matrix after solution casting by using a thermo or photo cross-linking agent.

Hajji et al.[131] studied the tensile behaviour of poly(S*co*-BuA)/tunicin whisker composites prepared from different manners. The authors classified processing methods in ascending order of their reinforcement efficiency (tensile modulus and strength): extrusion < hot pressing < evaporation. Poor results obtained by freeze drying followed by hot pressing arise from rough dispersion of the fillers, which creates film irregularities[132], whereas extrusion causes the gradual breakage of whiskers, which decreases their aspect ratio and their efficiency, which at the same time also limits the possibility of nanocomposite recycling. On the other hand, water evaporation technique provides time enough for whiskers to form a three dimensional hydrogen-bonded network; increasing in this way the mechanical performance of the nanocomposites.

C) The matrix structure and the competition between matrix/nanowhisker and nanowhisker/nanowhisker interactions.

Classical composite theory considers matrix/fibre interaction as a pivotal condition for optimal performance. However, in cellulose whisker based nanocomposites the opposite trend is observed. Dufresne[133,134] studied the effect of different cellulose whiskers in various rubbery latex matrices. The matrix material was typically a poly(styrene-co-n-butyl acrylate) (PBA) latex with a low glass-transition temperature. At low whisker concentrations, the reinforcing effect observed above *Tg* was found to be much higher than predicted for a composite only reinforced with discrete nanofillers by the mechanical composite model of Halpin-Kardos (Figure 3.13).

A percolation model has been used for the interpretation of the reinforcing effect of cellulose nanowhiskers since the high specific surface of whiskers and their numerous hydroxyl groups suggest a possible whisker self-association to form a percolated network through hydrogen bonds[117,135]. The network reinforcing concept was elegantly demonstrated in pioneering studies reported by Favier et al.[31,117]. The percolation model allows the determination of whiskers volume fraction from which

they start to connect one to each other by hydrogen bonds to form a rigid 3D network. This critical value of whisker concentration is defined as percolation threshold. For rod-like nanocrystals the percolation threshold is linked to their aspect ratio. Table 3.4 shows the influence of the aspect ratio of different cellulose whiskers on their percolation threshold[67]. The higher the aspect ratio of cellulose whiskers, the lower the percolation threshold; thus, the percolation threshold for tunicin whiskers with an aspect ratio of about 67 is just 1%, whereas this threshold increases up to 5.9% for cotton whiskers with a lower aspect ratio of 11.8. The formation of this whisker network is responsible for the extraordinary reinforcing effect observed at high temperatures. This percolation approach included in the series-parallel model of Takayanagi was found to fit satisfactory with the experimental data, especially for high filler content.

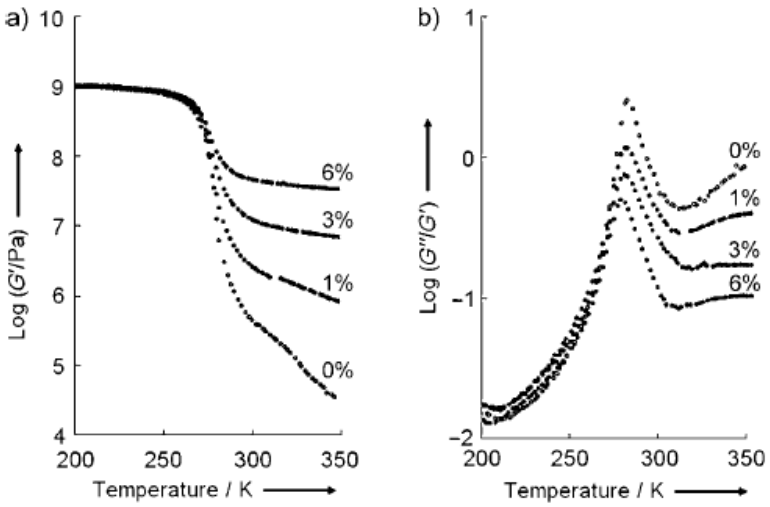

Figure 3.13. a) Evolution of the log of the shear modulus of a whisker reinforced composites for several whisker concentrations. The whiskers are hydrolysed from tunicates; the matrix is PBA latex (35% styrene, 65% butyl acrylate units). b) Plot of log (G´´/G´) against the temperatures in Figure a)[31].

The optimal enhancement of mechanical properties usually occurs at the limit of the percolation threshold, at which just enough reinforcing agent has been added to establish connectivity. A plateau in stiffness is often observed as more filler is added. On the other hand, if the nanowhisker content is too high, the matrix modulus may decrease as a consequence of poor whisker dispersibility and aggregate formation. This effect is observed particularly with whiskers that have a weak affinity for the matrix[128].

The matrix crystallinity is also affected by cellulose nanocrystals, as pointed out by Mathew and Dufresne[136], who reported an increase in the crystallinity of their plasticised starch matrix as the whisker content was increased. The incorporation of cellulose whiskers can lead to nucleation of crystallisation of the polymer matrix near the surface of the whiskers during cooling. This phenomenon known as transcrystallisation, led to an improvement of composite mechanical properties. The water resistance of the film was also affected by the whisker content, thus, at high whisker content (30%), the water uptake by a soy-protein thermoplastic film was reduced by 10%[137]. Dufresne et al.[26] invoked transcrystallisation of a PHA latex by cellulose whisker surfaces to explain the enhanced performance of the composite.

So far, in the nanocomposite field, cellulose whiskers were only used as geometrically and structurally well-defined model cellulosic fillers and no practical industrial application was envisaged. This is mainly ascribed to the duration of the preparation technique, especially in non-hydrosoluble matrices, where the modification of whisker surface is required[36]. Moreover, the surface modification can lead to a detriment of mechanical performance of nanocomposites as a result of disruption of the 3D crystal network. From an environmental point of view, these chemical treatments applied for whisker surface modification will reduce the environmental character associated with cellulose. In addition, cellulose nanowhisker can be considered as an efficient reinforcement since low nanowhisker contents lead to a considerable improvement of nanocomposite mechanical properties, however, which in principle can be taken as an advantage for recycling, it has been

demonstrated that this option is restricted due to the nanowhisker degradation and breakage. In addition, low amount of reinforcement involves higher polymer content, and therefore higher amount of polluter, since the polymer matrix is considered the real polluter of these composites as demonstrated in the previous chapter. The use of biodegradable polymer matrices could be a solution to improve their environmental impact. Therefore, the potential application of nanowhiskers is more related to functional properties such as optical and liquid crystalline properties rather than to their reinforcing capacity (Figure 3.14).

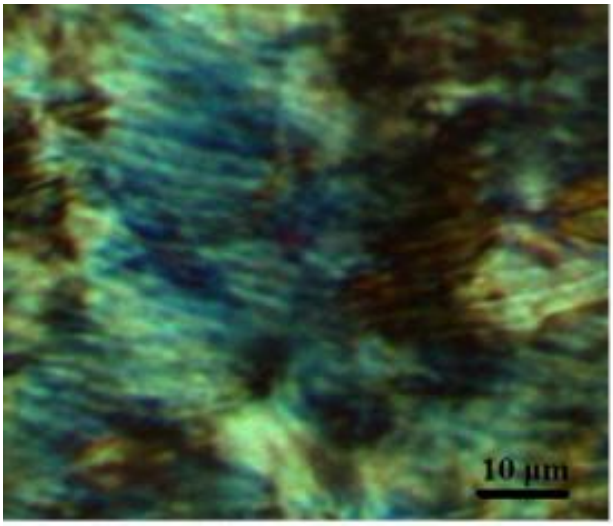

Figure 3.14. Optical micrograph (crossed polarisers) of the chiral nematic structure present in a dry film made of cellulose whiskers grafted with acrylamide[138].

3.2.2 NFC based nanocomposites

An alternative to decrease the polymer content in cellulose based nanocomposites, and thus their environmental impact, consists of increasing nanocellulose content by using NFC. Unlike cellulose whiskers nanocomposites, the production of NFC based nanocomposites with NFC volume fractions as high as 80% is feasible. Unlike cellulose nanocrystals, NFC exhibits both amorphous and

crystalline regions and presents a web-like structure. The reinforcing capability of NFC depends on its purification level and individualisation degree. NFC display similar morphologies but various dimensions depending on the cellulose source and the method used for their preparation. Typical aspect ratios of NFC are estimated in the 100-150 range; a value quite high compared to cellulose nanowhisker. As a consequence of their higher aspect ratio, NFC exhibits superior stress-transfer efficiency to cellulose nanowhiskers.

The first studies on nanocomposites with high cellulose content were published by Nakaigato and Yan[57,139]. A porous network of nanofibrillated cellulose was impregnated by liquid low molar mass polyphenol formaldehyde (PF) precursors and the liquid was polymerised. The resulting material was compressed under high pressure to produce high-strength cellulose nanocomposites. The flexural strength of these nanocomposites determined by three point bending test, was as high as 370 MPa[139]. This study was also designed to clarify how the degree of fibrillation of pulp fibres affects the mechanical properties of cellulose composites. It was found that surface fibrillation is not as effective in improving composite strength as complete fibre fibrillation[57]. More recently, the same authors used aqueous sodium hydroxide-treated NFC and phenolic resin to produce nanocomposites[140]. The tensile properties of NFC-resin nanocomposites were compared with those of wood pulp-resin composites and it was shown that the tensile strength of the NFC composites was significantly higher than that of the pulp composites, regardless of the treatment or resin content. In contrast, the Young's modulus values were practically the same. The advantage of cellulose based nanocomposites over cellulose microcomposites in terms of strength and ductility was also reported by these authors. Nanocomposite films of NFC and melamine formaldehyde (MF) resin were produced by Henriksson and Berglund[59]. The resulting nanocomposites showed average Young's moduli in tension as high as 16.6 GPa and average tensile strength as high as 142 MPa. The combination of these tensile properties with their high mechanical damping, makes these nanocomposites suitable for the production of loudspeaker membranes.

Besides the good mechanical performance, NFC combined with transparent resins lead to optical transparent nanocomposites since NFC does not scatter the light scattering as a consequence of its small dimensions, which is less than one-tenth of the wavelength of visible light. High composite transparency is required for some applications in the optoelectronics industry. Iwamoto et al.[58,61] reported that NFC-reinforced acrylic resin retains its transparency even at fibre contents as high as 70 wt.% because of the size of the nanofibres. By reducing the average fibre size (d ~15 nm) Abe et al.[141] reported the fabrication of optical transparent NFC-epoxy resin nanocomposites with high thermal conductivity and low thermal expansion. The average transmittance of this nanocomposite based on a NFC content of 58 wt.%, was 80% (400-800 nm) (Figure 3.15). The in-plane thermal conductivity of the nanocomposite was over 1.0 $W.m^{-1}$. The low thermal expansion (CTE) of these nanocomposites is attributed to the introduction of cellulose nanofibres since another useful feature of these fibres is their low CTE. NFC coefficient of thermal expansion[142] is comparable with that of quartz glass and its value can be as low as 0.1 $ppmK^{-1}$. An improvement in CTE of the nanofibres can be achieved by keeping the fibres in water-swollen state before disintegration into nanofibres.

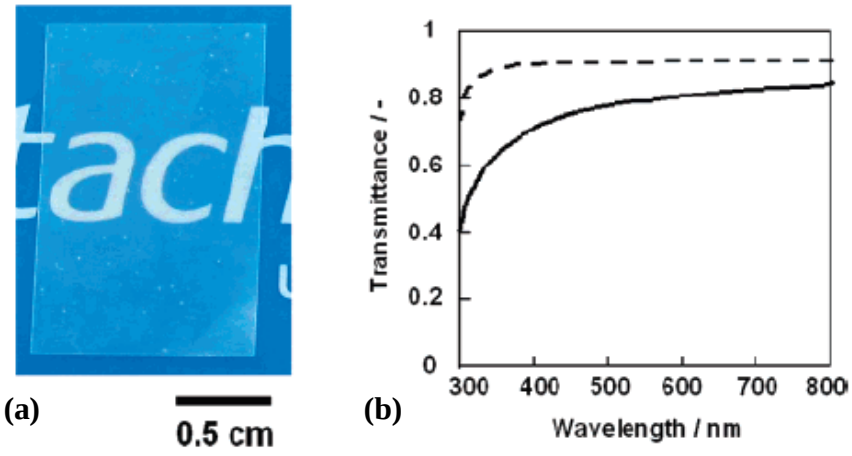

Figure 3.15. (a) Photograph of cellulose nanofibre/epoxy resin nanocomposite. (b) Transmission spectra of nanofibre/epoxy resin nanocomposite (solid line) and epoxy resin without nanofibres (dashed line)[141].

Following this pioneering work on never-dried pulp, Iwamoto et al.[143] studied the effect of hemicellulose on the nanofibrillation and mechanical properties of nanofibre reinforced composites, and reported that hemicelluloses hinder the coalescence of cellulose nanofibres (nanofibril bundles) during drying, and facilitate the nanofibrillation of once-dried pulp. Furthermore, hemicelluloses provide adhesion between nanofibres, contributing to the reduction of thermal expansion and enhancement of mechanical properties of the composites.

All these NFC composites prepared by impregnation with thermosetting resins showed high mechanical strength and stiffness but also brittle behaviour. For applications where ductility and toughness are required, more ductile polymer matrices should be used.

The low CTE combined with high strength and modulus make cellulose nanofibres a potential reinforcing material for roll-to-roll technologies (e.g., for fabricating flexible displays, solar cells, electronic paper, panel sensors and actuators). Recently, Okahisa et al.[144] reported the fabrication of an optical transparent nanocomposite with very low CTE while having high flexibility and ductile properties. This nanocomposite, consisting of a low Young´s modulus resin matrix reinforced with NFC, was used as substrate to deposit an organic light-emitting diode (OLED) layer to demonstrate their potential application as displays (Figure 3.16).

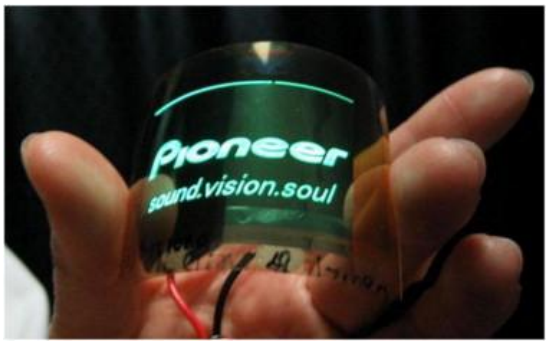

Figure 3.16. Luminescence of an organic light-emitting diode deposited onto a flexible, low-CTE and optically transparent wood–cellulose nanocomposite[144].

The production of biodegradable bio-nanocomposites is also feasible through a combination of NFC with biopolymers. Casting from aqueous solutions with starches, poy(vinyl alcohol) or hydroxypropyl cellulose is straightforward and always yields good reinforcing effects.

If high fraction of nanofibres is thoroughly dispersed in a highly plasticised starch matrix, the resulting biodegradable nanocomposite shows an attractive combination of strength, modulus, and work-to-fracture. It is worth highlighting the work carried by Svagan et al.[90] where homogeneous films with a NFC content in the range of 10-70 wt.% in a matrix of 50/50 amylopectin-glycerol blend were successfully produced. As the NFC content increases, the Young's modulus and the strength both increase while the strain-to-failure decreases. However, even at 70 wt.% of NFC reinforcement, the nanocomposite showed a modulus of 6.2 GPa, a tensile strength as high as 160 MPa, and a strain-to-failure of 8.1% (Figure 3.17). The work of fracture was as high as 9.4 MJ/m^3. This unique combination of strength and strain-to-failure in a viscous matrix composite is ascribed to the nanoscale network structure of the NFC.

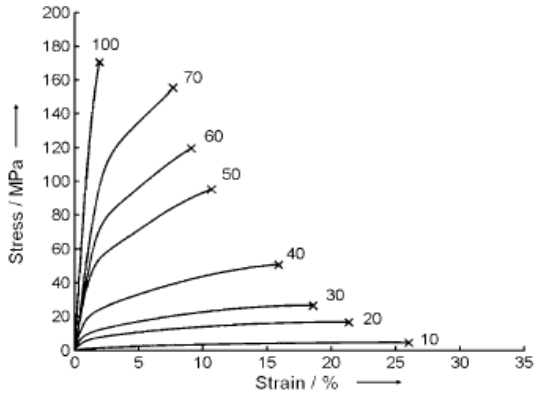

Figure 3.17. Stress-strain curves for a starch/glycerol (1/1) matrix reinforced with different wood-based NFC wt.% fractions[90].

Different processing approaches have been examined to address the critical problem of achieving a good dispersion of hydrophilic cellulose nanofibres in the hydrophobic polylactide (PLA) matrix. Iwatake et al.[145] dispersed NFC in excess acetone and mixed with a fully amorphous grade PLA dissolved in the same solvent. After evaporation of acetone, the mixture was compounded by a kneader, and thin films were obtained by compression moulding of the kneaded compounds. A 10 wt.% NFC load resulted in a modulus increase of 40% and strength gains of 25% over the neat PLA without a reduction in yield strain. Later, the method was extended to a semicrystalline grade of PLA[146] improving tensile modulus and strength in both amorphous and crystallised states, and also enhancing the heat resistance (storage modulus at high temperature), which was not possible with the fully amorphous PLA grade. Recently, Nakagaito et al.[60] established a straightforward process to produce NFC/PLA nanocomposites by compression moulding of sheets made of homogenously dispersed NFC and PLA fibres. The method similar to papermaking allowed good dispersions even at high NFC contents up to 90 wt.% and as a result the mechanical properties of the composites increase linearly as a function of NFC content. The modulus and strength was tripled as the NFC content increased from 10 to 70 wt.%. This method is quite simple with potential implementation at an industrial scale. Mathew et al.[147] used another method whereby nanofibres were added to a PLA melt in a twin-screw extrusion. The processing was complicated by a steam-removal problem, which was eventually solved; however, the reinforcement effect was negative, a result attributed to poor dispersion of the nanofibres[23,52]. Another approach to prepare NFC/PLA bio-nanocomposites is by using PLA in latex form. Following this approach, Larsson et al.[94] produced NFC/PLA nanocomposites with high cellulose content by using a wet mixing technique for a good dispersion of the components, followed by filtration and hot-pressing. The mechanical properties of bio-nanocomposites were improved even at high NFC content. A linear increase of strength, Young´s modulus and strain at break with NFC content was observed.

A more environmental way to produce 100% NFC based materials where no solvents and surface treatments are required due to the lack of polymer matrix is through casting or vacuum filtration of aqueous NFC dispersions obtained from natural fibre disintegration[66,139]. The processing method leads to NFC films where the intrinsic extraordinary mechanical performance of the hydrogen bonded NFC network is shown. When water is removed from NFC dispersions, strong interfibril interactions lead to the formation of porous films, known as cellulose nanopaper for its structural analogy to conventional paper. The nanopaper is a fibrous hydrogen bonded network as occurs in conventional paper but at nanometer level. Despite a porosity of 28%, the nanopaper[66] exhibited interesting mechanical properties including 214 MPa for tensile strength, high modulus (13.2 GPa) and work to facture (15 MJ/m^3). As a consequence of a nanofibre slippage mechanism, the strain to failure was unexpectedly high. The superior mechanical performance compared to conventional paper lies in higher fibril strength, more favourable interfibril adhesion properties, and much smaller and more homogenously distributed defects. The mechanical properties of the nanopaper were correlated with the viscosity average molar mass M_v of nanofibrils, which demonstrated the importance of using methods for the preparation of NFC that preserves the DP of cellulose. Saito et al.[84] recently reported higher strengths (310 MPa), similar strain to failure and lower modulus for another nanopaper system. For comparative purposes, typical strain to failure values for conventional high-strength papers are 3-4%, rather than 10% achievable with nanopaper. Optically transparent nanopaper (Figure 3.18) was achieved by careful polishing with an emery paper the nanopaper surface[148]. Once the surface roughness was minimalised, its transparency at a 600 nm wavelength reached 71.6%. The resulting nanopaper presents fascinating properties such as transparency (71.6%), high modulus (13 GPa) and strength (223 MPa) and minimal thermal expansion (8.5 $ppmK^{-1}$) and high foldability. The density of this nanopaper was 1.53 g/cm^3, which is close to the 1.59 g/cm^3 of a cellulose crystallite, indicating that small interfibrillar cavities were practically eliminated. The foldable, low CTE, and optically transparent nanopaper could be a perfect match as substrates for continuous roll-to-roll processing. Further studies consisted of coating the nanopaper with transparent

resins to smooth the surface, which demonstrated the potential to produce transparent materials by simple cost-effective processes and suggested the possibility of continuous roll-to-roll manufacturing methods.

Figure 3.18. Foldable optically transparent nanopaper[148].

All these nanopapers present a random-in-plane orientation, and therefore a limited mechanical performance. In order to fully exploit the mechanical potential of native cellulose nanofibrils, optically transparent nanopaper with preferred orientation of NFC has been recently prepared by cold drawing[149]. As expected, the mechanical properties of highly oriented nanopaper were much higher than those of isotropic nanopaper.

NFC is also applied to other kind of materials such as foams and aerogels. Aerogels are a class of material where the liquid phase of a gel is removed without substantial shrinkage. The NFC gels obtained from the deconstruction of natural fibres exhibit a 2 orders of magnitude higher storage modulus than those of cellulose nanocrystals. This difference is ascribed to entangled networks formed by long nanofibrils in NFC. These strong hydrogels allow the formation of highly porous

aerogels by direct water removal through freeze-drying, as demonstrated by Pääkkö[87]. Unlike in typical aerogel preparations, neither crosslinking or solvent exchange or supercritical dry is required to suppress the collapse during the aerogel preparation, reducing processing costs. The aerogels show high porosity (98%), very low density (~0.02 $g.cm^{-3}$) and high compressive strain (70%). For the first time, this method allowed the production of aerogels consisting of cellulose I. Until then, cellulose based aerogels have been obtained from regenerated cellulose (cellulose II). In this study, electrically conducting flexible aerogels were also produced by dipping the aerogels in an electrically conducting polyaniline–surfactant solution. Sehaqui et al.[93] prepared low-density aerogels based on NFC by tert-butanol freeze-drying. The ‘‘effective’’ diameter of the NFC nanofibres in the aerogels was around 10–18 nm corresponding to specific surface areas as high as 153–284 $m^2 \cdot g^{-1}$. These aerogels exhibited a ductile behaviour and high compressive strain, however their modulus and compression strength were lower than those of cellular NFC. They concluded that tert-butanol freeze-drying can be used to create ‘‘soft’’ aerogels. Recently, Zhang et al.[150] reported the production of chemically crosslinked aerogels by the addition of crosslinkers. The aerogels showed superabsorbent properties. They also found that the crosslinked aerogel exhibited fast shape recovery properties upon contact with water. The aerogel recovered more than 98% of their original shape in less than 10 s by immersing in water. Using this type of aerogel, new materials with different functionalities such as highly flexible magnetic aerogels and superhydrophobic foams, etc. have been prepared in recent years.

Biofoams based only on biological polymers are interesting as an alternative to petroleum-based polymer foams. Efforts are being made to use starch-based foams for packaging applications as a replacement for polystyrene based foams; however, starch is brittle without a plasticiser, and its mechanical properties are sensitive to moisture. Svagan et al.[90] have shown that through the use of a freeze-drying technique, NFC can reinforce starch foams. The advantage of using NFC instead of conventional wood-based pulp fibres is that the nanosized fibrils enable reinforcement of the thin cell walls in the starch foam; the larger dimensions of

wood-based fibres make them much less suitable for structural reinforcement. In contrast, freeze-dried starch biofoams show the potential of cellulose nanofibre. The energy absorption, which is estimated as the area under the stress-strain curve, is more than doubled as 40 wt.% of NFC are added. This is highly relevant for packaging application. The foam structure of a starch/glycerol/NFC composite is shown in Figure 3.19.

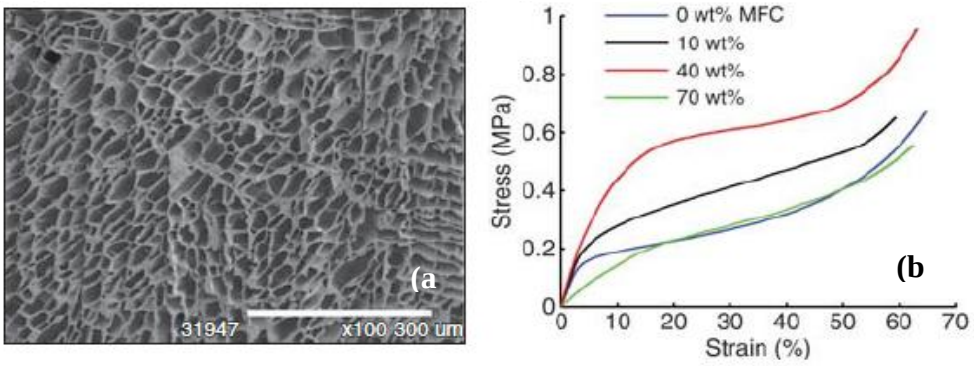

Figure 3.19. Bioinspired starch/cellulose nanofibre biofoams[90]. (a) Microcellular structure where the scale bar is 300 microns; (b) compressive stress-strain curves showing strong improvement in energy absorption (area under stress-strain curve) with NFC addition.

In conclusion, NFC can have a reinforcing role in composites for many applications, but processing can be considered a key issue that needs to be addressed for their production at an industrial scale.

.

3.2.3 BC based nanocomposites

Bacterial cellulose exhibits a strong network structure based on high-modulus cellulose ribbons that are less than 100 nm wide and are made of microfibrils 2–4 nm in diameter. BC is more ordered than standard cellulose and this order and lack of irregularities are responsible for their impressive properties such as a high Young´s

modulus of around 130-140 GPa, a tensile strength of 2 GPa and a thermal expansion of only $0.1x10^{-6}$ K^{-1} [35]. Moreover, since these fibres are almost pure cellulose and their dimensions are already in the nanometer scale, BC can be directly applied after simply purification, without further processing. Due to these properties, BC has been considered as an attractive reinforcement in nanocomposite materials.

The preparation of BC composites leads to a great variety of products. Composites can be formed by in situ modification of BC, that is, by the addition of the matrix to the culture medium, or by post-processing of BC synthesised conventionally. Typical composite partners are organic compounds, such as bioactive agents and polymerisable monomers, polymers, such as polyacrylates, resins, polysaccharides, and proteins, as well as inorganic substances, such as metals and metal oxides[23]. A characteristic example of post-processing of BC is the preparation of optically transparent nanocomposites by reinforcing transparent resins with BC. In 2005, Yano et al.[98] reported the first example of optically transparent cellulose nanocomposites at a BC content as high as 70 wt.%, with a mechanical strength about five times that of engineered plastics and a coefficient of thermal expansion similar to that of a single crystal of silicon. The nanocomposites were prepared by impregnation of dried BC sheets with resins followed by either curing process or by hot-pressing, depending on the resin employed. The light transmittance measured for BC/epoxy nanocomposite in the wavelength interval between 500 to 800 nm exceeded 80%. The reduction of light transmission because of the BC incorporation was less than 10%, compared to neat epoxy resin. Unlike conventional composites, the composite transparency does not depend on matching the refractive indexes of matrix and reinforcement, since the matrix transparency is preserved when reinforced with nanosized fibres. The addition of BC into the epoxy matrix involved a considerable decrease of the CTE, reaching a value of just $6x10^{-6}$ K^{-1}. An electroluminescent layer was successfully deposited on this transparent BC nanocomposite, as shown in Figure 3.20. However, the final nanocomposite was not flexible enough for roll-to-roll processing due to its high modulus of 21 GPa.

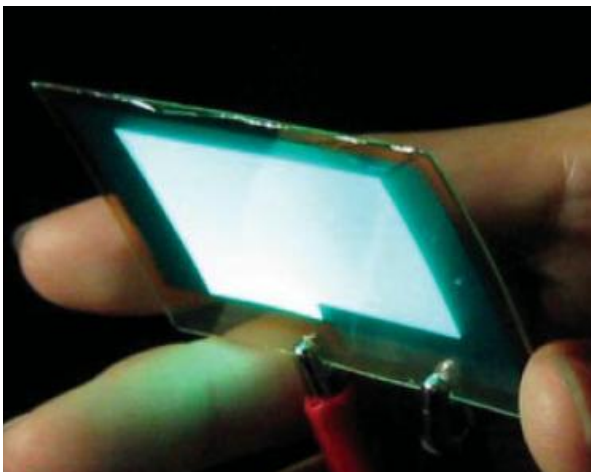

Figure 3.20. Luminiscence of an OLED deposited onto a transparent BC nanocomposite[151].

In 2008, the same authors developed a foldable and ultralow-CTE (4 ppm.K^{-1}) transparent nanocomposite[151]. Foldable properties and high thermal stability were achieved by reinforcing a low-Young's modulus transparent acrylic resin with just 5 wt.% of BC. The resulting nanocomposite was not only flexible but even foldable due to its low modulus of 335 MPa (Figure 3.21).

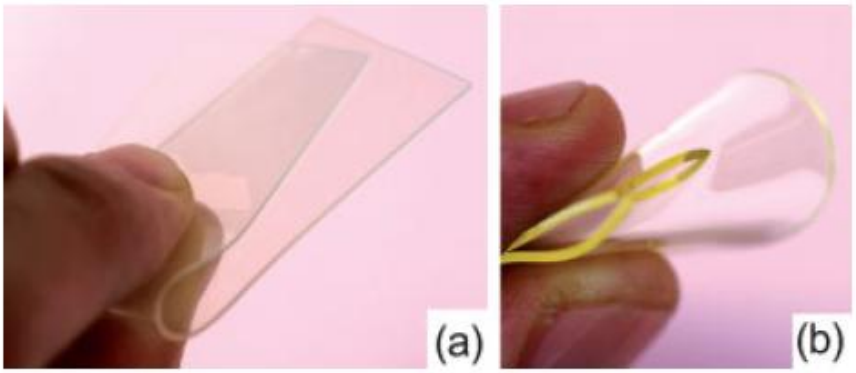

Figure 3.21. a) Foldable transparent BC nanocomposite. b) The more fragile neat acrylic resin sheet of the same thickness[151]

Jung et al.[152] prepared an electrically conductive transparent nanocomposite by depositing multiwalled carbon nanotubes (MWCNTs) on a composite made of BC and silk fibroin. BC membranes served as a template to uniformly disperse the MWCNTs. The transparent nanocomposite with 0.02 wt.% of MWCNT showed remarkable flexibility without any loss of its initial properties. Conductivity measurements demonstrated that the incorporation of carbon nanotubes is a suitable way to prepare electrically conductive BC membranes.

The growing trend towards the use of biodegradable polymers for the production of biocomposites is also present in nanomaterials. Thus, optically transparent bionanocomposite consisting of BC, were prepared by adding dried BC pellicle into a poly(l-lactic acid) (PLA) matrix. In spite of the incorporation of an opaque bacterial cellulose pellicle, the light transmission of the nanocomposite was quite high due to the size effect of the nanofibrillar BC. The addition of BC led to a partial crystallisation of PLA and an improvement of its mechanical performance. The tensile strength and Young's modulus of the BC/PLA nanocomposite was increased by 203% and 146%, respectively, compared with those of the PLA. The combination of good mechanical properties with transparency and biocompatibility make this nanocomposite suitable for applications such as medical devices and food packaging[153]. BC has recently been incorporated in hydroxyapatite (HAp)[154,155], poly(vinyl alcohol) (PVA)[156], cellulose acetate butyrate (CAB)[157] and also as a hybrid material in apple and radish pulp[158].

In a similar fashion to all-cellulose nanocomposites based on cellulose whiskers[159], the production of fully recyclable BC bio-nanocomposites has been recently reported by using the surface selective dissolution method[160]. Nanocomposites showed nearly twice the tensile strength of microcomposites, while similar high values of work-to-fracture compared to all-cellulose nanocomposites based on cellulose whiskers and nanopaper. It is worth highlighting the high strength observed for BC sheet itself, due to the extensive hydrogen bonded network formed

by high modulus nano-size cellulose ribbons. In fact, the mechanical performance of BC sheet is superior to that of many nanocomposites reported today.

The activity of the BC nanofibres as nanotemplates for the formation and fixation of different types of nanoparticles is of fundamental significance. The treatment of BC fleeces with titanium tetraisopropoxide ($Ti(O\textit{i}Pr)_4$), followed by its hydrolysis, resulted in titania-coated BC fibres. Upon removal of the BC by heating up to 500°C, TiO_2 nanotubes were obtained. In this case, the BC nanofibres acted as a support for titania and as a precursor[161]. The treatment of BC fleeces with aqueous silver nitrate and subsequent reduction with $NaBH_4$ dissolved in water resulted in the precipitation of silver as nanoparticles on the BC fibres. The freeze-dried silver-nanoparticle-impregnated bacterial cellulose exhibited strong antimicrobial activity against Escherichia coli (Gram-negative) and Staphylococcus aureus (Gram-positive)[162].

Alternative to conventional composite processing, BC nanocomposites can be performed in situ by the direct addition of the composite compounds into the culture medium. Thus, the incorporation of nanosilica to the culture medium led to BC/nanosilica nanocomposites[163]. For medical purposes such as healing of wounds, ulcers and burns, chitosan was incorporated into the culture medium to produce BC/chitosan nanocomposites[164]. Carboxymethylated-bacterial cellulose, as copper and lead ion removal membrane, has been obtained by adding the water-soluble carboxymethylated cellulose directly into the culture medium[165]. BC was also grown in the presence of potato and corn starch, and poly(vinyl alcohol) (PVA). The presence of PVA can influence the in-situ growth of BC through the formation of spherulites. Seifert et al.[104] found that the addition of cellulose derivatives and PVA into the culture medium gave place to biocomposites with better water retention and ion absorption. Recently, Gea et al.[166] reported a comparative study of the properties of BC/PVA nanocomposites prepared either in-situ or by impregnation of BC gels with a PVA solution. The in-situ growth technique resulted in a BC/PVA nanocomposites with a better combination of mechanical and optical properties due

to a more homogeneous microstructure while, at the same time, avoiding a subsequent impregnation process for the fabrication of the composite.

An important goal for cellulose nanocomposites is nanostructural control. Recently, Zhou et al.[167] introduced a hygroscopic cellulose derivative (hydroxyethyl cellulose (HEC)) in the water-based culture during bacterial cellulose biosynthesis. The HEC was adsorbed by the cellulose microfibrils during biosynthesis, so that each microfibril in the suspension was coated by HEC. Vigorous mechanical mixing was used, and a stable suspension of well-dispersed HEC-coated nanofibres was obtained. Compared with nanopaper, or a physical blend of HEC, the tensile strength of resulting random-in-plane nanocomposites was much improved and approached 300 MPa, due to the nanostructured morphology of the bionanocomposite where each nanofibre is compartmentalised by a thin matrix layer coating, similar to many biological composites, such as the wood cell wall. This suggests a new nanostructured concept for cellulose composites. Recently, this compartmentalisation approach has been applied for the production of wood NFC/HEC nanocomposites[95]. This bionanocomposite showed a unique combination of low yield stress, high ultimate strength, high toughness, thermomechanical stability, limited moisture absorption and high creep resistance as a result of the nanostructure characteristics of a cellulose nanofibre network coated by a ductile HEC coating.

As demonstrated BC has been applied for reinforcement of a great variety of polymers, due to its extraordinary characteristics, however the fermentation processes employed for its production are costly and the industrial scale production of BC for technical applications is so far not established. So far applications of bacterial cellulose have been mainly focused on medical purposes, such as the use of a cellulosic “scaffold” to direct the growth of tissue or bone and as a support for cell immobilisation[23,168,169].

3.3 References

[1] M. J. John and S. Thomas, Carbohydrate Polymers 71 (3), 343 **(2008)**.

[2] G. Bogoeva-Gaceva, M. Avella, M. Malinconico, A. Buzarovska, A. Grozdanov, G. Gentile, and M. E. Errico, Polymer Composites 28 (1), 98 **(2007)**.

[3] A. K. Mohanty, M. Misra, and G. Hinrichsen, Macromolecular Materials and Engineering 276-277 (1), 1 **(2000)**.

[4] S. Kamel, Express Polymer Letters 1 (9), 546 **(2007)**.

[5] D. Klemm, Schmauder, H., Heinze, T., *Cellulose*, in *Biopolymers*, A. Steinbüchel, Editor. Weinheim Wiley-VCH 6, 275-285, **(2003)**

[6] V. I. Kovalenko, Russian Chemical Reviews 79 (3), 231 **(2010)**.

[7] G. C. Davies and D. M. Bruce, Textile Research Journal 68 (9), 623 **(1998)**.

[8] A. Sturcova, G. R. Davies, and S. J. Eichhorn, Biomacromolecules 6 (2), 1055 **(2005)**.

[9] Y. C. Hsieh, H. Yano, M. Nogi, and S. J. Eichhorn, Cellulose 15 (4), 507 **(2008)**.

[10] I. Sakurada, Y. Nukushina, and T. Ito, Journal of Polymer Science 57 (165), 651 **(1962)**.

[11] T. Nishino, K. Takano, and K. Nakamae, Journal of Polymer Science Part B-Polymer Physics 33 (11), 1647 **(1995)**.

[12] M. Matsuo, C. Sawatari, Y. Iwai, and F. Ozaki, Macromolecules 23 (13), 3266 **(1990)**.

[13] K. Tashiro and M. Kobayashi, Polymer 32 (8), 1516 **(1991)**.

[14] R. J. Marhofer, S. Reiling, and J. Brickmann, Berichte Der Bunsen-Gesellschaft-Physical Chemistry Chemical Physics 100 (8), 1350 **(1996)**.

[15] S. J. Eichhorn and G. R. Davies, Cellulose 13 (3), 291 **(2006)**.

[16] S. J. Eichhorn, A. Dufresne, M. Aranguren, N. E. Marcovich, J. R. Copadona, S. J. Rowan, C. Weder, W. Thielemans, M. Roman, S. Renneckar, W. Gindl, S. Veigel, J. Keckes, H. Yano, K. Abe, M. Nogi, A. N. Nakagaito, A. Mangalam, J. Simonsen, A. S. Benight, A. Bismarck, L. A. Berglund, and T. Peijs., Journal of Materials Science 45 (1), 1 **(2009)**.

[17] S. K. Garkhail, R. W. H. Heijenrath, and T. Peijs, Applied Composite Materials 7 (5-6), 351 **(2000)**.

[18] M. J. A. van den Oever and H. L. Bos, Advanced Composites Letters 7 (3), 81 **(1998)**.

[19] J. Andersons, E. Sparnins, R. Joffe, and L. Wallstrom, Composites Science and Technology 65 (3-4), 693 **(2005)**.

[20] S. Garkhail, B. Wieland, J. George, N. Soykeabkaew, and T. Peijs, Journal of Materials Science 44 (2), 510 **(2009)**.

[21] T. Saito, R. Kuramae, J. Wohlert, L. A. Berglund, and A. Isogai, Biomacromolecules 14 (1), 248 **(2013)**.

[22] A. Kaushik and M. Singh, Carbohydrate Research 346 (1), 76 **(2011)**.

[23] D. Klemm, F. Kramer, S. Moritz, T. Lindstrom, M. Ankerfors, D. Gray, and A. Dorris, Angewandte Chemie-International Edition 50 (24), 5438 **(2011)**.

[24] B. G. Rånby and R. W. Noe, Journal of Polymer Science 51 (155), 337 **(1961)**.

[25] P. Terech, L. Chazeau, and J. Y. Cavaille, Macromolecules 32 (6), 1872 **(1999)**.

[26] A. Dufresne, M. B. Kellerhals, and B. Witholt, Macromolecules 32 (22), 7396 **(1999)**.

[27] X. M. Dong, T. Kimura, J.-F. o. Revol, and D. G. Gray, Langmuir 12 (8), 2076 **(1996)**.

[28] J. Araki, M. Wada, S. Kuga, and T. Okano, Colloids and Surfaces A: Physicochemical and Engineering Aspects 142 (1), 75 **(1998)**.

[29] Y. Chen, C. Liu, P. R. Chang, X. Cao, and D. P. Anderson, Carbohydrate Polymers 76 (4), 607 **(2009)**.

[30] J. Araki, M. Wada, S. Kuga, and T. Okano, Journal of Wood Science 45 (3), 258 **(1999)**.

[31] V. Favier, G. R. Canova, J. Y. Cavaillé, H. Chanzy, A. Dufresne, and C. Gauthier, Polymers for Advanced Technologies 6 (5), 351 **(1995)**.

[32] M. Martínez-Sanz, A. Lopez-Rubio, and J. M. Lagaron, Carbohydrate Polymers 85 (1), 228 **(2011)**.

[33] J. F. Revol, Carbohydrate Polymers 2 (2), 123 **(1982)**.

[34] J. Bras, D. Viet, C. Bruzzese, and A. Dufresne, Carbohydrate Polymers 84 (1), **(2011)**.

[35] D. J. Gardner, G. S. Oporto, R. Mills, and M. Samir, Journal of Adhesion Science and Technology 22 (5-6), 545 **(2008)**.

[36] M. A. S. Azizi Samir, F. Alloin, and A. Dufresne, Biomacromolecules 6 (2), 612 **(2005)**.

[37] X. Dong, J.-F. Revol, and D. Gray, Cellulose 5 (1), 19 **(1998)**.

[38] S. Beck-Candanedo, M. Roman, and D. G. Gray, Biomacromolecules 6 (2), 1048 **(2005)**.

[39] D. Bondeson, A. Mathew, and K. Oksman, Cellulose 13 (2), 171 **(2006)**.

[40] M. F. Rosa, E. S. Medeiros, J. A. Malmonge, K. S. Gregorski, D. F. Wood, L. H. C. Mattoso, G. Glenn, W. J. Orts, and S. H. Imam, Carbohydrate Polymers 81 (1), 83 **(2010)**.

[41] H. Kargarzadeh, I. Ahmad, I. Abdullah, A. Dufresne, S. Y. Zainudin, and R. M. Sheltami, Cellulose 19 (3), 855 **(2012)**.

[42] A. Isogai and Y. Kato, Cellulose 5 (3), 153 **(1998)**.

[43] J. Araki, M. Wada, and S. Kuga, Langmuir 17 (1), 21 **(2001)**.

[44] R. H. Marchessault, F. F. Morehead, and N. M. Walter, Nature 184, 632 **(1959)**.

[45] J. F. Revol, H. Bradford, J. Giasson, R. H. Marchessault, and D. G. Gray, Int. J. Biol. Macromol. 14 (3), 170 **(1992)**.

[46] J. Sugiyama, H. Chanzy, and G. Maret, Macromolecules 25 (16), 4232 **(1992)**.

[47] N. Lavoine, I. Desloges, A. Dufresne, and J. Bras, Carbohydrate Polymers 90 (2), 735 **(2012)**.

[48] A. F. Turbak, F. W. Synder, and K. R. Sandberg, Journal of Applied Polymer Science. Applied polymer symposium. 37 **(1983)**.

[49] K. L. Spence, R. A. Venditti, O. J. Rojas, Y. Habibi, and J. J. Pawlak, Cellulose 18 (4), 1097 **(2011)**.

[50] E. Dinand, H. Chanzy, and M. R. Vignon, Cellulose 3 (1), 183 **(1996)**.

[51] L. Heux, E. Dinand, and M. R. Vignon, Carbohydrate Polymers 40 (2), 115 **(1999)**.

[52] I. Siro and D. Plackett, Cellulose 17 (3), 459 **(2010)**.

[53] A. Alemdar and M. Sain, Bioresource Technology 99 (6), 1664 **(2008)**.

[54] G. Siqueira, J. Bras, and A. Dufresne, Biomacromolecules 10 (2), 425 **(2009)**.

[55] M. Hassan, A. Mathew, E. Hassan, N. El-Wakil, and K. Oksman, Wood Science and Technology 46 (1-3), 193 **(2012)**.

[56] A. Bendahou, H. Kaddami, and A. Dufresne, European Polymer Journal 46 (4), 609

[57] A. N. Nakagaito and H. Yano, Applied Physics a-Materials Science and Processing 78 (4), 547 **(2004)**.

[58] S. Iwamoto, A. N. Nakagaito, and H. Yano, Applied Physics A 89 (2), 461 **(2007)**.

[59] M. Henriksson and L. A. Berglund, Journal of Applied Polymer Science 106 (4), 2817 **(2007)**.

[60] A. N. Nakagaito, A. Fujimura, T. Sakai, Y. Hama, and H. Yano, Composites Science and Technology 69 (7-8), 1293 **(2009)**.

[61] S. Iwamoto, A. N. Nakagaito, H. Yano, and M. Nogi, Applied Physics A 81 (6), 1109 **(2005)**.

[62] M. E. Malainine, M. Mahrouz, and A. Dufresne, Composites Science and Technology 65 (10), 1520 **(2005)**.

[63] M. Andresen, L.-S. Johansson, B. r. S. Tanem, and P. Stenius, Cellulose 13 (6), 665 **(2006)**.

[64] K. Syverud and P. Stenius, Cellulose 16 (1), 75 **(2009)**.

[65] P. Stenstad, M. Andresen, B. r. Tanem, and P. Stenius, Cellulose 15 (1), 35 **(2008)**.

[66] M. Henriksson, L. A. Berglund, P. Isaksson, T. Lindstrom, and T. Nishino, Biomacromolecules 9 (6), 1579 **(2008)**.

[67] G. Siqueira, J. Bras, and A. Dufresne, Polymers 2 (4), 728 **(2010)**.

[68] T. Zimmermann, E. Pöhler, and T. Geiger, Advanced Engineering Materials 6 (9), 754 **(2004)**.

[69] A. López-Rubio, J. M. Lagaron, M. Ankerfors, T. Lindstrom, D. Nordqvist, A. Mattozzi, and M. S. Hedenqvist, Carbohydrate Polymers 68 (4), 718 **(2007)**.

[70] C. Aulin, S. Ahola, P. Josefsson, T. Nishino, Y. Hirose, M. Osterberg, and L. Wagberg, Langmuir 25 (13), 7675 **(2009)**.

[71] K. Abe, S. Iwamoto, and H. Yano, Biomacromolecules 8 (10), 3276 **(2007)**.

[72] T. Taniguchi and K. Okamura, Polymer International 47 291 **(1998)**.

[73] A. Dufresne, J. Y. Cavaille, and M. R. Vignon, Journal of Applied Polymer Science 64, **(1997)**.

[74] A. Chakraborty, M. Sain, and M. Kortschot, Holzforschung 59, 102 **(2005)**.

[75] B. Wang and M. Sain, Composites Science and Technology 67 (11-12), 2521 **(2007)**.

[76] A. Bhatnagar and M. Sain, Journal of Reinforced Plastics and Composites. 24, 1259 **(2005)**.

[77] T. Saito, Y. Nishiyama, J. L. Putaux, M. Vignon, and A. Isogai, Biomacromolecules 7 (6), 1687 **(2006)**.

[78] A. Isogai, T. Saito, and H. Fukuzumi, Nanoscale 3 (1), 71 **(2011)**.

[79] T. Saito, I. Shibata, A. Isogai, N. Suguri, and N. Sumikawa, Carbohydrate Polymers 61 (4), 414 **(2005)**.

[80] T. Saito, Y. Okita, T. T. Nge, J. Sugiyama, and A. Isogai, Carbohydrate Polymers 65 (4), 435 **(2006)**.

[81] T. Saito, S. Kimura, Y. Nishiyama, and A. Isogai, Biomacromolecules 8 (8), 2485 **(2007)**.

[82] M. Hirota, N. Tamura, T. Saito, and A. Isogai, Cellulose 16 (5), 841 **(2009)**.

[83] M. Hirota, N. Tamura, T. Saito, and A. Isogai, Carbohydrate Polymers 78 (2), 330 **(2009)**.

[84] T. Saito, M. Hirota, N. Tamura, S. Kimura, H. Fukuzumi, L. Heux, and A. Isogai, Biomacromolecules 10 (7), 1992 **(2009)**.

[85] T. Isogai, T. Saito, and A. Isogai, Cellulose 18 (2), 421 **(2011)**.

[86] T. Taipale, M. Osterberg, A. Nykanen, J. Ruokolainen, and J. Laine, Cellulose 17 (5), 1005201 **(2010)**.

[87] M. Paakko, M. Ankerfors, H. Kosonen, A. Nykanen, S. Ahola, M. sterberg, J. Ruokolainen, J. Laine, P. T. Larsson, O. Ikkala, and T. Lindstrom, Biomacromolecules 8 (6), 1934 **(2007)**.

[88] M. Henriksson, G. Henriksson, L. A. Berglund, and T. Lindstrom, European Polymer Journal 43 (8), 3434 **(2007)**.

[89] H. Sehaqui, A. Liu, Q. Zhou, and L. A. Berglund, Biomacromolecules 11 (9), 2195 **(2010)**.

[90] A. J. Svagan, M. A. S. Azizi Samir, and L. A. Berglund, Biomacromolecules 8 (8), 2556 **(2008)**.

[91] H. Sehaqui, M. Salajkova, Q. Zhou, and L. A. Berglund, Soft Matter 6 (8), 1824 **(2010)**.

[92] M. Paakko, J. Vapaavuori, R. Silvennoinen, H. Kosonen, M. Ankerfors, T. Lindstrom, L. A. Berglund, and O. Ikkala, Soft Matter 4 (12), 2492 **(2008)**.

[93] H. Sehaqui, Q. Zhou, and L. A. Berglund, Composites Science and Technology 71 (13), 1593 **(2011)**.

[94] K. Larsson, L. A. Berglund, M. Ankerfors, and T. Lindström, Journal of Applied Polymer Science 125 (3), 2460 **(2012)**.

[95] H. Sehaqui, Q. Zhou, and L. A. Berglund, Soft Matter 7 (16), 7342 **(2011)**.

[96] G. Nystrom, A. Razaq, M. Stromme, L. Nyholm, and A. Mihranyan, Nano Letters 9 (10), 3635 **(2009)**.

[97] R. Olsson, M. Samir, G. Salazar-Alvarez, L. Belova, V. Strom, L. Berglund, O. Ikkala, J. Nogues, and U. Gedde, Nature Nanotechnology 5 (8), 584 **(2010)**.

[98] H. Yano, J. Sugiyama, A. N. Nakagaito, M. Nogi, T. Matsuura, M. Hikita, and K. Handa, Advanced Materials 17 (2), 153 **(2005)**.

[99] A. N. Nakagaito, S. Iwamoto, and H. Yano, Applied Physics A 80 (1), 93 **(2005)**.

[100] H. El-Saieda, A. H. Bastaa, and R. H. Gobranb, Polymer-Plastics Technology and Engineering 43 (3), 797 **(2004)**.

[101] D. Klemm, D. Schumann, F. Kramer, N. Hessler, M. Hornung, H. P. Schmauder, and S. Marsch, *Nanocelluloses as innovative polymers in research and application*, in *Polysaccharides II*, D. Klemm, Editor. Berlin, Springer-Verlag Berlin 205, 49-96, **(2006)**

[102] P. Gatenholm and D. Klemm, MRS Bulletin 35 (3), 208 **(2010)**.

[103] M. Iguchi, S. Yamanaka, and A. Budhiono, Journal of Materials Science 35 (2), 261 **(2000)**.

[104] M. Seifert, S. Hesse, V. Kabrelian, and D. Klemm, Journal of Polymer Science Part A: Polymer Chemistry 42 (3), 463 **(2004)**.

[105] S. Hesse and T. Kondo, Carbohydrate Polymers 60 (4), 457 **(2005)**.

[106] H. R. Bungay and G. C. Serafica, US-6071727 **(2000)**.

[107] K. Frankenfeld, M. Hornung, B. Lindner, M. Ludwig, A. Muelverstedt, and H. P. Scmauder, DE-10022751 **(2001)**.

[108] N. L. F. Levy, E. C. Kurokawa, and P. A. S. Podlech, WO-2004050986 **(2004)**.

[109] L. F. X. Farah, P. A. S. Podlech, C. D. R. Archanjo, and L. A. Coral, WO-2006066377 **(2006)**.

[110] D. Kralisch, N. Hessler, D. Klemm, R. Erdmann, and W. Schmidt, Biotechnology and Bioengineering 105 (4), 740 **(2010)**.

[111] B. H. D. Klemm, H. P. Fink, and A. Bohn, Angewandte Chemie-International Edition 44 (22), 3358 **(2005)**.

[112] W. Czaja, D. Romanovicz, and R. m. Brown, Cellulose 11 (3-4), 403 **(2004)**.

[113] R. Jonas and L. F. Farah, Polymer Degradation and Stability 59 (1-3), 101 **(1998)**.

[114] L. L. Zhou, D. P. Sun, L. Y. Hu, Y. W. Li, and J. Z. Yang, Journal of Industrial Microbiology and Biotechnology 34 (7), 483 **(2007)**.

[115] J. Halpin and J. Kardos, Polymer engineering and science 16 (5), 344 **(1976)**.

[116] M. A. S. Azizi Samir, F. Alloin, M. Paillet, and A. Dufresne, Macromolecules 37 (11), 4313 **(2004)**.

[117] F. Favier, H. Chanzy, and J. Y. Cavaillé, Macromolecules 28 (18), 6365 **(1995)**.

[118] S. J. Eichhorn and R. J. Young, Cellulose 8 (3), 197 **(2001)**.

[119] D. Dubief, E. Samain, and A. Dufresne, Macromolecules 32 (18), 5765 **(1999)**.

[120] L. Chazeau, J. Y. Cavaille, G. Canova, R. Dendievel, and B. Boutherin, Journal of Applied Polymer Science 71 (11), 1797 **(1999)**.

[121] L. Chazeau, J. Y. Cavaille, and P. Terech, Polymer 40 (19), 5333 **(1999)**.

[122] L. Heux, G. Chauve, and C. Bonini, Langmuir 16 (21), 8210 **(2000)**.

[123] M. Grunert and W. T. Winter, Polymer Materials Science and Engineering 86, 367 **(2002)**.

[124] M. Grunert and W. T. Winter, Journal of Polymers and the Environment 10 (1-2), 27 **(2002)**.

[125] C. Goussé, H. Chanzy, G. r. Excoffier, L. Soubeyrand, and E. Fleury, Polymer 43 (9), 2645 **(2002)**.

[126] H. Yuan, Y. Nishiyama, M. Wada, and S. Kuga, Biomacromolecules 7 (3), 696 **(2006)**.

[127] B. Braun and J. R. Dorgan, Biomacromolecules 10 (2), 334 **(2008)**.

[128] Y. Habibi, A.-L. Goffin, N. Schiltz, E. Duquesne, P. Dubois, and A. Dufresne, Journal of Materials Chemistry 18 (41), 5002 **(2008)**.

[129] K. Gopalan Nair and A. Dufresne, Biomacromolecules 4 (6), **(2003)**.

[130] M. A. S. Azizi Samir, F. Alloin, J. Y. Sanchez, N. El Kissi, and A. Dufresne, Macromolecules 37 (4), 1386 **(2004)**.

[131] P. Hajji, J. Y. Cavaillé, V. Favier, C. Gauthier, and G. Vigier, Polymer Composites 17 (4), 612 **(1996)**.

[132] A. Dufresne, J. Y. Cavaille, and W. Helbert, Polymer Composites 18 (2), 198 **(1997)**.

[133] A. Dufresne, Recent research developments in macromolecular research 3, 455 **(1998)**.

[134] A. Dufresne, Canadian Journal of Chemistry 86 (6), 484 **(2008)**.

[135] V. Favier, J. Y. Cavaille, G. R. Canova, and S. C. Shrivastava, Polymer Engineering and Science 37 (10), 1732 **(1997)**.

[136] A. P. Mathew and A. Dufresne, Biomacromolecules 3 (3), 609 **(2002)**.

[137] Y. Wang, X. Cao, and L. Zhang, Macromolecular Bioscience 6 (7), 524 **(2006)**.

[138] J. Yang and D. Y. Ye, Chinese Chemical Letters 23 (3), 367 **(2012)**.

[139] A. N. Nakagaito and H. Yano, Applied Physics A 80 (1), 155 **(2005)**.

[140] A. Nakagaito and H. Yano, Cellulose 15 (2), 323 **(2008)**.

[141] Y. Shimazaki, Y. Miyazaki, Y. Takezawa, M. Nogi, K. Abe, S. Ifuku, and H. Yano, Biomacromolecules 8 (9), 2976 **(2007)**.

[142] T. Nishino, I. Matsuda, and K. Hirao, Macromolecules 37 (20), 7683 **(2004)**.

[143] S. Iwamoto, K. Abe, and H. Yano, Biomacromolecules 9 (3), 1022 **(2008)**.

[144] Y. Okahisa, A. Yoshida, S. Miyaguchi, and H. Yano, Composites Science and Technology 69 (11-12), 1958 **(2009)**.

[145] A. Iwatake, M. Nogi, and H. Yano, Composites Science and Technology 68 (9), 2103 **(2008)**.

[146] L. Suryanegara, A. N. Nakagaito, and H. Yano, Composites Science and Technology 69 (7-8), 1187 **(2009)**.

[147] A. P. Mathew, A. Chakraborty, K. Oksman, and M. Sain, *The structure and mechanical properties of cellulose nanocomposites prepared by twin screw extrusion*, in *Cellulose Nanocomposites,* ACS Symposium Series 938, 114-131, **(2006)**

[148]M. Nogi, S. Iwamoto, A. N. Nakagaito, and H. Yano, Advanced Materials 21 (16), 1595 **(2009)**.

[149] H. Sehaqui, N. Ezekiel Mushi, S. Morimune, M. Salajkova, T. Nishino, and L. A. Berglund, ACS Applied Materials & Interfaces 4 (2), 1043 **(2012)**.

[150] W. Zhang, Y. Zhang, C. Lu, and Y. Deng, Journal of Materials Chemistry 22 (23), 11642 **(2012)**.

[151] M. Nogi and H. Yano, Advanced Materials 20 (10), 1849 **(2008)**.

[152] R. Jung, H.-S. Kim, Y. Kim, S.-M. Kwon, H. S. Lee, and H.-J. Jin, Journal of Polymer Science Part B: Polymer Physics 46 (12), 1235 **(2008)**.

[153] Y. Kim, R. Jung, H.-S. Kim, and H.-J. Jin, Current Applied Physics 9 (1, Supplement), S69 **(2009)**.

[154] Y. Z. Wan, L. Hong, S. R. Jia, Y. Huang, Y. Zhu, Y. L. Wang, and H. J. Jiang, Composites Science and Technology 66 (11-12), 1825 **(2006)**.

[155] L. Hong, Y. L. Wang, S. R. Jia, Y. Huang, C. Gao, and Y. Z. Wan, Materials Letters 60 (13-14), 1710 **(2006)**.

[156] L. E. Millon and W. K. Wan, Journal of Biomedical Materials Research Part B: Applied Biomaterials 79B (2), 245 **(2006)**.

[157] W. Gindl and J. Keckes, Composites Science and Technology 64 (15), 2407 **(2004)**.

[158] Gea S, Torres FG, Troncoso OP, Reynolds CT, Vilaseca F, Iguchi M, and P. T, Journal of Biobased Materials and Bioenergy 22, 497 **(2007)**.

[159] W. Gindl and J. Keckes, Polymer 46 (23), 10221 **(2005)**.

[160] N. Soykeabkaew, C. Sian, S. Gea, T. Nishino, and T. Peijs, Cellulose 16 (3), 435 **(2009)**.

[161] S. Yamanaka and J. Sugiyama, Cellulose 7 (3), 213 **(2000)**.

[162] T. Maneerung, S. Tokura, and R. Rujiravanit, Carbohydrate Polymers 72 (1), 43 **(2008)**.

[163] S. Yano, H. Maeda, M. Nakajima, T. Hagiwara, and T. Sawaguchi, Cellulose 15 (1), 111 **(2008)**.

[164] D. Ciechanska, Fibres and Textiles in Eastern Europe 12 (4), 69 **(2004)**.

[165] S. Chen, Y. Zou, Z. Yan, W. Shen, S. Shi, X. Zhang, and H. Wang, Journal of Hazardous Materials 161 (2-3), 1355 **(2009)**.

[166] S. Gea, E. Bilotti, C. T. Reynolds, N. Soykeabkeaw, and T. Peijs, Materials Letters 64 (8), 901 **(2010)**.

[167] Q. Zhou, E. Malm, H. Nilsson, P. T. Larsson, T. Iversen, L. A. Berglund, and V. Bulone, Soft Matter 5 (21), 4124 **(2009)**.

[168] J. D. Fontana, A. M. Souza, C. K. Fontana, I. L. Torriani, J. C. Moreschi, B. J. Gallotti, S. J. Souza, G. P. Narcisco, J. A. Bichara, and L. F. X. Farah, Applied Biochemistry and Biotechnology 24-25 (1), 253 **(1990)**.

[169] W. Czaja, A. Krystynowicz, S. Bielecki, and R. M. Brown Jr, Biomaterials 27 (2), 145 **(2006)**.

4

All-cellulose composites by partial dissolution of cotton fibres

4.1 Introduction

Over the last few years, a number of researchers have been involved in investigating the exploitation of natural fibres as reinforcements in polymer composites[1-7]. The use of ligno-cellulosic fibres such as flax and hemp as reinforcements is increasing because they are renewable, low cost, can be incinerated at the end of their lifetime and have competitive mechanical properties.

When using natural fibres as reinforcement, an improvement in fibre-matrix adhesion is usually achieved by fibre surface- or matrix modifications, the use of compatibilizers, coupling agents or other surface modification methods, all adding cost to the fibres[8,9]. The most desirable solution to some of these problems is the development of self-reinforced polymer composites where the fibre and the matrix are composed of the same material, such as in the case of all-polypropylene composites that have been recently developed[10-13]. The fact that in these composites both the fibre and the matrix are chemically identical renders an excellent interfacial compatibility, hence providing fully-recyclable, environmentally friendly materials with good mechanical properties.

A combination of these two trends, namely the use of cellulosic fibres and the advantages of all-polymer composites, has recently led to extensive work on the development of all-cellulose composites since the pioneering work of Nishino and co-workers[14]. In their initial approach, the material was prepared by impregnating aligned ramie fibres with a cellulose solution followed by coagulation in methanol and drying. These all-cellulose composites showed a high tensile strength due to their high volume fraction (≥80%)[14,15]. This impregnation method has been used to produce all-cellulose composites based on rice husk[16], bacterial cellulose[17] and cellulose nanowhiskers[18]. However, the inherent difficulty associated with the impregnation of fibres with high viscosity resin systems triggered the development of a new method for the processing of these composites. The outer cell wall of most ligno-cellulose fibres is porous and consists of poorly oriented crystalline cellulose microfibrils, while in the secondary cell wall, microfibrils are helically arranged with a high level of orientation (Figure 2.9, Chapter 2)[5,19-22]. Nishino and co-workers[23] developed a new process for the preparation of all-cellulose composites, where the disoriented surface layer of the cellulosic fibres was selectively dissolved and subsequently precipitated in situ to form a matrix around the undissolved fibre cores. These remaining oriented fibre cores preserve their original structure providing a reinforcing effect to the composite[19]. The resulting all-cellulose composites showed excellent mechanical properties similar or even better than those prepared by

traditional impregnation methods[14,15,23-25]. This method constitutes not only a simplification of the composite preparation, but also provides a significantly improved fibre/matrix interface. The surface selective dissolution method results not only in very high fibre volume fractions, but also in a gradual change in the properties of the fibre, forming an interphase or interfacial region which minimises voids and stress concentrations as in sharp, well-defined fibre/matrix interfaces[26]. The concept of all-cellulose composites has been explored for a wide range of cellulose materials including wood pulp fibres[27,28], filter and Kraft paper[23,29-31], micro-crystalline cellulose[24,32-34], sisal[35,36], ramie[24], regenerated cellulose (Lyocell) and cellulose fibres spun from anisotropic phosphoric acid solution (Bocell)[37], and bacterial cellulose[38].

In the process developed by Nishino and co-workers[23] the surface dissolution of the fibres was carried out by immersion of cellulose samples in a solvent system consisting of lithium chloride dissolved in *N*,*N*-dimethylacetamide (LiCl/DMAc). In recent years, this solvent system has become very popular due to its capability to dissolve polysaccharides which are not water soluble such as cellulose, chitin, etc[39-46]. Originally, the LiCL/DMAc system was developed by Austin in the late 1970s to dissolve chitin[42]. Its use was quickly extended to cellulose by McCormick[43] and Turbak et al.[44] These preliminary studies together with other works on cellulose dissolution in LiCl/DMAc demonstrated the exclusivity and uniqueness of this solvent system[44,45]. The fact that cellulose dissolves in LiCl/DMAc without degradation or other undesirable reactions[41,46,47] makes this solvent system particularly suitable for the processing[48,49] characterisation[40,50-53] and derivatisation[54-56] of cellulose.

After two decades of use, the dissolution mechanism of cellulose in LiCl/DMAc is still not perfectly understood despite of numerous scientific efforts. However, it is well-known that the dissolution of cellulose directly depends on the accessibility of the hydroxyl groups of their anhydroglucose units to be attacked[41]. For this reason, cellulose needs to undergo a so-called ‘‘activation procedure’’

during which cellulosic fibres are penetrated with a polar solvent in order to disrupt and break the intermolecular hydrogen bonds of the cellulose structure. This activation step is crucial for opening up the cellulose chains into its most relaxed conformation, and thus enhancing the diffusion kinetics of the solvent to the tightly packed crystalline regions during dissolution process. In other words, the increased molecular mobility of cellulose through activation allows the LiCl/DMAc solvent to penetrate the cellulose structure more easily. In fact, without activation, it can take several months for the dissolution to proceed regardless of the crystallinity of the cellulose. Heat activation, first proposed by Ekmanis et al.[57], is based on the fact that near its boiling point, a solvent has a sufficiently high vapour pressure to penetrate into the fibre and swell it[53]. Although some authors reported this activation as more convenient since it requires less LiCl in the subsequent dissolution step and because it is a one-step procedure, Dawsey et al.[45], Terbojevich et al.[58] and, more recently, Dupont[39] observed some oxidative degradation of cellulose at high temperatures. Taking into account these disadvantages, in this work the activation treatment was carried out by a solvent exchange method, which consists of the sequential immersion of cellulosic fibres in water, acetone and DMAc. Interestingly, this activation step before the actual dissolution does not affect cellulose crystallinity.

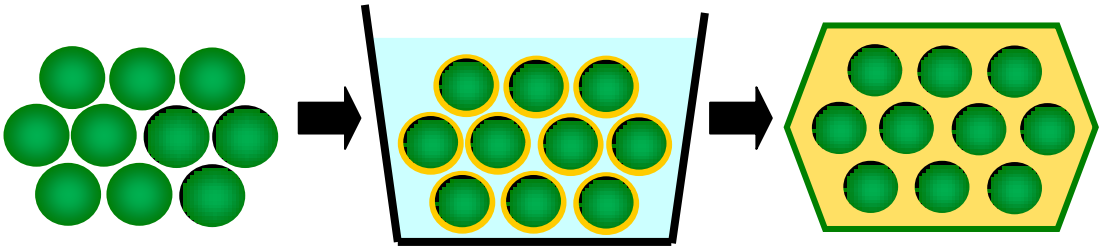

Figure 4.1. Schematic picture of the fibre surface dissolution process for the production of all-cellulose composites.

The different steps involved in the processing of the all-cellulose composites are depicted in Figure 4.1. Initially, cellulose chains are tightly packed through H-bonds between contiguous chains. In the solvent exchange activation step, first water swells and opens the structure through the replacement of inter- and intra-molecular

hydrogen links by hydrogen bonds formed with water. A subsequent immersion step in acetone is required for a good dissolution of the fibres in LiCl/DMAc, since the presence of water in the ionic liquid in the dissolution step was shown to significantly decrease the solubility of cellulose, because its presence hinders complexation with cellulose through competitive hydrogen-bonding, thus inhibiting solubilisation[59]. The necessity of allowing enough time for a good desorption of the water from the more crystalline regions of the cellulose in the solvents used in subsequent steps is crucial for an optimal activation. The subsequently introduced DMAc impedes the inter- and intra-hydrogen bonds to reform, keeping the fibres away from each other, thus making them readily available for a subsequent attack during the dissolution stage. Solvent exchange has proven to enhance the molecular mobility of cellulose, thus facilitating the access of solvent molecules to the cellulose and accelerating the dissolution of cellulose in LiCl/DMAc[60].

Apart from the activation pre-treatment, the relative proportions of LiCl and cellulose are critical for optimal dissolution. 'Ideal' concentrations of LiCl by weight of cellulose were reported within a range as wide as 2 to 12% [43,44]. In solutions with too low LiCl and/or too high cellulose concentrations, the solvent was unable to completely rupture the strong hydrogen bonds in the cellulose[61].

For cotton fibres, 8% LiCl was found to be the minimum amount necessary to achieve complete dissolution[53,62]. Other parameters in the dissolution process such as cellulose concentration as well as supramolecular structure of the polymer, its molar mass, and sample preparation for the activation step greatly influence the dissolution process. In the present work randomly oriented all-cellulose composites were obtained by surface dissolution using cotton fibre pads as cellulose source and the solvent exchange method as the activation treatment. Cotton is a relatively strong natural fibre with a high cellulose content between 88 to 96%, and tensile strengths between 300 to 600 MPa, Young's moduli of 6 to 12 GPa and an elongation to break of 7 to 9% [63]. The dissolution time as well as activation time will be studied and related to structural and mechanical properties of the final composites, in order to

optimise the mechanical performance of the all-cellulose composites. In addition, the effect of a different cotton sources will be discussed.

4.2 Experimental methodology

4.2.1 Sample preparation

Two types of commercial cotton cellulose have been used in the present work (Types A and B). Cotton pads were cut and fixed in a metal mesh frame in order to maintain the dimensions of the sample during processing. As explained in the introduction, activation of the fibres was carried out by immersion of cotton pads consecutively in distilled water, acetone and N,N'-dimethylacetamide (DMAc), each for 1 or 24 hrs at room temperature. All these operations were performed in sealed beakers; special care was taken to prevent moisture in the cases that involved DMAc since the presence of moisture will affect the dissolution of the fibres by LiCl/DMAc through competitive hydrogen-bonding of water with the cellulose microfibrils. Then, these activated pads were subjected to a dissolution treatment by immersion in 75 ml of a solution containing 8 wt.% of LiCl in DMAc for selected periods of time: 6, 12, 18, 24 and 48 hrs. Both LiCl and DMAc are highly hygroscopic, and water has to be excluded from the solvent system, since its presence hinders complexation with cellulose[44] and promotes the formation of polymer aggregates[64]. After these immersion times, the partially dissolved fibres were removed from the solvent system and then exposed to ambient conditions for 15 hrs where the dissolved cellulose started to precipitate/gel. In order to extract the solvent, the gelified samples were transferred into hermetic boxes and treated with distilled water by solvent exchange. This procedure was carried out for 48 hrs; the water solution was frequently renewed to make sure that the solvent exchange was complete. During this process, the partially dissolved layers of cotton fibres were precipitated as a cellulose matrix, thus yielding all-cellulose composites. The process of cellulose regeneration

is an important step in processing all-cellulose composites as it controls the degree of crystallinity (and hence, microstructure) of the cellulose matrix phase. Thus, the microstructure of the regenerated cellulose matrix in all-cellulose composites can vary from crystalline to amorphous as a function of the precipitation rate. Finally, these samples were then pressed between sheets of absorbing paper in a hot-press (at a temperature of 120 °C and pressure of 40 MPa) in order to obtain flat and dry samples. Different parameters in the processing of the composites such as the activation time and the fibre dissolution time as well as the cotton source have been systematically studied in an attempt to yield composite materials with the best overall mechanical properties.

4.2.2 Characterisation of the materials

The microstructure and morphology of the all-cellulose composites were analysed by means of scanning electron microscopy (SEM), using a JEOL JSM 6300 microscope at an accelerating voltage of 10 kV. Prior to examination, the surface of the samples was sputtered with a thin layer of gold.

The X-ray diffraction patterns of the composites were obtained by using a X'PERT PRO (Phillips) diffractrometer at 40 kV, 40 mA and CuKα radiation. The air scattering was subtracted to the X-Ray profiles of the samples. Reflections were were assigned according to the crystalline phase of cellulose I. The apparent crystallinity, χ_{cr} (%), has been determined by the Segal method (Equation 4.1)[65], using the intensity of the (200) reflection (I_{200}) and the minimum between the (200) and (110) reflections (I_{AM}). I_{200} represents both crystalline and non-crystalline material while I_{AM} represents only the fraction of non-crystalline material.

$$\chi_{cr} = (I_{200} - I_{AM}) / I_{200} \quad \text{(Equation 4.1)}$$

where I_{200} is the height of the reflection assigned to (200) planes, typically located at $2\theta = 22.7°$. I_{AM} is the height measured at the minimum between the (200) and (110) reflections, which is where the maximum occurs for fully-amorphous cellulose.

Thermogravimetric analyses (TGA) of the all-cellulose composites were performed using a TA Instrument TGA Q500 thermal analyzer. Approximately 5 mg of each sample were used for the analysis since under these conditions the heat transfer limitations can be neglected. The analyses were carried out under nitrogen atmosphere at a heating rate of 20 °C/min over a temperature range of 25–1000 °C.

Tensile tests of strips of all-cellulose composites, with approximately 3.5 mm in width and 25 mm in length, were performed using an Instron 5584 tensile tester at room temperature with a 1 kN load cell. The cross-head speed was 1.5 mm/min and the gauge length was fixed to 15 mm. At least 5 specimens of each sample were tested, and the values were averaged.

4.3 Results and discussion

As mentioned in the introduction, the processing of the all-cellulose composites requires subsequent steps of activation of the fibres, dissolution and finally precipitation. In an attempt to optimise the processing protocol and thus the performance of the obtained composites, different processing parameters have been studied in the present work.

It is expected that longer activation times lead to a more relaxed conformation of the polymer chains, implying that the cellulose chains are more accessible to the solvent, favouring the selective dissolution of the fibre skins. Therefore, in order to study the effect of the activation time on the dissolution process, two activation times

of 1 and 24 hrs have been selected for the preparation of our composites. For each of these, the optimum dissolution time in LiCl/DMAc was investigated.

Hereafter, samples will be referred to by the type of cotton used, followed by the activation time (preceded by 'a') and by the dissolution time (preceded by 'd'). For example, sample A-a1h-d6h refers to a composite prepared from cotton source A and an activation time of 1 h in each solvent (1 h in water, 1 h in acetone and 1 h in DMAc) and then followed by a dissolution time for 6 hrs in 8% LiCl DMAc. Table 4.1 summarizes the different experiments that have been carried out.

Results will be presented in separate sections, first those for the composites prepared with cotton A for 1 h activation time, then 24 hrs activation time; finally the effect of the cotton source will be analysed.

Table 4.1. Composites studied in this chapter and prepared under different conditions.

	Cellulose source	**Activation time**	**Dissolution time**	**Crystallinity (%)**
Raw	Cotton A	0h	0h	80.6
A-a1h-d6h	Cotton A	1h	6hrs	66.1
A-a1h-d12h	Cotton A	1h	12hrs	41.4
A-a1h-d18h	Cotton A	1h	18hrs	22.2
A-a1h-d24h	Cotton A	1h	24hrs	0
A-a1h-d48h	Cotton A	1h	48hrs	---
A-a24h-d6h	Cotton A	24hrs	6hrs	---
A-a24h-d12h	Cotton A	24hrs	12hrs	---
A-a24h-d18h	Cotton A	24hrs	18hrs	25.5
B-a1h-d18h	Cotton B	1h	18hrs	19.8
Raw	Cotton B	0h	0h	77.7

4.3.1 All-cellulose composites with 1 h of activation.

Figure 4.2 shows the XRD patterns of composites prepared after 1 h of activation as a function of the dissolution time in LiCl/DMAc. For comparison, the XRD pattern of the raw material (cotton A) is also shown.

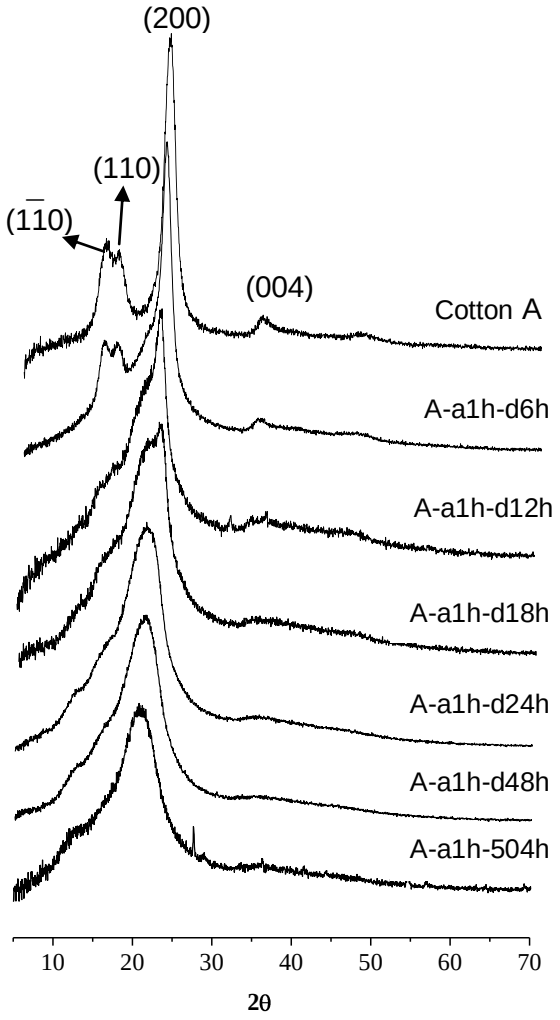

Figure 4.2. X-ray diffraction patterns of composites prepared with an activation time of 1 h.

It can be clearly seen that the intensity of the reflections corresponding to the crystalline phase of cellulose I[(1-10), (111), (200) and (004)] progressively decreases upon increasing dissolution time. Besides, an increase of the intensity of the peak at 21° 2θ, corresponding to the non-crystalline or amorphous cellulose phase, is simultaneously observed, demonstrating that the partially dissolved layers of cotton fibres were regenerated as an amorphous or non-crystalline matrix phase. As a result of a fast precipitation, the time for the cellulose chains to order themselves into a lower energy crystalline phase was not enough, resulting in an amorphous phase. Therefore, the increase of the intensity of the peak corresponding

to the amorphous cellulose with the dissolution time provides evidence that longer immersion times lead to larger fractions of the cellulose fibres being dissolved to form a non-crystalline cellulose matrix phase. This observation directly results in a reduction of the overall crystallinity of the composites, as can be seen in Table 4.1 and Figure 4.3. A linear reduction of the sample crystallinity as a function of dissolution time is found up to 24 hrs. From this time on, dissolution of the fibres is almost complete, as can be seen by the lack of reflections of the crystalline phase in the XRD patterns, revealing a small fraction of fibres remaining in the composite. For this reason, the crystallinity of the composites obtained after dissolution time of 24 hrs and longer could not be reliably calculated.

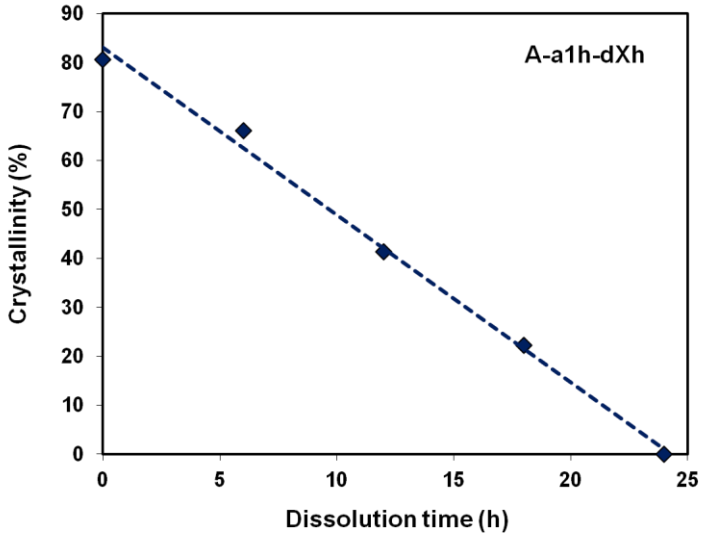

Figure 4.3. Crystallinity of composites (1 h activation time) as a function of the dissolution time.

The thermal behaviour of the different composites compared with the raw cotton material is shown in Figure 4.4. Three different steps of weight loss can be observed. The first weight loss occurs at around 100 ºC and corresponds to the desorption of adsorbed water in the raw material. This initial weight loss is more intense for the composites and ends at a higher temperature, around 170 ºC, which corresponds, in this case, to the elimination of remaining solvent in the composites

since this temperature is close to the boiling point of DMAc. The second stage, which takes place in the 265-400 ºC temperature range, is assigned to the decomposition of cellulose. In the case of raw cotton fibres, only one peak is observed with a maximum degradation rate at 380 ºC. In contrast, the degradation of cellulose in the composites is split in two different steps, one at a lower temperature around 330 ºC, which is assigned to the decomposition of the non-crystalline cellulose matrix formed by the selective dissolution of the cotton fibres, and another at a higher temperature, around 370 ºC, corresponding to the decomposition of the cellulose fibres remaining in the composites. The amorphous cellulose matrix exhibits lower thermal stability than cellulose fibres due to its non-crystalline structure.

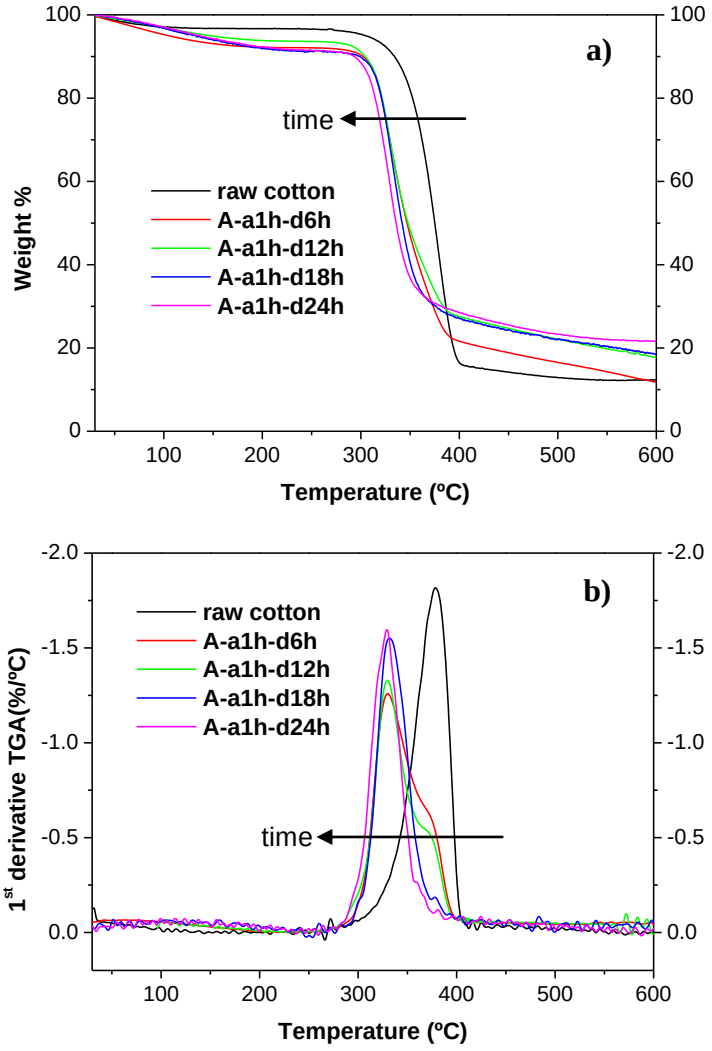

Figure 4.4. TGA (a) and DTG (b) curves of cellulose composites prepared with an activation time of 1 h.

A clear trend can be observed by looking at the relative intensity of the weight loss at the two steps as a function of the dissolution time. Longer dissolution times lead to a decrease of the weight loss of the cellulose fibres and consequently to an increase of that of the non-crystalline matrix. These results support the evidence observed by XRD that the non-crystalline phase increases with the dissolution time. It is worth mentioning that in the composites obtained after 24 hrs of dissolution time and so on, the second stage is formed only by one peak, but in this case with a maximum intensity at 330 ºC, corresponding to degradation of the cellulose matrix. This is explained since such an extremely long dissolution time results in an almost complete dissolution of the cellulose fibres. The third stage, covering the temperature range 450–800 ºC, may be due to oxidation of volatile products and charred residues.

The mechanical behaviour of the different all-cellulose composites was studied by tensile tests. Figure 4.5 shows the mechanical properties of the all-cellulose composites as a function of dissolution and activation times. In this section, only 1 h activated samples are analysed in detail. In addition, the SEM pictures of the composites prepared with 1 h of pre-treatment are shown in Figure 4.6 in order to get a profound understanding of the mechanical behaviour as a function of their microstructure. Figure 4.5 shows that the composite obtained after 18 hrs of dissolution exhibits the best overall mechanical properties. At this dissolution time, the amount of outer layer of the cotton fibres dissolved to form the matrix is enough to bond the remaining core fibres efficiently together, as can be seen in Figure 4.6-d, since no cracks and voids are present near the interface between the fibres and the matrix, hence resulting in a good interfacial bonding and stress transfer from the matrix to the reinforcement. In samples obtained after 6 and 12 hrs of dissolution time, a smaller fraction of fibre surface is dissolved to create the cellulose matrix, as was revealed by XRD and TGA results, and the presence of cracks and voids between the fibres indicates that not a sufficient amount of matrix is formed to provide a good interfacial bonding between the fibres (see Figures 4.6-b and 4.6-c).

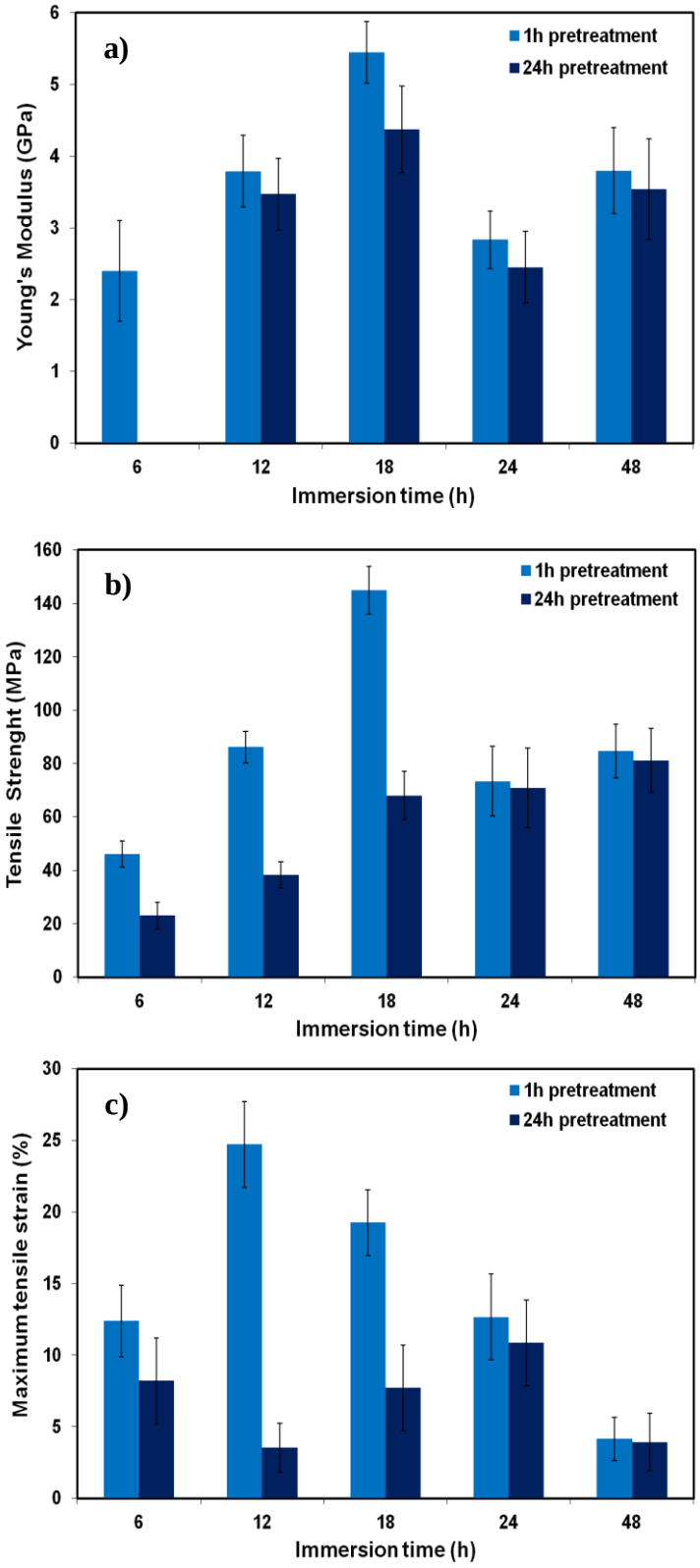

Figure 4.5. Mechanical properties of all-cellulose composites prepared after 1 h (light blue) or 24 hrs (dark blue) activation times as a function of dissolution time: a) Young´s modulus, b) tensile strength, and c) maximum tensile strain.

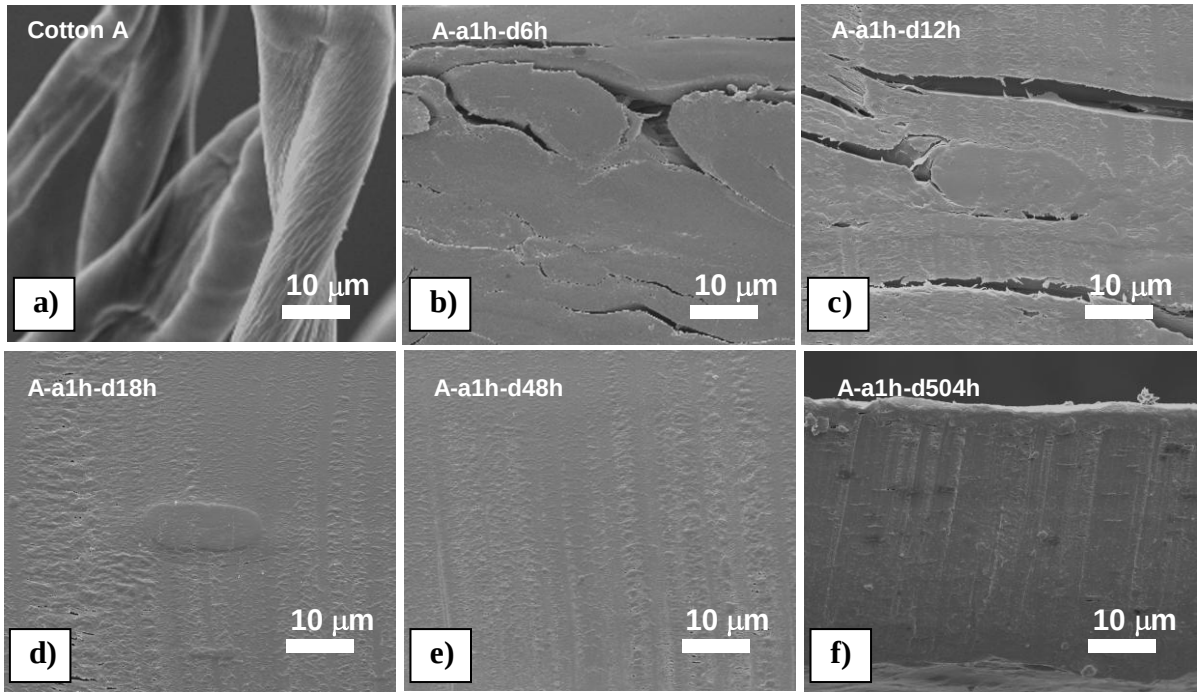

Figure 4.6. SEM images of cotton fibres (a) and all-cellulose composites prepared with an activation time of 1 h and a dissolution time of 6 (b), 12 (c), 18 (d), 48 (e) and 504 hours (f). (Magnification x5000).

A significant reduction in mechanical performance is observed for samples prepared with dissolution times exceeding 18 hrs. In this case, the poor mechanical properties are not due to poor interfacial bonding between fibres (see Figures 4.6-e and 4.6-f) but due to the significant reduction in remaining fibre volume fraction. SEM pictures of these samples show the near absence of fibres in these composites. Indeed, no difference in mechanical properties is found between samples obtained with 24 and 48 hrs of immersion time, what suggests that nearly all fibres were completely dissolved after 24 hrs.

The mechanical properties of the obtained all-cellulose composites as a function of their overall crystallinity are displayed in Figure 4.7. A clear maximum in both tensile strength and Young´s modulus can be observed for a crystallinity of approximately 20%, which corresponds to the A-a1h-d18h sample. The existence of

these maximums imply a balance between reinforcement provided by the presence of remaining cellulose fibre cores and the creation of sufficient matrix to bond these cores together to form all-cellulose composites with good mechanical properties. Such balance is achieved in our case for the A-a1h-18h composite.

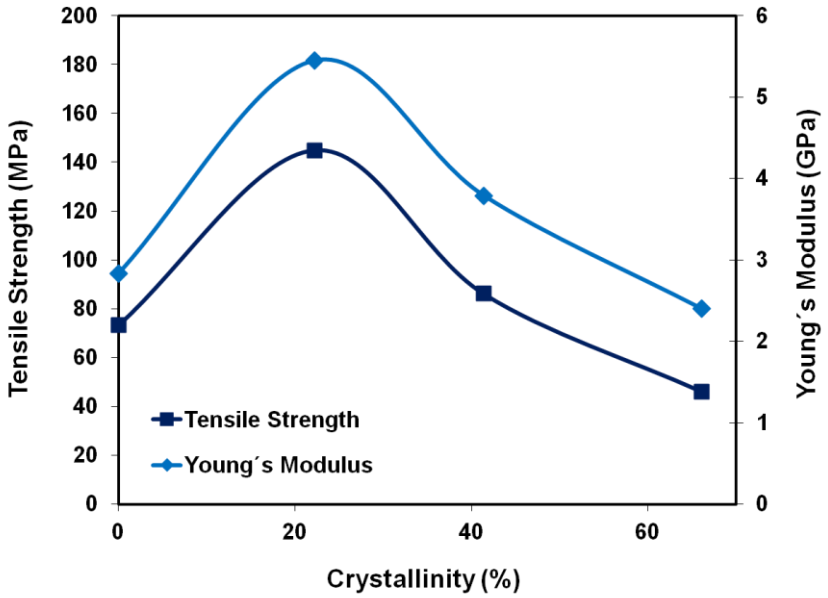

Figure 4.7. Evolution of the mechanical properties of the all-cellulose composite materials (obtained with 1 h activation time) as a function of their crystallinity.

It is worth mentioning that the sample which exhibited the highest tensile strength and Young´s modulus (A-a1h-d18h) presents also a very high maximum tensile strain (around 20%) (see Table 4.2). The mechanical properties of raw cotton fibres[66] are also listed in Table 4.2 for the sake of comparison. It can be observed that, despite the fact that the cotton fibres in the all-cellulose composite are randomly oriented, typically leading to a decrease in mechanical reinforcement by a factor of 0.2 to 0.3, the effective Young's modulus achieved by the A-a1h-d18h composite is nearly the same as that of the single cotton fibre, while the tensile strength is reduced only by a factor of 0.25 to 0.5. The maximum tensile strain achieved is much higher than that of raw cotton fibre, as much as twice the value of the raw fibre. Therefore, it can be concluded that the optimisation of the dissolution process created all-

cellulose composites with good overall mechanical properties such as stiffness, strength and toughness. Indeed, the mechanical performance of our cotton based all-cellulose composites is higher than that of other natural fibres composites made with PP as matrix (Table 4.2, entries 5 and 6[66]), although still worse than all-cellulose composites made with other cellulose raw materials (Table 4.2, entry 7[23]).

Table 4.2. Mechanical properties of the cotton fibre (1), of the best all-cellulose composite obtained in this work (2, A-a1h-d18h) and that obtained with cotton B (3, B-a1h-d18h), of randomly oriented glass-fibre reinforced PP composites (4, PP/glas)[66], of PP/flax (5) and PP/sisal (6) composites[66] and of all-cellulose composites prepared with filter paper (7)[23].

Entry	Sample	Young's modulus (GPa)	Tensile strength (MPa)	Elongation at break (%)
1	**Cotton fibre**	6 – 12	300 – 600	7.0 – 8.0
2	**A-a1h-d18h**	5.5	144.9	19.3
3	**B-a1h-d18h**	3.8	67.5	9.7
4	**PP/glass**	6	100	---
5	**PP/flax**	5.1	47	---
6	**PP/sisal**	3.7	38	---
7	**All-cellulose composite (filter paper)**	8.3	211	---

4.3.2 All-cellulose composites with 24 hrs of activation.

The influence of activation time on the final mechanical performance of all-cellulose composites is described in this section. As explained in the introduction, the aim of the activation treatment is to facilitate the dissolution process which directly depends on the accessibility of the hydroxyl groups of the anhydroglucose units to be attacked[67]. In addition, the activation process brings about an increase in the molecular mobility of cellulose, which allows the LiCl/DMAc solvent to penetrate its structure more easily. In order to get an optimal activation, sufficient time must be allowed for a good desorption of water from the more crystalline regions of cellulose. It was proposed that the subsequent penetration of the DMAc into cellulosic fibres

hindered the inter- and intra-hydrogen bonds to reform[39]. However, recent work by Ishii et al. based on solid-state NMR and FTIR spectroscopy showed that DMAc impedes the formation of intermolecular hydrogen bonds while favouring intramolecular hydrogen bonds[68]. Besides, these authors suggested that the increase of the amount of small pores induced by the DMAc treatment leads to enlargement of the surface area and consequently facilitates the access of solvent to the cellulose solid[69]. Recently, the same authors reported that DMAc molecules solvating the cellulose molecular chain at the surface of solid cellulose facilitates the penetration of the LiCl/DMAc complex into the cellulose solid[68].

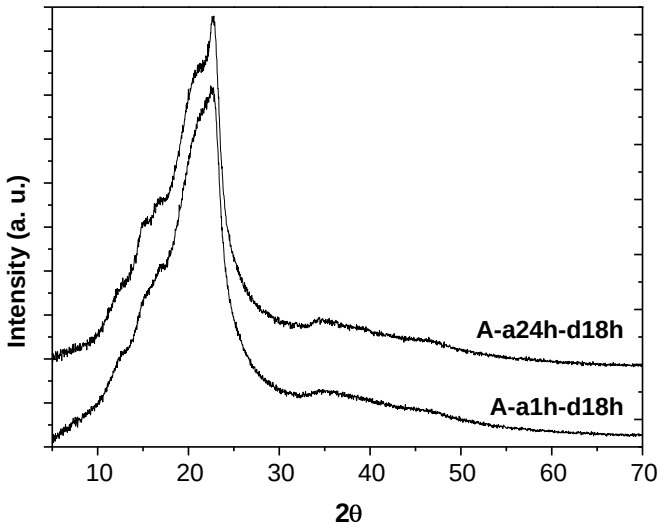

Figure 4.8. XRD patterns of cellulose treated samples at different pre-treatment times and dissolution time of 18 hrs.

Unexpectedly, composites prepared after a 24 hrs pre-treatment showed the same trend than those obtained after 1 h of activation time, although the mechanical properties were generally worse (Figure 4.5). The XRD pattern (Figure 4.8) of the A-a24h-d18h sample showed a slightly higher overall crystallinity than that of the corresponding sample after 1 h of pre-treatment (see Table 4.1), indicating that partial dissolution of the fibres by LiCl/DMAc is hindered by increasing the pre-

treatment time to 24 hrs, thus involving a higher amount of fibre reinforcement. As a result, the poor mechanical performance observed for the 24 hrs pre-treated samples can only be explained by a poor interfacial bonding between the cotton fibres due to the lack of sufficient matrix phase in these composites.

The unexpected poor mechanical properties of the composites obtained with longer pre-activation times could be due to a higher exposure to DMAc during the 24 hrs pre-activation treatment, which eventually could lead to the effective occlusion of certain amounts of DMAc that could remain entrapped in the composite after the fast coagulation of the cellulose matrix. Yun et al.[70] showed that such entrapped DMAc results in negative effects on the surface morphology and mechanical performance since it can hinder cellulose to form a homogeneously stacked layer-by-layer structure by weakening intermolecular hydrogen bonds between cellulose chains. However, this can be ruled out in our case since the TGA of samples obtained after 1 or 24 hrs of pre-treatment showed a similar amount of DMAc, as evidenced by the similar weight loss at a temperature around 170 ºC, which corresponds to the desorption of retained DMAc.

The SEM study of the microstructure of these composites (Figure 4.9) provides an explanation for the unexpected behaviour as all these materials show a very heterogeneous microstructure, where two different regions can be clearly differentiated regardless the dissolution time. One region shows completely dissolved fibres (Figure 4.9-C1), with only non-crystalline cellulose matrix present, while another region shows only slightly dissolved cellulose fibres with insufficient matrix between them to provide a good interface (Figure 4.9-C2). The lack of reinforcement in the first region together with the absence of a good interfacial bond between fibres in the second region explains the poor mechanical properties of these composites. The heterogeneous dissolution pattern of all these samples obtained after 24 hrs of pre-treatment can be explained by the very fast initial dissolution of the most-accessible outer areas of the composites, hindering the dissolution of the

remaining inner region, thus leading to a heterogeneous composite with areas with completely dissolved and undissolved fibres.

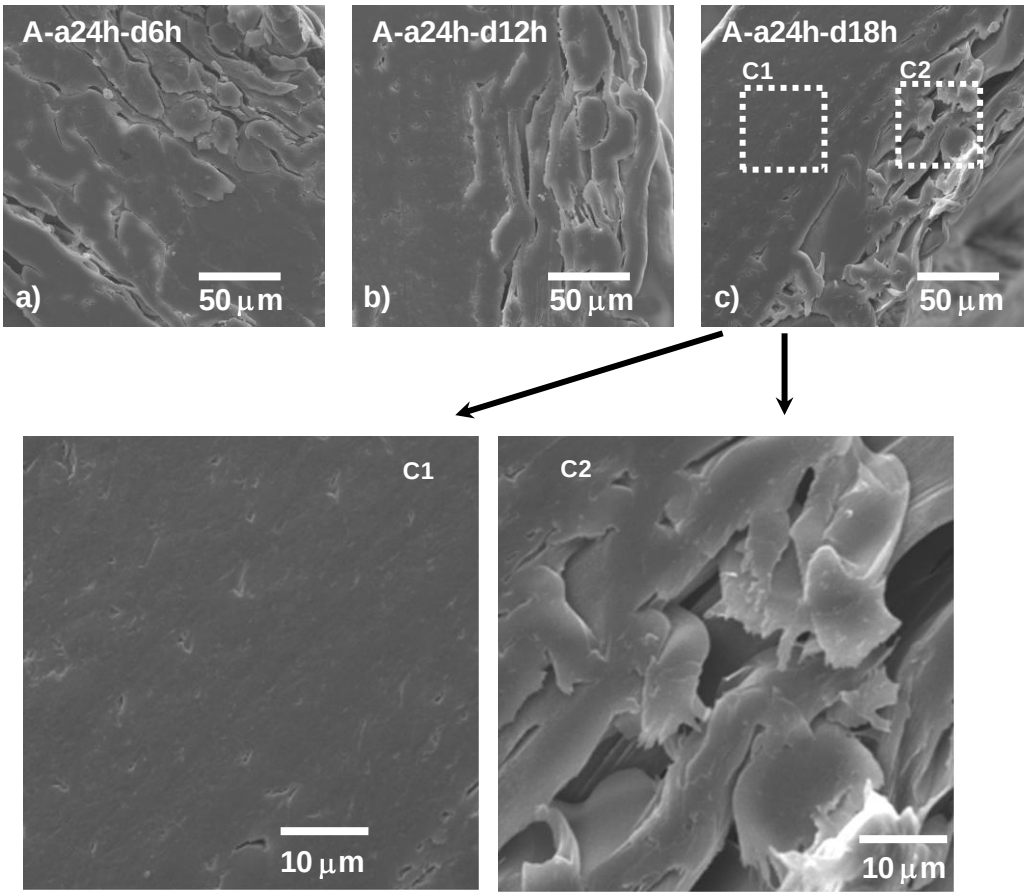

Figure 4.9. SEM images of all-cellulose composites prepared with an activation time of 24 h and a dissolution time of 6 (a), 12 (b) and 18 hours (c). (C1-C2) SEM pictures at higher magnification of the two identified areas in the composite (A-a24h-18h) (c).

4.3.3 Composites prepared with different cotton sources.

Finally, the effect of a different cotton source employed as raw material was studied. For this, a cotton B source with a slightly lower initial crystallinity (77.7%) than cotton A (80.6%) was used. Optimal conditions observed for the previous

samples were employed, i.e. 1 h of activation and 18 hrs of dissolution. The obtained all-cellulose composite based on cotton B had a crystallinity only slightly lower (19.8%) than that of cotton A (22.2%). The mechanical properties of this new all-cellulose composite is, however, worse than the corresponding ones based on cotton A (Table 4.2). Obviously, the lower initial crystallinity of the raw material involved leads to a major dissolution of the fibres, resulting in higher matrix content in the final composite and lower mechanical properties. Moreover, cotton B´s lower initial crystallinity also implies inferior mechanical properties of the raw cotton fibre after dissolution. Besides the crystallinity, other features of the raw cotton pad B that could explain the poorer mechanical properties of the resulting all-cellulose composite are: its composition; cotton quality; the presence of impurities or additives; and manufacturing process.

4.4 Conclusions

The relationships between structure and properties of all-cellulose composites obtained by partial dissolution of cotton fibres in LiCl/DMAc have been investigated. Three parameters have been studied: (i) dissolution time, (ii) activation time and (iii) cellulose source. These parameters all influence the mechanical properties of the resulting all-cellulose composite material through their effect on the dissolution process of the raw cotton fibres and the structure of the obtained composites in terms of the interfacial bonding between the remaining cellulose fibre cores.

A dissolution time of 18 hrs leads to composites with the best overall mechanical properties in terms of stiffness, strength and ductility. At these optimal conditions, the amount of fibre surfaces dissolved is adequate to provide sufficient interfacial adhesion to the composite, while still a considerable fraction of remaining fibre cores remains, thus providing reinforcement to the material.

An increase of the activation time to 24 hrs led to composites with worse mechanical properties than those obtained with 1 h. This behaviour is explained by the occurrence of a heterogeneous dissolution process of the fibres, leading to composite materials with regions of completely dissolved fibres (providing no reinforcement) and another region with nearly undissolved fibres (providing no interfacial adhesion).

In addition, we have observed that the initial crystallinity of the cotton source affected the processing and properties of the all-cellulose composites. The best composite obtained in this work has a comparable Young's modulus and tensile strength than that of cotton fibres, while the maximum tensile strain is greatly improved, leading to materials with promising properties, out-performing most isotropic glass- and natural fibre reinforced plastics.

4.5 References

[1] S. K. Garkhail, R. W. H. Heijenrath, and T. Peijs, Applied Composite Materials 7 (5-6), 351 **(2000)**.

[2] R. Heijenrath and T. Peijs, Advanced Composites Letters 5 (3), 81 **(1996)**.

[3] T. Peijs, S. Garkhail, R. Heijenrath, M. van den Oever, and H. Bos, Macromolecular Symposia 127, 193 **(1998)**.

[4] A. Stamboulis, C. A. Baillie, S. K. Garkhail, H. G. H. van Melick, and T. Peijs, Applied Composite Materials 7 (5-6), 273 **(2000)**.

[5] M. J. John and S. Thomas, Carbohydrate Polymers 71 (3), 343 **(2008)**.

[6] T. Peijs, Materials Technology 15 (4), 281 **(2000)**.

[7] L. A. Berglund and T. Peijs, Materials Research Society Bulletin 35 (3), 201 **(2010)**.

[8] G. Jayamol, M. S. Sreekala, and T. Sabu, Polymer Engineering & Science 41 (9), 1471 **(2001)**.

[9] R. A. Shanks, A. Hodzic, and D. Ridderhof, Journal of Applied Polymer Science 99 (5), 2305 **(2006)**.

[10] I. M. Ward and P. J. Hine, Polymer 45 (5), 1413 **(2004)**.

[11] T. Peijs, Materias Today 6 (4), 30 **(2003)**.

[12] N. Cabrera, B. Alcock, J. Loos, and T. Peijs, Proceedings of the Institution of Mechanical Engineers Part L-Journal of Materials-Design and Applications 218 (L2), 145 **(2004)**.

[13] B. Alcock, N. O. Cabrera, N. M. Barkoula, J. Loos, and T. Peijs, Composites Part A: Applied Science and Manufacturing 37 (5), 716 **(2006)**.

[14] T. Nishino, I. Matsuda, and K. Hirao, Macromolecules 37 (20), 7683 **(2004)**.

[15] C. Qin, N. Soykeabkaew, N. Xiuyuan, and T. Peijs, Carbohydrate Polymers 71 (3), 458 **(2008)**.

[16] Q. Zhao, R. Yam, B. Q. Zhang, Y. K. Yang, X. J. Cheng, and R. Li, Cellulose 16 (2), 217 **(2009)**.

[17] W. Gindl and J. Keckes, Composites Science and Technology 64 (15), 2407 **(2004)**.

[18] M. Grunert and W. T. Winter, Journal of Polymers and the Environment 10 (1-2), 27 **(2002)**.

[19] X. Lu, M. Q. Zhang, M. Z. Rong, G. Shi, and G. C. Yang, Composites Science and Technology 63 (2), 177 **(2003)**.

[20] A. K. Mohanty, M. Misra, and L. T. Drzal, *Natural fibers, Biopolymers, and Biocomposites*. Boca Raton, CRC Press **(2005)**.

[21] D. Klemm, H. Schmauder, and T. Heinze, *Cellulose*, in *Biopolymers*, ed. A. Steinbüchel. Weinheim, Wiley-VCH 6, 275-285, **(2003)**.

[22] H. A. Krassig, *Cellulose: structure accesibility and reactivity*, in *Polymer Monographs*. Amsterdam. Gordon and Breach Science Publishers, 167-323 **(1993)**.

[23] T. Nishino and N. Arimoto, Biomacromolecules 8 (9), 2712 **(2007)**.

[24] W. Gindl and J. Keckes, Polymer 46 (23), 10221 **(2005)**.

[25] N. Soykeabkaew, N. Arimoto, T. Nishino, and T. Peijs, Composites Science and Technology 68 (10-11), 2201 **(2008)**.

[26] S. J. Eichhorn, A. Dufresne, M. Aranguren, N. E. Marcovich, J. R. Copadona, S. J. Rowan, C. Weder, W. Thielemans, M. Roman, S. Renneckar, W. Gindl, S. Veigel, J. Keckes, H. Yano, K. Abe, M. Nogi, A. N. Nakagaito, A. Mangalam, J. Simonsen, A. S. Benight, A. Bismarck, L. A. Berglund, and T. Peijs., Journal of Materials Science 45 (1), 1 **(2009)**.

[27] H. Matsumura and W. G. Glasser, Journal of Applied Polymer Science 78 (13), 2254 **(2000)**.

[28] H. Matsumura, J. Sugiyama, and W. G. Glasser, Journal of Applied Polymer Science 78 (13), 2242 **(2000)**.

[29] A. J. de Menezes, D. Pasquini, A. A. D. Curvelo, and A. Gandini, Cellulose 16 (2), 239 **(2009)**.

[30] A. J. de Menezes, D. Pasquini, A. A. D. Curvelo, and A. Gandini, Carbohydrate Polymers 76 (3), 437 **(2009)**.

[31] A. Gandini, A. A. D. Curvelo, D. Pasquini, and A. J. de Menezes, Polymer 46 (24), 10611 **(2005)**.

[32] W. Gindl, K. J. Martinschitz, P. Boesecke, and J. Keckes, Composites Science and Technology 66 (15), 2639 **(2006)**.

[33] W. Gindl and J. Keckes, Journal of Applied Polymer Science 103 (4), 2703 **(2007)**.

[34] B. J. C. Duchemin, R. H. Newman, and M. P. Staiger, Composites Science and Technology 69 (7-8), 1225 **(2009)**.

[35] L. Xun, Q. Z. Ming, Z. R. Min, and C. Y. Gui, Polymers for Advanced Technologies 14 (10), 676 **(2003)**.

[36] X. Lu, M. Q. Zhang, M. Z. Rong, D. L. Yue, and G. C. Yang, Polymers & Polymer Composites 12 (4), 297 **(2004)**.

[37] N. Soykeabkaew, T. Nishino, and T. Peijs, Composites Part a-Applied Science and Manufacturing 40 (4), 321 **(2009)**.

[38] N. Soykeabkaew, C. Sian, S. Gea, T. Nishino, and T. Peijs, Cellulose 16 (3), 435 **(2009)**.

[39] A. L. Dupont, Polymer 44 (15), 4117 **(2003)**.

[40] A. M. Striegel, Carbohydrate Polymers 34 (4), 267 **(1997)**.

[41] C. L. McCormick, P. A. Callais, and B. H. Hutchinson, Macromolecules 18 (12), 2394 **(1985)**.

[42] P. Austin, US-4059457 **(1977)**.

[43] C. L. McCormick, US-4278790 **(1981)**.

[44] A. F. Turbak, A. El Kafrawy, F. W. Snyder Jr., and A. B. Auerbach, US-4352770 **(1982)**.

[45] T. R. Dawsey and C. L. McCormick, Journal of Macromolecular Science-Reviews in Macromolecular Chemistry and Physics C30 (3-4), 405 **(1990)**.

[46] A. F. Turbak, Tappi Journal 67 (1), 94 **(1984)**.

[47] T. Matsumoto, D. Tatsumi, N. Tamai, and T. Takaki, Cellulose 8 (4), 275 **(2001)**.

[48] Y. Nishio, S. K. Roy, and R. S. Manley, Polymer 28 (8), 1385 **(1987)**.

[49] Y. Nishio and R. S. Manley, Macromolecules 21 (5), 1270 **(1988)**.

[50] M. Hasegawa, A. Isogai, and F. Onabe, Journal of Chromatography 635 (2), 334 **(1993)**.

[51] J. F. Kennedy, Z. S. Rivera, C. A. White, L. L. Lloyd, and F. P. Warner, Cellulose Chemistry and Technology 24 (3), 319 **(1990)**.

[52] A. M. Striegel and J. D. Timpa, Carbohydrate Research 267 (2), 271 **(1995)**.

[53] A. A. Silva and M. L. Laver, Tappi Journal 80 (6), 173 **(1997)**.

[54] C. L. McCormick and T. R. Dawsey, Macromolecules 23 (15), 3606 **(1990)**.

[55] A. M. Regiani, E. Frollini, G. A. Marson, G. M. Arantes, and O. A. El Seoud, Journal of Polymer Science Part a-Polymer Chemistry 37 (9), 1357 **(1999)**.

[56] K. Suzuki, S. Kurata, and I. Ikeda, Polymer International 29 (1), 1 **(1992)**.

[57] J. T. Ekmanis, AF, Lab Highlights, 251, Waters Chromatography Division, Millipore, Milford **(1986)**.

[58] M. Terbojevich, A. Cosani, G. Conio, A. Ciferri, and E. Bianchi, Macromolecules 18 (4), 640 **(1985)**.

[59] R. P. Swatloski, S. K. Spear, J. D. Holbrey, and R. D. Rogers, Journal of the American Chemical Society 124 (18), 4974 **(2002)**.

[60] D. Ishii, D. Tatsumi, and T. Matsumoto, Biomacromolecules 4 (5), 1238 **(2003)**.

[61] T. Roder, B. Morgenstern, and O. Glatter. *Polarized and depolarized light scattering on solutions of cellulose in N,N-dimethylacetamide lithium chloride*, in

Workshop on Data Evaluation in Light Scattering of Polymers (LS '99). Bad Schandau, Germany. Wiley-V C H Verlag Gmbh **(1999)**.

[62] J. D. Timpa, Journal of Agricultural and Food Chemistry 39 (2), 270 **(1991)**.

[63] J. Biagiotti, D. Puglia, and J. M. Kenny, Journal of Natural Fibers 1 (2), 37 **(2004)**.

[64] A. Potthast, T. Rosenau, R. Buchner, T. Roder, G. Ebner, H. Bruglachner, H. Sixta, and P. Kosma, Cellulose 9 (1), 41 **(2002)**.

[65] L. Segal, J. J. Creely, A. E. Martin, and C. M. Conrad, Textile Research Journal 29, 786 **(1959)**.

[66] A. K. Bledzki and J. Gassan, Progress in Polymer Science 24 (2), 221 **(1999)**.

[67] W. Koch, Herlinger, H., Textil Praxis international 39 (9), 902 **(1984)**.

[68] D. Ishii, D. Tatsumi, and T. Matsumoto, Carbohydrate Research 343 (5), 919 **(2008)**.

[69] D. Ishii, Y. Kanazawa, D. Tatsumi, and T. Matsumoto, Journal of Applied Polymer Science 103 (6), 3976 **(2007)**.

[70] S. Yun, Y. Chen, J. N. Nayak, and J. Kim, Sensors and Actuators B-Chemical 129 (2), 652 **(2008)**.

5

Binder-free all-cellulose composites

5.1 Introduction

Natural fibre reinforced plastics (NFRPs) are becoming more and more attractive for both environmental and economic reasons. Despite the advantages associated to NFRPs, the low interfacial adhesion between biofibres and hydrophobic polymer matrices because of the poor compatibility between them[1-3] poses a serious problem for their widespread application, since the different strategies currently employed to improve their compatibility usually involve an increase in processing cost and time[4] as well as a decrease of the "green" character associated with cellulose fibres. The development of cost effective and environmentally friendly methods for

the fibre and/or matrix modifications is necessary, since one of the main market attraction of natural fibre composites is their competitive price[5]. An alternative solution to enhance the fibre-matrix adhesion while notably improving the environmental impact regarding polymeric matrix and composite recyclability is provided through the development of all-cellulose composites[6]. As explained in the previous chapter, the fact that in these composites both the fibre and the matrix are chemically identical renders an excellent interfacial compatibility, hence providing fully recyclable and environmentally friendly materials with good mechanical properties[4,7]. Due to the environmental benefits and the high mechanical performance of these materials, this approach was followed for the production of all-cellulose composites by partial dissolution of cotton fibres[8] as described in Chapter 4. Nevertheless, although most of the typical problems found in conventional NFRPs are overcome in all-cellulose composites, their processing method still involves the use of environmentally hazardous chemical substances, such as solvents like N,N-dimethyl acetamide or N-methylmorpholine-N-oxide.

Since plant fibres have a lower environmental impact than polymers or polymer binders, the ideal composite material would be solely based on natural fibres and hence have no polymer matrix so that a 100% biobased material would be obtained, consequently decreasing its environmental impact[9] (see Figure 2.13 in Chapter 2), while at the same time creating also a fully recyclable material, which as previously mentioned represents the most favoured waste management option (see Figure 2.14 in Chapter 2). In addition, the elimination of a polymer matrix or binder would not only involve the elimination of the necessary polymer production step (see Figure 2.12 in Chapter 2) but would also eliminate the addition of coupling agents or fibre treatments, which would all increase the environmental impact. So a crucial question emerges: is it possible to obtain high-performance cellulose based materials without matrix? If so, the challenge would be to find out how to produce such a material.

To find an answer to this question, the structure of one of the best-performing cellulose materials available, Bacterial Cellulose (BC), is worth analysing. BC films consist of a very strong network structure based on high-modulus (~130 GPa)[10] nano-sized cellulose ribbons, which allows them to form an extensive hydrogen bonding network[11-13] (Figure 5.1). This extensive hydrogen-bonded network, which is responsible for its high mechanical performance, is achieved thanks to an extremely high specific-surface area between the nano-ribbons.

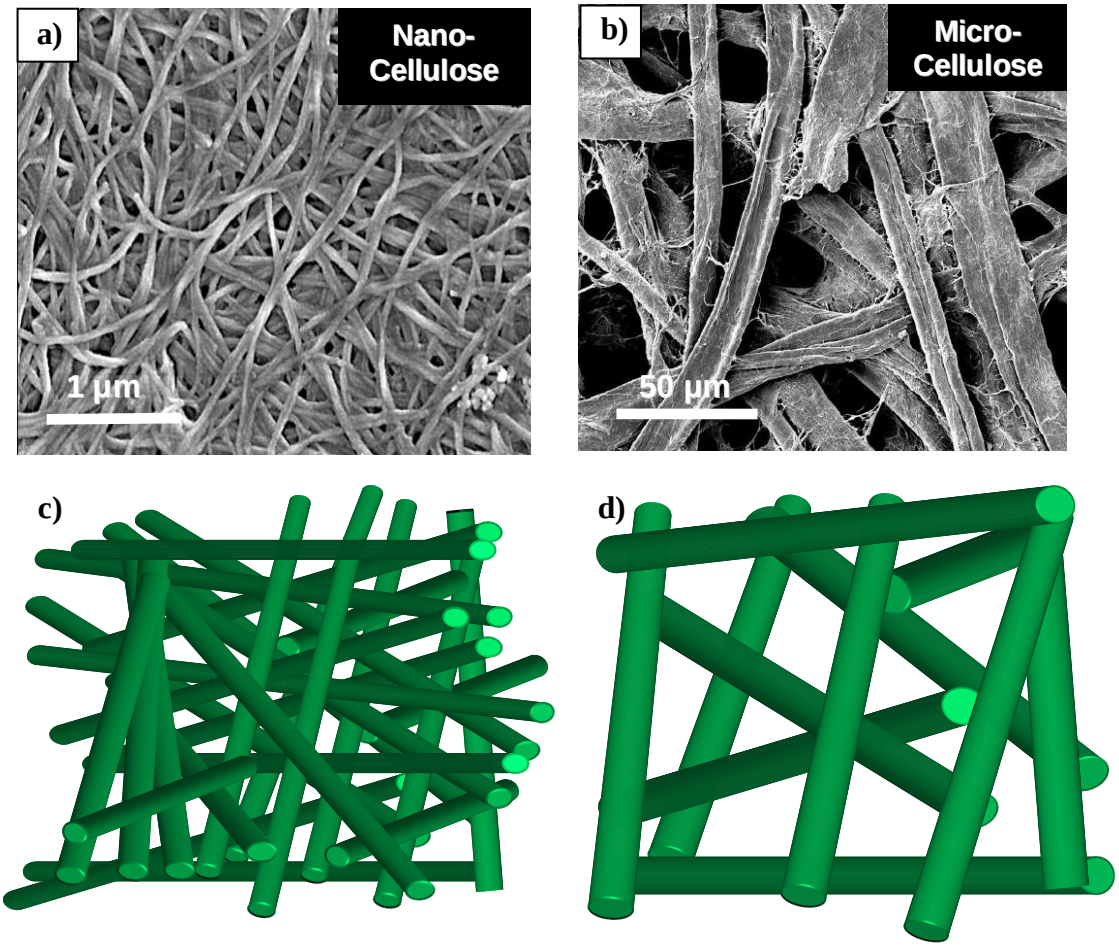

Figure 5.1. SEM pictures (a-b) and schematic drawing (c-d) of the hydrogen-bonded network structure of nano-cellulose (a and c) versus micro-cellulose (b and d).

In comparison, the Van der Waals or hydrogen-bonding network in micro-sized cellulose paper is notably less extensive due to the lower specific-surface area

of the fibres. Therefore, comparing the nano-structured network of BC and the micro-structured cellulose network of conventional paper, it seems that one of the key aspects in determining the mechanical performance of these two types of cellulose is related to the extension of the hydrogen-bonding network, and as such to the specific-surface area.

Based on these ideas, an increase of the contact surface area of the cellulose fibres could provide a way of producing high-performance cellulose materials without the need of a matrix. To produce matrix- or binder-free materials, the Van der Waals or hydrogen-bonded network should be enhanced by creating more fibrillated cellulose fibres, thus increasing its specific-surface area. Evidences of the importance of a high specific surface area of cellulose fibres in biocomposite mechanical performance are provided by the outstanding mechanical properties of films based on nanosized cellulose[14-17] although they are considerable lower than what would be expected theoretically for such reinforcement[18] (Young´s modulus of 100-160 GPa[13] and estimated strength of 1.6-3 GPa[19]). Nanofibrillated cellulose (NFC) exhibits extraordinary properties such as high specific surface area, good mechanical properties, and the ability to form strong hydrogen bonded networks derived from its nanostructure consisting of long crystalline cellulose nanofibrils with diameters in the nanometer scale, however, until now the high energy consumption required for its isolation has prevented its wide-spread industrialisation[20,21]. Recently, several methods including chemical[22-25] and/or enzymatic[26,27] pre-treatments, have been developed in order to decrease the energy demands and facilitate the fibrillation process, however, these pre-treatments usually consist of multi-step processes where fibres are not only subjected to several aggressive chemical treatments, but also to mechanical process such as refining. In addition, these pre-treatments typically involve long processing times and the use of a variety of non-environmentally friendly chemical substances. Even though chemical and enzymatic pre-treatments can be used to promote fibre disintegration, the required mechanical treatments for NFC production are still highly energy intensive and costly[28].

The need to produce at an industrial scale, fully recyclable and biodegradable materials based on the exploitation of the high intrinsic hydrogen bonding capability of fibrillated cellulose fibres has motivated the development of high-performance binder-free cellulose composites through an environmentally friendly processing method. In this work, this new processing protocol based on the refinement of raw cellulose materials such as plant fibres and cellulose wastes without the application of any kind of pre-treatments, has been designed and optimised. Compared with other methods, this procedure provides higher yields of nanofibrillated cellulose fibres at lower operational costs, since the elimination or reduction of lignin and hemicellulose content is not required. This procedure greatly improves the one followed in the previous chapter since it avoids the use of chemical substances such as solvents. Unlike conventional all-cellulose composites that consist of cellulose I (fibre) and II (matrix), the cellulose composites without matrix produced by this method are made entirely of cellulose I.

5.2 Experimental methodology

5.2.1 Sample preparation

Different natural fibre sources including plants and wastes with high cellulose content could be used for the production of these materials. Here, flax fibres kindly supplied by EKOTEX have been used in this work. Figure 5.2 shows the outline of the experimental procedure followed in order to manufacture the cellulose based materials. First, the raw materials were subjected to a refining treatment using a Valley or Hollander Beater where the fibres were cut and fibrillated in the presence of a high amount of water (98%). The second step involved filtering of the refined pulp to partially remove the water in order to get the desired consistence of the samples for the next processing step. The initial cross-linking among the fibres occurred when the samples were subjected to a room temperature pressing (10 bar)

where further removal of water took place. This partially dewatered precursor (50% water content) was finally dried using a hot press where the application of pressure combined with moderately high temperature allowed the complete removal of all retained water, giving flat samples. In this procedure, in an attempt to facilitate the elimination of water and to maintain the dimensions of the sample during the drying process, the samples were placed between two breather membranes, and the set-up was positioned between two perforated aluminium plates. The drying process consisted of three consecutive stages, first the sample was subjected to a pressure of 40 bar at 140 °C for 1500 sec, followed by a second stage where the pressure was increased to 80 bar, at the same temperature and for a further 1500 sec; finally, the sample was cooled down to room temperature.

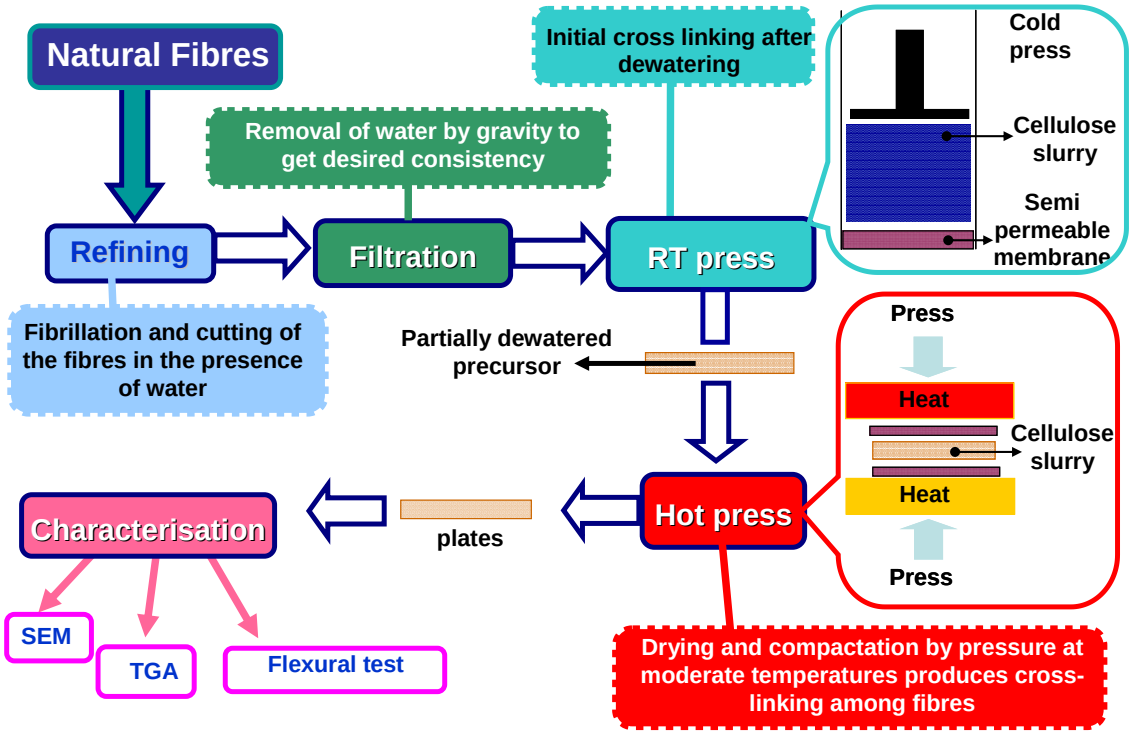

Figure 5.2. Schematic experimental procedure for the production of binder-free all-cellulose composites.

After optimising different processing parameters such as refining time, temperature, time and pressure during hot pressing, for the successful manufacture of binder-free cellulose composites, the influence of the initial flax fibre length on the mechanical performance of the resulting composites was studied. Flax fibres with different fibre length of 5, 10 and 20 mm were used for the manufacture of all-cellulose composites. The experimental conditions applied for the successful production of these composites from different initial fibre lengths are summarised at Table 5.1

Table 5.1. Outline of the main processing parameters set for the successful manufacture of binder-free cellulose composites from different initial fibre length.

Refining time (h)	**Pressure at room temperature (bar)**	**Hot Press Parameters**		
		Phase 1	**Phase 2**	**Phase 3**
6	10	T=140 °C P=40 bar t=1500 s	T=140 °C P=80 bar t=1500 s	T=20 °C P=80 bar t=600 s

5.2.2 Characterisation of the materials

The microstructure and morphology of the all-cellulose composites was analysed by scanning electron microscopy (SEM), using a JEOL JSM 6300 microscope at an accelerating voltage of 10 kV. Prior to examination, the surface of the samples was sputtered with a thin layer of gold to make them conductive.

Three-point bend tests of the all-cellulose composite panels were performed using an Instron 5584 universal tester at room temperature with a 1 kN load cell. The cross head speed was 5 mm/min. The specimens were cut into strips following ASTM D790–02 standard (procedure A). At least 5 specimens of each sample were tested, and the values were averaged.

The density of the different binder-free composites and of the flax fibres was measured by means of a Micromeretics helium Pycnometer model AccuPyc 1330, which uses the gas displacement technique to determine absolute density of solids. The sample holder had a volume of 1 cm^3. The measurements were performed at a run fill pressure of 135 kPa and at an equilibration rate of 35 $Pa \cdot min^{-1}$. Porosity was then calculated from the measured density following equation 5.1:

$$\text{Porosity} = 100 \cdot \frac{\rho_f - \rho_c}{\rho_f} \qquad \text{(Equation 5.1)}$$

where ρ_f is the density of flax fibres and ρ_c corresponds to the density of the binder-free composites.

The water absorption behaviour of the different all-flax composites was monitored at regular intervals. Prior to carrying out the test, the samples were dried in an oven at 60 °C until constant weight. The specimens were submerged in a Grant Y-38 distilled water bath at 23 °C) and weighed in a high precision balance at selected periods of time. The water absorption (MC = moisture content) was determined by the weight difference (equation 5.2):

$$\text{MC}(\%) = 100 \cdot \frac{W - W_d}{W} \qquad \text{(Equation 5.2)}$$

where W and W_d are the weight of wet and dried composites, respectively. Times ranging from 0 to 3000 min were studied.

5.3 Results and discussion

5.3.1 Effect of refinement on fibre microstructure

Prior to the production of the panels, the effect of the refinement treatment in the Valley or Hollander Beater on the fibre microstructure was studied by SEM. Figure 5.3 shows the microstructure of the raw flax fibre (a), and of the pulps obtained after 4 (b) and 6 (c) hrs of refining (after drying in an oven at 80 °C overnight). A progressive fibrillation of the fibres with time can be clearly seen. After 4 hrs, the initial fibre diameter is reduced and as a consequence of the fibrillation of the outer layers branches are created on the fibre surface, leading to an increase of the specific surface area, and a potential enhancement of the hydrogen-bonded fibre network (Figure 5.3-b). Further refinement (6 hrs) yields highly branched fibres with diameters around 1 µm and fibrils in the nanometer scale (Figure 5.3-c). The presence of such a highly fibrillated material will potentially favour extensive hydrogen-bonding between the fibres, thus overcoming the limitations of the absence of a matrix.

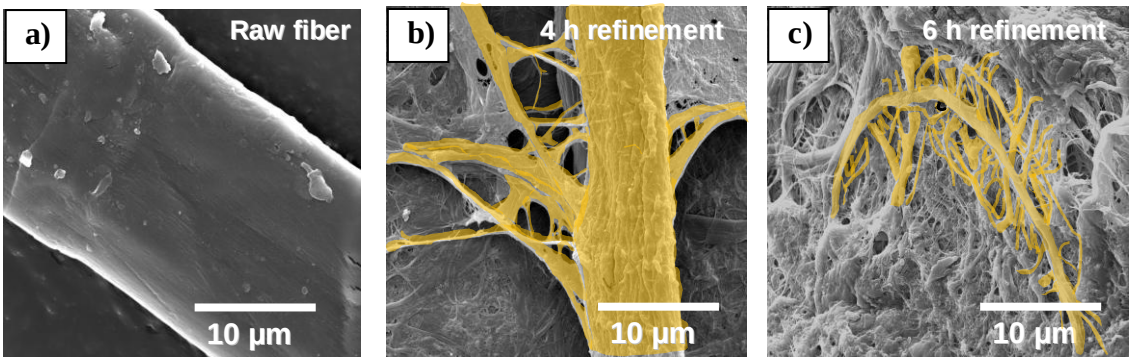

Figure 5.3. Effect of refinement treatment on cellulose fibres: a) initial raw flax fibre; b) fibrillation of the fibres after 4 hrs of refinement; and c) fibrils formed after 6 hrs of refinement.

5.3.2 Effect of refinement on composite mechanical performance and microstructure

After the previous study of fibrillation of the pulps at different refinement times, the effect of these refining times on mechanical properties of the consolidated panels was evaluated. Refining times of 1.5, 3, 4, 5, 6 and 12 hrs were studied. The influence of these refinement times on the flexural properties of the binder-free cellulose panels is shown in Figure 5.4.

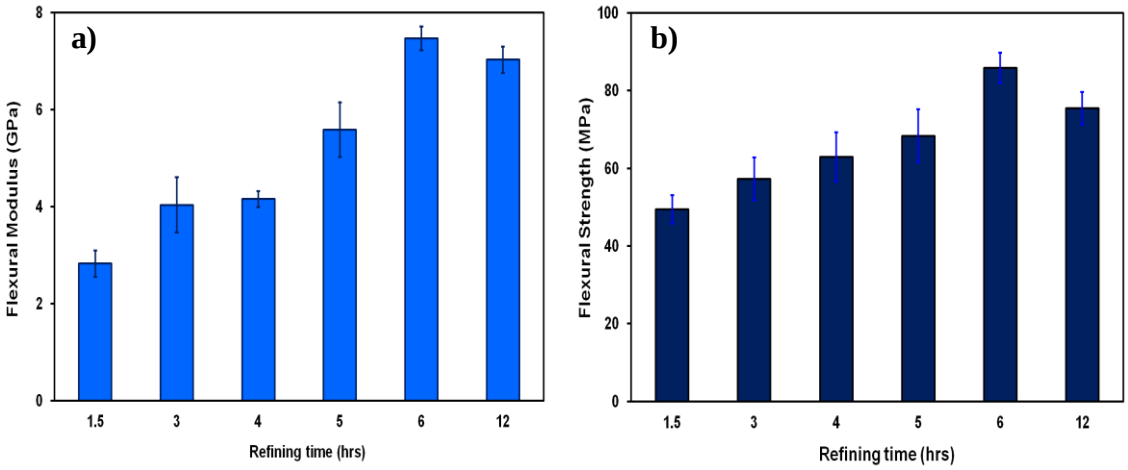

Figure 5.4. Flexural modulus (a) and strength (b) of the binder-free all-cellulose composites as a function of refining time.

An increase of refinement time leads to a clear improvement of both flexural modulus and strength. Such an improvement in mechanical performance is progressive with refinement time up to 6 hrs, yielding highest values for both flexural modulus and strength of 7.5 GPa and 86 MPa, respectively. In order to assess if longer refinement times would bring even better mechanical properties, a sample was subjected to a much longer refinement time of 12 hrs. However, this increase in refinement treatment did not yield any further improvement of the mechanical performance. In fact, a slight reduction in flexural properties was observed; this might be due to the massive mechanical treatment to which this

sample has been subjected and which can lead to destruction of the fibre microstructure and a resulting loss of its mechanical performance.

In an attempt to understand the influence of refining time on the microstructure of the panels, the fracture surface of binder-free cellulose composites was studied by SEM (Figure 5.5). A low magnification of the fracture surface of samples obtained after 1.5 (a), 4 (b) and 6 hrs (c) of refining time shows the layered structure present in all the composites; however, no notable differences were observed at this magnification among the different materials. In order to understand the relationship between mechanical behaviour and microstructure, a higher magnification is required (Figure 5.5: d-f). At a relatively low refining time of 1.5 hrs (d), the fibrillation process has just started, and consequently the flax fibres remain almost intact, as can be observed in Figure 5.5-g. Therefore, the absence of fibrils hinders the effective cross-linking between fibres, hence yielding a high void content and poorly compacted material. This high void content is responsible for less fibre-fibre interactions and explains the relatively poor mechanical properties of this composite. An increase of the refining time to 4 hrs yields an enhanced degree of fibrillation, as can be clearly appreciated from the detailed microstructure of this composite (Figure 5.5-h). Indeed, this enhanced level of fibrillation allows for a more extensive hydrogen-bonded network between fibres and renders more compact materials with lower void contents and as a result improved mechanical properties. However, this degree of fibrillation is still not enough to yield maximum compaction since voids are still present (Figure 5.5-e). The optimum refining time was found at 6 hrs with highly fibrillated fibres (Figure 5.5-i), leading to a very dense material with negligible voids and a very strong network structure with optimal interfibre bonding between micro-sized fibres through nano-sized fibrils (Figure 5.5-f). This strong hydrogen-bonded fibrillated network is responsible for the outstanding mechanical performance of this self-binding cellulose composite.

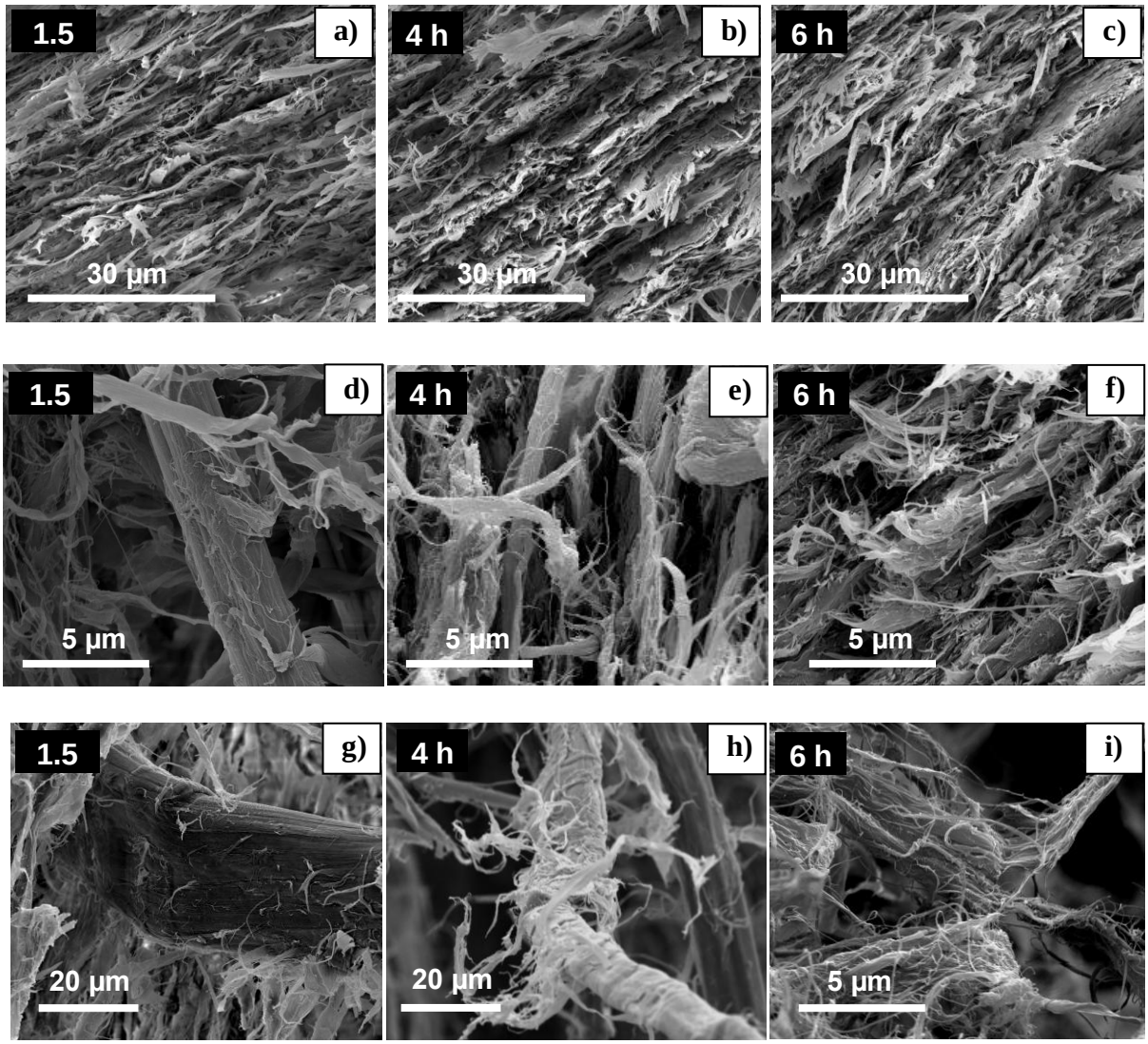

Figure 5.5. SEM pictures of the binder-free all-cellulose composites as a function of the refining time (a, d and g: 1.5 hrs; b, e and h: 4 hrs; c, f and i: 6 hrs), showing a general view of the surface (a-c), a detail of the structure (d-f) and of the fibres (g-i), evidencing an increase in fibrillation level with refining time. Note that the magnification in (i) is different from those in (g) and (h).

It is well documented that porosity is one of the main factors influencing the mechanical performance of natural fibre composites[29,30]. In order to assess and quantify the void content of the different binder-free composites, the density of the samples and raw flax fibres was measured to estimate their porosity following equation 5.1. Figure 5.6-a shows the evolution of composite density and porosity as a

function of refinement time, compared to that of neat flax fibres. A strong increase in density is observed during the first 3 hrs of refining; further refinement leads to a further increase, but to a lower extent, reaching a maximum at 6 hrs of treatment (ρ_{6h} = 1.62 g/cm^3). As expected, this value is still lower than the corresponding number for flax fibres (ρ_{flax} = 1.93 g/cm^3). As shown previously by SEM, the composite obtained after 1.5 hrs of refinement presents a high void content corresponding to a high porosity of 20.46%. A notable decrease in porosity of these materials is achieved after another 1.5 hrs of refining (17.07%). Similar to the density behaviour, longer refinement times slightly reduce the porosity of the composites, reaching a final value of 16.14% (6 hrs). At the first stages of the refinement treatment – up to 3 hrs – the initial fibrillation favours the cross-linking between the fibres, promoting the creation of a hydrogen-bonded network and renders a close packing of the fibres, which explains the remarkable increase of the panel density (and decrease of the porosity). Additional refining – from 3 to 6 hrs – creates a large amount of nanofibrils which further strengthens the hydrogen- or Van der Waals bonded fibre network, leading to a slight increase in density, and lower porosity. The flexural strength and modulus of the composites can be directly related to their density and inversely to the void content (porosity) present in the cellulose panels (Figure 5.6-b). Microvoids cause high stress-concentrations and are detrimental to mechanical properties. As expected, more porous materials exhibit lower mechanical properties. The strong increase of both flexure modulus and strength with increasing refinement time from 4 to 6 hrs, despite having similar porosities (16.63 and 16.14%, respectively), can be explained by the abundant presence of nanofibrils, leading to an enhanced hydrogen-bonded fibre network, as previously discussed.

Finally, the water absorption of the best-performing binder-free composite (6 hrs refining) was studied (Figure 5.7). Generally maximum water absorption occurs up to 10 hrs of immersion, after which voids are saturated with water, leading to a decrease in water absorption rate and a nearly constant weight with a water content of 37%.

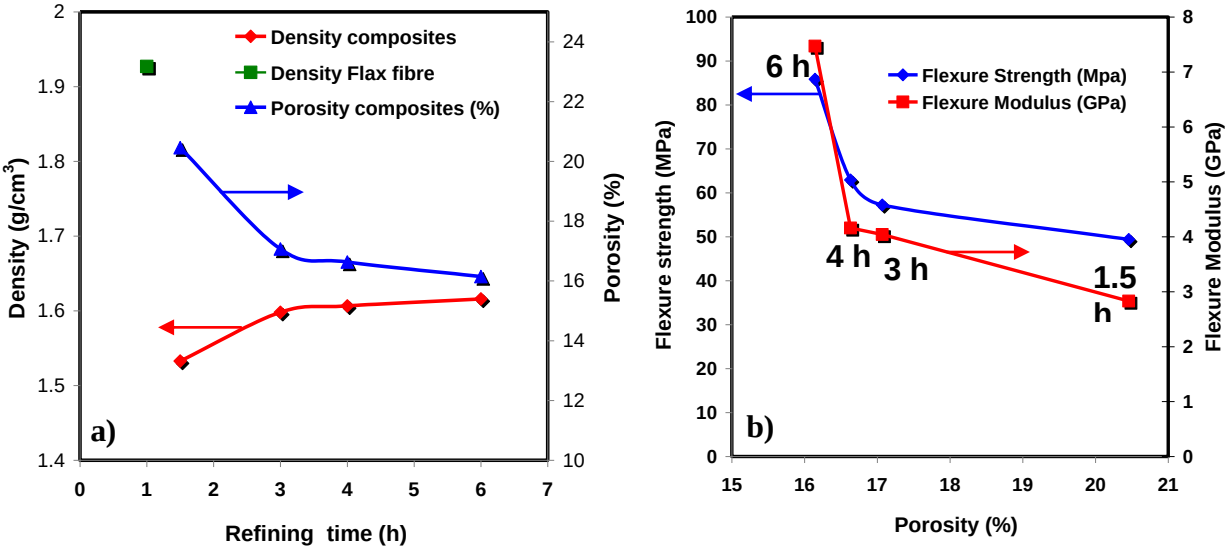

Figure 5.6. Density and porosity of the binder-free all-cellulose composites as a function of refining time (a). Relationship between the mechanical properties and the porosity of the binder-free all-cellulose composites (b).

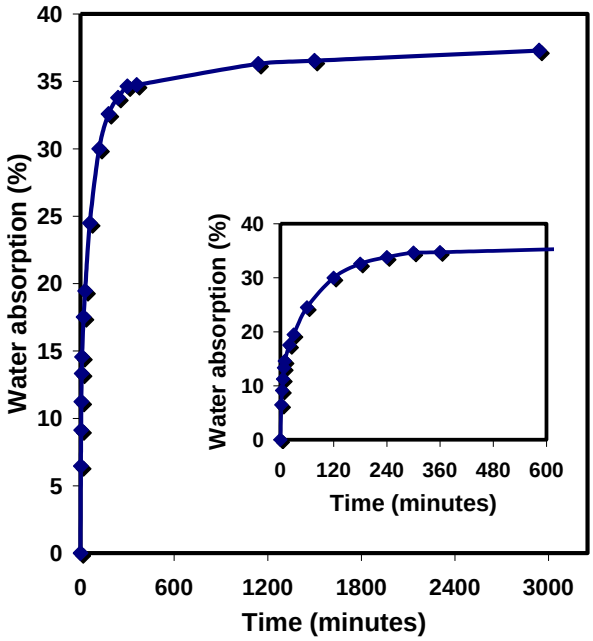

Figure 5.7. Water absorption of binder-free all-cellulose composite obtained after 6 hrs of refining. Inset: detail of the water absorption at short times.

5.3.3 Influence of initial fibre length on composite mechanical performance.

Three-point bending tests were carried out to study the effect of different initial flax fibre lengths on the mechanical performance of the self-binding cellulose composites. The influence of the initial fibre length prior to mechanical refinement on the flexural properties of the all-cellulose composites is displayed in Figure 5.8.

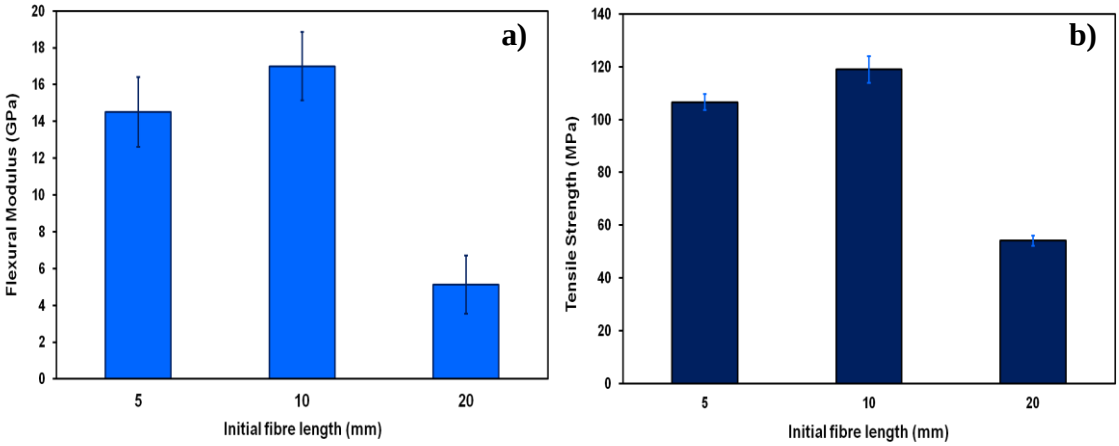

Figure 5.8. Flexural modulus (a) and strength (b) of the binder-free all-cellulose composites as a function of the initial flax fibre length.

Initial fibre lengths are not preserved in the final composites because the refining process does not only lead to fibre fibrillation, but also to fibre shortening. It is however expected that an increase in initial fibre length will also result in an increase of the final fibre length after fibrillation, leading to materials incorporating longer flax fibres and potentially higher strengths. Indeed, increasing the initial fibre length to 10 mm leads to a clear improvement of both flexural modulus and strength; however an increase of the initial flax fibre length to 20 mm did not yield any further property improvements. In fact, panels based on the longest flax fibres exhibited the poorest flexural properties exhibiting a flexural modulus and strength of 5.1 GPa and 54 MPa, respectively. The highest mechanical properties were obtained for composites produced from flax fibres with an initial length of 10 mm, and flexural

strength and modulus values as high as 119 MPa and 17 GPa, respectively, where achieved. The improvement in mechanical properties observed with increasing initial fibre length from 5 to 10 mm can be ascribed to enhanced fibre efficiency and its improved ability to distribute and transfer stresses as a result of the longer fibres. For similar reasons, long fibres of high aspect ratio are desirable for reinforcing composite materials as they are more effective in transferring loads and stopping cracks. However, in contrast to this a further increase in fibre lengths to 20 mm did not bring any additional improvements in mechanical properties. This unusual behaviour might be due to two possible reasons. First, the refining process of long fibres is typically more difficult than for shorter ones because of the numerous fibre entanglements in long fibres. The presence of a large amount of entanglements can hinder effective fibre fibrillation in the Hollander beater, leading to non-fibrillated fibres possessing insufficient specific surface area to form a dense material with an extensive self-binding network. This would explain the poor mechanical performance of these composites. Moreover, the probability of randomly oriented out-of-plane fibres crossing each other also increases as fibre length is increased. This will result in a lower in-plane stiffness in the X-Y plane and a subsequent increase in stiffness in the Z-direction[31,32]. In addition, such out-of-plane fibres can be bent during compression moulding in the hot press, reducing further their reinforcing efficiency. The presence of a large number of bent and out-of-plane oriented fibres in the panels as a result of longer fibre lengths can bring about a considerable reduction in flexural properties and could partly explain the mechanical behaviour of composites produced from 20 mm flax fibres. Finally, the high void content in these materials as a result of ineffective packing of long fibres might be another reason for their inferior mechanical properties.

The water absorption of the binder-free cellulose panels produced from different initial flax fibre lengths was determined at regular time intervals. The trend observed for all panels was similar to the one displayed in Figure 5.7. Panels only showed slight differences in water saturation levels. The binder-free all-cellulose composites produced from 5, 10 and 20 mm flax fibres reached water saturation level

of 38%, 35% and 37%, respectively. It is worth pointing out that despite differences in mechanical performance, all composites reached similar saturation levels. Table 5.2 lists water absorption data (after 24 hrs) of different wood-based materials reported in the literature. In comparison, the water absorption of our optimal binder-free all-cellulose composite is lower or similar to traditional panel products such as randomly oriented strandboard and medium density fibreboard (MDF), evidencing the high level of densification achieved in these materials.

Table 5.2. Water absorption (after 24 hrs of immersion) of different wood-based materials found in the literature and of our binder-free all-cellulose panel (produced from an initial fibre length of 10 mm and after 6 hrs of refining).

Material	Compressed pine wood panels[33]	Sapwood[34]	Randomly Oriented Standboard[35]	MDF1[36]	MDF2[37]	Binder-free composite
Water absorption (%)	55	66	75	57-67	19-26	35

5.3.4 Comparison with other fibre board materials

The current work proposes a new concept for developing self-binding cellulose panel products. In these materials, there is no need for a polymer resin or binder to bond the different fibres together. It was shown that optimal fibrillation of fibres is key for the creation of high-quality self-binding cellulose materials, since the refinement process increases the Van der Waals or hydrogen-bonding capacity between the fibres.

Initial fibre length plays an important role in the optimisation of these materials and has a strong effect on the final mechanical performance. The reason for this is that there is an optimal fibre length for efficient fibrillation. Fibres of 20 mm lengths show less effective fibrillation during mechanical refinement as a result of

the presence of more fibre entanglements. This results in less dense materials of lower mechanical performance. Panels based on fibres with an initial length of 10 mm showed good fibrillation and a 130% increase in flexural modulus and 40% increase in flexural strength. Therefore, initial fibre length has proven to be an essential parameter for achieving optimal mechanical properties for these nanofibrillated cellulose materials.

In general, nanofibrillated cellulose films will show superior mechanical properties to our binder-free all-cellulose panels due to the higher purity and finer structure of the nanofibrillated cellulose. Moreover, these cellulose nanopaper films have a true 2D in-plane fibre arrangement, while thicker all-cellulose panels may have also a fraction of fibres arranged in a more 3D out-of-plane fashion. Yano and Nakahara[14] prepared NFC films by compression mouldings with flexural strengths of 250 MPa, which is more than twice the flexural strength achieved for our self-binding all-cellulose composites. However, as previously mentioned, the main key issue for NFC commercialisation is to develop low cost energy efficient fibrillation methods compatible with industrial scale production. In contrast to most cellulose nanofibre fibrillation processes, the method used here does not require chemical pre-treatments, purification processes or the use of other non-environmentally friendly chemical substances. The current method is based on relatively simple mechanical fibrillation making this technology of great interest for industrialisation.

Table 5.3 shows a comparison of the flexural mechanical properties of some conventional natural fibre reinforced plastics, cellulose based panel products and the current binder-free cellulose panels. Clearly the flexural properties of our all-cellulose materials out-perform those of conventional NFRPs. Their outstanding mechanical performance and low water absorption, combined with their fully biobased nature, recyclability and biodegradability and lower production costs, make these materials interesting alternatives for conventional reinforced plastics, wood fibre composites and other fibreboards for building applications.

Table 5.3. Comparison of the flexural mechanical properties of conventional natural fibres reinforced plastics and the binder-free all-cellulose material (produced from flax fibre of 10 mm and after 6 hrs of refining, highlighted in grey background).

Property	Oriented Standboard[38]	Medium-Density Fiberboard[38]	PVC/WF[38]	HDPE/WF[38]	PP/WF[38]	PP/ Hemp[39]	PE/ Hemp[39]	Binder-free all-cellulose
Flexural strength (MPa)	20-28	35	42	20	48	55	25	119
Flexural modulus (GPa)	5-8	3.5	5.2	3.8	3.3	2.6	1.4	17

5.4 Conclusions

A new concept for cellulose based engineering materials has been introduced which allows for the production of high-performance materials made entirely from plants or other biobased waste sources. These biobased materials use no pre-treatment, no solvents and, most importantly, no resins or bonding agents. Instead bonding between fibres is achieved solely through Van der Waals or hydrogen-bonding between highly fibrillated (both internally and externally) cellulose fibres, making these self-binding materials environmentally friendly and recyclable. In fact, such cellulose materials could be recycled, similar to paper, by simple repulping processes into new all-cellulose materials. Here the concept was demonstrated for flax fibres and it has been shown that the level of refinement of the fibres is crucial for a sufficient level of bonding and network formation between fibres, and as a result good mechanical properties. The selection of an optimal initial flax fibre length has shown to be of pivotal importance for creating panel products with optimal mechanical properties. The flexural properties of these binder-free cellulose panels are highly impressive as they out-perform those of most conventional natural fibre reinforced plastics and wood panel products.

Moreover, since these materials are 100% biobased and have no matrix or resin binder, and therefore exhibit less polluting agents, their environmental impact is expected to be low. At the same time these materials are, in contrast to conventional panelboard products like MDF, fully recyclable and biodegradable, and represent as such an interesting new biobased alternative for traditional building materials.

5.5 References

[1] R. Malkapuram, V. Kumar, and Y. S. Negi, Journal of Reinforced Plastics and Composites 28 (10), 1169 **(2009)**.

[2] M. J. John and S. Thomas, Carbohydrate Polymers 71 (3), 343 **(2008)**.

[3] M. Q. Zhang, M. Z. Rong, and X. Lu, Composites Science and Technology 65 (15-16), 2514 **(2005)**.

[4] N. Soykeabkaew, N. Arimoto, T. Nishino, and T. Peijs, Composites Science and Technology 68 (10-11), 2201 **(2008)**.

[5]G. Bogoeva-Gaceva, M. Avella, M. Malinconico, A. Buzarovska, A. Grozdanov, G. Gentile, and M. E. Errico, Polymer Composites 28 (1), 98 **(2007)**.

[6] T. Nishino, I. Matsuda, and K. Hirao, Macromolecules 37 (20), 7683 **(2004)**.

[7] T. Nishino and N. Arimoto, Biomacromolecules 8 (9), 2712 **(2007)**.

[8] R. Arévalo, O. Picot, N. Soykeabkaew, and T. Peijs, Journal of Biobased Materials and Bioenergy 4 (2), 129 **(2010)**.

[9] L. Shen and M. K. Patel, Journal of Polymers and the Environment 16 (2), 154 **(2008)**.

[10] D. Klemm, D. Schumann, F. Kramer, N. Hessler, M. Hornung, H. P. Schmauder, and S. Marsch, *Nanocelluloses as innovative polymers in research and application*, in *Polysaccharides II*, ed. D. Klemm. Berlin, Springer-Verlag Berlin. 205, 49-96, **(2006)**.

[11] S. Yamanaka, K. Watanabe, N. Kitamura, M. Iguchi, S. Mitsuhashi, Y. Nishi, and M. Uryu, Journal of Materials Science 24 (9), 3141 **(1989)**.

[12] T. Nishino, K. Takano, and K. Nakamae, Journal of Polymer Science Part B-Polymer Physics 33 (11), 1647 **(1995)**.

[13] S. J. Eichhorn, A. Dufresne, M. Aranguren, N. E. Marcovich, J. R. Copadona, S. J. Rowan, C. Weder, W. Thielemans, M. Roman, S. Renneckar, W. Gindl, S. Veigel, J. Keckes, H. Yano, K. Abe, M. Nogi, A. N. Nakagaito, A. Mangalam, J. Simonsen, A. S. Benight, A. Bismarck, L. A. Berglund, and T. Peijs., Journal of Materials Science 45 (1), 1 **(2009)**.

[14] H. Yano and S. Nakahara, Journal of Materials Science 39 (5), 1635 **(2004)**.

[15] T. Zimmermann, E. Pöhler, and T. Geiger, Advanced Engineering Materials 6 (9), 754 **(2004)**.

[16] M. Henriksson, L. A. Berglund, P. Isaksson, T. Lindstrom, and T. Nishino, Biomacromolecules 9 (6), 1579 **(2008)**.

[17] H. Sehaqui, N. Ezekiel Mushi, S. Morimune, M. Salajkova, T. Nishino, and L. A. Berglund, ACS Applied Materials & Interfaces 4 (2), 1043 **(2012)**.

[18] M. A. Hubbe, O. J. Rojas, L. A. Lucia, and M. Sain, Bioresources 3 (3), 929 **(2008)**.

[19] T. Saito, R. Kuramae, J. Wohlert, L. A. Berglund, and A. Isogai, Biomacromolecules 14 (1), 248 **(2013)**.

[20] I. Siro and D. Plackett, Cellulose 17 (3), 459 **(2010)**.

[21] D. Klemm, F. Kramer, S. Moritz, T. Lindstrom, M. Ankerfors, D. Gray, and A. Dorris, Angewandte Chemie-International Edition 50 (24), 5438 **(2011)**.

[22] T. Saito, I. Shibata, A. Isogai, N. Suguri, and N. Sumikawa, Carbohydrate Polymers 61 (4), 414 **(2005)**.

[23] T. Saito, S. Kimura, Y. Nishiyama, and A. Isogai, Biomacromolecules 8 (8), 2485 **(2007)**.

[24] M. Hirota, N. Tamura, T. Saito, and A. Isogai, Carbohydrate Polymers 78 (2), 330 **(2009)**.

[25] T. Isogai, T. Saito, and A. Isogai, Cellulose 18 (2), 421 **(2011)**.

[26] M. Henriksson, G. Henriksson, L. A. Berglund, and T. Lindstrom, European Polymer Journal 43 (8), 3434 **(2007)**.

[27] M. Paakko, M. Ankerfors, H. Kosonen, A. Nykanen, S. Ahola, M. sterberg, J. Ruokolainen, J. Laine, P. T. Larsson, O. Ikkala, and T. Lindstrom, Biomacromolecules 8 (6), 1934 **(2007)**.

[28] T. Suopajarvi, H. Liimatainen, and J. Niinimaki, Cellulose 19 (1), 237 **(2012)**.

[29] J. Varna, R. Joffe, L. A. Berglund, and T. S. Lundstrom, Composites Science and Technology 53 (2), 241 **(1995)**.

[30] S. F. M. Almeida and Z. S. N. Neto, Composite Structures 28 (2), 139 **(1994)**.

[31] J. L. Thomason and M. A. Vlug, Composites Part A: Applied Science and Manufacturing 27 (6), 477 **(1996)**.

[32] J. L. Thomason, M. A. Vlug, G. Schipper, and H. G. L. T. Krikor, Composites Part A: Applied Science and Manufacturing 27 (11), 1075 **(1996)**.

[33] O. Unsal, S. N. Kartal, Z. Candan, R. A. Arango, C. A. Clausen, and F. Green Iii, International Biodeterioration & Biodegradation 63 (5), 548 **(2009)**.

[34] E. Baysal, A. Sonmez, M. Colak, and H. Toker, Bioresource Technology 97 (18), 2271 **(2006)**.

[35] J. W. Kirkpatrick and H. M. Barnes, Bioresource Technology 97 (15), 1959 **(2006)**.

[36] Y. Zheng, Z. L. Pan, R. H. Zhang, B. M. Jenkins, and S. Blunk, Industrial Crops and Products 23 (3), 318 **(2006)**.

[37] A. D. Çavdar, M. Ertas, H. Kalaycıoglu, and M. H. Alma, Materials and design 31 (5), 2561 **(2010)**.

[38] H. H. Jiang and D. P. Kamdem, Journal of Vinyl & Additive Technology 10 (2), 59 **(2004)**.

[39] I. Taha and G. Ziegmann, Journal of Composite Materials 40 (21), 1933 **(2006)**.

6

Binder-free all-cellulose composites: Kraft and hemp reinforced recycled paper composites.

6.1 Introduction

As previously mentioned in Chapter 5, different natural fibre sources including plants and wastes with high cellulose content could be used for the production of binder-free all-cellulose composites. The use of flax fibres as raw

material provided fully recyclable and biodegradable panel products with impressive flexural properties that out-perform those of most conventional natural- or wood fibre panel products. However, the application of natural fibres such as flax and hemp for the manufacture of these products at an industrial scale could pose several problems related to their availability, storage and particularly price. Most of these natural fibres are annual plants and therefore have seasonal availability and a relatively short harvesting period. Consequently, these fibres must be acquired over a short period of time and stored for the rest of the year. During such a long storage period, natural fibre properties may deteriorate, thus providing lower yields. In addition, storage requires a lot of (mostly manual) handling of the bulky stalk bundles, which involves an increase of the raw material price. The fact that the harvesting of these natural fibres is often manual will also significantly raise cost. All these drawbacks and particularly the high price of hemp and flax fibres compared to other natural fibres, has generated interest in alternative cellulose sources from waste such as recycled paper. The use of recycled paper as a raw material for biobased materials could provide a cost-effective raw material source for binder-free all-cellulose composites due to their low cost and availability throughout the year, thus eliminating possible problems associated with storage. However, it is well-known that recycled fibres present inferior strength properties and lower bonding capability compared to those of virgin fibres (fresh from pulping fibres) as a consequence of the different chemical and physical changes undergone during pressing, drying, printing, storage, re-pulping and deinking[1]. Most of the changes that reduce the strength properties of the recycled fibres arise from the drying process, since it brings partially irreversible closure of small pores in the fibre wall, as well as an increased resistance to swelling during rewetting[2]. The phenomenon associated with this partially irreversible loss of flexibility and swelling capacity of fibres after drying is known as hornification. The hornification occurs when the hydrogen bonds that were formed between cellulose chains in the cell wall during drying cannot be broken during the rewetting process, resulting in only partial swelling since some chains remain bonded[3, 4]. The loss of swelling capability of recycled fibres leads to reduced fibre flexibility, lesser interfibre contacts, and therefore reduced interfibre network

bonding[5]. Therefore, drying influences fibre strength, fibre swelling and bonding potential[6], which are the main factors that govern the mechanical properties of self-bonding cellulose composites. Different approaches can be followed for the recovering of the bonding potential of recycled fibres including re-refining and blending with virgin fibre pulps[7].

In an attempt to produce binder-free all-cellulose composites at reduced cost, the use of highly fibrillated recycled paper fibres as a raw material has been proposed in this work. Due to the lower strength and bonding capability of these fibres compared to ligno-cellulose fibres, hemp or bleached kraft fibres have been incorporated in the recycled paper pulp matrix with the aim of enhancing the mechanical properties. Firstly, the reinforcing effect of the addition of non-fibrillated and semi-fibrillated hemp fibres to a recycled paper matrix was studied as a function of hemp fibre content. Subsequently, an optimum fibre content was defined for both hemp and kraft fibres. Finally, the effect of the degree of fibrillation of these reinforcements on the mechanical properties of the binder-free recycled paper composites was assessed as a function of fibre type.

6.2 Experimental methodology

6.2.1 Preparation of binder-free all-cellulose composites based on hemp fibres and recycled paper.

In this work, highly fibrillated recycled paper has been used for the production of binder-free cellulose composites. This never-dried recycled paper pulp with the required degree of fibrillation was produced by DRUMAPARM (Austria). In order to increase the mechanical performance of these recycled paper materials, hemp fibres were incorporated into the recycled paper pulp prior to panel processing. Hemp fibres with a fibre length of 5 mm were kindly supplied by EKOTEX Ltd.

(Czech Republic). Figure 6.1 shows images of the recycled paper pulp (a) and hemp fibres (b) as received.

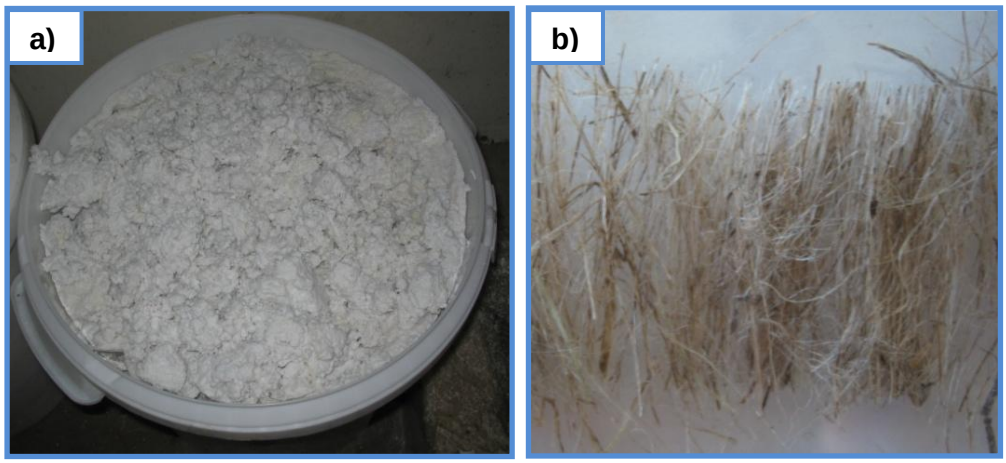

Figure 6.1. Images of recycled paper pulp (a) and hemp fibres (b).

The experimental procedure followed for the manufacture of binder-free hemp fibre reinforced recycled paper composites is similar to the one described in Chapter 5 except for some minor differences (see Figure 5.2 in Chapter 5). Here, the refining process was replaced by the incorporation of hemp fibres into the recycled paper pulp. In order to study the reinforcing effect of non-fibrillated and semi-fibrillated hemp fibres into recycled paper based composite materials two different approaches were applied for the incorporation of hemp fibres into the paper matrix. The first method consisted of directly mixing the hemp fibres with the paper pulp in a mixer device (Figure 6.2-a) for 15 min without the application of any refining treatment since the recycled paper pulp was already refined. After mixing, this homogenous mixture was subjected to a room temperature press (10 bar) to create a partially dewatered precursor (Figure 6.3) that was finally dried under pressure in a hot press. In a second approach, hemp fibres and recycled paper pulp were simultaneously mixed and refined in a Hollander beater (also termed Valley beater, Figure 6.2-b) for 5 min at very low solid content (98% water). The resulting suspension was filtered in order to achieve the required consistency for the

subsequent pressing at room temperature. The partially dewatered precursor obtained was finally dried in a hot press at 140 ºC.

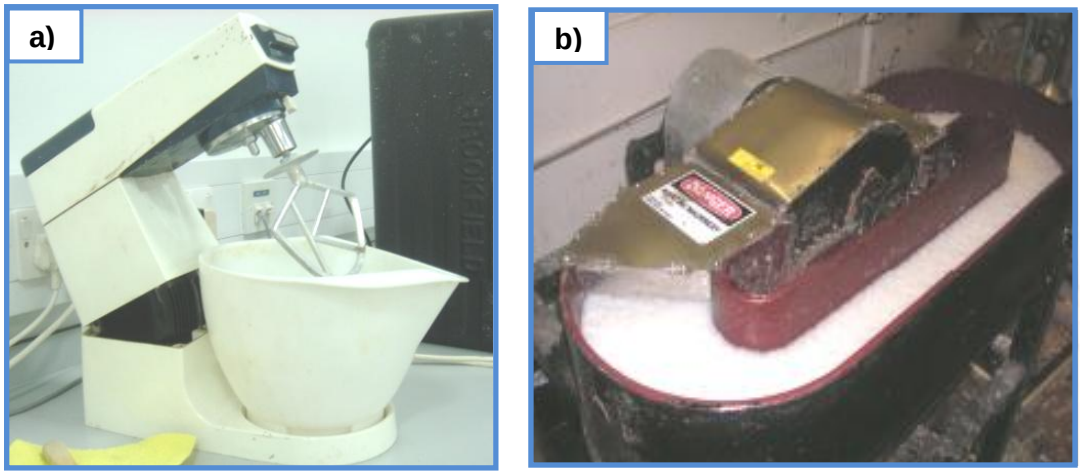

Figure 6.2. Pictures of mixer device (a) and Hollander or Valley beater (b).

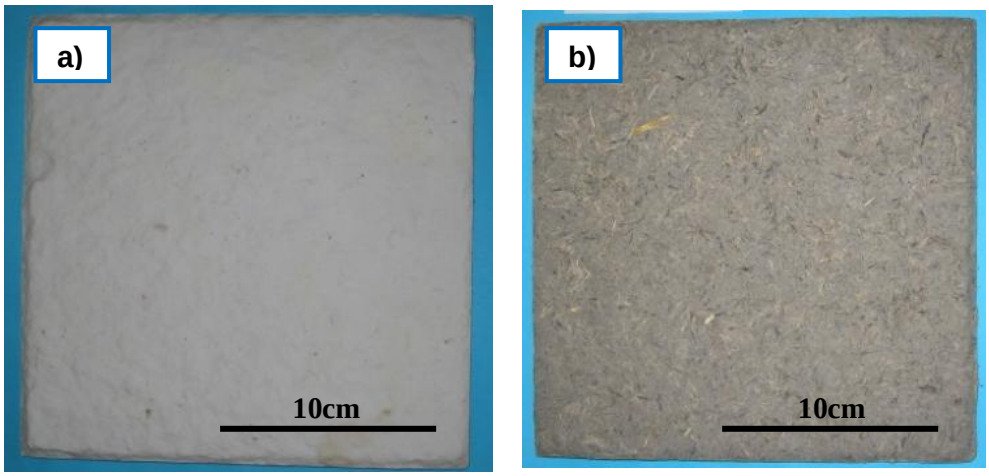

Figure 6.3. Images of partially dewatered precursors based on recycled paper pulp (a) and a blend of non-fibrillated hemp fibres and recycled paper pulp in a 50/50 wt.% ratio (b).

The hemp fibre content in recycled paper materials was varied from 0 to 70 wt.% for both processing methodologies. In addition, drying conditions of the paper

based composites were modified due to their lower compression strength compared to flax based materials which manifested itself by the appearance of cracks in the compression moulded panels after drying as shown in Figure 6.4-a. The optimum parameters applied for drying these paper based panel materials in the hot press are summarised at Table 6.1. The recycled paper based materials dried under these new conditions did not show any cracks or processing defects as shown in Figure 6.4-b.

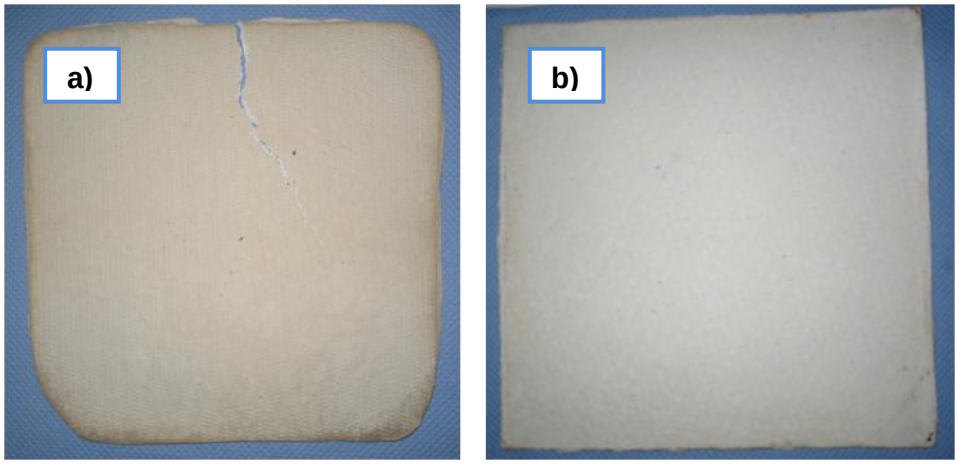

Figure 6.4. Images of binder-free recycled paper materials obtained after drying a) according to the conditions applied for flax based materials and b) under modified conditions specially optimised for paper based composites.

Table 6.1. Hot press conditions (T= temperature; P= pressure and t= time) applied for the successful drying of recycled paper composites.

Hot Press Parameters		
Phase 1	**Phase 2**	**Phase 3**
T=140 °C	T=140 °C	T=20 °C
P=20 bar	P=40 bar	P=40 bar
t=1200 s	t=1200 s	t=600 s

After determining the optimum hemp fibre content that led to the binder-free recycled paper composite materials with optimal mechanical performance, the influence of the degree of fibrillation of hemp fibres on the mechanical properties of these composite materials was studied for that optimal composition. Here, the corresponding amounts of hemp fibres and recycled paper pulp to the optimum weight ratio were mixed and refined simultaneously in Valley or Hollander beater for different periods of time ranging from 5, 10, 15, 20, 25 and 30 min. The production of panels made from these composite blends fibrillated at different refining times was carried out following the previously described procedure.

6.2.2 Preparation of binder-free all-cellulose composites based on bleached kraft fibres and recycled paper.

In this section, bleached kraft pulps were used as reinforcement in binder-free recycled paper composites. Bleached kraft fibres with a fibre length between 2-3 mm were provided in sheet form by Norske Skog (Norway). Figure 6.5 shows an image of the bleached kraft fibre sheet as received.

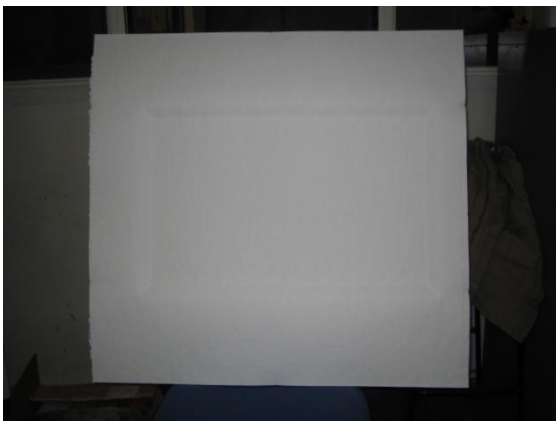

Figure 6.5. Image of bleached kraft fibre sheet.

In this case, the kraft fibres were disintegrated and refined in Valley beater for 15 min prior to the addition of the recycled paper pulp. Both kraft fibres and paper pulp were mixed in Valley beater for 30 min. This blend was subsequently filtered and pressed at room temperature. Finally the partially dewatered precursor was dried using compression moulding under conditions listed in Table 6.1. In order to define the optimum kraft fibre content, kraft/recycled fibre blends were prepared at different weight ratios including 0/100, 30/70, 50/50 and 70/30 wt/wt.%.

Once the optimum kraft fibre content was determined, the effect of the degree of fibrillation of the kraft fibres on the mechanical properties of the binder-free kraft/recycled paper composites was studied for that composition. Kraft and recycled fibres were mixed and refined in Valley beater for different periods including 5, 10, 15, 20, 25 and 30 min and the resulting blends were used for the production of self-binding all–cellulose composites.

6.3 Characterisation of the materials

The degree of fibrillation of kraft and hemp fibres was indirectly evaluated by the determination of the drainability of the pulp suspensions through the Schopper-Riegler method[8]. This test measures the rate of water drainage from the pulp fibres and gives an indication of the degree of fibrillation and hydration of fibres. Figure 6.6 shows the Schopper-Riegler apparatus employed for performing such tests together with a working schematic. The functioning of this device is quite simple as can be deduced from Figure 6.6. The technology is based on the principle that finer pulp suspensions are more hydrated, slowing down the water drainage through the filter and allowing most of the water to pass through orifice B. The low amount of water collected from orifice A indicates the ºSR value of the pulp in the graduated collector vessel. The ºSR value corresponding to highly fibrillated pulp fibres will be higher than the one of low fibrillated pulp. For lightly beaten pulp suspensions, the

water drainage through the filter is fast, and consequently, water is accumulated in the cone. In this case, most of the drained water will pass through orifice A instead of B, leading to a lower ºSR value.

Pulp suspensions of hemp and kraft fibres were prepared according to the standard operational procedure SOP PAP 24. At least 5 suspensions of each pulp were tested, and the ºSR values were averaged.

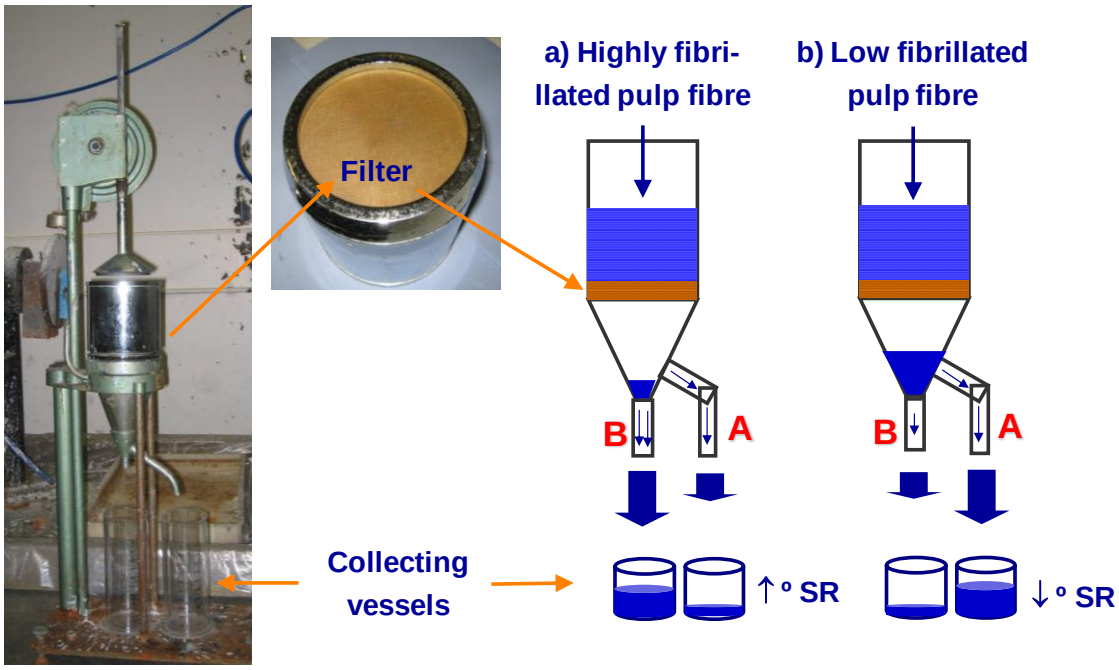

Figure 6.6. Image of the Schopper-Riegler test.

The morphology of kraft fibres as a function of the refining time was also observed using an Olympus BX60 optical microscope.

Three-point bend tests of binder-free all-cellulose panels were performed using an Instron 5584 universal tester at room temperature with a 1 kN load cell (Figure 6.7-b). The cross head speed was 5 mm/min. In order to reveal potential anisotropy in these materials, specimens were cut into strips in both longitudinal and

transverse directions according to ASTM D790–02 standard (procedure A) (Figure 6.7-a). At least 8 specimens of each sample were tested, and the values were averaged.

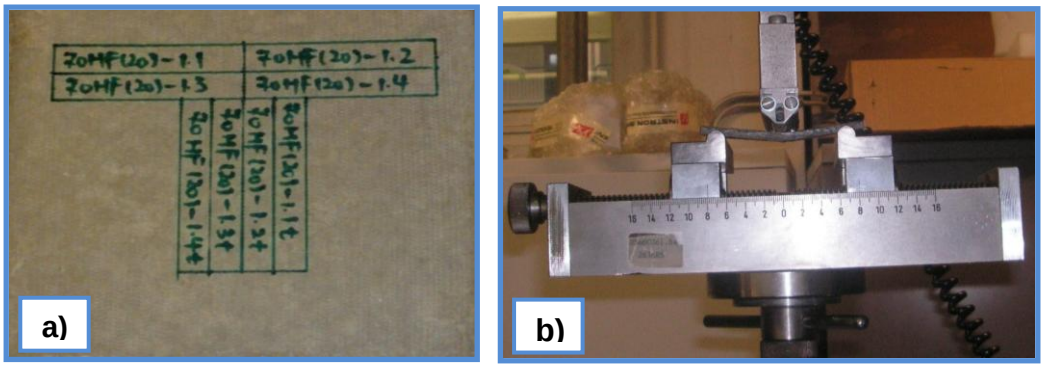

Figure 6.7. a) Image of samples drawn according to ASTM D790–02 standard (procedure A) in both longitudinal and transverse directions of a hemp/paper based panel cut for subsequent flexural testing, and b) Image of a sample subjected to a three-point bend test.

The microstructure and morphology of the binder-free all-cellulose composites were analysed by scanning electron microscopy (SEM), using a JEOL JSM 6300 microscope at an accelerating voltage of 10 kV. Prior to examination, the surface of the samples was sputtered with a thin layer of gold to make them conductive.

The water absorption of the best performing binder-free all cellulose composite was monitored at regular intervals. Prior to carrying out these tests, the samples were dried in an oven at 60 °C until constant weight. The dried specimens were then submerged in a Grant Y-38 distilled water bath at 23 °C and weighed using a high precision balance at selected periods of time. The water absorption (MC = moisture content) was determined from the weight difference (equation 6.1):

$$MC(\%) = 100 \cdot \frac{W - W_d}{W} \qquad \text{(Equation 6.1)}$$

where W and W_d are the weight of wet and dried composites, respectively. Times ranging from 0 to 48 hrs were studied.

6.4 Results and discussion

6.4.1 Binder-free hemp fibre reinforced recycled paper composites

Reinforcing effect of non-fibrillated hemp fibres

Binder-free composites based on non-refined hemp fibres with a fibre length of 5 mm and a recycled paper matrix were prepared at hemp fibre contents ranging from 0, 10, 30, 50 and 70 wt.%. The mechanical properties of the resulting composites were studied by three-point bend tests. The effect of the non-fibrillated hemp fibre content on the flexural properties of hemp reinforced recycled paper is shown in Figure 6.8. In contrast to binder-free flax composites, the material based solely on recycled paper exhibited extremely poor mechanical properties due to the shorter and lower strength fibres of recycled paper. Flexural modulus and strength of these recycled paper based panels were 2.7 GPa and 34 MPa, which is already competitive with wood plastic composites (WPC) or medium density fibre boards (MDF). The addition of up to 30 wt.% hemp fibres lead to a slight improvement of the stiffness of the panels reaching a value of 3.5 GPa. However, a strong decrease of the flexural modulus was observed at higher hemp fibre contents (Figure 6.8-a). The flexural strength of the recycled paper composites with non-refined hemp fibres as a function of hemp content is shown in Figure 6.8-b. Surprisingly, here the addition of hemp fibres showed no improvements, in fact the addition of non-refined fibres had a rather detrimental effect on the bending strength of the panels for the whole composition range. However, this effect was again more pronounced at higher fibre contents. The origin of this behaviour is related to the lack of refinement of the hemp

fibres and the absence of nanofibrils on the hemp fibre surface which could lead to effective cross-linking with the recycled paper matrix fibres. In the case of non-refined fibres none of this cross-linking effectively takes place, hence leading to poorly compacted materials with a high void content and poor interfacial adhesion. Especially the poor interfacial adhesion between hemp and paper fibres prevents effective stress transfer from the paper matrix to the hemp fibres, making that these fibres mainly act as defects. The reduction in the flexural strength observed with the incorporation of non-refined hemp fibres in these materials could be due to a combination of high void content together with weak interfaces caused by poor fibre-fibre cross-linking. As such, the addition of non-fibrillated hemp fibres to recycled paper failed to prove true reinforcement, hindering the formation of a continuous hydrogen-bonded cellulose network which is essential for achieving good mechanical properties in these types of materials.

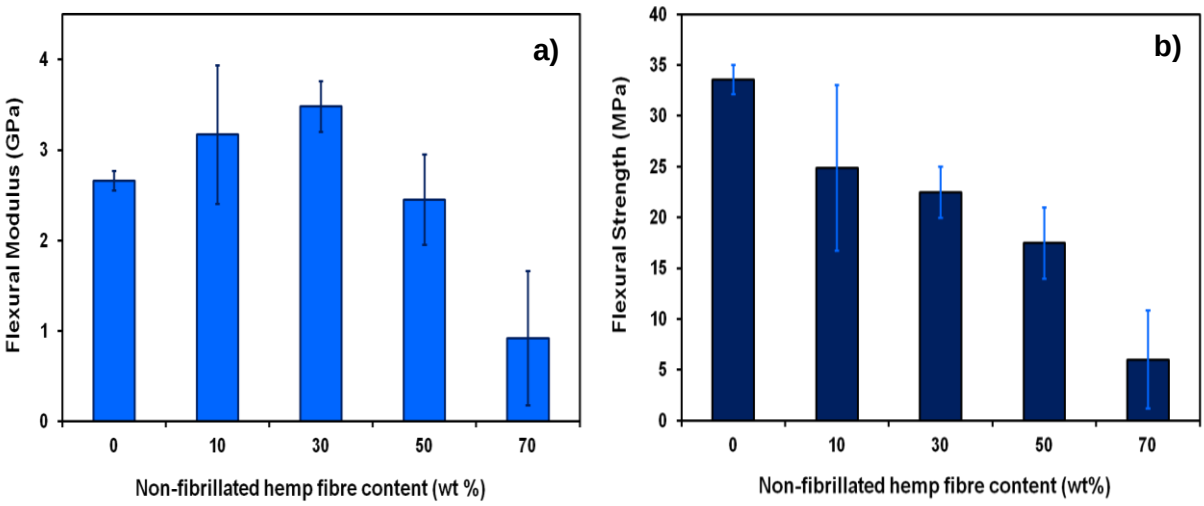

Figure 6.8. Flexural properties of self-binding non-fibrillated hemp/recycled paper composites as a function of hemp fibre content.

Logically, this worsening in mechanical properties will be more significant for higher fibre contents, thus, justifying the poorer mechanical performance observed for paper based composites reinforced with 50 and 70 wt.% hemp fibres. The isotropic nature of these panels was assessed by determining the flexural properties of the specimens cut in both longitudinal and transverse directions. Figure 6.9-a shows typical three-point bending curves obtained for longitudinal and transverse samples of paper based composites containing 30 wt.% hemp fibres. Identical mechanical behaviour was observed for both test directions, indicating that these panels are isotropic and possess a homogenous distribution of randomly oriented hemp fibres. All hemp and paper based materials exhibited planar-isotropic behaviour except for the one with the highest hemp fibre content. As shown in Figure 6.9-b, the flexural properties of the recycled paper composite reinforced with 70 wt.% hemp fibres showed a strong directional dependence, indicating anisotropy probably as a result of a heterogeneous distribution of the hemp fibres in the recycled paper matrix. In general, the difficulty of achieving homogenous distributions at high fibre loadings, usually leads to heterogeneous and anisotropic materials as shown for the 70 wt.% hemp reinforced paper composite.

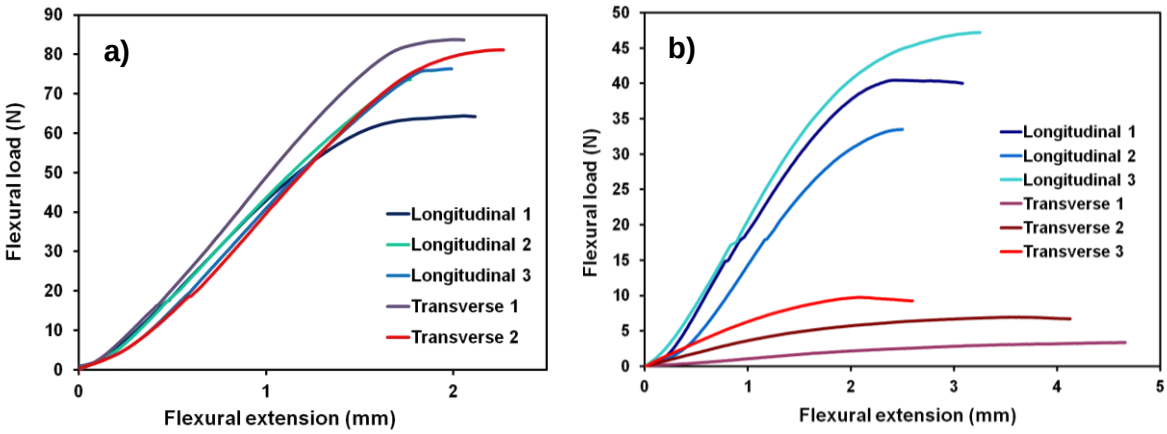

Figure 6.9. Typical flexural load-displacement curves for longitudinal and transverse samples of paper based composites containing a) 30 and b) 70 wt.% non-fibrillated hemp fibres.

Reinforcing effect of semi-fibrillated hemp fibres

In order to establish if a mild refinement of the hemp fibres can provide sufficient fibrillation and improved interfacial interactions with the recycled paper pulp, hemp fibres and recycled paper pulp were simultaneously mixed and fibrillated in Valley beater for 5 min. The mechanical properties of these self-binding composites based on recycled paper and semi-fibrillated hemp fibres were again studied by three-point bend test. All panels with different hemp fibre contents showed isotropic mechanical behaviour since their flexural properties did not vary with sample directionality (Figure 6.9-a), thus demonstrating that this processing method also achieves homogenous hemp fibre distributions even at very high hemp fibre contents unlike the mixing procedure in the previous section. Flexural properties of hemp/recycled paper composite materials as a function of hemp content are shown in Figure 6.10. An increase of the flexural properties with hemp fibre content can be seen until a maximum is reached followed by a drastic drop. The maximum values attained at 30 wt.% fibre content were 4.5 GPa and 42 MPa for flexural modulus and strength, respectively. The observed loss in mechanical performance at high hemp fibre contents can be ascribed to an increase in void content brought about by an insufficient amount of highly fibrillated recycled paper fibres surrounding the reinforcing hemp phase. Clearly also here the mechanical properties of these self-binding cellulose composites rely on their Van der Waals and hydrogen-bonded fibre network, which in turn, depends on the specific fibre surface area. Since in these materials a greatly enhanced network is achieved by increasing the specific surface area of the fibres, the amount of fibre-fibre interactions are increased by the fibrillation process. The addition of a large amount of semi-refined fibres with a relatively low specific surface area reduces the number of interfibre interactions and leads to materials with high void content in a rather weak fibre network, hence giving reduced mechanical properties for composites with 50 and 70 wt.% hemp fibres.

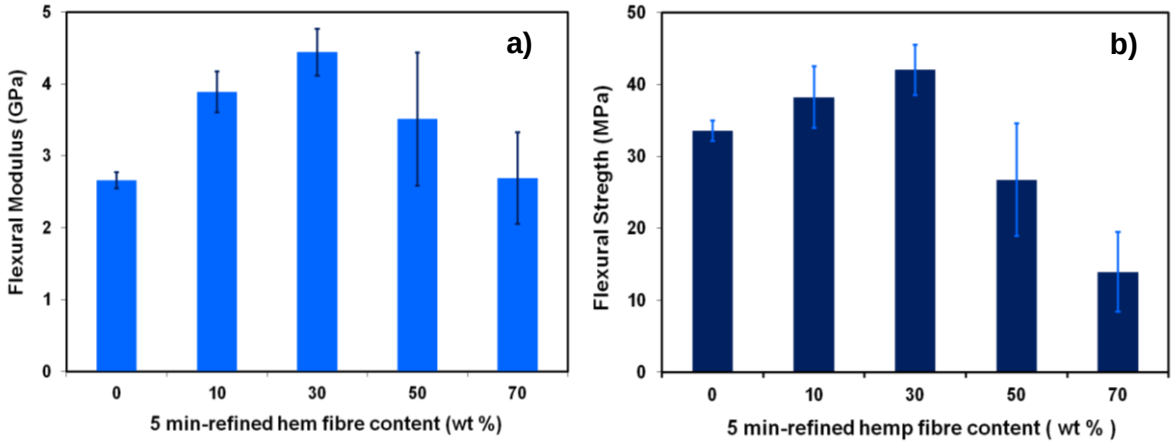

Figure 6.10. Flexural properties of binder-free semi-fibrillated hemp/recycled paper composites as a function of hemp fibre content.

The influence of semi-fibrillated hemp fibres on their reinforcing effect is illustrated in Figure 6.11.

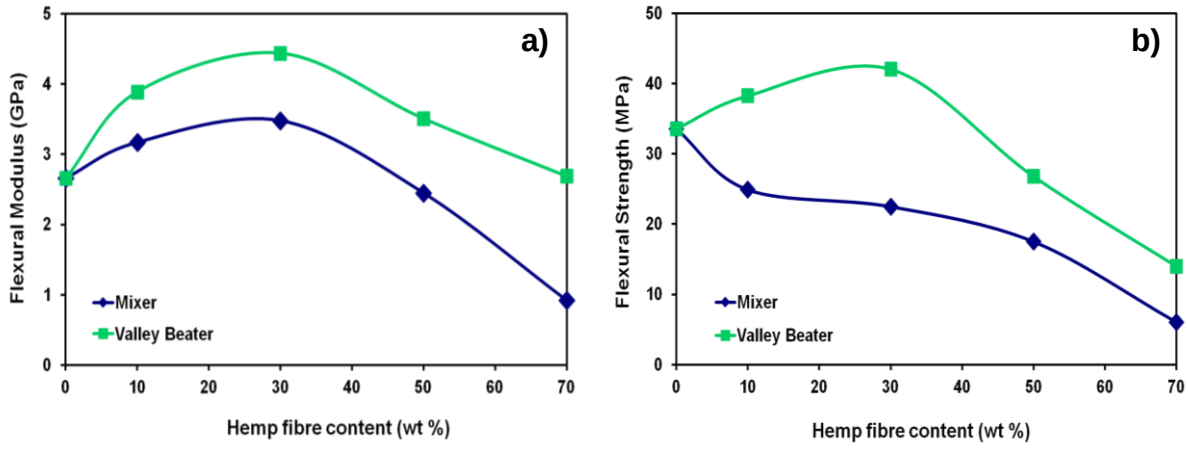

Figure 6.11. The influence of the mixing method on the flexural modulus (a) and strength (b) of binder-free hemp/recycled paper composites at different fibre contents.

The use of non-fibrillated hemp fibres in recycled paper composites led to a modest improvement in panel stiffness of 25% but resulted in a strong reduction in

flexural strength. The addition of semi-refined hemp fibres (5 min) provided, however, a more impressive 66% improvement in flexural modulus and a 25% increase in flexural strength, thus evidencing the importance of fibre fibrillation for reinforcing this type of materials.

Influence of degree of hemp fibre fibrillation

The effect of the degree of fibrillation of the hemp fibres on the mechanical properties was studied for the recycled paper composites reinforced with 30 wt.% hemp fibres since this composition showed optimal mechanical performance and homogeneity as demonstrated in the previous section. Corresponding amounts of hemp fibres and recycled paper pulp for this optimum weight ratio were again mixed and refined simultaneously in Valley beater for different periods of time including 5, 10, 15, 20, 25 and 30 min. The influence of refining time on flexural properties of the self-binding hemp/recycled paper composites is shown in Figure 6.12. The flexural properties of the materials based on pure recycled paper are also included in the chart with the aim of assessing the reinforcing effect of 30 wt.% hemp fibres fibrillated at different refining times.

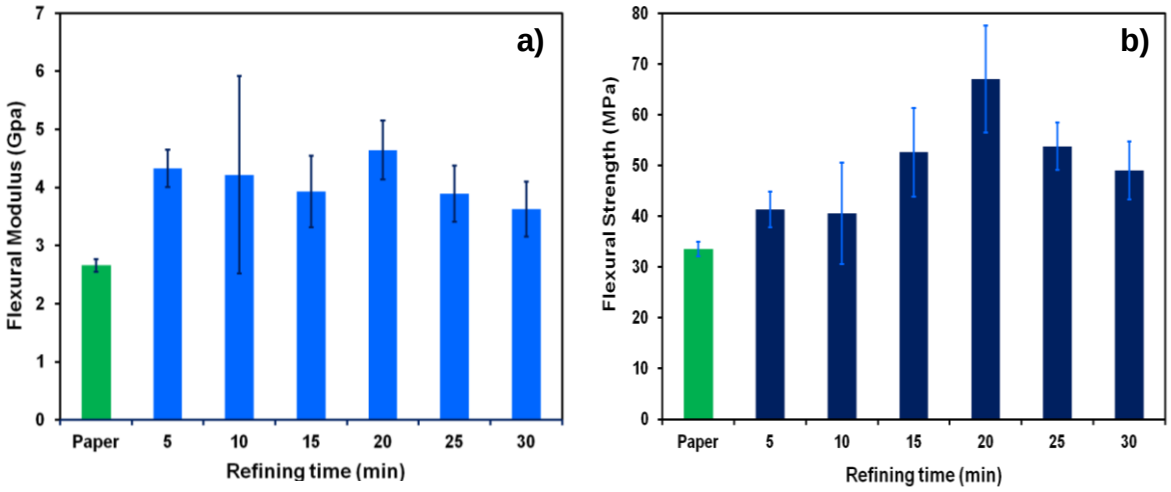

Figure 6.12. Effect of the refining time on the flexural properties of binder-free recycled paper composites reinforced with 30 wt.% hemp fibres. For comparison purposes, the mechanical properties of materials made solely of recycled paper are also included (green).

A slight increase of the flexural modulus with refining time can be observed until it reaches a maximum value of 4.6 GPa at a refining time of 20 min (Figure 6.12-a). Longer refining times lead to a progressive reduction in panel stiffness. Despite the flexural strength following a similar trend to that of the flexural modulus, the effect of fibre refining time on this mechanical property was more pronounced. A maximum value of 67 MPa in panel bending strength was achieved for composites reinforced with hemp fibres refined for 20 min (Figure 6.12-b). The increase of the refining time from 5 to 20 min resulted in an improvement of 15% in panel stiffness, while bending strength increased by 62% compared with pure recycled paper panels.

These results are in general agreement with composite reinforcing mechanisms which typically show that improved fibre-matrix adhesion has a far greater effect on composite strength than on composite stiffness. Moreover, it seems also to be in agreement with general short fibre composite theory, which predicts that typically higher fibre aspect ratios are needed to achieve maximum composite strengths compared to composite stiffness[9, 10]. Refinement can lead to an increase in hemp fibre aspect ratios which in turn can have a more pronounced effect on composite strength rather than stiffness (Figure 6.13). The relatively small increase in stiffness after the initial 5 min of refining might be due to the fact that property build-up with increasing fibre aspect ratio in composites is quicker for composite stiffness than for composite strength. Typically for short fibre composites, fibre aspect ratios (i.e. fibrillation) need to be higher for maximum strength than for maximum stiffness. An increase from 5 to 20 min refining time brings an increase of the degree of fibrillation of hemp fibres, and so of their specific surface area, thus favouring hemp fibre interaction with the surrounding paper matrix. This improved hemp-recycled paper interaction will not only bring about improved fibre-matrix adhesion due to more effective hemp-paper cross-linking through an increase in hydrogen bonds, but also a considerable reduction in void content, which will also greatly contribute to the improvement in flexural strength for the 20 min refined samples. Although longer refining times should provide a further improvement in hemp-recycled paper adhesion, it would also bring about an excessive deconstruction

of the reinforcing fibre structure as well as a reduction in fibre length and thus aspect ratio, explaining the loss in mechanical properties after 25 and 30 min of refining.

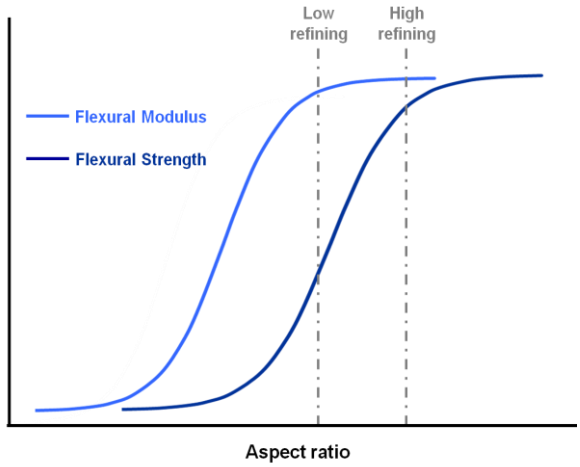

Figure 6.13. Typical influence of fibre aspect ratio on the short fibre composite stiffness and strength according to micromechanical composite theory.

In order to study the degree of fibrillation of the hemp fibres as a function of refining time, hemp pulp suspensions were tested by the Schopper-Riegler method. In order to determine the ºSR value corresponding to an optimum degree of fibrillation for hemp fibres, hemp pulp suspensions were prepared at different refining times (Figure 6.14).

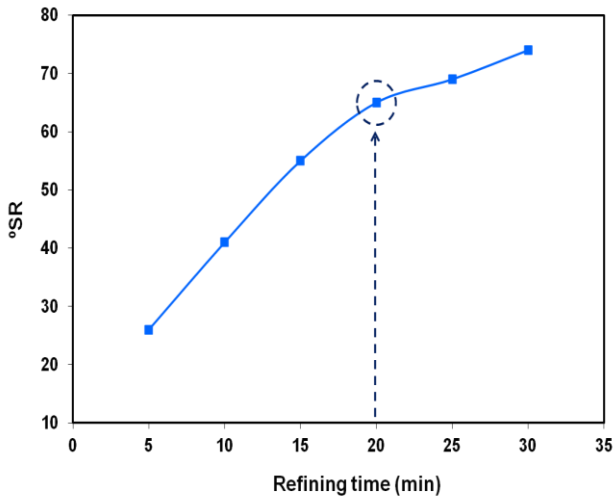

Figure 6.14. Effect of the refining time on the ºSR values for hemp pulps. The optimum degree of fibrillation for hemp fibres in binder-free recycled paper based composites is encircled.

A progressive increase of the drainage resistance with refining time can be clearly observed, indicating the effectiveness of the refining treatment in fibrillation and hydration of hemp fibres. The ºSR value corresponding to the optimum degree of fibrillation for hemp fibres was found to be 65.

For a further understanding of the influence of refining time on reinforcement microstructure and hemp-paper adhesion, fracture surfaces of these self-binding cellulose composites were studied by SEM (Figure 6.15). At a low refining time of 5 min (Figure 6.15-a), almost intact hemp fibres are seen surrounded by a compacted matrix phase consisting of highly fibrillated recycled paper fibres. The absence of fibrils on the hemp fibre surface hinders an effective adhesion between the coarse hemp fibres and finer recycled paper fibres. This in turn may lead to the significant debonding observed along the hemp-paper interface (Figure 6.15-b), which explains the low mechanical properties of this composite. The SEM images corresponding to the hemp-paper composite obtained after 10 min of refining (Figure 6.15:c-d) indicate that the fibrillation process has started for some of the hemp fibres providing more effective adhesion between hemp and recycled paper fibres through hemp nanofibrils (Figure 6.15-d), leading to an improvement in mechanical properties. However, the presence of some non-refined hemp fibres can still be observed (Figure 6.15-c). Although an increase of 5 min in refining time leads to an enhancement of hemp-paper adhesion, and thus better compaction of the material as a result of a higher degree of fibrillation, still some non-refined fibres are visually present (Figure 6.15-e). An optimum refining time was found at 20 min since it provides a sufficient degree of fibrillation of most hemp fibres, achieving improved hemp-paper bonding while preserving the hemp fibre microstructure and reinforcing efficiency, leading to a compact material with negligible void content which explains its high mechanical performance (Figure 6.15-f). The SEM image corresponding to the binder-free hemp-recycled paper composites obtained after 25 min of refining (Figure 6.15-g) shows excessive fibrillation of hemp fibres, resulting in a loss in hemp reinforcing efficiency, and as a result a reduction in mechanical properties. Finally, further refining leads to a well compacted material with improved adhesion between hemp

nd recycled paper fibres but lower mechanical properties due to a loss in reinforcing efficiency as a result of a too high level of fibrillation (Figure 6.15-h).

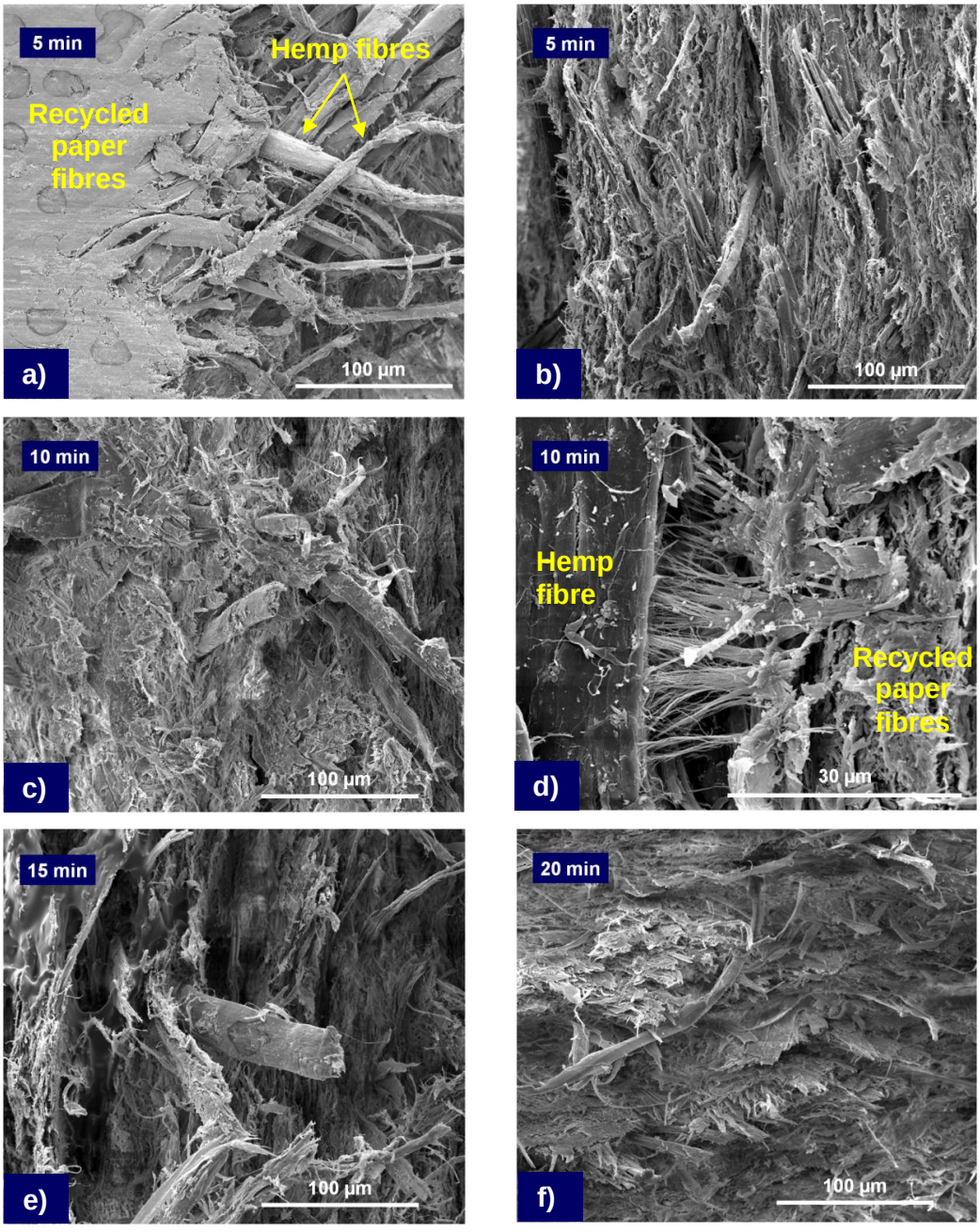

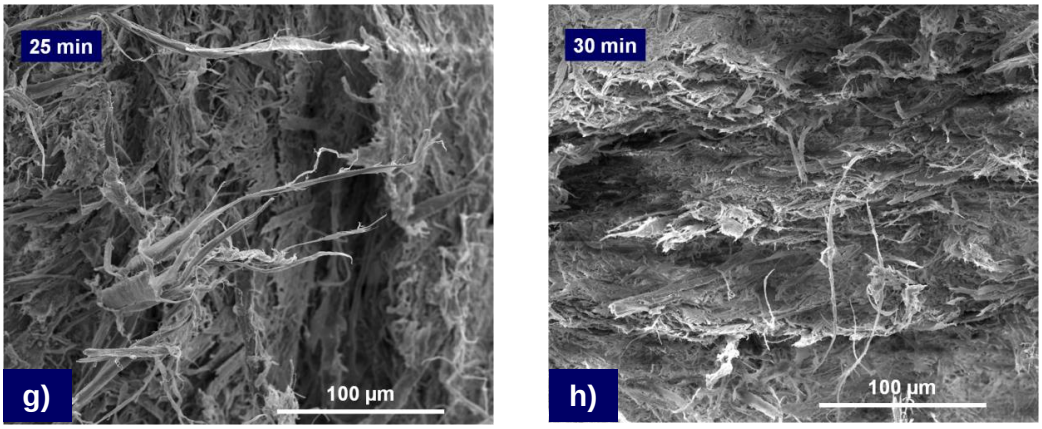

Figure 6.15. SEM images of the microstructure of binder-free recycle paper composites reinforced with 30 wt.% hemp fibres refined for 5 (a-b), 10 (c-d), 15 (e), 20 (f), 25 (g) and 30 (h) min.

Overall, the addition of a 30 wt.% of hemp fibres refined for 20 min in a recycled paper pulp matrix resulted in a 100% improvement in flexural strength (67 MPa) and a 75% increase in flexural modulus (4.6 GPa). This significant improvement in panel strength seems more related to optimum fibrillation, leading to improved hemp-paper adhesion while preserving their fibrous reinforcing structure, whereas the enhancement in flexural modulus is mainly the result of the increase in hemp fibre content.

6.4.2 Binder-free bleached kraft fibre reinforced recycled paper composites

Reinforcing effect of semi- fibrillated bleached kraft fibres

In order to determine the optimum kraft fibre content for the reinforcement of recycled paper based composite materials, different weight ratios of kraft fibres

previously refined for 15 min, including 10, 30, 50, and 70 wt.% were mixed with the recycled paper pulp in Valley beater for 30 min. The mechanical properties and the anisotropy of these self-binding composites were studied as a function of kraft fibre content. The study of the flexural properties in both longitudinal and transverse panel directions revealed isotropic behaviour for all panels regardless of the kraft fibre content, demonstrating a homogeneous distribution of kraft fibres into the recycled paper pulp. The effect of the addition of different weight ratios of partially refined kraft fibres on the panel's flexural properties is displayed in Figure 6.16.

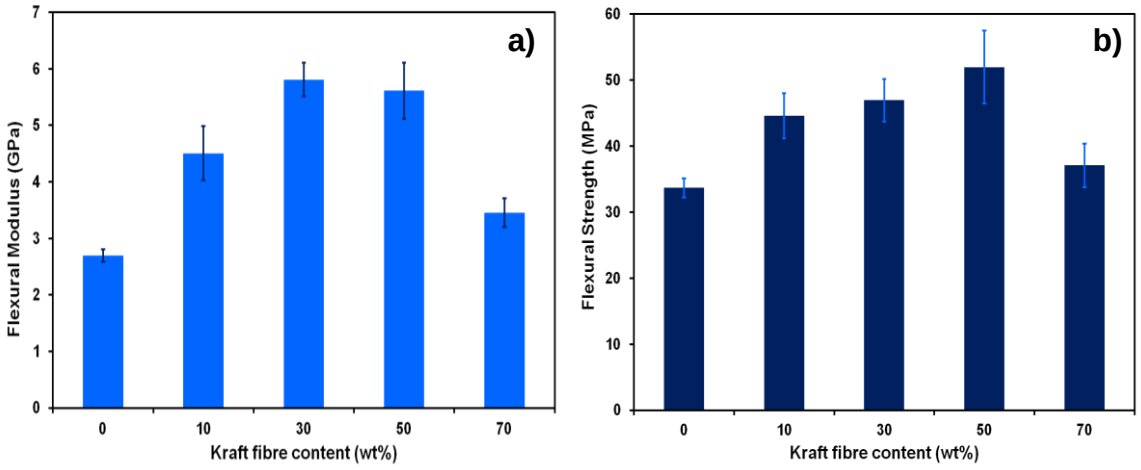

Figure 6.16. Flexural properties of binder-free semi-fibrillated kraft/recycled paper composites as a function of kraft fibre content.

A strong increase of the flexural modulus with kraft fibre content can be clearly observed until it reaches a maximum value of 5.8 GPa at 30 wt.% fibre content. A further increase of the kraft fibre content up to 70 wt.% leads to a progressive reduction of the panel stiffness. Unlike the flexural modulus, a maximum bending strength of 52 MPa was achieved for a kraft fibre content of 50 wt.%. As previously described, this loss in mechanical performance at high fibre contents is presumably due to the high void content in these materials and insufficient highly fibrillated recycled paper fibres to connect to the reinforcing phase.

Influence of the degree of fibrillation of bleached kraft fibres

The influence of the degree of fibrillation of bleached kraft fibres on their reinforcing effect was studied for a blend of kraft fibre/recycled paper pulp in a 30/70 wt.% ratio. Although a binder-free recycled paper composite containing 50 wt.% kraft fibres showed a slightly higher flexural strength than those of 30 wt.% kraft fibres, the poor reproducibility as evidenced by the large scatter for both flexural modulus and strength (Figure 6.16) combined with the higher amount of reinforcement required for that composition were the main reasons for discarding the results obtained for this fibre content. Therefore, kraft fibres and recycled paper pulp in a 30/70 wt.% ratio were mixed and refined simultaneously in Valley beater for different periods of time including 5, 10, 15, 20, 25 and 30 min. The influence of refinement time on the flexural properties of kraft/recycled paper composites is shown in Figure 6.17. The effect of kraft fibrillation on flexural properties of the self-binding kraft/recycled paper composites was not evident up to 20 min of refining, at which a strong improvement of both modulus and strength was observed. At 25 min of refining time, the flexural properties reach maximum values of 5.9 GPa and 75 MPa for stiffness and strength, respectively.

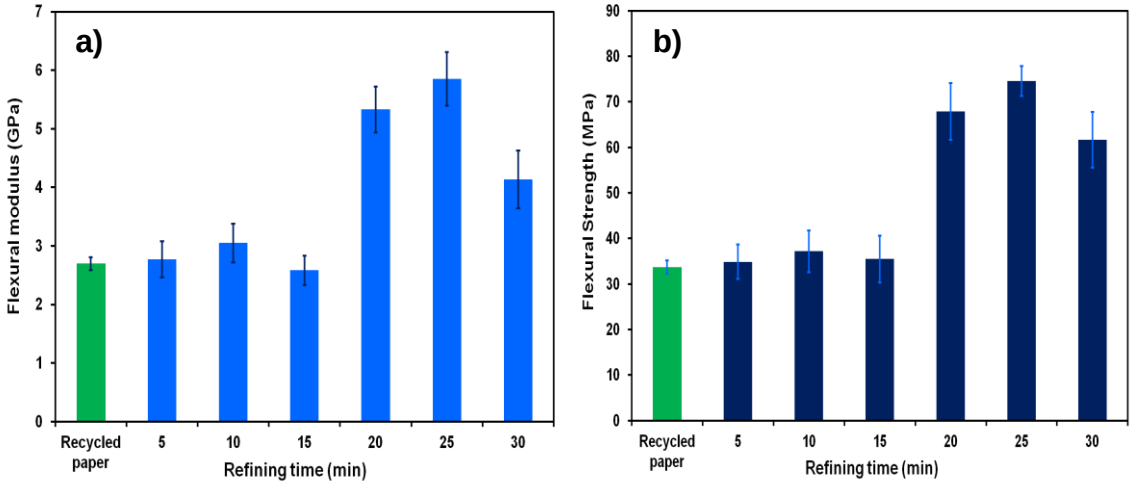

Figure 6.17. Effect of the refining time on flexural properties of binder-free recycled paper composites reinforced with 30 wt.% bleached kraft fibres. For comparison purposes, the mechanical properties of materiala made solely of recycled paper are also included (green).

The loss of mechanical performance observed for composites prepared with refining times of 30 min is due to excessive fibrillation, leading to fibre damage. Similar to hemp/recycled paper composites, the enhancement in flexural properties is mainly due to increased interfacial bonding and more effective interfibre crosslinking achieved through increased levels of kraft fibre surface fibrillation. However, in contrast to hemp based systems, where the increase in mechanical properties was gradual, a more sudden increase in properties was observed for kraft based composites after 15 min of refinement. This could be attributed to the difficulty of fibrillating once-dried bleached kraft pulp and the strong hydrogen bonding between fibres generated during typical pulp drying processes after removal of the matrix[11]. Seth[12] studied the physical properties and response to refining of never-dried and dried kraft pulps and reported that never-dried pulps require less energy to reach a certain degree of fibrillation due to higher swelling and conformability of never-dried fibres. Therefore, pulps should only be dried if they need to be stored or transported as in this case. In addition, the removal of hemicellulose results in the replacement of relatively flexible cellulose–hemicellulose–cellulose bonds by more rigid cellulose–cellulose bonds, thus increasing the refining energy required for a given degree of fibrillation[13]. Therefore, the results suggest that effective fibrillation of bleached kraft fibres starts after 15 min refining.

In order to support this statement, the degree of fibrillation of kraft fibres was determined by the Schopper-Riegler method at different periods of time (Figure 6.18). For the first 15 min only a slight increase in the degree of fibrillation of kraft fibres can be observed thus explaining the negligible effect of these fibres on mechanical properties. However, a further increase in refining times lead to a drastic improvement in fibre fibrillation, explaining the sudden increase in composite properties for refinement times of 20 and 25 min. Excessive fibrillation of kraft fibres (ºSR value of 58) achieved at 30 min refining is the reason for the subsequent loss in reinforcing efficiency. Hence, the optimum degree of fibrillation of kraft fibres for use as reinforcements in recycled paper based composites corresponds to a ºSR value of 35 and is achieved after a refining of 25 min. The optimum ºSR value of

kraft fibres refined for 25 min was considerably lower than the one of hemp fibres due to the higher resistance to fibrillation shown for once-dried kraft pulp fibres.

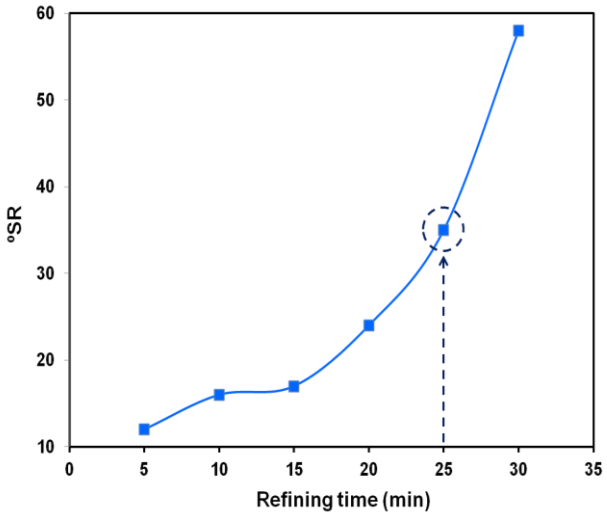

Figure 6.18. Effect of the refining time on the ºSR value of kraft pulps. Optimum fibrillation of kraft fibres for the production of self-binding kraft/recycled paper composites is encircled.

The morphology of the kraft fibres as a function of refining time was observed by optical microscopy (Figure 6.19).

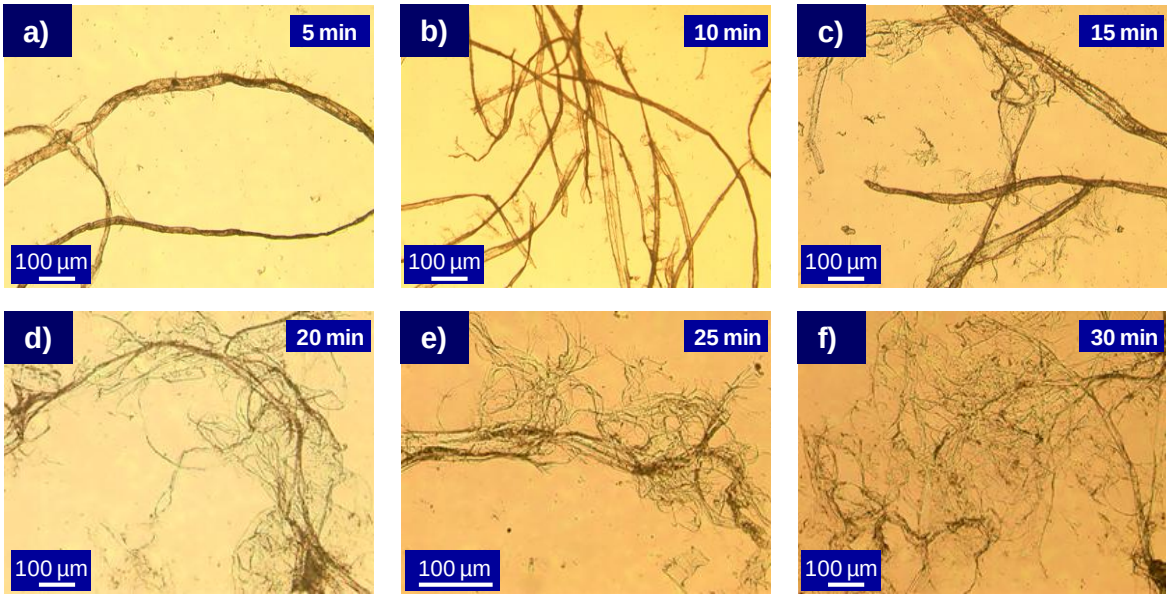

Figure 6.19. Effect of the refining time on the morphology of the kraft fibres. OM images of kraft fibres refined for 5 (a), 10(b), 15(c), 20(d), 25(e), and 30 min (f).

The OM images clearly support the results obtained through the Schopper-Riegler method, evidencing that effective refining is obtained after 15 min of treatment. It is also worth highlighting that 30 min of refining leads to excessive degradation of the initial fibre structure, thus resulting in a loss of reinforcing efficiency.

In an attempt to get a deeper understanding of the mechanical behaviour as a function of refining time, the fracture surface of these kraft/recycled paper composites was analysed by SEM (Figure 6.20). The magnification of the images was selected according to the desired region that needed highlighting. On the left (a, c, e, g, i and k), SEM images show the reinforcement embedded in a matrix phase based on highly fibrillated recycled paper fibres, whereas a detail of reinforcement fibrillation is illustrated on the right (b, d, f, h, j and l). The SEM images corresponding to the kraft/recycled paper composites obtained after 5 (Figure 6.20: a-b), and 10 min (Figure 6.20: c-d) of refining indicate that the fibrillation process has not yet started, thus preventing good kraft-paper adhesion. At a refining time of 15 min, a few fibrils appear on kraft fibre surfaces (Figure 6.20-e), however large voids around these fibres indicate that this degree of fibrillation is still not sufficient for achieving effective kraft-recycled paper fibre crosslinking (Figure 6.20-f). A further 5 min increase in refining time provides an enhancement of the kraft fibre specific surface area (Figure 6.20-h), allowing an increase in fibre-fibre interactions resulting in improved kraft-recycled paper adhesion and better consolidation, which in turn will lead to enhanced mechanical properties. However, also here the presence of non-fibrillated kraft fibres can still be observed (Figure 6.20-g). A highly densified structure, consisting of fibrillated kraft fibres surrounded by recycled paper fibres, is achieved after 25 min of refining (Figure 6.20-i). At this refining time, the level of fibrillation of the kraft fibres is sufficient to render improved kraft-paper fibre bonding while preserving their fibrous microstructure and so its reinforcing ability, thus justifying the high mechanical performance of these composites (Figure 6.20-j). SEM images corresponding to kraft/recycled paper composites obtained after 30 min of refining (Figure 6.20-l) show excessive fibrillation as well as high

microstructural damage of kraft fibres, leading to loss in reinforcing efficiency and reduced composite properties. The distinction between kraft fibres and recycled paper fibres in this composite structure becomes less clear due to the high degree of fibrillation of the kraft fibres (Figure 6.20-k).

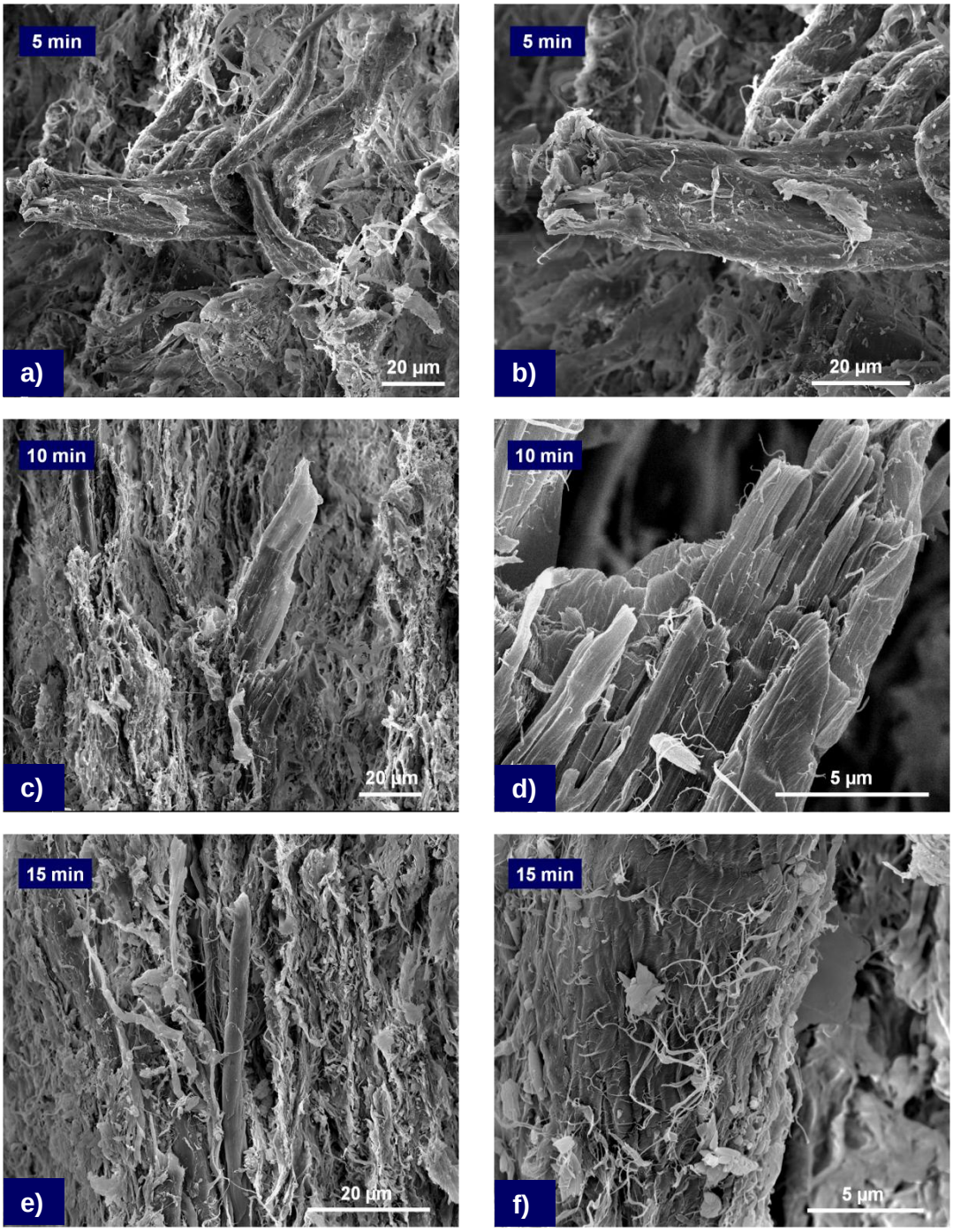

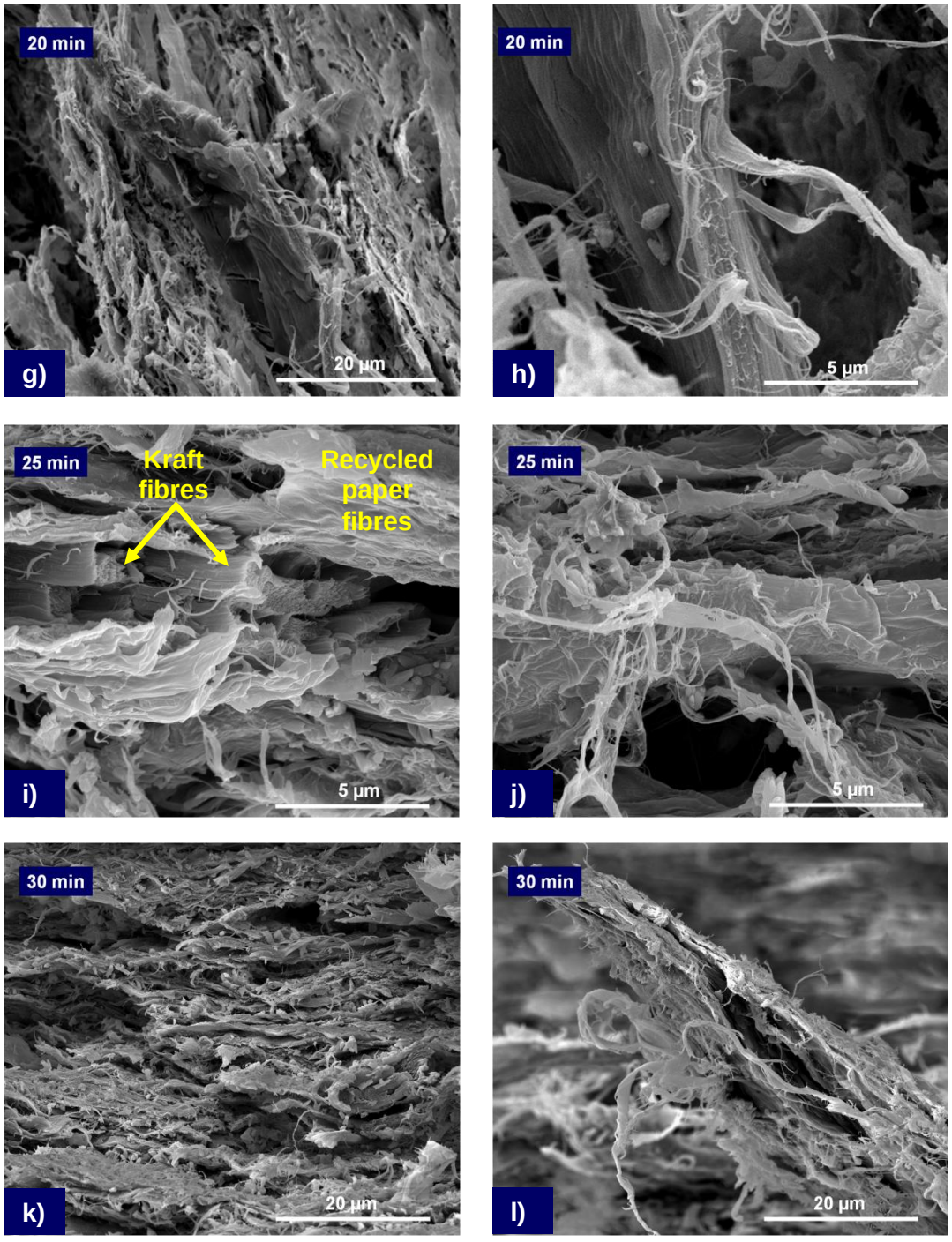

Figure 6.20. SEM images of fracture surfaces of the binder-free recycled paper composites reinforced with 30 wt.% kraft fibres refined for 5 (a-b), 10 (c-d), 15(e-f), 20(g-h), 25(i-j), and 30 min (k-l).

Finally, the water absorption behaviour of well-compacted binder-free kraft/recycled paper composite panels was studied at regular intervals. (Figure 6.21). For these studies compositions were selected that were well densified and showed optimal mechanical properties.

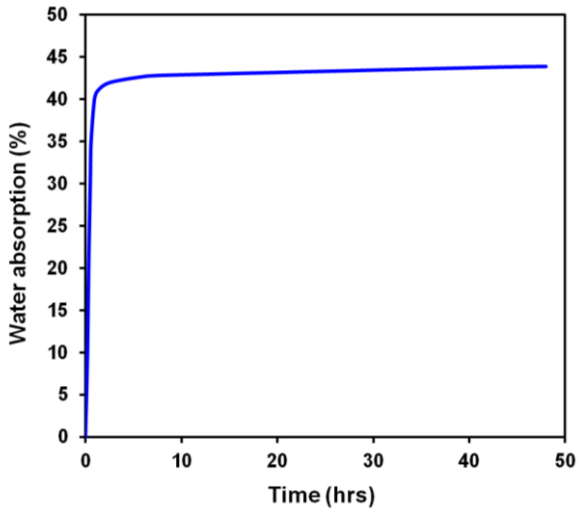

Figure 6.21. Water absorption of binder-free recycled paper composite reinforced with a 30 wt.% of kraft fibres fibrillated for 25 min.

The initial high water absorption rate occurs by the filling of material pores with water during the first 6 hrs of immersion. Once these pores are saturated with water, the absorption significantly decreased leading to an almost constant weight and a water saturation level of 43%. These recycled paper based composites reinforced with 30 wt.% of kraft fibres fibrillated for 25 min showed a water absorption behaviour similar to self-binding all-flax composites, but their water saturation level was around 8% higher. Having said that, after 24 hrs of immersion, the water content of these all-cellulose kraft/recycled paper composites is still lower or similar to wood panel products such as randomly oriented strandboard and MDF (see Table 5.2 in Chapter 5). This is particularly impressive as here the entire

material is based on cellulose and there is no polymer resin present to protect the fibres.

6.5 Conclusions

Potentially low-cost binder-free all-cellulose composites were successfully developed using recycled paper as a matrix reinforced with hemp or kraft fibres using the environmentally friendly processing method described in Chapter 5. Partial fibrillation of the reinforcing fibres (hemp or kraft) was crucial for obtaining good reinforcing efficiency of these fibres in the recycled paper matrix since the addition of non-refined fibres had a strongly detrimental effect on composite strength as a result of a lack of adhesion between the hemp or kraft fibres and the recycled paper matrix. Surface fibrillation of the hemp or kraft reinforcement increased their specific surface area, thus allowing for greater fibre-fibre interactions, leading to improved adhesion as well as a better densification and lower void content of the composites.

The addition of 30 wt.% of semi-refined reinforcements into recycled paper pulp led to a strong improvement of their mechanical properties for both hemp and kraft fibre composites. Optimal fibrillation of the cellulose reinforcement was key for achieving a maximum reinforcing effect. Fibres with a lower degree of fibrillation did not possess sufficient specific surface area to achieve strong bonding with the recycled paper pulp matrix, leading to poor compaction and low mechanical performance. Conversely, long refining times resulted in loss of reinforcing efficiency as a result of excessive destruction of the fibre structure as well as aspect-ratio. An optimum degree of fibrillation for hemp fibres was reported at a drainage resistant ºSR value of 65, which was attained after 20 min of refining, while an optimal ºSR value of only 35 was reached after 25 min refining for kraft fibres.

In summary, the addition of a 30 wt.% of kraft fibres refined for 25 min in recycled paper pulp resulted in a 123% improvement in panel strength (75 MPa) and a 119% increase in panel stiffness (5.9 GPa) compared to pure recycled paper panels. Although the mechanical properties of both hemp and kraft fibre reinforced recycled paper composites were lower than those reported for the all-flax composites in Chapter 5, these fully biobased composites still out-performed many conventional wood fibre and natural fibre composites (See Table 5.3 in Chapter 5).

In this work, the feasibility of producing low cost fully recyclable and biodegradable binder-free all-cellulose composites has been demonstrated through the successful manufacture of self-binding biobased composites based on recycled paper pulp and hemp or kraft fibres through a simple and environmentally friendly mechanical fibrillation method. Since these materials use also waste streams rather than more expensive ligno-cellulose fibre streams this can lead to highly cost-effective panel products that can compete with existing products such as MDF and wood plastic composites (WPC).

6.6 References

[1] N. Wistara and R. Young, Cellulose 6 (4), 291 **(1999)**.

[2] M. A. Hubbe, R. A. Venditti, and O. J. Rojas, BioResources 2 (4), 739 **(2007)**.

[3] W. D. Wanrosli, Z. Zainuddin, and S. Roslan, Industrial Crops and Products 21 (3), 325 **(2005)**.

[4] J. L. Minor, R. H. Atalla, and T. M. Harten, Journal of Pulp and Paper Science 19 (4), 152 **(1993)**.

[5] M. Ahmad Azizi, H. Jalaluddin, T. Paridah Md, R. Hossein, I. Rushdan, S. Seyed Rashid Fallah, and M. Ainun Zuriyati, Modern Applied Science 4 (9), 21 **(2010)**.

[6] R. L. Ellis and K. Sedlachek, TAPPI Journal 76 (2), 143 **(1993)**.

[7] R. C. Howard, Journal of Pulp and Paper Science 16 (5), 143 **(1990)**.

[8] *Methods for determination of the drainability of pulp Schopper-Riegler method,* BS 6035-1:1981.

[9] J. L. Thomason and M. A. Vlug, Composites Part A: Applied Science and Manufacturing 27 (6), 477 **(1996)**.

[10] J. L. Thomason, M. A. Vlug, G. Schipper, and H. G. L. T. Krikor, Composites Part A: Applied Science and Manufacturing 27 (11), 1075 **(1996)**.

[11] K. Abe, S. Iwamoto, and H. Yano, Biomacromolecules 8 (10), 3276 **(2007)**.

[12] R. S. Seth, Solutions (Tappi) 1 (1), 1 **(2010)**.

[13] H. Pande and D. N. Roy, Pulp and Paper Canada 99 (11), **(1998)**.

7

Effect of refining time on fracture behaviour of binder-free all-flax composites

7.1 Introduction

As previously mentioned in Chapter 5, the key to the production of high performance binder-free all-cellulose composites is to create a strong Van der Waals and/or hydrogen bonded network between fibres by increasing their specific surface area and thus, their self-bonding capability through a refining process. Mechanical properties were found to increase with increasing fibre refinement, due to an increase

in network density. In the present chapter, the fracture behaviour of self-binding all-cellulose composites will be examined. Since refinement time is a key processing parameter in controlling the mechanical properties of these materials the fracture resistance of these materials will be studied as a function of refinement time, and will be based on a) measuring the fracture resistance under mode I loading conditions and b) observing the failure mechanisms during crack growth. Crack growth in cellulose networks can be complicated by the occurrence of fibre bridging during crack growth and resembles fracture or tearing of paper[1-4]. Fibre bridging as a toughening mechanism results in a large fracture process zone and gives significant rise to the fracture resistance with crack extension (*R*-curve behaviour)[5,6]. Therefore, the fracture of these materials should not in general be characterised in terms of Linear Elastic Fracture Mechanics (LEFM) which assumes that the fracture process zone is very small in comparison with all length dimensions (including the crack size) of the specimen[7]. In contrast, when the size of the fracture process zone is comparable to or larger than any of the specimen dimensions, the fracture process zone should be analysed using Non-Linear Fracture Mechanics[6]. However, such a modelling approach is well beyond the scope of this thesis; instead, here, a simplified method based on a Double Cantilever Beam (DCB) specimen loaded with pure bending moments was used to evaluate the effect of refinement time on the fracture behaviour of the binder-free all-cellulose composites.

7.2 Experimental methodology

The fracture properties are determined through the use of a Double Cantilever Beam (DCB) sandwich specimen as shown in Figure 7.1. It consists of the all-cellulose composite glued inside the grooves of two steel beams that are mounted on a special fixture (described in section 7.2.3), which applies pure bending moments[8]. The use of the steel beams in such sandwich specimens has a practical issue as these

stiff elastic beams facilitate the mounting of the specimen to the fixture avoiding local failure at the point of fixation.

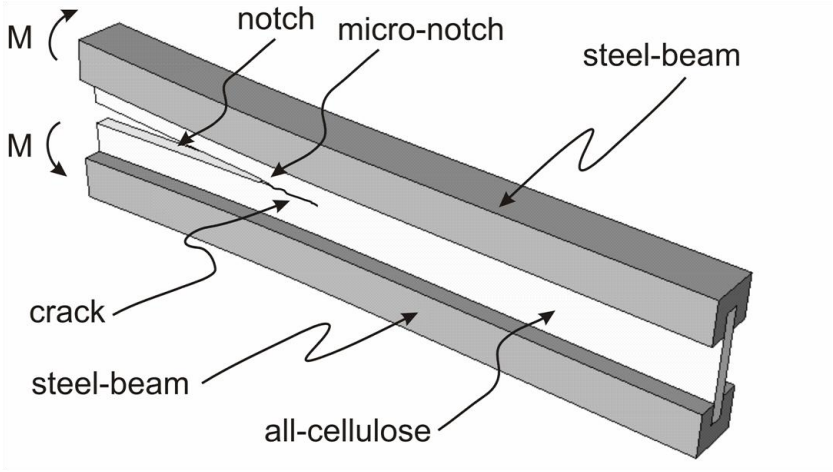

Figure 7.1. Double Cantilever Beam (DCB) specimen loaded with pure bending moments.

7.2.1 Sample preparation

Binder-free all-flax composites were produced at different refining times including 1.5, 3, 4, 5 and 6 hrs, according to the experimental protocol described in Chapter 5.

7.2.2 Specimen geometry

Rectangular specimens with a central notch along the largest dimension were cut from binder-free all-flax composite panels at dimensions approximately 10 mm x 65 mm x *b* mm, where width *b* varied from 1.2 to 2 mm depending on the refining time. The notch length (see Figure 7.1) was 25 mm and the height was approximately 1 mm (notch radius = 500 µm). Fracture mechanics testing requires a sharp pre-

crack, which is usually achieved by cyclic loading. However, fatigue pre-cracking is quite difficult and time consuming. Therefore here a sharp crack was sawed manually at the root of the notch with a thin steel band that had its edge finely ground using a 1 µm diamond slurry[9,10]. The micro-notch at the root of the initial notch obtained this way can be seen in Figure 7.2-a, while Figure 7.2-b shows the micro-notch in detail. The micro-notch has a root radius less than 1.5 µm which, it is argued, suffices for accurate fracture mechanics measurements. Figure 7.2-c shows a cross-sectional view of the notch and micro-notch geometry from a fractured specimen. It can be seen that the micro-notch length along the cross-section is uniform.

After preparation of the micro-notch, the binder-free all-flax composite panels were placed inside the grooves of two steel beams and glued using a two-part epoxy adhesive (Scotch-WeldTM DP460 from 3M) to form the Double Cantilever Beam (DCB) test specimen, which is shown in Figure 7.1. The height, H, of the steel beams was 5.95 mm and the width, B, 4.85 mm. The depth of the grooves, *t*, was 1.5-2.0 mm.

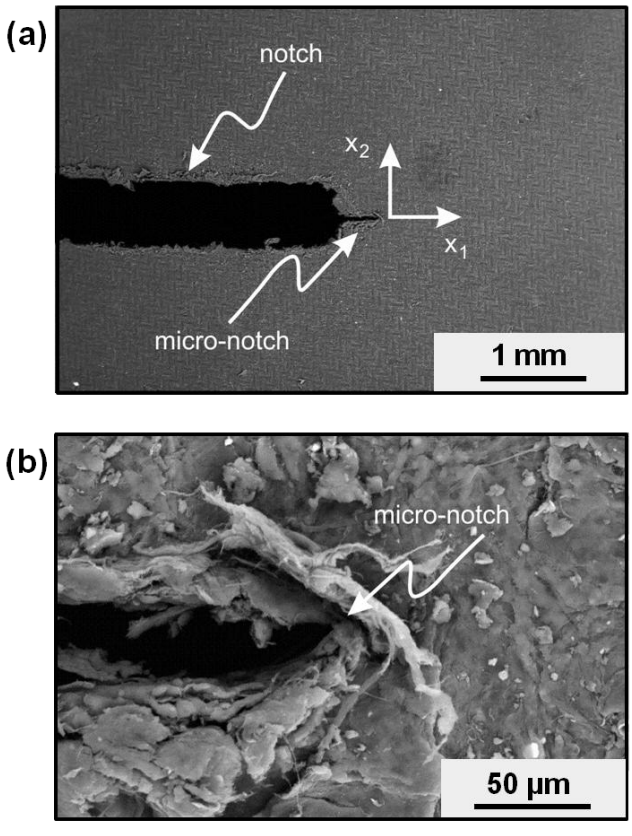

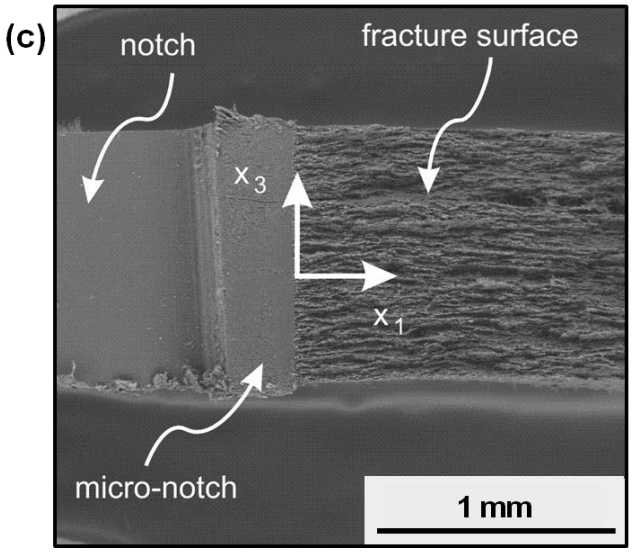

Figure 7.2. (a) SEM micrograph of the notch geometry, (b) close view of the micro-notch at the root of the machined macro-notch and (c) cross-sectional view of the notch geometry after fracture. (all-flax composite obtained after 6 hrs of refining).

7.2.3 Loading arrangement and instrumentation

Pure bending moments are applied to the DCB specimen using a special fixture as described by Sørensen et al.[8,11], which can be operated inside the chamber of an environmental scanning electron microscope (ESEM) for in situ observation of the crack growth. In an ESEM, the specimens do not need to be coated with conductive layers as in a conventional SEM since the new surfaces created by crack growth ”charge up”, thus hindering their observation in detail.

All the tests were conducted at room temperature and at vapour pressure of 50 Pa. The fixture was mounted on the *XYZ* stage of the microscope (Zeiss Evo 60 EP-SEM) and thus by translating the stage in the specimen plane (*XY*) the crack growth increments (defined below) could be measured.

7.2.4 Loading procedure

The DCB specimens were subjected to a monotonically increasing loading in the ESEM. Images of the initial crack tip/micro-notch were recorded at different load levels (moments) as shown in Figure 7.3. As the moment increases, the opening of the crack tip increases. These openings represent the opening of the crack tip fracture process zone. At a certain load level, crack growth takes place at the tip of the micro-notch (Figure 7.3-a).

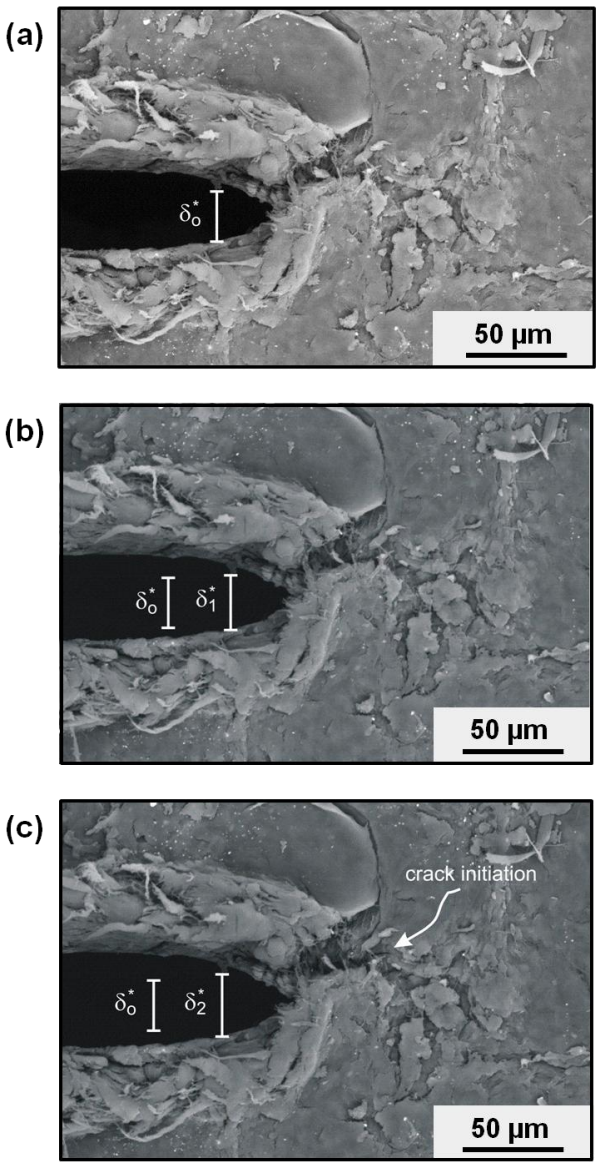

Figure 7.3. Backscatter electron micrographs showing the opening of the crap tip for binder-free all-flax composite produced with 6 hrs of refining.

Applied load was further increased and images were taken to measure the opening of the initial crack tip as illustrated in Figure 7.4. These openings correspond to the openings of the fibre bridging zone. The applied load was increased until complete failure of the specimens. In the bridging zone there are fibres or bundle of fibres that connect the crack faces, and thus forces can still be transmitted, hence increasing the fracture resistance with crack growth (*R*-curve behaviour).

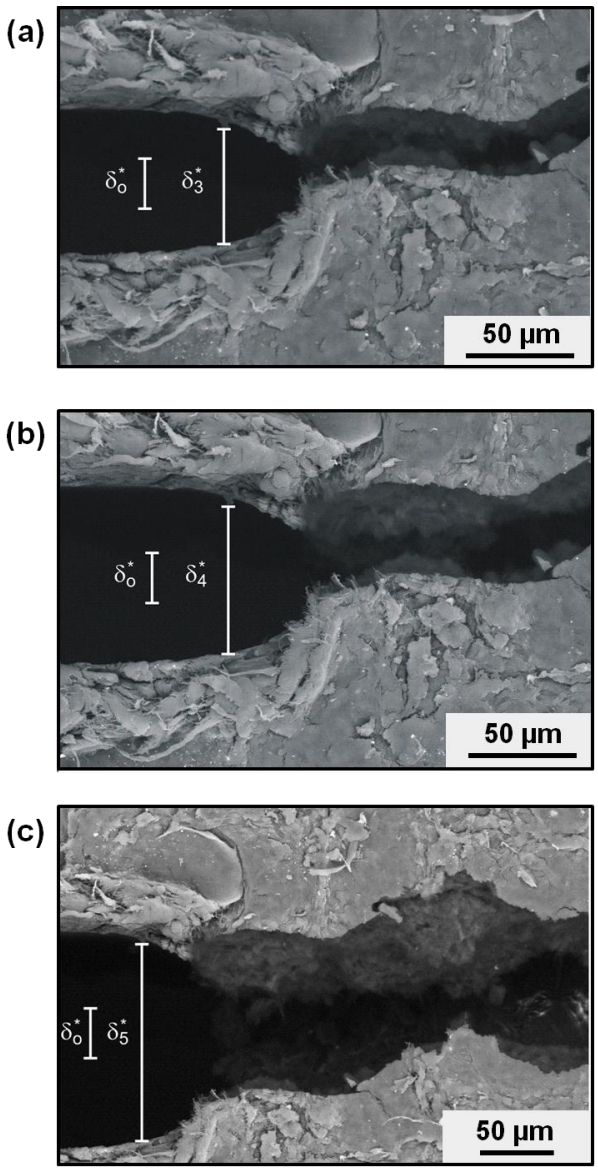

Figure 7.4. Backscatter electron micrographs showing the opening of the fibre bridging zone for the all-flax composite produced from 6 hrs of refining.

In parallel with measurements of the end opening of the fracture process zone, the crack extension was measured as a function of the applied moment to obtain fracture resistance curves (traditional *R*-curves).

For a number of specimens, after crack initiation and subsequent crack growth, the specimens were partially unloaded. The new crack tip was located and then the crack growth was monitored with increasing load to observe the failure mechanisms in front and at the wake of crack tip. This procedure was repeated several times per specimen. For these experiments, no measurements are reported since the bridging zone is affected by the specimen unloading.

7.2.5 Characterisation method

As it was mentioned in the introduction, when the fracture process zone is comparable or larger than any specimen length dimension, Non-Linear Fracture Mechanics should be used[7]. The use of Non-Linear Fracture Mechanics is however complicated in the present work due to: a) the specimen geometry, and b) the composites stress-strain behaviour. The DCB specimen of Figure 7.1 is a bimaterial sandwich specimen for which an analytical but complicated expression for the fracture energy is only available for the case where both materials are linear elastic[12]. However, the binder-free all-flax composites have a non-linear mechanical response, and thus the solution of Bao et al.[12] should be modified to account for this non-linearity. This can prove to be a complicated task and in general there is no analytical expression possible. Thus, a simplified method was preferred to compare the fracture properties of the binder-free all-flax composites as a function of refining time, which involved plotting the measured applied moments as a function of the crack end-opening and as function of the crack extension.

The solution of Bao et al.[12] can be written in the following form:

$$G = f\ (geometry, elastic\ properties)\ M^2 \quad \text{(Equation 7.1)}$$

where f is a complicated function that depends on the geometry of the DCB sandwich specimen and the elastic properties of the steel and the all-cellulose composite. As it was mentioned, Equation 7.1 is not valid when one or both materials of the DCB sandwich specimen have a non-linear stress-strain response. However, since the Young's modulus of the steel beams is much larger than the Young's modulus of the cellulose composites, the fracture energy in Equation 7.1 is dominated by the steel beams and thus the binder-free all-flax composites can be assumed to be linear elastic. With this assumption, Equation 7.1 can be used and the error introduced is very small. It can be learned from Equation 7.1 that the fracture energy is proportional to the square of the applied moment and thus we can simply use the applied moments to analyse the fracture behaviour and study the effect of the refining time, avoiding in this way to having to calculate the constant function f.

7.3 Results and discussion

7.3.1 Fracture resistance

Representative applied moments curves as function of the normal end-opening, δ*, are shown in Figure 7.5 for the five different refining times. In all cases, the applied moment increases from a relatively low value, corresponding to deformation and damage initiation at the crack tip region (see Figure 7.3). At some level of applied moment, crack initiation occurs at the crack tip, followed by crack growth. During crack initiation and crack growth the applied moment continues to increase due to the fibre bridging at the wake of the crack tip (see Fig. 7.4). When the bridging zone is fully developed, the applied moment reaches a steady-state value,

which is higher for lower refining times. The end-opening at which the steady-state is attained is also increasing for lower refining times although this observation is not very clear from Figure 7.5 due to scatter in the experimental results.

A fully developed bridging zone is attained when the fibres at the position of the initial crack tip start to break (Figure 7.3). As the specimen continues to be loaded, the crack grows and a number of fibres and bundle of fibres enter the bridging zone but at the same time an equivalent number of fibres and fibre bundles fail at the end of the bridging zone. As a result, the sum of forces transmitted to the crack faces by the bridging fibres is constant and the bridging zone purely translates along the specimen length. Thus there is no increase in the applied moment. This can be clearly seen in Figure 7.5.

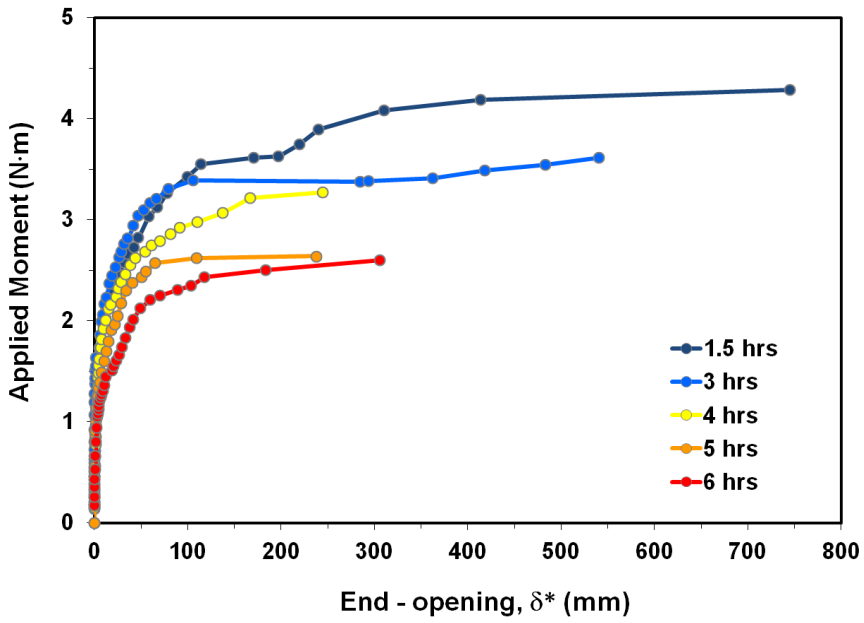

Figure 7.5. Applied moments curves, *M*, as a function of the end-opening δ^* for binder-free all-flax composites produced at different refining times.

7.3.2 *R*-curve

Figure 7.6 shows the representative *R*-curves (applied moment as a function of the crack extension) for the different binder-free all-flax composites. It can be seen that significant crack growth takes place before the steady-state is attained illustrating the significance of the bridging mechanisms in increasing the fracture resistance.

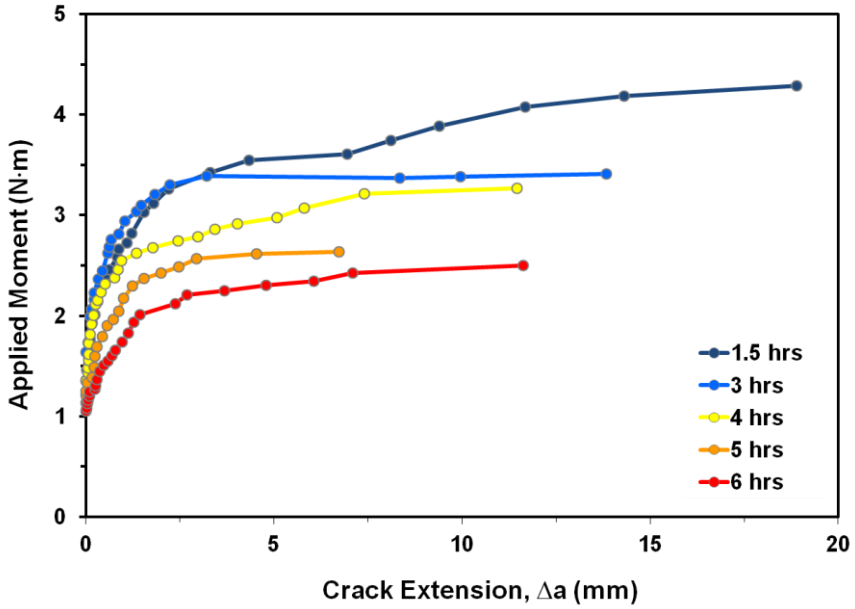

Figure 7.6. Applied moment curves, *M*, as a function of the crack extension, Δa, for binder-free all-flax composites obtained at five different refining times.

7.3.3 Crack initiation

As explained in Chapter 5, the degree of fibrillation of the flax fibres increases with the refining time. The enhanced fibrillation degree of flax fibres achieved after 6 hrs of refining, allows a more extensive Van der Waals or hydrogen-bonded network between the fibres. Such a strong network structure would result in

higher applied moment (higher fracture resistance) for crack initiation. At a low refining time of 1.5 hrs, the fibrillation process has just started and the flax fibres remain almost intact. In this case, due to the absence of sub-micron sized fibrils, the effective cross-linking between the fibres is limited. Such a weak bonding between the fibres would result in lower applied moment (lower fracture resistance) for crack initiation. To verify this, the crack end-opening at the onset of crack growth, was measured quite accurately by observing the initial micro-notch at high magnification as shown in Figure 7.3-c as a function of the applied moment. The measured end-opening for crack initiation for the binder-free all-flax composites with 6 hrs refining time was between 6-7 µm, whereas for binder-free all-flax composites with 1.5 hrs refining time this was 3-4 µm. A larger opening for crack initiation also means higher applied moments, and thus higher fracture resistance. These results are in agreement with the flexural bending results showed in Figure 5.4 of Chapter 5, where the improvement of the flexural strength of these binder-free composites with refining time was demonstrated. Fracture in three-point bending specimens, unlike the DCB specimens loaded with pure bending moments used in this chapter, is unstable e.g. when fracture occurs, the specimen fails catastrophically and the bending flexural strength is related to the fracture resistance for crack initiation.

7.3.4 Fracture observations – bridging zone

As mentioned above, the increase of refining time results in an increase in fibre fibrillation. However, higher refining times not only lead to a reduction in fibre diameter but also to shorter fibres and thus, a smaller fracture resistance increase with crack growth can be seen in Figure 7.5. The fracture resistance in the bridging zone (at the wake of the crack-tip) is controlled by the length of the fibres and the adhesion between them. As the crack opens, short fibres are less effective in bridging the crack faces and therefore the increase in applied moment (fracture resistance) is less pronounced. In addition, the enhanced bonding between the fibres in the binder-

free all-flax composites with increased fibrillation also contributes in a smaller increase in applied moment (fracture resistance). Several authors have published that weaker interfacial bonding between the fibres results in higher fracture resistance in long and short glass fibre composites[13, 14]. Strong bonding between fibres can lead to fibre failure, whereas when the bond is weak, the fibres do not fail and thus can still transmit stress between the crack faces.

Figure 7.7 shows a sequence of micrographs of a binder-free all-flax composite obtained from 5 hrs of refining for increasing applied moment. It clearly shows the fibre bridging limitation in the bridging zone. The same can be seen in Figure 7.4 for the material with 6 hrs of refining time. In both panels the fibres were extensively fibrillated and therefore, their fibre length was considerable reduced, which makes these fibres less effective in increasing the fracture resistance.

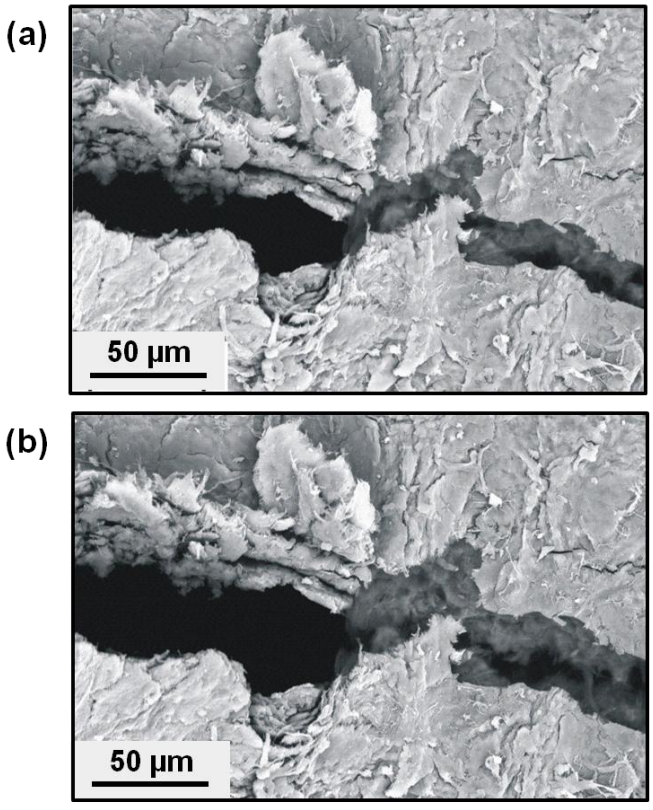

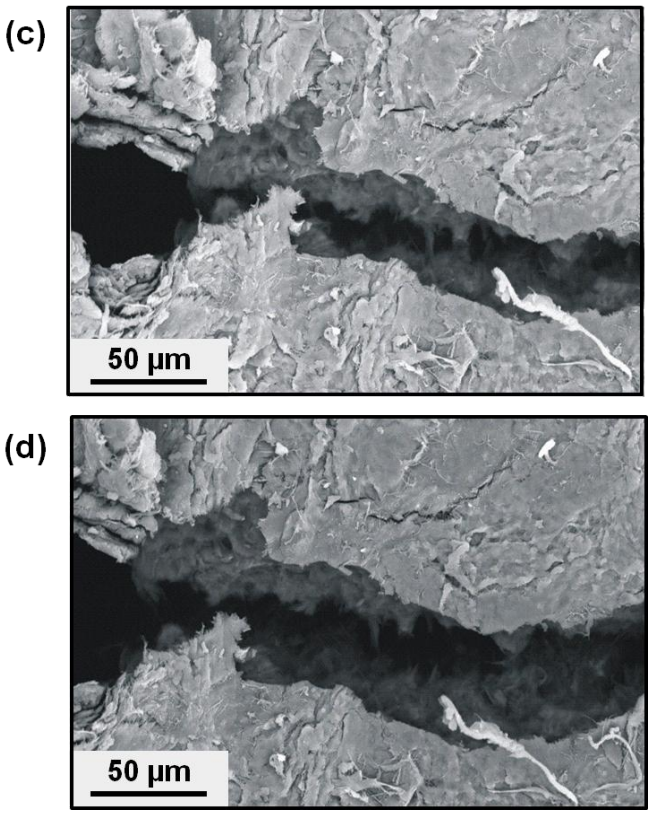

Figure 7.7. Backscatter electron micrographs showing the end-opening of the fracture process zone at increasing applied moment for the binder-free all-flax composite produced by a refining of 5 hrs.

On the other hand, for a short refining time of 1.5 hrs, extensive fibre bridging takes place (Figure 7.8) due to the greater fibre length of these low fibrillated flax fibres. Almost intact fibres can be seen in the bridging zone. Even for large crack openings (Figure 7.9), the fibres are still transmitting stresses between the crack faces. These observations are in agreement with the results of Figure 7.5 and the increase in the fracture resistance with decreasing fibre fibrillation. Furthermore, the presence of large fibres in the bridging zone should result in higher cohesive stresses as shown in Figure 7.8.

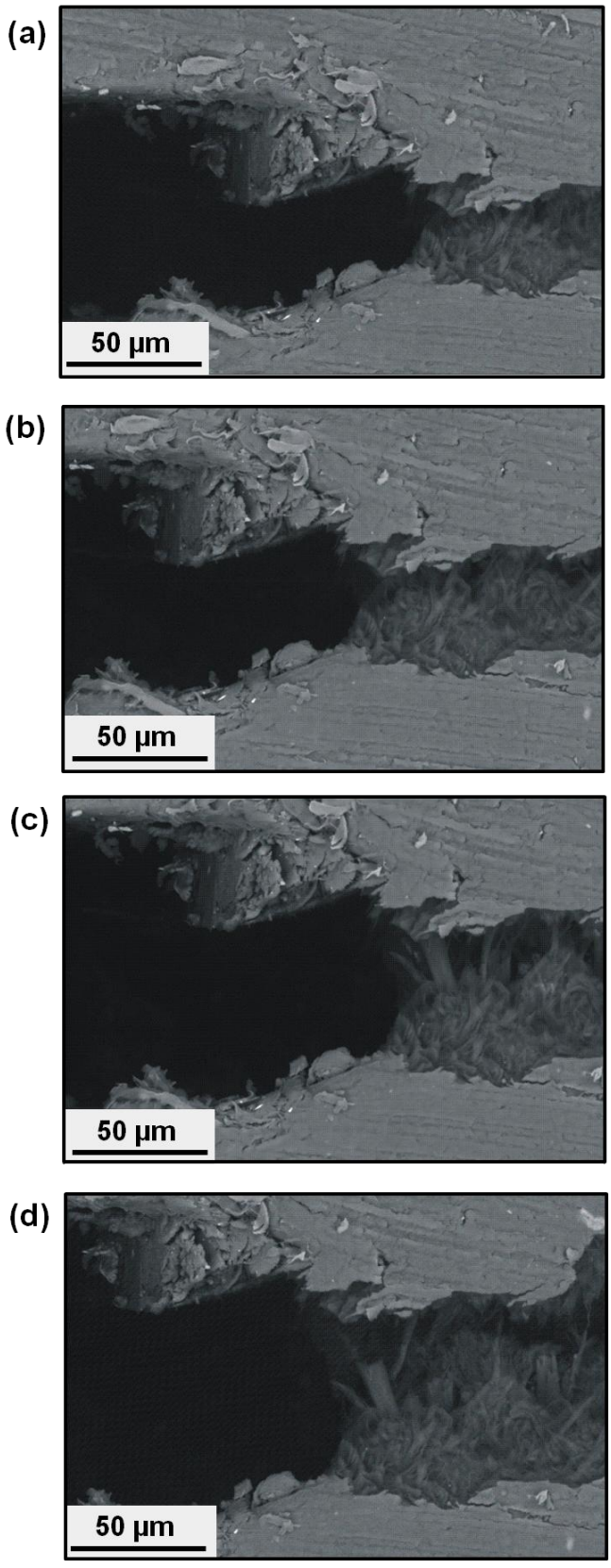

Figure 7.8. Backscatter electron micrographs showing the end-opening of the fracture process zone at increasing applied moment for the binder-free all-flax composite produced by a refining of 1.5 hrs.

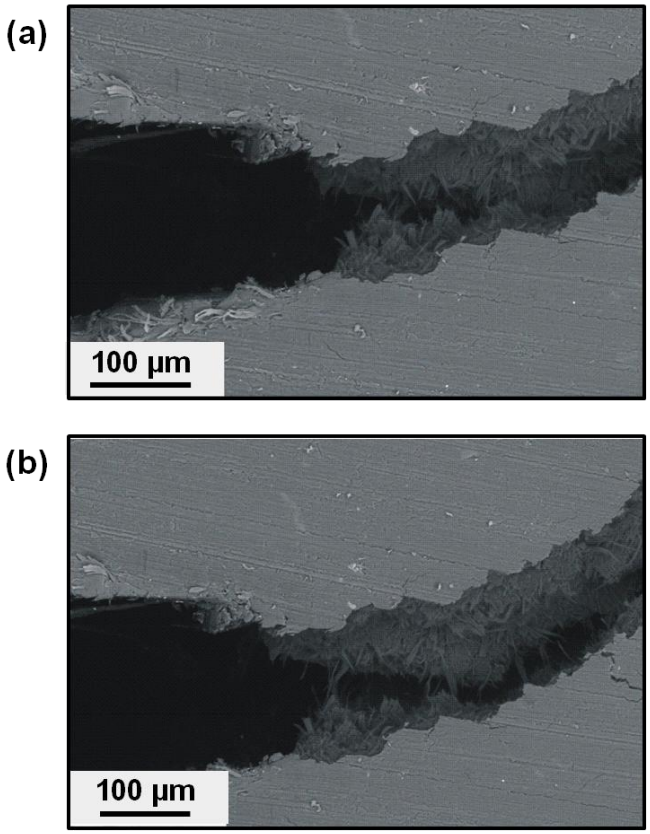

Figure 7.9. Backscatter electron micrographs showing fibre bridging the crack faces at large end-openings while the moment is increasing for the binder-free all-flax composite obtained after a refining of 1.5 hrs.

7.4 Conclusions

A sandwich DCB specimen loaded with pure bending moments was used for mode I fracture mechanics characterisation of binder-free all-flax composites. Using a simple method, which was shown to yield equivalent conclusions to rigorous fracture mechanics analysis, the effect of the refining time on the fracture properties could be determined. By performing the experiments inside the chamber of an

environmental scanning electron microscope, interesting information about the failure mechanisms was obtained.

Similar to paper, the mechanical properties of these materials are originated from the formation of intra and intermolecular bonds between the cellulose fibrils. The applied moment (fracture resistance) for both crack initiation and crack opening increased with fibre fibrillation. This was due to the presence of a stronger Van der Waals or hydrogen bonded network structure in binder-free all-flax composites with higher refining time. However, the steady-state applied moment (fracture resistance) decreased with increasing fibre fibrillation since an increase of refining time results not only in a reduction in fibre diameter but also in shorter fibres. This, combined with the formation of a stronger network between refined flax fibres, resulted in a lower applied moment (fracture resistance) with increasing refining times.

7.5 References

[1] S. Heyden and P. J. Gustafsson, JOURNAL OF PULP AND PAPER SCIENCE 25 (5), 160 **(1998)**.

[2] H. Kettunen and K. Niskanen, JOURNAL OF PULP AND PAPER SCIENCE 26 (1), 35 **(2000)**.

[3] P. Isaksson, P. A. Gradin, and A. Kulachenko, International Journal of Solids and Structures 43 (3-4), 713 **(2006)**.

[4] P. Isaksson and R. Hagglund, International Journal of Solids and Structures 44 (18-19), 6135 **(2007)**.

[5] D. Broek, *Elementary engineering fracture mechanics*. 4th edition, ed. Dordrecht, Boston, Martinus Nijhoff Publishers**(1986)**.

[6] Z. Suo, G. Bao, and B. Fan, Journal of the Mechanics and Physics of Solids 40 (1), 1 **(1992)**.

[7] M. F. Kaninen and C. H. Popelar, Advanced fracture mechanics, New York: Oxford University Press **(1985)**.

[8] B. F. Sørensen, A. Horsewell, O. Jørgensen, A. N. Kumar, and P. Engbæk, Journal of the American Ceramic Society 81 (3), 661 **(1998)**.

[9] S. Goutianos, H. L. Frandsen, and B. F. Sørensen, Journal of the European Ceramic Society 30 (15), 3173 **(2010)**.

[10] J. J. Kruzic, S. J. Kuskowski, and R. O. Ritchie, Journal of Biomedical Materials Research Part A 74A (3), **(2005)**.

[11] B. F. Sørensen, P. Brethe, and P. Skov-Hansen, Journal of the European Ceramic Society 16 (9), 1021 **(1996)**.

[12] G. Bao, S. Ho, Z. Suo, and B. Fan, International Journal of Solids and Structures 29 (9), 1105 **(1992)**.

[13] S. Feih, J. Wei, P. Kingshott, and B. F. Sørensen, Composites Part A: Applied Science and Manufacturing 36 (2), 245 **(2005)**.

[14] S. P. Fernberg and L. A. Berglund, Composites Science and Technology 61 (16), 2445 **(2001)**.

8

Conclusions and future work

8.1 Conclusions

Nowadays, problems associated with the environment such as the shortage of landfill space, the depletion of petroleum resources, the emissions during incineration and hazards to living beings combined with the growing environmental awareness have motivated an extensive research in environmentally friendly materials in order to replace materials considered harmful to the environment. Natural fibres represent exceptional candidates for the production of biomaterials due to their low cost, worldwide availability, low density, competitive specific mechanical properties, sustainability, combustibility and biodegradability. Their competitive mechanical properties together with superior environmental benefits has spurred exploitation as an alternative to conventional reinforcements in composite

materials, such as glass fibres, over the last few years. Comparative life cycle assessment (LCA) studies have demonstrated that NFRPs are environmentally superior to GRP in most applications for the following reasons: natural fibre production results in lower environmental impacts compared to high-temperature glass fibre production; NFRPs require higher fibre content for equivalent performance, reducing the amount of polluting polymer matrix; lightweight NFRPs improve fuel efficiency and reduce emissions during their use phase, especially in automotive applications; and end-of-life incineration of natural fibres results in energy recovery[1]. A further advantage arises when natural fibres are combined with a biodegradable matrix, such as polyhydroxybutyrate (PHB), polylactic acid (PLA) or starch, since an additional disposal option becomes available through composting.

Despite the advantages associated with NFRPs, the low interfacial adhesion between biofibres and hydrophobic polymer matrices because of the poor compatibility between them[2-4] poses a serious problem for their widespread application, since the different strategies currently employed to improve their compatibility usually involves an increase in processing cost and time[5] as well as a reduction of the "green" character associated with cellulose fibres. The development of cost effective and environmentally friendly methods for the fibre and/or matrix modifications is necessary, since one of the main market attraction of natural fibre composites is their competitive price[6]. An alternative solution to enhance the fibre-matrix adhesion while notably improving the environmental impact regarding polymeric matrix and composite recyclability is provided through the development of all-cellulose composites[7]. The fact that in these composites both the fibre and the matrix are chemically identical renders an excellent interfacial compatibility, hence providing fully recyclable and environmentally friendly materials with good mechanical properties[5,8].

The aims of this thesis were to produce all-cellulose composites through two different experimental procedures as well as to assess the properties of the resulting materials.

The first strategy applied for the production of all-cellulose composites was based on a selective dissolution method where the cellulose fibre skins were partially dissolved to form a matrix phase that bonds the fibres together, while the strong core fibres were maintained to impart a real reinforcing effect to the composites. All-cotton composites were successfully prepared by partial dissolution of cotton fibres in (LiCl/DMAc). Solvent exchange was used as activation pretreatment, involving subsequent immersion of the fibres in water, acetone and DMAc. The influence of three parameters on the mechanical properties of the all-cotton composites was investigated: (i) dissolution time, (ii) activation time and (iii) cellulose source. These three parameters had a strong effect on the dissolution process of the raw cotton fibres and on the structure of the obtained composites in terms of the interfacial bonding between the remaining cellulose fibre cores. The optimisation of the activation and dissolution times was key for the production of high-performance all-cellulose composites by this method. The activation pre-treatment performed under the optimum conditions allowed achieving a homogenous dissolution of the cotton fibres surfaces, while longer pre-treatments than the optimum one resulted in a heterogeneous dissolution process of the fibres, leading to composite materials with regions of completely dissolved fibres (providing no reinforcement) and another region with nearly undissolved fibres (providing no interfacial adhesion). At the optimum dissolution time, the amount of cotton fibre surfaces selectively dissolved to form the matrix phase was adequate to provide sufficient interfacial adhesion to the composite, while the remaining fibre cores maintained most of their initial strength. In addition, the final properties of the all-cellulose composites were influenced by the initial characteristics of the cellulose source. The best-performing all-cellulose composite obtained by this method had a Young's modulus and tensile strength of 5.5 GPa and 145 MPa, respectively, leading to materials with promising properties, out-performing most isotropic glass- and natural fibre reinforced plastics.

However, although this method provides a great advance towards the production of high quality biobased materials, it still involves the use of environmentally hazardous solvents.

For this reason, a new environmentally friendly concept was developed for the production of all-cellulose composites: "binder- or matrix-free all-cellulose composites". This concept for all-cellulose panel materials made entirely from plants and biobased waste sources use water as a processing aid, no pre-treatment, no solvents and, most importantly, no resins or bonding agents as in the case of e.g. phenolic resin based MDF or natural fibre reinforced plastics. Instead bonding between fibres is achieved solely through Van der Waals or hydrogen-bonding as occurs in conventional paper. Compared to conventional paper, binder-free all-cellulose composites present a denser network structure as a result of a greater interaction between fibres with higher specific surface area (Figure 8.1). Such an extensive fibrous network is responsible for the high mechanical performance of these binder-free all-cellulose composites. Therefore, the key for producing binder-free materials is to enhance the Van der Waals or hydrogen-bonding capability of the cellulose fibres by increasing their specific surface area. A promising way to increase the cellulose network density is through the use of nanofibrillated cellulose, however until recently the high energy consumption required for its isolation has prevented its industrialisation. For this reason, an alternative processing method for a large scale production of fully recyclable and biodegradable materials based on the exploitation of the intrinsic high Van der Waals or hydrogen bonding capability of nanofibrillated cellulose has been designed and optimised. This environmentally friendly processing protocol based on the refinement of raw cellulose materials such as plant fibres and cellulose wastes does not require the application of pre-treatments and/or purification processes and the use of non-environmentally friendly chemical substances, resulting in high yields at low processing cost, which makes industrialisation easy.

In this process, the optimisation of the fibre refining time was key for the creation of a strong network structure based on an enhanced inter-fibre crosslinking through nano-sized fibrils, and as a result the production of very compact all-cellulose materials with low void contents. The interfacial bonding area between the fibres was considerable increased due to the high specific surface area of the fibres

and the presence of a high amount of nanofibrils achieved through an optimal refining process.

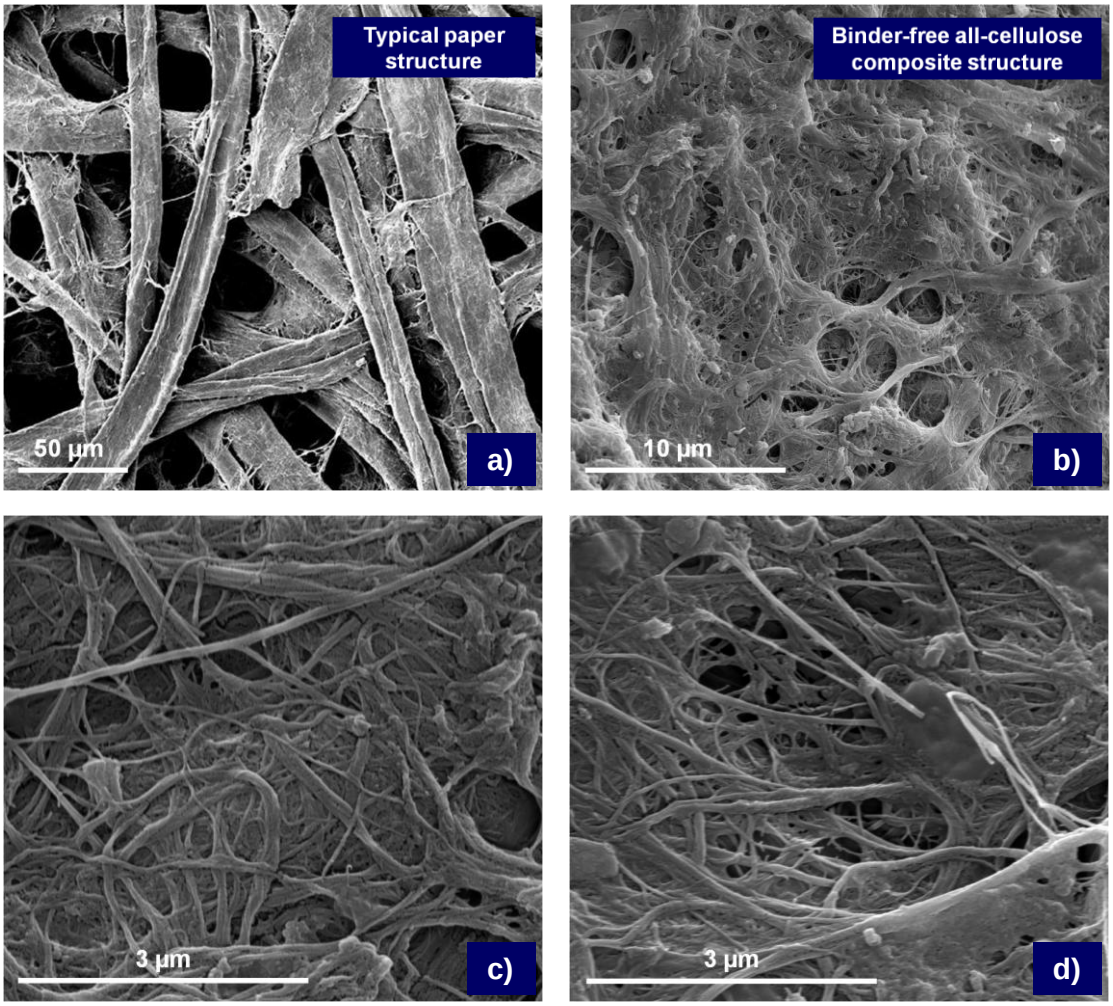

Figure 8.1. SEM images of the Van der Waals or hydrogen-bonded network structure of conventional paper (a) versus binder-free all-cellulose composites (b-d). Note that the magnifications in (b), (c) and (d) differ from that in (a).

The initial fibre length was also demonstrated to play an important role in the production of these materials due to its strong effect on mechanical performance. Long fibres with high aspect ratios are desirable for reinforcing composite materials as they are more effective in transferring loads and stopping crack growth, however,

in this type of materials, fibres longer than the optimum led to less compacted materials with lower mechanical performance since the presence of fibre entanglements hindered the effective fibrillation of fibres.

The use of flax fibres as raw material for the production of binder-free all-cellulose composites provided panel products with impressive flexural properties (values as high as 119 MPa and 17 GPa were achieved for both flexural strength and modulus, respectively) that out-perform those of most conventional natural fibres reinforced plastics and wood panel products. Their outstanding mechanical performance and low water absorption, combined with their fully biobased nature, recyclability and biodegradability and lower production costs, make these materials exceptional alternatives of conventional reinforced plastics, wood fibre composites and other chipboards for building applications.

However, the application of natural fibres such as hemp and flax for the manufacture of these materials at an industrial scale could possess several problems related to their seasonal availability, storage and price. Consequently, an alternative cellulose source, recycled paper, was proposed for a more cost-efficient production of binder-free all-cellulose composite. Due to the low cost and availability throughout the year of recycled paper fibres, the use of this cellulose source as a raw material will not only involve a considerable reduction of the material processing costs, but also the elimination of the possible storage problems. Binder-free all recycled paper fibre panels were successfully obtained through the previous experimental procedure with slight modifications. In contrast to binder-free all-flax composites, the material based solely on recycled paper exhibited extremely poor mechanical properties as a result of the poor mechanical properties of recycled paper fibres. Hemp or bleached kraft fibres were therefore incorporated into the recycled paper pulp in an attempt to enhance the mechanical properties of the binder-free recycled paper based materials.

The partial external fibrillation of the reinforcing fibres (hemp and kraft fibres) was crucial for providing a reinforcing effect in recycled paper based materials since the addition of non-refined fibres proved to have a detrimental effect on the mechanical properties as a result of their lack of adhesion with the recycled paper fibres, and the disruption of the hydrogen bonded network between these recycled fibres.

An optimal degree of fibrillation of the reinforcement was essential for achieving a maximum reinforcing effect. Fibres with a lower degree of fibrillation than the optimum one do not have enough specific surface area to form a strong network with the recycled paper fibres, leading to poorly compacted materials of low mechanical performance. However, similarly, at refining times exceeding the optimal one, also a loss of reinforcing efficiency was observed due to excessive degradation of the fibre structure.

The addition of 30 wt.% of partially refined kraft or hemp reinforcement into the recycled paper pulp led to a strong improvement of the composite flexural properties for types of reinforcing fibres. Although the mechanical properties of these composites were lower than those achieved for all-flax composites, they still out-perform those of most conventional reinforced plastics, evidencing the feasibility of producing fully recyclable and biodegradable binder-free all-cellulose composites at low cost.

Finally, the fracture properties of binder-free all-flax composites were studied as a function of refining time. Both the fracture resistance for crack initiation and the peak cohesive stress increased with fibre fibrillation since the increase of the fibre specific surface area with the refining time allowed the formation of a stronger Van der Waals or hydrogen bonded fibre network structure. However, the steady-state fracture resistance decreased with increasing fibre fibrillation due to a considerable reduction in fibre length at longer refinement times. This, combined with the

formation of a stronger network between the refined flax fibres, resulted in a reduction in fracture resistance with increasing refining times.

8.2 Future work

Depending on the application, a further characterisation of these binder-free all-cellulose composites should be performed in order to guarantee their suitability for such application. For building applications, fire resistance, insulation behaviour, wear and impact resistances, etc. need to be further studied.

Another important aspect for future research is related to the recyclability of these binder-free all-cellulose composites. Since these materials have a structure similar to the one of the conventional paper, they should be recyclable using a simple repulping process. This could lead to new binder-free all-cellulose materials, giving these materials a significant environmental benefit of natural fibre reinfocerd plastics or panel board materials such as MDF, where incineration is the main end-of-life senario. Therefore, a study of the effect of the recycling process on the properties of the recycled binder-free materials is essential to assess the viability of material recycling. In addition, the determination of the maximum number of recycling cycles which these materials can undergo without considerable degradation of their properties needs to be identified.

8.3 References

[1] S. V. Joshi, L. T. Drzal, A. K. Mohanty, and S. Arora, Composites Part A: Applied Science and Manufacturing 35 (3), 371 **(2004)**.

[2] R. Malkapuram, V. Kumar, and Y. S. Negi, Journal of Reinforced Plastics and Composites 28 (10), 1169 **(2009)**.

[3] M. J. John and S. Thomas, Carbohydrate Polymers 71 (3), 343 **(2008)**.

[4] M. Q. Zhang, M. Z. Rong, and X. Lu, Composites Science and Technology 65 (15-16), 2514 **(2005)**.

[5] N. Soykeabkaew, N. Arimoto, T. Nishino, and T. Peijs, Composites Science and Technology 68 (10-11), 2201 **(2008)**.

[6] G. Bogoeva-Gaceva, M. Avella, M. Malinconico, A. Buzarovska, A. Grozdanov, G. Gentile, and M. E. Errico, Polymer Composites 28 (1), 98 **(2007)**.

[7] T. Nishino, I. Matsuda, and K. Hirao, Macromolecules 37 (20), 7683 **(2004)**.

[8] T. Nishino and N. Arimoto, Biomacromolecules 8 (9), 2712 **(2007)**.